Author:
Flynn, Ben

Title:
Loss of ultradian glucocorticoid pulses modulates glucocorticoid receptor and transcriptional regulation in the liver

University of BRISTOL

Loss of ultradian glucocorticoid pulses modulates glucocorticoid receptor and transcriptional regulation in the liver.

By

Benjamin P Flynn

Bristol Medical School

June 2019

Supervisors: Dr. Becky Conway-Campbell & Prof. Stafford Lightman

A dissertation to the University of Bristol in accordance with the requirements of the degree of Doctor of Philosophy in the Faculty of Health Sciences.

Word Count: 44,346

Abstract

Circulating adrenal glucocorticoids exhibit characteristic circadian and ultradian rhythms, important for maintaining homeostasis and regulating multiple physiological processes. Glucocorticoids exert genomic actions on target cells via a ligand activated transcription factor, the glucocorticoid receptor (GR). In the liver, GR regulates transcription of many critical determinants of carbohydrate and fat metabolism. Furthermore, glucocorticoids been implicated in metabolic disorders including insulin resistance, hyperlipidaemia and non-alcoholic fatty liver disease. Despite the increasing prevalence of metabolic disease in western society, the relative contribution of glucocorticoid rhythm disturbance, particularly ultradian dysregulation, has been largely unexplored.

Using GR ChIP-Seq of livers taken from corticosterone treated adrenalectomised (ADX) rats, I have found that ultradian replacement induces ~3,000 GR binding events at the pulse peak, all of which are lost at the pulse nadir. I have further demonstrated that constant corticosterone infusion results in prolonged GR binding. To assess effects on gene transcription, I have also performed RNA polymerase II ChIP-Seq with an antibody specific for the actively transcribing form of the complex. Using pSer2 RNA polymerase II binding as proxy for active gene transcription, I found similarly synchronised, predominantly down-regulated transcriptional modulation in response to corticosterone pulses. Whereas in response to constant corticosterone, prolonged and mostly upregulated transcription was detected.

Notably, functional pathway analysis showed that differentially regulated targets were involved in glucose, carbohydrate, cholesterol, fatty acid, lipid, proliferative and necrotic pathways. My findings support the hypothesis that glucocorticoid pattern dysregulation leads to dysregulation of key metabolic targets in the liver, potentially contributing to the development of metabolic syndrome.

Finally, I present the development of a novel rodent corticosterone replacement model that incorporates both circadian and ultradian rhythms for use in longer duration studies where I plan to test the metabolic outcome of chronic glucocorticoid dysregulation. This approach shows great potential for ultradian research, particularly for translational studies.

Dedication and Acknowledgements

I would first and foremost like to express my sincerest gratitude to my supervisors Dr. Becky Conway-Campbell and Professor Stafford Lightman. Your ongoing support and advice have been invaluable. I would particularly like to thank Becky for her endless help, effort and expertise.

Thankyou also to Professor David Murphy and Dr. Liang-Fong Wong for your advice and support during my yearly progress reviews. Your comments and insights were extremely helpful.

I would further like to thank my work colleagues. First, Yvonne Kershaw and Dr. Matthew Brinie for all your help and amazing contributions, not only experimentally but also keeping me sane and amused. George Horn, Clare Kennedy and Dr. Georgina Hazell for always being there for a good moan and a great time. I could not ask for a better clique. Dr. Felicity Stubbs for her invaluable advice writing my thesis as well as telling me stories only from her I would believe. Everyone else past and present within the group, it has been a pleasure to work with you. Finally, a debt I can never repay to all the animals used within this project, as without them, none of this was possible.

To my family, a big thank you for your ongoing support and love. My mum (Bernadette) for always pushing me to be the best I can, my dad (Martin) for his breadth of knowledge and encouraging joy in unusual facts, particularly as his own pass the point of incredulity and to my sister (Naomi), whom has made me the resilient, calm and driven. Without all your influences I would not be the man I am, thank you.

Lastly, to Sophie. Your support and contribution to my life from the day I met you has been incalculable. You make me a better person and without you I don't know how I would have finished this thesis. You continue to make every day a joy. You mean the world and I love you.

I would also like to thank my collaborators, the national institute of Health, Maryland USA whom sequenced the ChIP samples at and Dr. Gordon Hagers group. Specifically, to Dr. Sohyoung who helped with preliminary QC analysis and was instrumental for trans-Atlantic communication.

I would like to thank my sponsors; The Wellcome Trust, Medical Research Council and the Needham Charitable Trust for supporting this project and providing me with my scholarship and costs of all materials and consumables

Author’s declaration

I declare that the work in this dissertation was carried out in accordance with the requirements of the University's *Regulations and Code of Practice for Research Degree Programmes* and that it has not been submitted for any other academic award. Except where indicated by specific reference in the text, the work is the candidate's own work. Work done in collaboration with, or with the assistance of, others, is indicated as such. Any views expressed in the dissertation are those of the author.

SIGNED: ..... DATE:.....

Table of Contents

University of BRISTOL

Table of Figures

Abbreviations

11β-HSD1	11 β-hydroxysteroid dehydrogenase type 1
11β-HSD2	11 β-hydroxysteroid dehydrogenase type 2
ACC	Acetyl coenzymeA carboxylase
Acetyl-CoA	Acetyl coenzymeA
ACTH	Adrenocorticotropic hormone
AD-1	Activation domain 1
AD-2	Activation domain 2
AD-3	Activation domain 3
ADX	Adrenalectomy
AF	Regulatory region
AF1	N-terminal transactivation region
AF2	C-terminal transactivation region
aka	Also known as
AKT	Activation function-1
AMPK	Adenosine 5’ monophosphate-activated protein kinase
AP1	Activator protein 1
aPKCι/λ	Atypical protein kinase Cι/λ
ApoAI	Apolipoprotein AI
ApoAIV	Apolipoprotein AIV
ApoB	Apolipoprotein B
ApoE	Apolipoprotein E
AR	Androgen receptor
ATP	Adenosine triphosphate
AVP	Arginine vasopressin
b	Base
BMAL	Brain and muscle ARNT-like 1
CBP	CREB binding protein
CBG	Corticosteroid binding protein
CDK1	Cyclin dependent kinase 1
CDK5	Cyclin dependent kinase 5
CEBPA	CCAAT enhancer binding protein alpha
ChIP	Chromatin immunoprecipitation

CK2	Casein kinase 2
CLOCK	Circadian locomotor output cycles kaput
COUP	Chicken ovalbumin upstream transcription factor
CRE	cAMP response element
CREB	Cyclic adenosine 3’,5’-monophospate response element-binding protein
CRH	Corticotropin releasing hormone
CRTC2	CREB-regulated transcriptional co-activator 2
DBD	DNA binding domain
Dex	Dexamethasone
DHS	DNase hypersensitive sites
DNA	Deoxyribonucleic acid
EDTA	Ethylenediaminetetraacetic acid
ER	Endoplasmic reticulum
F2,6BP	Fructose 2,6 bisphosphate
F6P	Fructose-1,6-bisphosphate
FASN	Fatty acid synthase
FAIRE	Formaldehyde-assisted isolation of regulatory elements
FBP1	Fructose 1,6-bisphosphatase
FBPase2	Fructose bisphosphatase 2
FDR	False discovery rate
FOX	Forkhead transcription factor
FOXM1	Forkhead box M1
G6P	Glucose-6-phosphate
G6PC	Glucose-6-phosphatase
GC	Glucocorticoid
GILZ	Glucocorticoid induced leucine zipper
GPAT3	Glycerol-3-phosphate acyltransferase 3
GPAT4	Glycerol-3-phosphate acyltransferase 4
GR	Glucocorticoid receptor
GRE	Glucocorticoid response element
GRU	Glucocorticoid response unit
GSK3β	Glycogen synthase kinase 3β
HAT	Histone acetyltransferase
HDAC	Histone deacetylase

HDAC2	Histone deacetylase 2
HDL	High density lipoprotein
HES1	Hairy enhancer split 1
HFD	High fat diet
hGR	Human glucocorticoid receptor
HIPK2	DNA damage-responsive kinase 2
HLDL	High density lipoprotein
HNF	Hepatic nuclear factor
hnRNA	Heterogeneous ribonucleic acid
HPA	Hypothalamic pituitary adrenal
HR	Hinge region
hr	Hour
hsp	Heat shock protein
I.P.	Intraperitoneal
I.V.	intravenous
IDR	Irreproducible discovery rate
IGF1	Insulin like growth factor 1
IPA	Ingenuity pathway analysis
JNK	c-Jun N-terminal kinase
kb	Kilobases
LBD	Ligand binding domain
LDL	Low density lipoprotein
LPL	Lipoprotein lipase
Lys	Lysine
MARK2	Microtubule affinity-regulating kinase 2
MED14	Mediator complex subunit 14
MetS	Metabolic Syndrome
min	Minute
MMTV	Mouse mammary tumor virus
MR	Mineralocorticoid receptor
MT2	Metallothionein 2
MTP	Microsomal triglyceride transfer protein
MYC	MYC proto-oncogene, BHLH transcription factor
mTOR	Mammalian target of rapamycin

NAFLD	Non-alcoholic fatty liver disease
NASH	Non-alcoholic steatohepatitis
NCOA1	Nuclear receptor coactivator 1
NCOA2	Nuclear receptor coactivator 2
nGRE	Negative glucocorticoid response element
NF1	Nuclear factor 1
NFκB	Nuclear factor kappa-light-chain-enhancer of activated B cells
NLS	Nuclear localisation signal
NTD	N-terminal domain
OAA	Oxaloacetate
PC	Pyruvate carboxylase
PCK1	Phosphoenolpyruvate carboxykinase
PCT	Patterned cort time point
PEP	Phosphoenolpyruvate
PEPCK	Phosphoenolpyruvate carboxykinase
PER	Period circulating regulator
PEST	Proline, glutamic acid, serine and threonine
PFK2	Phosphofructokinase 2
PFKFB1	Phosphofructokinase 2/ fructose 2,6 bisphosphate
PPAR	Peroxisome proliferator-activated receptor
PR	Progesterone Receptor
Pre-Pol	Multi polypeptide transcription preinitiation complex
pSer2 Pol2	Ribonucleic acid polymerase II complex, serine 2 phosphorylated
PSer5 Pol2	Ribonucliec acid polymerase II complex, serine 5 phosphorylated
PTEN	Phosphate and tensin homolog
PVN	Paraventricular nucleus
RIA	Radioimmunoassay
RNA	Ribonucleic acid
RNA Pol2	Ribonucleic acid polymerase II
ROR	Retinoic acid-receptor-related orphan receptors
RT-qPCR	Real time quantitative polymerase chain reaction
SCD	Stearoyl-CoA desaturase
SCN	Suprachiasmatic nucleus
SD	Standard deviation

SDS	Sodium dodecyl sulphate
sec	Second
Ser	Serine
Seq	Next generation sequencing
Sds	Serine dehydratase
sGC	Synthetic glucocorticoid
SIK2	Salt-inducible kinase 2
SIRT1	Sirtuin1
SLC37A4	Solute carrier family 37 member 4
SNP	Single nucleotide polymorphism
SREBP-1	Sterol regulatory element binding transcription factor 1
STAT	Signal transducer and activator of transcription
SUMO	Small ubiquitin-related modifier
SWI/SNF	SWItch/ sucrose non-fermentable
TAD	Topologically associated domains
TAT	Tyrosine aminotransferase
TBP	TATA binding protein
TG	Triglyceride
TGM	transglutaminase
Thr	Threonine
TNFα	Tumor-necrosis factor α
TSS	Transcriptional start site
TTS	Transcription termination sites
VEH	Vehicle
VLDL	Very low density lipoprotein
VLDLR	Very low density lipoprotein receptor
WAT	White adipose tissue
ZT	Zeitgeber

Chapter 1 Introduction

GC rapid synthesis and secretion from the adrenal glands fluctuates over a 24-hour period; maximal levels recorded prior to the onset of the active period and gradually decreasing within the circulation to negligible levels within the inactive period. This pattern of secretion is under the regulation of a neuroendocrine circuit first described within the 1950s by Hans Seyle, termed the hypothalamic pituitary adrenal (HPA) axis (Selye, 1950; Lightman and Conway-Campbell, 2010). Further investigation discovered upon series, short time point blood sampling, that GC levels are not constant within the circulating blood plasma, but consists of a series of pulses whose amplitude varies in a circadian fashion (Windle, Wood, Lightman, *et al.*, 1998; Windle, Wood, Shanks, *et al.*, 1998; Walker, Terry and Lightman, 2010). Despite this being an intrinsic oscillatory and well conserved mechanism within mammals, research into dysregulated GC rhythm primarily asses longer time points of up to 6-12hrs that do not investigate function or loss of the ultradian intra-rhythm of GC signalling.

Dysregulation from usual endogenous dynamics occur due to the ability of the HPA axis to respond to a range of stimuli including the stress response (Selye, 1950; Lightman and Conway-Campbell, 2010; Sarabdjitsingh *et al.*, 2010). Whilst acute activation is thought to be protective, such as within the classic fight or flight response, chronic activation is associated with the development of a range of metabolic phenotypes such as obesity, type II diabetes and dyslipidaemia to name a few (Deuschle *et al.*, 1997; J. Haller *et al.*, 2000; Lightman, 2016; Oster *et al.*, 2016; Kalafatakis *et al.*, 2018). Similar presentations are observed within individuals whose activity is out of synchrony with their endogenous rhythm, such as workers with variable shift patterns and patients who suffer from hypercortisolism (Nieman and Ilias, 2005; Chandola, Brunner and Marmot, 2006; Buliman *et al.*, 2016). Additionally, despite the tailoring of synthetic steroid use to recapitulate circadian GC rhythm, similar side effects are observed over a chronic time scale and has shown to be a primary cause of type II diabetes development (Simmons *et al.*, 2012; Charmandari, Nicolaides and Chrousos, 2014).

Despite emerging evidence of the importance of ultradian rhythms to homeostatic function, it remains relatively un-known how dysregulation of both the circadian and ultradian elements of GC dynamics may affect metabolic as well as cognitive homeostatic function (Flynn, Conway-Campbell and Lightman, 2018; Kalafatakis *et al.*, 2018).

1.1 The glucocorticoid receptor

1.1.1 Glucocorticoid receptor structure

GCs regulate transcription of specific genes via liganded activation of the glucocorticoid receptor (GR). The GR (encoded by the gene NR3C1) is a ligand-activated transcription factor that belongs to the

oxosteroid sub-family of steroid hormone receptors within the nuclear receptor superfamily. Other steroid hormone receptors include the mineralocorticoid receptor (MR) (encoded by the gene NR3C2), progesterone receptor (PR) (encoded by the gene NR3C3) and androgen receptor (AR) (encoded by the gene NR3C4) ('A Unified Nomenclature System for the Nuclear receptor superfamily', 1999; Bledsoe *et al.*, 2002). Steroid hormone receptors are comprised of three main functional domains. The N-terminal domain (NTD), DNA binding domain (DBD) and ligand binding domain (LBD) (Figure 1.1). This structure is well conserved across mammalian species.

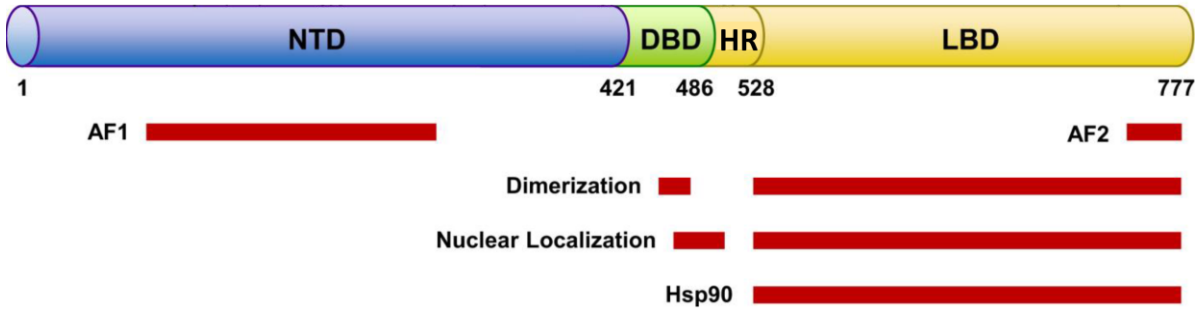

Figure 1.1 Schematic of the GR protein.

Diagram describes the GR three major domains; the N-terminal domain (NTD) (blue) and a central highly conserved DNA binding domain (DBD) which is separated from the ligand binding domain (LBD) by a hinge region (HR). GR regions important for dimerization, nuclear localisation, chaperone binding (e.g HSP90) and transactivation function (AF1 and AF2) are also indicated. Figure adapted from Robert H. Oakley and Cidlowski 2013.

The N-terminal domain (NTD) is the least well conserved structural domain. It is a highly modifiable domain for post-translational events such as phosphorylation, and contains a large transactivation region (AF1) through which the GR interacts with a variety of chromatin remodellers and transcription factors such as the SWItch/ sucrose non-fermentable (SWI/SNF) complex, TATA binding box protein (TBP), cyclic adenosine 3',5'-monophosphate- response element binding protein (CREB) binding protein (CBP) and p300, modulating GR transcriptional regulation (Giguère *et al.*, 1986; Godowski *et al.*, 1987; Bodwell *et al.*, 1991; Dieken and Miesfeld, 1992; Dahlman-Wright *et al.*, 1995; Almlöf *et al.*, 1998; Wallberg *et al.*, 2000).

The DBD contains a nuclear localisation sequence (NLS1) as well as a p-box of zinc finger motifs, termed the D-loop. These zinc fingers directly interact with short consensus 6bp palindromic DNA sequences separated by a 3bp spacer (5'-AGAACA-nnn-TGTTCT-3') (within certain base predictive tolerances), termed glucocorticoid response elements (GRE)s (Figure 1.2) (Scheidereit *et al.*, 1983; Luisi *et al.*, 1991; La Baer and Yamamoto, 1994; Savory *et al.*, 1999; Meijsing *et al.*, 2009). Each zinc finger of a GR homodimer recognises one half of the palindromic GRE sequence, therefore allowing

full sequence recognition by the complex (Dahlman-Wright *et al.*, 1991; Oakley *et al.*, 1999; Hudson, Youn and Ortlund, 2013). However, this model is further complicated by increasing evidence of higher order oligomerisation, such as the discovery of GR tetramers as well as heterodimers with other oxosteroid receptors such as MR (Trapp *et al.*, 1994; Mifsud and Reul, 2016; Presman *et al.*, 2016).

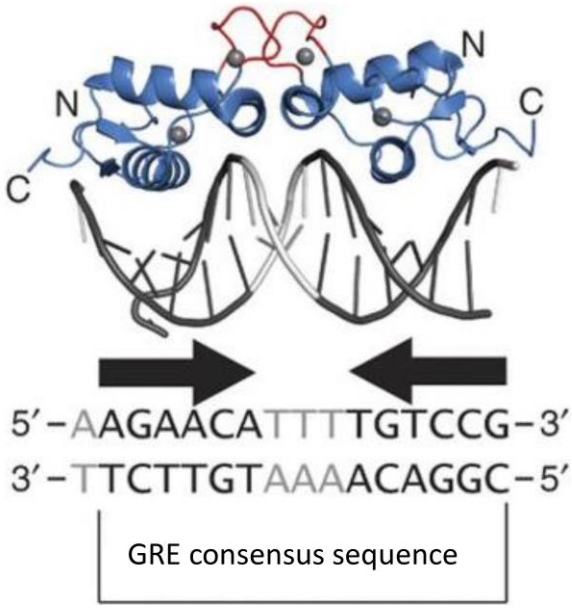

Figure 1.2 DBD interactions with DNA and within the GR homodimer.

GR binds as a homodimer in an inverted manner (classical model) to a GRE consensus sequence within the DNA via zinc finger within the P-box of the DBD (blue). Within the D-loop of each GR, the second zinc finger forms a dimerization interface (red). GRE consensus sequence required for GR recognition in bold. Figure modified from Hudson, Youn and Ortund 2013.

Finally, the LBD contains a second nuclear localisation region (NLS2) consisting of a canonical three layered helical hydrophobic pocket formed from 11-12 α-helices and four β-sheets. These are held in a conformational state by a multimeric complex of chaperones including heat shock proteins (hsp) hsp40, hsp70, hsp90 and p23 as well as immunophilins such as FKBP51, FKBP52, CYP44 and PP5 (Bourguet *et al.*, 1995; Renaud *et al.*, 1995; Xu *et al.*, 1999). The multimeric complex plays a key role in maintaining the correct conformational state, opening a hydrophobic pocket in the LBD to increase binding affinity for ligands such as glucocorticoids (GCs) and preventing proteasome mediated degradation (Bresnick *et al.*, 1989; Picard *et al.*, 1990). Upon ligand binding to the LBD hydrophobic pocket, the GR undergoes a conformational change, exposing the NLS1 and NLS2 as well as stabilizing or de-stabilizing a secondary activatory region (AF2). This regulates the ability of GR to associate with co-regulators of transcriptional function (Wurtz *et al.*, 1996; Savory *et al.*, 1999; Bledsoe *et al.*, 2002; Kauppi *et al.*, 2003). Deletion studies have shown that NLS2 mediated import of the GR to the nuclear compartment is ligand dependent (Picard and Yamamoto, 1987; Savory *et al.*, 1999).

1.1.2 GR post-translational modifications

Over 20 residues (mostly serine and threonine) have been identified within the human GR (hGR) structure to undergo post-translational modification, this includes phosphorylation of up to six serine (Ser) residues within the AF1 region (Ser-113, Ser-134, Ser-141, Ser-203, Ser-211 and Ser-226) (Figure 1.3) (Oakley and Cidlowski, 2013; Kino, 2018). Most phosphorylation events occur as a result of ligand binding and have distinct and varied effects on GR function. For example, phosphorylation of Ser-203, Ser-226 and Ser-404 is required for hGR nuclear translocation, while cyclin dependent kinase 5 (Cdk5) dependent phosphorylation of Ser-203, Ser-211 and Ser226 facilitates recruitment of co-regulators such as the histone acetyl-transferases (HAT), CBP and p300, and adenosine triphosphate (ATP) dependent chromatin remodelling factors such as the SWI/SNF complex (Itoh *et al.*, 2002; Wang, Frederick and Garabedian, 2002; Kino *et al.*, 2007; Blind and Garabedian, 2008; Galliher-Beckley, Williams and Cidlowski, 2011).

Other regulatory mechanisms involve acetylation at Lys-494 and Lys-495, which facilitates GR recruitment of histone deacetylase 2 (HDAC2), a factor known to interact with the tertiary structure of DNA and facilitate transcription (Ito *et al.*, 2006; Nader, Chrousos and Kino, 2009). Post-translational modifications can also repress GR mediated transcription. Genetic mutations which substitute aspartic acid residues for Serine residues at positions 226 and 404, produce a GR mutant that is incapable of being phosphorylated at these sites and cannot recruit p300, CBP or the nuclear factor kappa-light-chain-enhancer of activated B cells (NFκB) p65 subunit. These mutations have also been shown to attenuate glucocorticoid induced cell death of osteoblasts as well as play a distinct role within depression associated with GC resistant pathology (Miller *et al.*, 2005; Chen, Rogatsky and Garabedian, 2006; Blind and Garabedian, 2008; Chen *et al.*, 2008; Galliher-Beckley *et al.*, 2008; Simic *et al.*, 2013).

Post-translational modification has also been shown to play a role in circadian rhythms as described within (Chapter 1.2.3) Histone acetyltransferases such as CBP, P300, circadian locomotor output cycle kaput (CLOCK) and brain and muscle ARNT-like1 (BMAL1) can directly acetylate GR residues in a daily oscillating manner synchronised to the rise and fall of total blood serum corticosterone levels. This has been shown to directly regulate the induction of glucocorticoid induced leucine zipper (*GILZ*) and inhibition of glucose-6-phosphatase (*G6PC*) transcription and regulating gluconeogenesis within the liver (Nader, Chrousos and Kino, 2009).

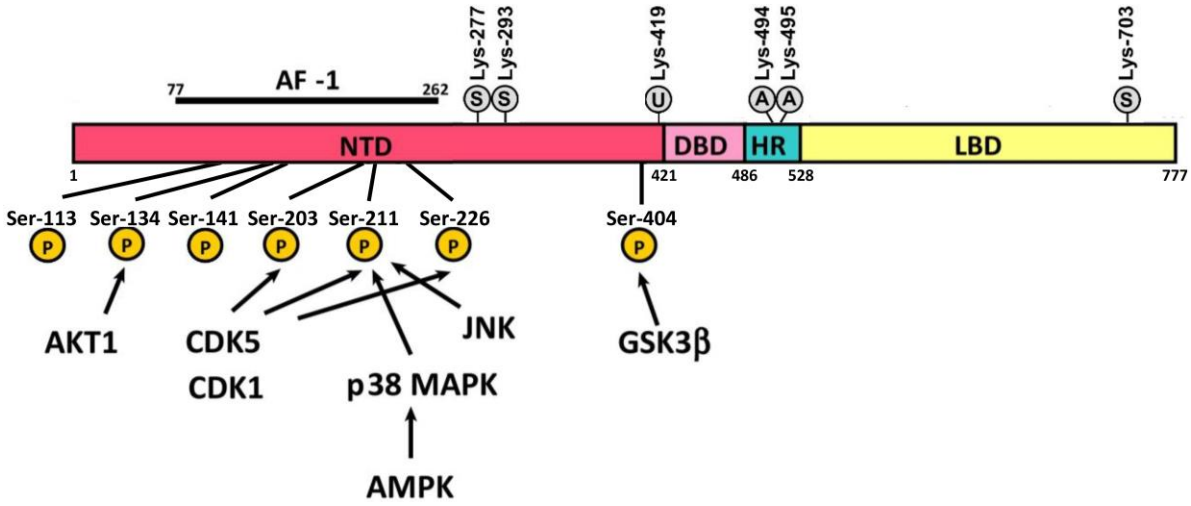

Figure 1.3 Post-translational modification of the GR by phosphorylation, acetylation, ubiquitination and SUMOylation.

*Within the NTD of the human GR transcript, 7 serine residues are indicated as phosphorylation targets (P) within the AF1 region. Serine residues (Ser) directly phosphorylated by cyclin dependent kinase 1 (CDK1) and 5 (CDK5), activation function-1 (AKT1) as well as adenosine 5' monophosphate-activated protein kinase (AMPK) indirectly via c-Jun N-terminal kinase (JNK) are indicated. Ser-404 outside of the AF1 is phosphorylated by glycogen synthase kinase 3*β *(GSK3*β*) is also indicated. Lysine (Lys) residues Lys-277 and Lys-293 within the NTD and Lys-703 towards the c-termini of the LBD are targeted for SUMOylation (S) residues Lys-419 within the NTD for ubiquitination (U) and Lys-494 and Lys-495 within the HR are targeted for acetylation (U) are also indicated. All numbers refer to human GR structure. Figure modified from Oakley and Cidlowski, 2013; Kino, 2018.*

Proteasomal degradation of the GR is also initiated by a post-translational modification, in this case ubiquitination. Phosphorylation of proline, glutamic acid, serine and threonine residues (PEST) sequences often precede ubiquitination of proteins by a series of proteins commonly referred to as E1 activating, E2 conjugating and E3 ligase enzymes (Jadhav and Wooten, 2009). Mutational studies of (Lys) 426 residue within a (PEST) sequence were found to alter the degree of ubiquitination and reduce proteasomal degradation of hGR within HeLa and COS cell lines (Wallace and Cidlowski, 2001; Wallace *et al.*, 2010). Overexpression of the Ubiquitin E3 ligase, carboxyl terminus of hsp70-interacting protein decreases GR transcript levels, indicating a chaperone complex role in proteasomal degradation (Ballinger *et al.*, 1999; Vandevyver, Dejager and Libert, 2014). Conversely, inhibition of the 26S proteasome complex by the aldehyde peptide MG132 results in increased GR protein levels and retention within the nucleus (Wallace and Cidlowski, 2001; Deroo *et al.*, 2002; Han *et al.*, 2009; Wilkinson, Verhoog and Louw, 2018). Similarly, GR binding to DNA or ligands can induce small ubiquitin-related modifiers (SUMO) to covalently attach via an ATP-dependent process to residues

Lys-277, 293 within the NTD and Lys-703 in the LBD of the CTD, initiating proteasomal degradation (Le Drean *et al.*, 2002; Tian *et al.*, 2002; Holmstrom *et al.*, 2008; Oakley and Cidlowski, 2013). SUMOs share 20% homology to ubiquitin and are regulated by the homologous factors SUMO2/ SUMO3 (95% homology) and SUMO1 (50% homology) factors (Mahajan *et al.*, 1997; Kamitani *et al.*, 1998; Tatham *et al.*, 2001). Classically, SUMOylation is associated with proteasomal degradation during cellular heat shock mechanisms (Wallace and Cidlowski, 2001; Tatham *et al.*, 2011). However, as SUMOylation of NTD sites affect co-regulator recruitment, transcriptional effects are varied and highly context dependent (Davies *et al.*, 2008; Druker *et al.*, 2013; Paakinaho *et al.*, 2014).

1.1.3 GR splice variants and translational isoforms

The GR is coded by a single gene consisting of 9 exons within humans. Multiple variants and isoforms, however, are present with distinct features and actions of potential importance to function (Figure 1.4). GR variants are produced from a range of splice events between exons 5-9 within the LBD coding region of the gene, and are categorized as GR-α, GR-β, GR-A and GR-P. A further variant, GR-γ, occurs due to splicing within exon 3-4 of the DBD coding region of the gene. Relative levels of isoforms can be tissue dependent, but GR-α is expressed most abundantly and is commonly described when investigating GR function (Hollenberg *et al.*, 1985; de Castro *et al.*, 1996; Oakley, Sar and Cidlowski, 1996; Rivers *et al.*, 1999; Haarman *et al.*, 2004; Nieman and Ilias, 2005; Choi *et al.*, 2006).

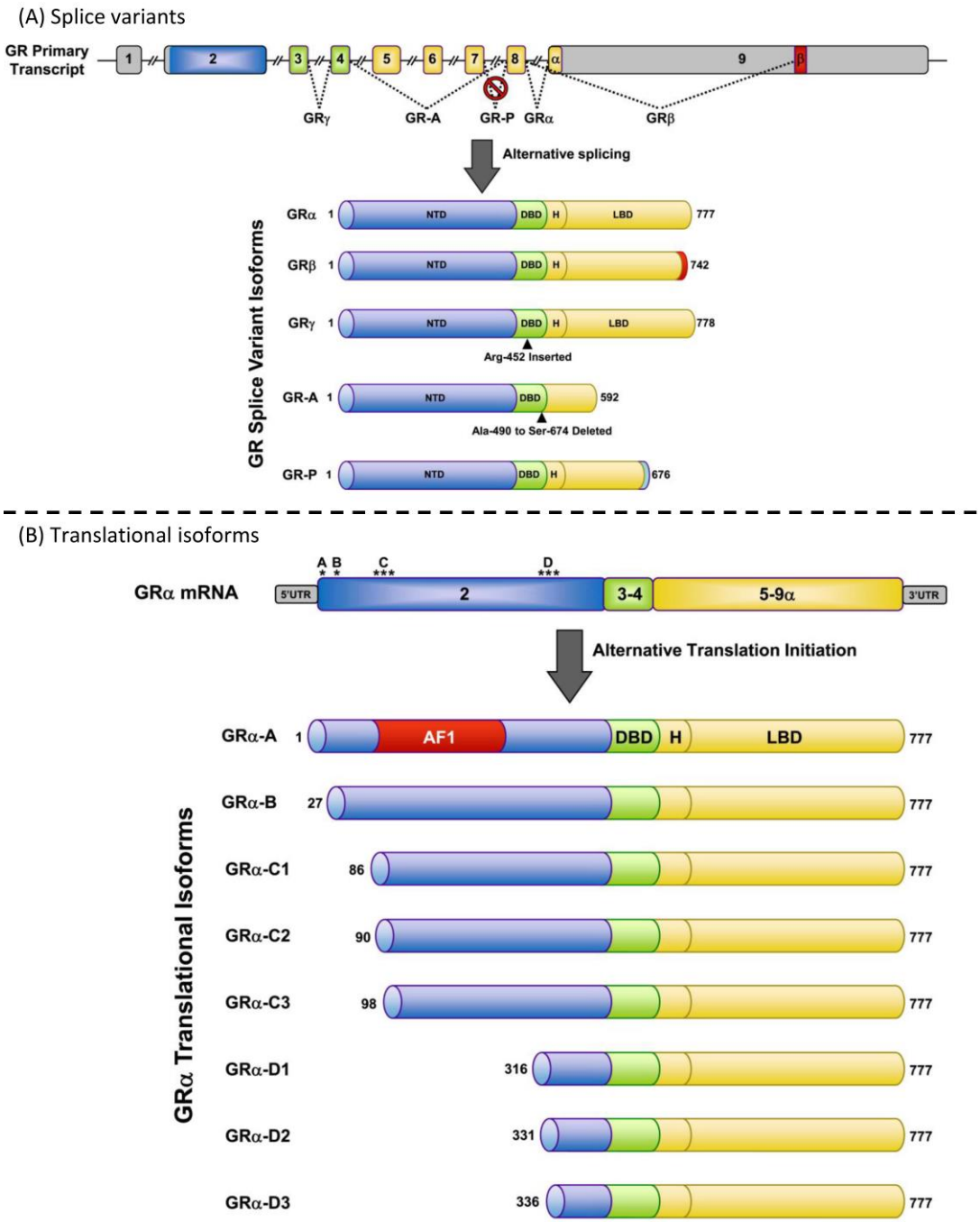

Figure 1.4 Splice variants and translational isoforms of the GR.

(A) Exon number found within the GR primary transcript and location of splicing events that create alternative splice variants. (B) Schematic of GRα translational isoforms with translational start site (*) indicated to produce variable lengths. All numbers refer to human GR structure. Figure adapted from Oakley and Cidlowski, 2013.

GRβ has an identical amino acid sequence to GRα up to amino acid 727, but this splice variant is joined further downstream within exon 9. Creating a non-homologous carboxyl-terminal sequence as well as reducing the overall length from 777 to 742 amino acids (Hollenberg *et al.*, 1985). Due to the location

of the splicing events, the ability to bind ligand is lost due to the removal of helix 12 within the LBD (Bamberger *et al.*, 1995; de Castro *et al.*, 1996; Kino *et al.*, 2009). However, unlike GRα, GRβ is primarily located within the nucleus and can occupy GREs in a ligand independent manner, potentially as a heterodimer with GRα, to act as dominant negative inhibitor of transcription (Bamberger *et al.*, 1995; Oakley, Sar and Cidlowski, 1996; Oakley *et al.*, 1999). Increased GRβ / GRα ratios have been implicated in inflammation, major depressive disorder and GC resistance. Notably, GRβ was found to be increased in liver during the re-feeding phase of fasted rats and is associated within insulin action within mouse embryonic fibroblast cells (Hinds *et al.*, 2010; Carvalho *et al.*, 2014; John *et al.*, 2016).

Information on the function and distribution of remaining variants are limited. However, insertion of an arginine residue at position 454 (exon3-4) is known to produce GRγ which does not affect the LBD coding region but does reduce the transactivation potential compared to GRα (Rivers *et al.*, 1999). Whereas, splicing between exons 5-7 and 8-9 of the LBD coding region have been shown within isolated myeloma cells produces GR-A and GR-B respectively which may mediate function via modulation of GRα induced transcription (Moalli *et al.*, 1993; Gaitan *et al.*, 1995; Krett *et al.*, 1995; de Lange *et al.*, 2001; Oakley and Cidlowski, 2013).

Additionally, a variety of GRα translational start sites within the NTD is known to produce up to seven additional isoforms with the nomenclature GRα-A, -B, -C1, -C2, C3, -D1, -D2 and D3 (Lu and Cidlowski, 2005) (Figure 1.1). Evidence has indicated in their liganded un-bound state, isoforms A-C are found in the cytoplasm whilst the two D isoforms can be found within the nucleus. As these translational isoforms reduce the length of the NTD from the N-terminus, alterations or loss of the AF1 region as well as sites for targeted for post-translational modifications could affect each isoforms capability to recruit certain co-regulators and their transactivator/ transinhibitory potential. It has been proposed as a mechanism for GRα-A, -B and -C isoform mediated specific regulation of apoptotic genes within human osteosarcoma bone cells and T lymphoblastic leukaemia cells (Lu *et al.*, 2007; Wu *et al.*, 2013).

1.1.4 Ligand induced translocation of the GR

In the absence of ligand, newly synthesised GR is sequestered within the cytoplasm. Upon ligand binding, conformational changes within the GR cause members of the chaperone multimeric complex to dissociate, exposing AF regions and the ligand-inducible NLS. Cytoplasmic GRs are shuttled into the nucleus by the Importin α/β nuclear import pathway and along microtubule tracks (Savory *et al.*, 1999; Bledsoe *et al.*, 2002; Kauppi *et al.*, 2003; Pratt *et al.*, 2004). Hsp90 is known to interact with FKBP52 and dynein and in turn the microtubule-associated protein doublecortin-like to actively translocate GR into the nucleus (Czar *et al.*, 1995; Elbi *et al.*, 2004; Fitzsimons *et al.*, 2008). Upon inhibition of either hsp90 or FKBP52, GR diffusion rates are lowered from active to passive gradient diffusion

(Galigniana *et al.*, 1998; Elbi *et al.*, 2004). Hsp90 also appears to be required for GR recruitment of cofactors such as CREB, p300 and CBP, and there are reports indicating a role for these multimeric chaperone proteins during rapid GR dynamics (Conway-Campbell *et al.*, 2011). In contrast, inhibition of hsp70 had no effect on rapid translocation (Yang and DeFranco, 1994). After ligand loss, GR undergoes extremely slow translocation back into the cytoplasm. Therefore, unliganded GR can be found within a biochemically defined, low salt extractable, subcellular fraction sometimes referred to as the nucleoplasm (Yang, Liu and DeFranco, 1997; Conway-Campbell *et al.*, 2007). Upon GC re-exposure, GR re-binds ligand and is present within a high-salt extractable DNase-sensitive chromatin rich cellular fraction (Yang, Liu and DeFranco, 1997; Liu and DeFranco, 1999). Taken together, these findings indicate that the GR can be maintained within the nucleoplasm and become repeatedly activated with multiple cycles of ligand exposure. Further evidence shows that clearance from the nucleus is proteasome dependent (Stavreva *et al.*, 2004, 2009; Wang and DeFranco, 2005; Conway-Campbell *et al.*, 2007, 2011).

1.1.5 DNA structure and organisation of the genome

Ligand activated GR can interact directly with DNA in a tissue and cell specific manner (John *et al.*, 2008, 2011; Grøntved *et al.*, 2013) to regulate gene transcription. Within eukaryotic cells, the genome is organised into a highly complex structure termed chromatin that is separated into 'nucleosomes' of highly compacted DNA, coiled typically ~1.7 times around an octamer core of histone proteins (H2A, H2B, H3 and H4) (Kornberg, 1974; Hayes, Clark and Wolffe, 1991; Kornberg and Lorch, 1999). The density of chromatin is variable throughout the genome and can regulate the ability of factors to either bind or interact with the DNA template. It has been shown that nucleosomes packed to within 30nm structures are transcriptionally inactive, postulated to be due to inaccessibility of the molecular transcriptional machinery (Bednar *et al.*, 1998). The chromatin configuration and corresponding densities are modulated by the post-translational status and the variants of histones, the recruitment of chromatin re-modelling factors and the degree of DNA methylation (Biddie *et al.*, 2011; George, Lightman and Biddie, 2011). Regions of increased chromatin density are termed heterochromatin and described as 'closed' due to their transcriptionally inactive state, whereas less dense, 'open' regions of chromatin that are transcriptionally active are termed euchromatin (Archer *et al.*, 1991; Bednar *et al.*, 1998; John *et al.*, 2008). Regions of euchromatin are usually comprised of highly methylated and acetylated histones (Barski *et al.*, 2007; Bannister and Kouzarides, 2011). Mechanistic experiments in yeast have indicated that hyperacetylation of the H4 N-terminal tail can destabilize inter-nucleosomal contacts (30 nanometer fiber-like connections between histones) which have been shown to be important for maintaining higher order structures and therefore limiting access of the transcriptional

machinery (Shogren-Knaak *et al.*, 2006). Conversely, histone deacetylases (HDACs) have been linked to a loss in transcription (Ito *et al.*, 2006). The organisation of hetero- and euchromatin regions present fundamentally important tissue and cell specific mechanisms for directed nuclear factor binding. Separating binding sites into cell specific regions that are in either a 'closed' or 'open' chromatin state or sites that can be modified into an open or closed stated by external stimuli via intracellular signalling and co-factor assembly. Assessment of chromatin density in response to GR binding by formaldehyde-assisted isolation of regulatory elements (FAIRE) next generation sequencing (Seq) and DNase footprinting have indicated that hormone-induced reductions in chromatin density occur at nearly all GRE containing GR binding sites (John *et al.*, 2011; Burd *et al.*, 2012). Further, 90% of all GR binding sites have been detected within pre-accessible, 'open' chromatin regions, which are highly cell-specific (John *et al.*, 2008; Reddy, Pauli and Sprouse, 2009; Biddie *et al.*, 2011; Burd *et al.*, 2012). Nuclear factors such as the GR are able to initiate the remodelling of chromatin density via the recruitment of co-factors such as the HATs CBP and p300 and the ATP dependent chromatin remodellers such as the SWI/SNF complex (Lee and Archer, 1994; Archer and Lee, 1997; Kinyamu and Archer, 2004). Nuclear factors that initiate the 'opening' of the chromatin landscape in this way have been described as 'pioneer' factors. It is further postulated similar mechanisms are involved within epigenetic regulation as well as acute and chronic changes of genome transcription and regulation (Archer *et al.*, 1991; John *et al.*, 2008, 2011; Reddy, Pauli and Sprouse, 2009; Jubb *et al.*, 2017).

1.1.6 Models of GR mediated transcription

Upon ligand binding, GR is classically thought to translocate through the nuclear pore, rapidly diffuse throughout the nucleus and bind as a homodimer to specific regulatory elements across the genome. However, the homodimer is not essential for transcriptional regulation. GR monomers have been observed binding to both full GRE palindromic and half sites with differing transcriptional effects (Eriksson and Wrange, 1990; Grøntved *et al.*, 2013; Schiller *et al.*, 2014; Lim *et al.*, 2015; Pooley *et al.*, 2017). In fact, it has been postulated monomeric binding is more common than the homodimer form. There is also evidence that GR forms tetramers, potentially via looping of GR dimers bound at opposing sites within the genome (Presman *et al.*, 2016).

Upon binding to regulatory sites within DNA, liganded GR can recruit numerous co-factors important to transcriptional regulation with intrinsic and synergistic acetylation, methylation and phosphorylation mechanisms. These interactions have been shown to be rate limiting as well as significantly enhancing or repressive of transcriptional capacity for a single transcription factor (De Bosscher *et al.*, 2000; Tetel, 2009; Reiter, Wienerroither and Stark, 2017). In the simplest model, the co-factor complex will recruit the multi polypeptide transcription preinitiation complex (pre-Pol),

positioning ribonucleic acid (RNA) polymerase II (RNA Pol2) at the core promoter (a minimal DNA sequence required for the start of transcription) (Wang, Carey and Gralla, 1992; Wiley, Kraus and Mertz, 1992). Primarily, canonical TATA sequences within promoter regions direct the pre-Pol via interactions with the TATA box binding protein subunit, which in mammalian genes are typically 30b upstream of the transcriptional start site (TSS) (Ponjavic *et al.*, 2006). This is however, a simplified model, as genome wide studies indicate other initiator sequences and CpG islands can also be transcriptionally active (Sandelin *et al.*, 2007). In instances where the DNA cannot spontaneously unwind or non-template strands are not complementary, the helicase XPB subunit will melt approximately 11-15bp of the promoter, positioning the template strand within the active cleft to begin synthesis of RNA (Wiley, Kraus and Mertz, 1992; Holstege, Fiedler and Timmers, 1997; Tirode *et al.*, 1999; Hahn, 2004; Luse, 2014).

It has long been known that a classical promoter GR binding site is not required for transcriptional regulation and binding sites are often located many kilobases (kb) from the regulated TSS. These are sometimes referred to as 'enhancer' sites (Lee *et al.*, 1987). In fact 93% of dexamethasone (Dex) induced GR binding sites in mouse 3134 cells were further than 2.5kb away from the TSS (John *et al.*, 2011). Similarly, in HeLa cells only 7% of GR binding events were within 10kb promoter regions and in macrophages, lipopolysaccharide induced <6% within 20kb proximal promoter regions (Rao *et al.*, 2011; Uhlenhaut *et al.*, 2013). This highlights the question; how do long-distance interactions occur between GR binding and their transcriptionally dependent sites? The most accepted model relies on folding and organisation of the chromatin architecture within topologically associated domains (TADs). Within this 'looping' model, GR binding sites that are a very long distance (often many kbs) from a target gene's TSS, loop to within close proximity and are therefore in chromosomal contact (Dixon *et al.*, 2012; Nora *et al.*, 2012; Sexton *et al.*, 2012). It is theorised, co-regulated genes and appropriate regulating transcription factors all loop from a variety of locations to occupy the same spatial region or nuclear hub, termed 'transcription factories' (Jackson *et al.*, 1998; Osborne *et al.*, 2004; Schoenfelder *et al.*, 2010; Aguilar-Arnal and Sassone-Corsi, 2015). This has been shown via observations of the co-factor p300 which is considered to be a hallmark of active enhancers and commonly interacts with both GR and NFκB (Chakravarti *et al.*, 1996; Gerritsen *et al.*, 1997; Wang, Carroll and Brown, 2005; Heintzman *et al.*, 2009). It has been demonstrated, using circular chromosome conformation capture coupled with next generation sequencing, that upon stimulation both GR and NFκB localise to transcriptionally active TADs. But genes within these TADs do not always have a promoter located transcription factor interaction (Kuznetsova *et al.*, 2015). TADs and long-range interactions as well as short-range loops have been shown to be functionally important to mammalian biology. For example, circadian changes in transcriptional regulation of active genes

condensed within sub-sets of genomic TADs have been observed 12hrs apart within C57BL/6J mouse liver which could be modified by altering circadian cues. Implicating the role of the molecular circadian regulators such as BMAL1 (Aguilar-Arnal *et al.*, 2013; Zhao *et al.*, 2015; Kim *et al.*, 2018). GR facilitates this model of transcription by its ability to recruit co-factors such as CBP, p300 and nuclear co-activator 1 (NCOA1) & 2 (NCOA2) (a.k.a. SRC-1 and TIF2/GRIP1 respectively) with intrinsic and synergistic HAT activity modifying the chromatin architecture (Beato *et al.*, 1989; Lee *et al.*, 1993; Grunstein, 1997; Reinke and Hörz, 2003; Conway-Campbell *et al.*, 2011). Complexes can be built via NCOA1 & 2 interaction with the GR via an activation domain. This same domain will also interact with CBP, p300 and RNA helicase A of the Pre-pol and are essential for GR mediated transactivation (Hong *et al.*, 1996; Nakajima *et al.*, 1997; Spencer *et al.*, 1997; Onate *et al.*, 1998; Szapary, Huang and Simons, 1999). NCOA1 has a second activation domain which promotes transcription and a third which interacts with the SWI/SNF chromatin remodelling complex, enabling synergistic promotion of transcription and chromatin re-modelling (Hong *et al.*, 1997; Koh *et al.*, 2001; Belandia *et al.*, 2002; Daujat *et al.*, 2002; Chinenov *et al.*, 2008). Transcription can also be mediated by multiple GR binding sites, as was first described at the dual GR binding site regulated gene, tyrosine amino transferase (*TAT*) in 1987 (Jantzen *et al.*, 1987).

In certain situations, GR recruitment can also be repressive. These mechanisms are less well known but the recruitment of co-repressors such as sirtuin1 (SIRT1) and GSK3β have been implicated in certain situations. Recruitment of the co-repressor SIRT1 can induce inaccessibility of the chromatin to co-activators and the RNA Pol2 complex due to its intrinsic HDAC activity (Vaziri *et al.*, 2001; Ito *et al.*, 2006; Finkel, Deng and Mostoslavsky, 2009; Moore, Dai and Faller, 2012; Suzuki *et al.*, 2018). Post-translational modification of GR can also mediate transrepression as de-acetylation has been shown to promote binding of methyl-binding proteins which in turn recruit HDACs (Vaissière, Sawan and Herceg, 2008). Also, GSK3β modifies the phosphorylation state of GR, that can induce binding of the guanine nucleotide-binding protein β and has been postulated to be a mechanism of GR mediated transrepression of NFκB regulated targets (Kino *et al.*, 2005; Galliher-Beckley *et al.*, 2008; Kino, 2018).

Transcriptional repression can also be induced by GR binding to so called negative GRE (nGRE) consensus sequences identified as 5'-CTCC$(N)_{0\text{-}2}$GGAGA-3' (Pei, 1996; Meijer *et al.*, 2000; Surjit *et al.*, 2011). This proposed response element interacts with two ligand bound monomer GRs on opposing sides of the DNA helix in a head to tail configuration (see Figure 1.2 for classic GRE homodimer binding and Figure 1.5 for nGRE monomer GR binding schematics) (Hudson, Youn and Ortlund, 2013). nGREs enact a transrepressive effect via recruitment of the repressive inhibitors NCoR and SMRT (Surjit *et al.*, 2011; Hudson, Youn and Ortlund, 2013). It has also been identified via biochemical analysis, that

binding of a monomer to one side of the nGRE sequence, reduces the affinity for the second monomer. Thereby increasing the potential for purely single monomer binding as opposed to dual (Hudson, Youn and Ortlund, 2013). The exact role of nGREs, however, remains to be fully elucidated as it has been reported mutation of discovered sequences upstream of the 5-HT1a promoter did not affect GR mediated repression nor was their a defined link between dexamethasone (Dex) induced repression within 3134 mouse mammary adenocarcinoma cell lines (Meijer *et al.*, 2000; Presman *et al.*, 2014). nGREs have been shown to provide a role within the HPA axis, mediating repression of CRH and POMC genes via associated GR binding (Surjit *et al.*, 2011; Meijer, Buurstede and Schaaf, 2019). It has further been postulated that as the nGREs have also been characterised well within macrophages, then perhaps nGRE action is a cell and tissue context dependent mechanism of repression (Uhlenhaut *et al.*, 2013; Jubb *et al.*, 2016).

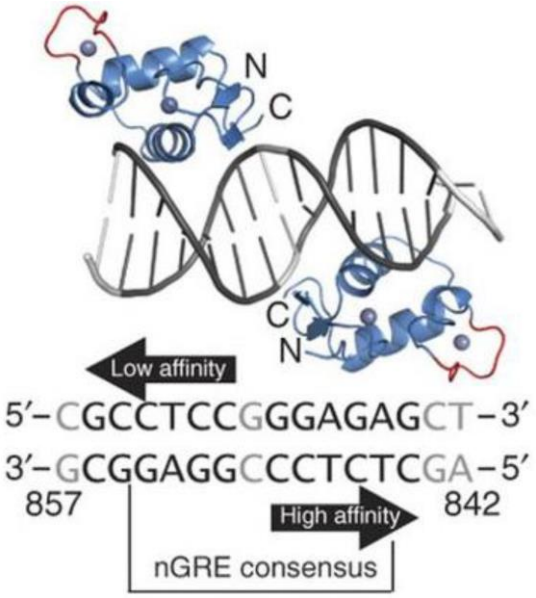

Figure 1.5 nGRE binding of monomer GR

A monomeric GR will bind to a negative GRE consensus sequence via a zinc finger within the P-box of the DBD (blue). A second monomeric GR can bind on the opposing side of the DNA helix in the same manner. There is no direct interaction between GRs within the dimerization interfaces (red). nGRE consensus sequence required for GR recognition in bold. Figure modified from Hudson, Youn and Ortlund, 2013.

GR mediated transcriptional control can also work in a composite fashion. Multiple observations were made of overlapping as well as adjacent response elements for differing nuclear factors whose presence was required for transcriptional output (Biddie *et al.*, 2011; Grøntved *et al.*, 2013; Uhlenhaut *et al.*, 2013). GR and activator protein 1 (AP1) was one of the first and most highly investigated

examples of transcriptional dependent composite interactions (Diamond *et al.*, 1990; Biddie *et al.*, 2011). Interestingly, these same studies indicated the composite interactions of GR and AP1 occurred at AP1 response element regions devoid of GREs. In these situations, it is hypothesized GR is 'tethered' by another co-factor, which is bound to the DNA template (Schule *et al.*, 1988; Newton and Holden, 2007; Biddie *et al.*, 2011). Similar observations have been made with other transcription factors including signal transducer and activation of transcription (STAT)5 and NFκB to mediate transrepressive effects (Jonat *et al.*, 1990; Schule *et al.*, 1990; Yang-Yen *et al.*, 1990; Ray and Prefontaine, 1994; Stöcklin *et al.*, 1996; Hudson, Youn and Ortlund, 2013). NFκB is a known mediator of inflammation via cytokine transcriptional induction. GCs are a potent anti-inflammatory and will interact with NFκB via tethering or as composite binding. Synergistic transcriptional regulation has also been shown with STAT3 & STAT5 tethered composites (Stoecklin *et al.*, 1997; Aittomäki *et al.*, 2000). It has been theorised synergistic transcription mediated at regulatory regions could be dependent on the tethered factor bound to the DNA (Stoecklin *et al.*, 1997; Zhang *et al.*, 1997; Takeda *et al.*, 1998; Engblom *et al.*, 2007). This was recently shown by observing tethered STAT3 and GR complexes; DNA bound GR complexes tethered to STAT3 induced transcription, whereas when the complex was bound via STAT3 transcription was repressed (Langlais *et al.*, 2012).

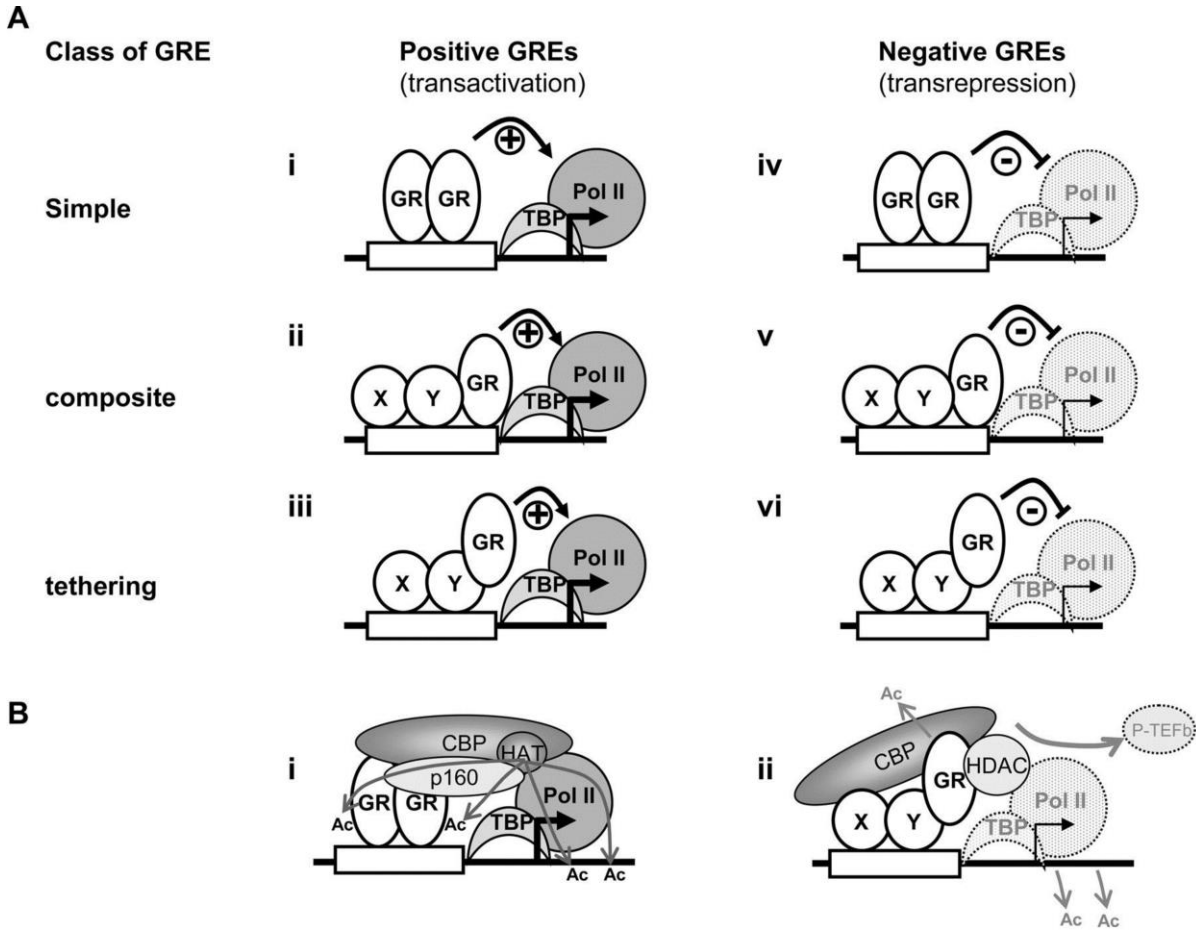

Figure 1.6 Diagram of the main pathways of GR mediated transcription.

(A) Within the simple model of GR transactivation, GR binds as a homodimer to response elements (white box) within a DNA (black line) 'promoter' region of a gene and transcription can be increased (transactivation) (i). GR can also recruit other co-factors (X and Y) as part of a composite complex and bind to specific response elements within a shared region (ii). Or GR can be tethered to other DNA bound co-factors without the need for direct interaction with the GR DNA binding domain (iii). Inhibition (transrepression) maybe observed at response elements that can be termed negative GREs for each simple (iv), composite (v) and tethering (vi) model described. GR transactivatory action is mediated by the TATA binding protein and RNA polymerase 2 (Pol II). (B) GR transactivatory action can be mediated by the recruitment of factors such as CREB binding protein (CBP) and a p160 protein family member (p160) and histone acetylases transferases (HAT). The co-factor complex intrinsic histone acetylase action promotes opening of the chromatin structure to allow access to the transcriptional machinery such as TBP and PolII (i). This action is opposed if the complex recruit's histone de-acetylases (HDAC) that deacetylate histones, closing the chromatin to transcriptional machinery. This has been described within a tethered model with NFκB amongst other nuclear receptors. Figure adapted from (Newton and Holden, 2007).

1.2 The pituitary-adrenal axis

1.2.1 Corticosterone

In the 1930s, small amounts of steroid hormones were extracted and isolated from the adrenal cortex, however it was only in 1949 that synthetic production of steroid compounds facilitated full scale clinical investigation and treatment of their potent anti-inflammatory effects. Originally termed compound B and compound E, corticosterone and cortisol (mainly cortisol) were observed to have remarkable efficacy in treating inflammatory conditions such as rheumatoid arthritis and rheumatic fever and to this day remain one of the most prescribed medicines (Kendall *et al.*, 1936; Mason, Hoehn and Kendall, 1938; Hench and Kendall, 1949; Kendall, 1949).

Corticosterone is the predominate circulating GC found in rodents, whereas in humans it is approximately 20 fold lower than cortisol (Underwood and Williams, 1972; Nishida *et al.*, 1977; Karssen *et al.*, 2001; Raubenheimer *et al.*, 2006). Despite its prevalence in total circulating blood plasma levels, up to 90% of GCs are bound to the major transport protein, corticosteroid binding globulin (CBG), reducing free corticosterone levels to approximately 4% of total levels (Chan *et al.*, 2013). The half-life of circulating corticosterone is variable within biological systems, however studies in healthy young adult female rats have calculated total corticosterone half-life to be approximately 8.6 ± 1.4 min within 10min blood serum sampling (Windle, Wood, Shanks, *et al.*, 1998; Lightman, 2006). This represents a significantly shorter half-life than the predominant human GC cortisol, which has been determined to between 62-97min (Weitsman *et al.*, 1971; Weitzman, 1976; Veldhuis *et al.*, 1989).

Free corticosterone and cortisol readily diffuse into cells due to their highly lipophilic nature, however, it was noted in 1953 that cortisone incubated in various rat tissues *in vitro*, could be converted to cortisol in a process identified to be the result of the of 11β-hydroxysteroid dehydrogenase enzymatic action (Amelung *et al.*, 1953). The type I isoform (11β-HSD1) is the most widely expressed isoform throughout the body and is concentrated within the liver (Tannin *et al.*, 1991). 11β-HSD1 is a bi-directional enzyme, but predominantly acts as an oxidoreductase, converting inactive cortisone and 11-dehydrocorticosterone to the biologically active cortisol and corticosterone (Duperrex *et al.*, 1993; Low *et al.*, 1994). Whereas the type II isoform (11β-HSD2) only works unidirectionally producing inactive 11-keto-metabolites (Agarwal *et al.*, 1994). Depending on their selective expression of 11β-HSD1 and 11β-HSD2, this mechanism enables cells to control the amounts of active GC ligand, regardless of circulating free corticosterone levels.

1.2.2 Anatomy of the hypothalamic-pituitary-adrenal axis

Hans Selye (1950) was among the first to highlight the importance of the HPA axis in the homeostatic regulation of the adrenal cortex stress response, leading to further implications in immunological, cognitive and metabolic regulation (Selye, 1950; McEwen, 2007; Lightman and Conway-Campbell, 2010). The HPA axis is modulated by a variety of inputs such as aversive stimuli (either physical or mental) or stress (Pariante and Lightman, 2008; Oster *et al.*, 2016). The primary input is from the suprachiasmatic nucleus (SCN) within the anterior hypothalamus of the brain, also termed the 'master clock'. The SCN mediates HPA axis regulation via innervations into the parvocellular subdivision of the paraventricular nucleus (PVN) as well as the hypothalamic medial preoptic area and dorsomedial nucleus (Figure 1.7) (Berk and Finkelstein, 1981; Vrang, Larsen and Mikkelsen, 1995). Parvocellular neuronal projections secrete corticotropin-releasing hormone (CRH) and arginine vasopressin (AVP) via the median eminence into the hypophyseal portal circulation to the anterior pituitary (Swanson *et al.*, 1983; Sawchenko, Swanson and Vale, 1984) (Figure 1.7). Predominantly, binding of CRH to corticotrophs induces production and secretion of pro-opiomelanocortin and adrenocorticotropic hormone (ACTH) into the pulmonary network (Kiss, Mezey and Skirboll, 1984; Pariante and Lightman, 2008). ACTH is transported around the body, diffusing into tissues such as the zona fasciculata of the adrenal cortex inducing synthesis and secretion of a range of steroids classed as GCs. ACTH release occurs in a highly synchronised, oscillating manner with an intrinsic 10min delay between release from the pituitary and the secretion of GCs from the adrenals (Follenius *et al.*, 1987; Carnes *et al.*, 1989; Veldhuis *et al.*, 1990; Jasper and Engeland, 1991; D E Henley *et al.*, 2009; Rankin *et al.*, 2012; Walker *et al.*, 2012). Adrenal GCs are transported around the body via the circulatory system and their lipophilic nature allows diffusion into nearly all tissues of the body, including the brain (M. T. Jones, Hillhouse and Burden, 1977). Therefore rising GC levels can act directly on CRH neurons within the PVN of the hypothalamus, as well as on ACTH producing corticotrophs of the anterior pituitary gland to rapidly and directly inhibit CRH production and ACTH secretion in a classical negative feedback loop (M T Jones, Hillhouse and Burden, 1977; Sawchenko, 1987; Harbuz and Lightman, 1989).

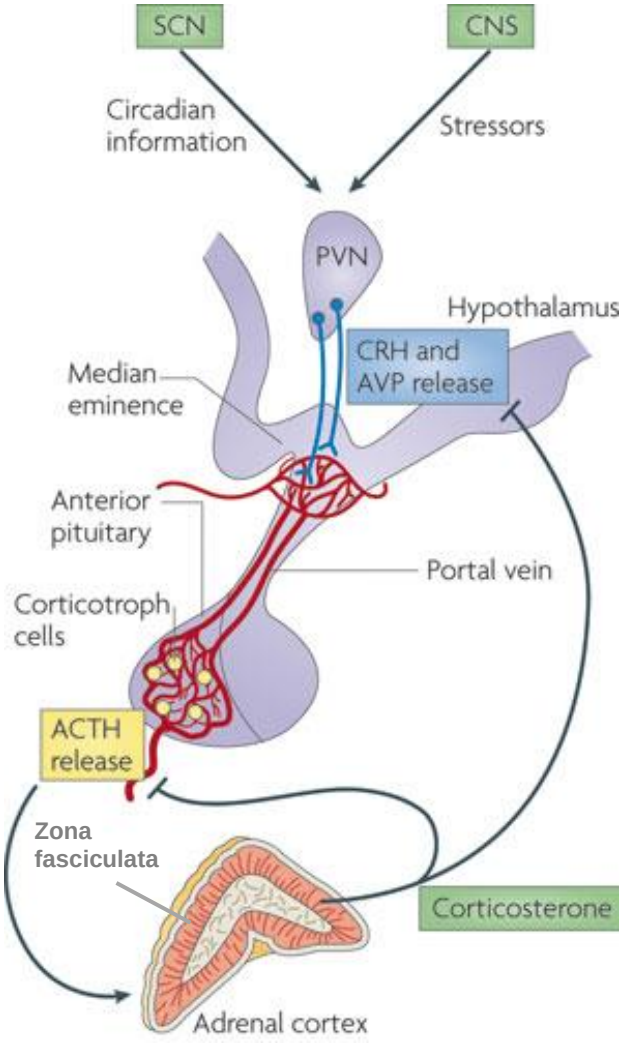

Figure 1.7 Hypothalamic-pituitary-adrenal axis schematic.

Activation of the HPA axis, by circadian cues or stress, results in activation of parvocellular neurons in the PVN and increased secretion of CRH and AVP into the hypophyseal portal blood system. ACTH is secreted from corticotrophs in the anterior pituitary and targets the zona fasciculata of the adrenal cortex increasing GC production and release into the peripheral circulation. Figure adapted from Lightman and Conway-Campbell, 2010.

1.2.3 Circadian rhythms

The daily rotation of the earth as well as its annual rotation around the sun causes distinct and varied changes in light, temperature and availability of food. Therefore, mammalian systems have developed innate circadian (circa=around, di=day) mechanisms to adapt to daily and seasonal changes in the photoperiod, mediating a wide range of behaviour and hormonal release as well as regulating body temperature, activity and sleep (Weitzman, 1976; Refinetti and Menaker, 1992). These systems are dynamically regulated and can be altered by extension/ shortening of the photoperiod which the HPA axis plays an integral regualtory role (Edmonds and Adler, 1977; Waite *et al.*, 2012). In unstressed

healthy mammals, GCs such as corticosterone and cortisol are synthesized and released from the adrenal glands at maximal capacity prior to waking. Maximal levels continue to be produced and secreted well into the onset of the active part of the day before gradually decreasing throughout the active period and returning to negligible levels during the inactive period and early sleep phase. This cycle continues with a period of 24hrs (Windle, Wood, Shanks, *et al.*, 1998; Lightman *et al.*, 2002; Lightman and Conway-Campbell, 2010; Russell *et al.*, 2010). In 1972 it was discovered that bilateral destruction of the hypothalamic SCN ablated diurnal oscillations of plasma corticosterone, as well as circadian drinking and activity periodicity in rats (Moore and Eichler, 1972; Stephan and Zucker, 1972). Study of SCN hypothalamic slices confirmed an innate ability to produce spontaneous neural activity at a rate of approximately 24hrs and showed that transplant into SCN lesioned hamsters could restore circadian activity. Furthermore, the donor periodicity was preserved despite phase shift experiments within the host prior to implantation (Inouye and Kawamura, 1979; Welsh *et al.*, 1995; Silver *et al.*, 1996). In the absence of light or other Zeitgeiber (Zt) cues, the 'free running' circadian period was determined to be slightly longer than 24 hours indicating the SCN has a phase advance activity. The maintenance of the 24hr rhythm has been found to be primarily regulated by light via impulses from activated retinal ganglion cells, along the retinohypothalamic tract and into the SCN (Aschoff, 1965; Czeisler *et al.*, 1999; Hattar, 2002). Interestingly, SCN stimulation by light and output into the PVN do not differ between diurnal and nocturnal animals. Within SCN ablated rats, AVP infusion into the PVN and dorsomedial hypothalamic regions inhibited raised corticosterone levels within circulating blood during the active period. This effect could be reversed with an AVP antagonist, raising circulating corticosterone within the circadian inactive period (Kalsbeek *et al.*, 1992; Kalsbeek, van der Vliet and Buijs, 1996). Opposing effects were observed in the diurnal rodent *Arvicanthis ansorgei* with the same experimental model, suggesting photic regulation of the SCN is conserved, but the downstream effect of AVP on the HPA axis is inhibitory in nocturnal and excitatory in diurnal mammals (Kalsbeek *et al.*, 2008).

1.2.4 Ultradian rhythms

Frequent blood micro sampling methodologies have led to the detection of a pronounced rhythm underlying the circadian rhythm; an intra-rhythm of rising and falling phases, the amplitude of which followed the circadian 24hour period. This 'ultradian' rhythm has been shown to be highly conserved across all mammals studied, including rats (Carnes *et al.*, 1989, 1994; Windle, Wood, Lightman, *et al.*, 1998; Sarabdjitsingh *et al.*, 2010; Walker *et al.*, 2012), hamsters (Loudon *et al.*, 1994), dogs (Benton and Yates, 1990), sheep (Engler *et al.*, 1990), horses (Cudd *et al.*, 1995), rhesus monkeys (Holaday, Martinez and Natelson, 1977; Sarnyai *et al.*, 1995), goats (Carnes *et al.*, 1992) and humans (Krieger *et*

al., 1971; Weitzman, 1976; Veldhuis *et al.*, 1989, 1990; Young, Carlson and Brown, 2001; D E Henley *et al.*, 2009; Russell *et al.*, 2010). However, there are variations in pulse frequency and duration as rat ultradian corticosterone frequency is roughly 56-60min, whereas human cortisol pulse frequency is roughly 95-180min (Figure 1.8) (Follenius *et al.*, 1987; Veldhuis *et al.*, 1989; Jasper and Engeland, 1991). The difference may be due to specific regulation of the HPA axis as well as differing blood plasma half-lives of corticosterone (8-9min) and cortisol (62-97min) (Weitzman, 1976; Veldhuis *et al.*, 1989; Windle, Wood, Lightman, *et al.*, 1998) .

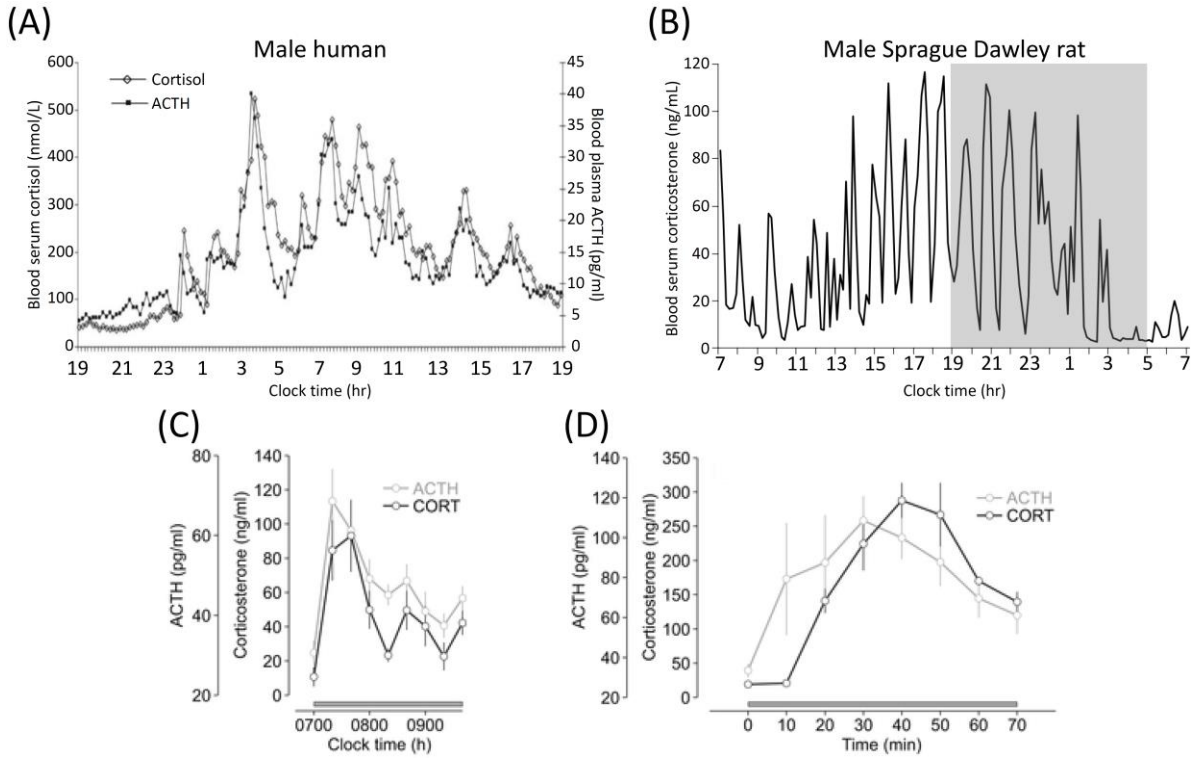

Figure 1.8 Ultradian models of human cortisol and rat corticosterone pulses and their relationship with ACTH.

(A) 10min blood samples were collected over a 24hr period in a healthy human male and total blood serum cortisol and ACTH concentrations measured. Circadian changes are present with increases in circulating cortisol between 24-9hrs (maximal ACTH and cortisol levels are approximately 550nmol/L and 45ng/ml respectively just before 4hr) before overall levels decrease to nadir by approximately 19hrs. Within overall circadian changes, supra-pulses of ACTH and slightly delayed phase shifted cortisol pulses are discernible within the raised cortisol period. Human cortisol and ACTH were measured by solid-phase, competitive chemiluminescent enzyme immunoassay. Figure adapted from D E Henley et al., 2009. (B) Similar circadian and ultradian changes in total circulating corticosterone are observable within the male rat but with an increased frequency of approximately 1hr. Rats are also nocturnal, therefore corticosterone rises start from approximately 11hrs, maximal at 17hrs

(~120ng/ml) and gradually decreases to nadir at 4hrs. Rat lighting schedule was on at 05:00 and off at 19:00 (14:10), food and water access ad libitum, total blood serum corticosterone levels assessed using an in house radio immunoassay (RIA) (n=8-10). Figure adapted from Seale et al ., 2004. (C) Average ACTH (grey line) and corticosterone (black line) oscillations in response to constant CRH infusion (0.5µg/hr) (grey bar) within male Sprague Dawley rats over a 3hr period and (D) over a 1hr period. Both measurements indicate a synchronised but slightly delayed phase shift in ACTH and corticosterone levels. Total blood serum corticosterone levels were assessed using RIA (n=3-7 per time point). Figure adapted from Walker et al ., 2012.

The ultradian rhythm is an intrinsically oscillating system due to the interplay between feed forward and feedback pathways of the HPA axis. Even though multiple studies have reported pulsatile AVP and CRH secretion within the HPA axis, recent studies have shown ultradian GC secretion can be preserved in response to constant CRH and constant light (Figure 1.8) (Engler *et al.*, 1989; Carnes *et al.*, 1990; Walker, Terry and Lightman, 2010; Waite *et al.*, 2012; Walker *et al.*, 2012). It is in fact a two-step delay, the first delay is between ACTH secretion and induction of GC secretion from the adrenal glands within feed forward mechanisms, whilst the second delay occurs between rising GC levels within the circulation, acting on the brain and pituitary to inhibit ACTH release with the negative feedback loop of the HPA axis. Together this data indicates GC release is naturally oscillatory, due to delayed feed forward and feedback mechanisms intrinsic within the HPA axis, whilst the CRH activatory drive primarily regulates pulse amplitude in an overall circadian manner (Walker *et al.*, 2012).

1.2.5 A functional role for corticosterone rhythms in regulation of stress response, physiology and behaviour

HPA axis activation and subsequent GC release has been shown to be a highly plastic system. Not only is it dependent on the type and duration of the stressful stimuli but also on the circadian phase. When an animal encounters a stressful situation, either real or perceived, during the circadian inactive phase when the CRH drive is naturally low and circulating ACTH and adrenal GCs are minimal, the HPA axis is highly responsive with rapid and robust activation of hypothalamic CRH and AVP neurons within the PVN (although multiple further interactions and sites exist), closely followed by increased ACTH secretion then a surge of adrenal GC synthesis and release. However, when a mammal encounters a stressful event during the circadian active phase, rapidly oscillating phases of HPA activation and inhibition are already underway, and these become very important for regulating outcome (Kyrou, Chrousos and Tsigos, 2006; Pariante and Lightman, 2008; Sarabdjitsingh *et al.*, 2010). Stress induced GC rises have many implications for memory acquisition, cognition and analgesia as well as metabolism, mobilising glucose stores within the liver via induction of gluconeogenesis and lipolysis

whilst inhibiting energy consuming functions such as digestion, reproduction, growth and certain immune functions (Kyrou, Chrousos and Tsigos, 2006). Thus, providing easily accessible energy for 'fight / flight' mechanisms.

However, stress induced HPA axis activation can also be dependent on the ultradian phase of GC release. Indicating a role for ultradian stress mediated activation (Kyrou, Chrousos and Tsigos, 2006; Pariante and Lightman, 2008; Sarabdjitsingh *et al.*, 2010). When ultradian corticosterone rhythmicity is lost, such as during constant corticosterone infusion into ADX rats, physiological (ACTH), neurological (neuronal activation) and behavioural stress responses were blunted (Sarabdjitsingh *et al.*, 2010). Even within the intact, oscillating ultradian endogenous GC release, the amplitude of the stress-induced GC release has been shown to be dependent on the timing of the stressful encounter relative to the phase of the adrenal GC pulse. In female rats, total blood corticosterone levels measured 20min after a 114 decibel (12,000-60,000Hz) noise stress were increased from 136 ±9ng/ml to 377 ±87ng/ml, which also marginally increased the subsequent pulse nadir interval even though no difference in corticosterone clearance was observed. This increased the average interpulse corticosterone peak period from 48±2min (non-stressed controls) to 70±3min (after the noise stress). Interestingly, if a noise stressor coincided with the falling phase of a corticosterone pulse, the stress induced GC release was blunted (Windle, Wood, Shanks, *et al.*, 1998). Similar behavioural effects have been observed when rats were exposed to a male intruder, the degree of self-initiated aggression was increased during a rising phase of endogenous corticosterone than during a falling phase (J Haller *et al.*, 2000; J. Haller *et al.*, 2000). These observations were made in response to an acute stress, however, the period of perceived stress will also affect GC release dynamics as a chronic 30min restraint stress of male rats induced prolonged raised total blood corticosterone levels for at least 60min after the insult (Kitchener *et al.*, 2004). In conclusion, the GC response to stress is highly dynamic, dependent not only on the nature of the stressor but also the endogenous corticosterone ultradian rhythm.

These intriguing results, which strongly indicate a functional consequence of rapidly fluctuating GC hormones, lead to the question of whether other GC targets and processes also respond in an ultradian manner? It is already known that GCs mediate numerous effects on downstream tissues such as the brain, liver, skeletal muscle and others, to regulate a wide range of behavioural and metabolic processes (Pariante and Lightman, 2008; Lightman and Conway-Campbell, 2010; Sarabdjitsingh *et al.*, 2010; Walker *et al.*, 2012; Oster *et al.*, 2016). What is not known is how ultradian GC dynamics further modulate outcome. I hypothesise that an oscillating system can carry more information due to the increased flexibility to modulate signal profiles.

1.2.6 Ultradian GR regulation

Even though 90% of circulating corticosterone and cortisol is bound to CBG, oscillating free levels of GCs have been measured by microdialysis in blood plasma, intra-adrenal extracellular fluid as well as the hippocampus of rats (Ballard *et al.*, 1975; Jasper and Engeland, 1991; Droste *et al.*, 2008, 2009). Other studies using multiple simultaneous microdialysis measurements have shown subcutaneous tissues do experience GC pulses highly synchronised with those observed in circulating blood (Qian *et al.*, 2012). The fact tissues experience changes in GC levels at the uppermost zenith of an ultradian pulse has been postulated to re-enforce a 'digital' like signal to responsive cellular networks. This has further implications when one considers the relative affinities of responsive receptors. The MR has a 6-10 fold higher affinity for GC ligand than the GR, indicating GRs will be activated within the upper range of GC pulses whereas MR could be responsive in a pro-longed manner to GR ligand activation and may not react in a pulsatile manner (Reul and Kloet, 1985; van der Laan, de Kloet and Meijer, 2009; Mifsud and Reul, 2016). As indicated by western blots of nuclear extracts, GR and MR translocation within the nucleus of hippocampal cells of ADX rats, was observed in response to hourly bolus intravenous injections of corticosterone. Upon hourly corticosterone replacement via intravenous (I.V.) infusions, total circulating corticosterone levels were maximal by 1min, however, despite this relatively large dose (100µg), corticosterone was cleared from the blood plasma by 60min in a similar interphase period to endogenous ultradian frequency. Increased GR and MR nuclear levels were reported in response to corticosterone infusion, maximal at 10min and 15min respectively. However, nuclear GR levels were found to decrease to basal levels by 60min in synchrony to circulating corticosterone dynamics, MR remained elevated within the nucleus (Conway-Campbell *et al.*, 2007). The model was expanded upon by investigating how these mock 'ultradian' like pulses induced GR recruitment to a known GRE upstream of the clock gene Period1 (*Per1*) as well as measuring heterogeneous ribonucleic acid (hnRNA) production within the liver of the rat. As was postulated, GR did bind transiently in response to the infusion model, reaching maximal binding levels by 10min in response to corticosterone administration and returning to basal levels by 60min at the GRE (Figure 1.9-A). This corticosterone synchronised GR recruitment could be reinstated repeatedly by multiple infusions at hourly intervals, with no loss in maximal binding. Interestingly, hnRNA levels were similarly responsive to the corticosterone 'pulses', albeit in a slightly delayed manner, peaking 30min after each corticosterone peak (Stavreva *et al.*, 2009).

Expanding upon these experiments *in vitro*, corticosterone synchronised pulsatile dynamic GR binding and dissociation was observed at not just a single, but multiple binding sites. In a series of live imaging experiments to a tandem array of mouse mammary tumor virus (MMTV) promoter-reporter gene

cassettes within 3617 adenocarcinoma mouse cells, fluorescently tagged GR translocated into the nucleus and bound to the concatemerized GREs within the MMTV array after 20min stimulation of 100nM corticosterone. Similarly to *in vivo* data, GR would fully dissociate within 40min of total corticosterone washout and could be repeated by successive mock 'ultradian' pulses of hormone (Figure 1.9-B). RNA Pol2 occupancy was shown to be similarly oscillatory indicating pulsatile transcriptional recruitment. Observed pulsatile responses were not intrinsic as the induction of oscillating 'ultradian' hnRNA production of SOUX, GILZ (aka TSC22D3), transglutaminase (TGM2) and Metallothionein (MT2) in response to 8 cycles of corticosterone application and washout, became dysregulated upon constant corticosterone stimulation *in vitro* (Figure 1.9-C) (Stavreva *et al.*, 2009). Together, these findings indicate that GR recruitment and resultant transcriptional regulation of target genes is highly dynamic in its response to pulses of corticosterone exposure both in cultured cells and *in vivo*.

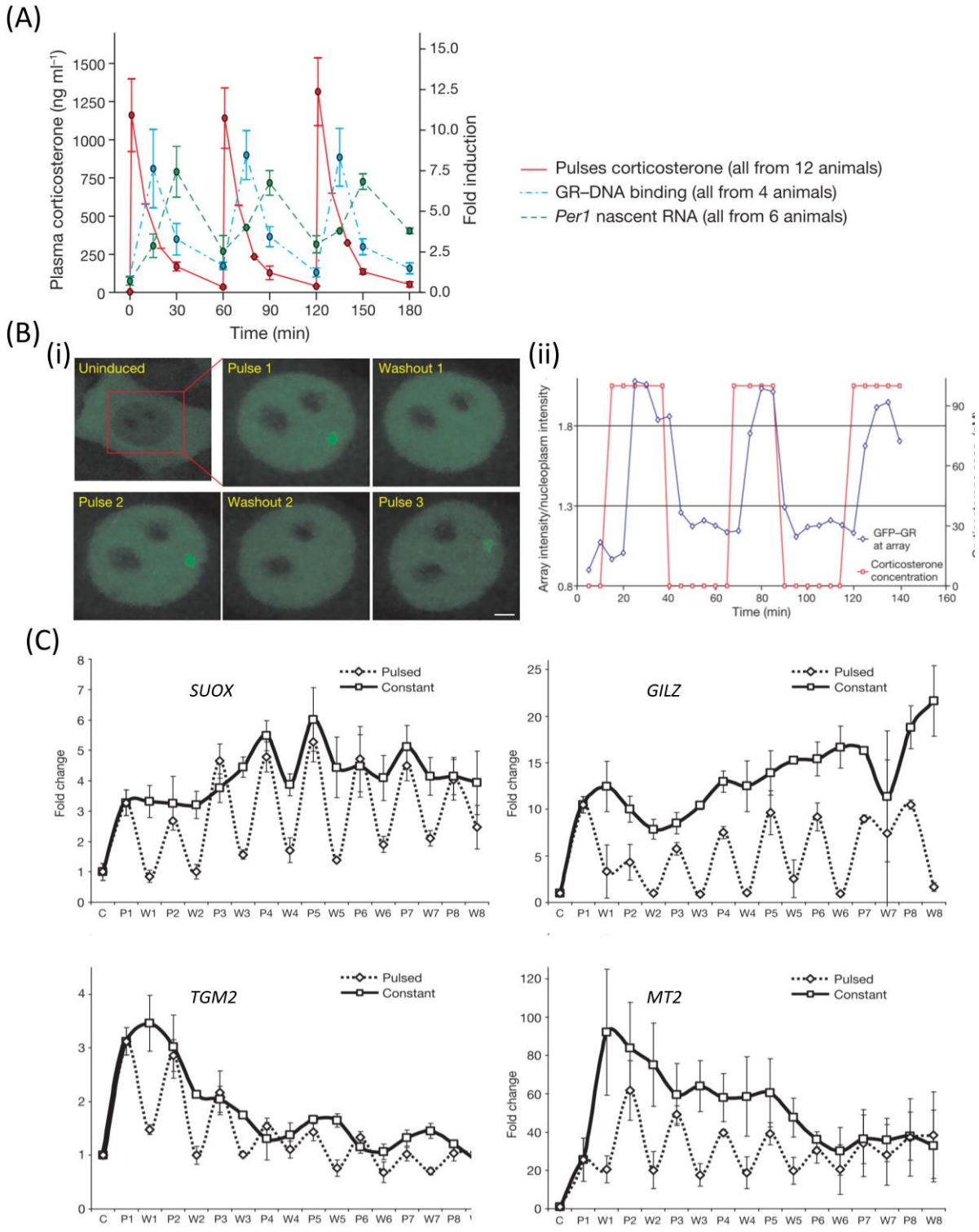

Figure 1.9 A series of mock 'ultradian' pulses of corticosterone induce synchronised GR recruitment/ dissociation from the DNA template and resultant mRNA production at select targets in vivo and in vitro.

(A) Three intravenous bolus injections of corticosterone at 0, 60 and 120min in an ADX male rat induced maximal circulating corticosterone levels by 1min, which cleared from the circulation within 60min (red). Synchronized increases and decreases in GR binding (blue) to the proximal GR binding

site of the clock gene Period1 (Per1) was detected, followed by pulses of heteronuclear RNA (hnRNA) (green) at phasic intervals between corticosterone pulses. Maximal phasic dynamics of GR and hnRNA levels were detected at 10min and 30min respectively, before returning to basal levels by 60min. Circulating total corticosterone was measured using radioimmunoassay, GR binding was measured using quantitative ELISA-based assay and heterogenous nuclear RNA (hnRNA) was measured by RT-qPCR analysis. (B) In a series of live cell imaging studies, green fluorescent protein tagged GR recruitment to the MMTV array in 3617 cell lines was induced by a 15min corticosterone administration and lost 40min after hormone washout. This was repeatable over three pulses of corticosterone (i) and GFP-GR MMTV array intensity against corticosterone concentrations plotted over time (ii). (C) Nascent transcript fold change to control were assessed via RT-qPCR analysis of selected up-regulated genes within 3134 cell lines in response to a series of eight 15min corticosterone administrations followed by 40min post hormone washout period (dotted lines). Results indicated pulsed corticosterone administration induced corticosterone synchronised increases in hnRNA of SUOX, GILZ, TGM2 and MT2. Oscillating hnRNA levels were lost in response to a constant exposure to corticosterone within froth media (black line). Control (C), induction (P) and withdrawal (W) are indicated along the x-axis. All error bars represent s.e.m. and figures are adapted from Stavreva et al., 2009.

1.2.7 Glucocorticoid regulation of gluconeogenesis

GCs were so named at the beginning of the 19th century by their ability to alter blood glucose levels. Upon further research, additional roles within metabolism was recognised, revealing regulation of lipolysis, triglyceride, fatty acid and carbohydrate homeostasis as well as glucose.

Glucose homeostasis is maintained by a myriad of endocrine signalling such as by insulin, glucagon and GC hormones. Indeed, glucocorticoids alter blood glucose levels by reducing uptake and glucose oxidation in skeletal muscle and white adipose tissues (WAT) whilst stimulating gluconeogenesis (mainly in the liver) and energy store mobilisation in response to a stressor (Kuo *et al.*, 2015). Focusing within the liver, GR action has been shown to regulate the gluconeogenic genes pyruvate carboxylase (PC), phosphoenolpyruvate (PEPCK1), PFKFB1 (a bi-directional enzyme consisting of 6-phosphofructio-2-kinase (PFK2)/fructose bisphosphatase2 (FBPase2) action), glucose-6-phosphatase (G6PC) and solute carrier family 37 member 4 (SLC37A4) (Figure 1.10).

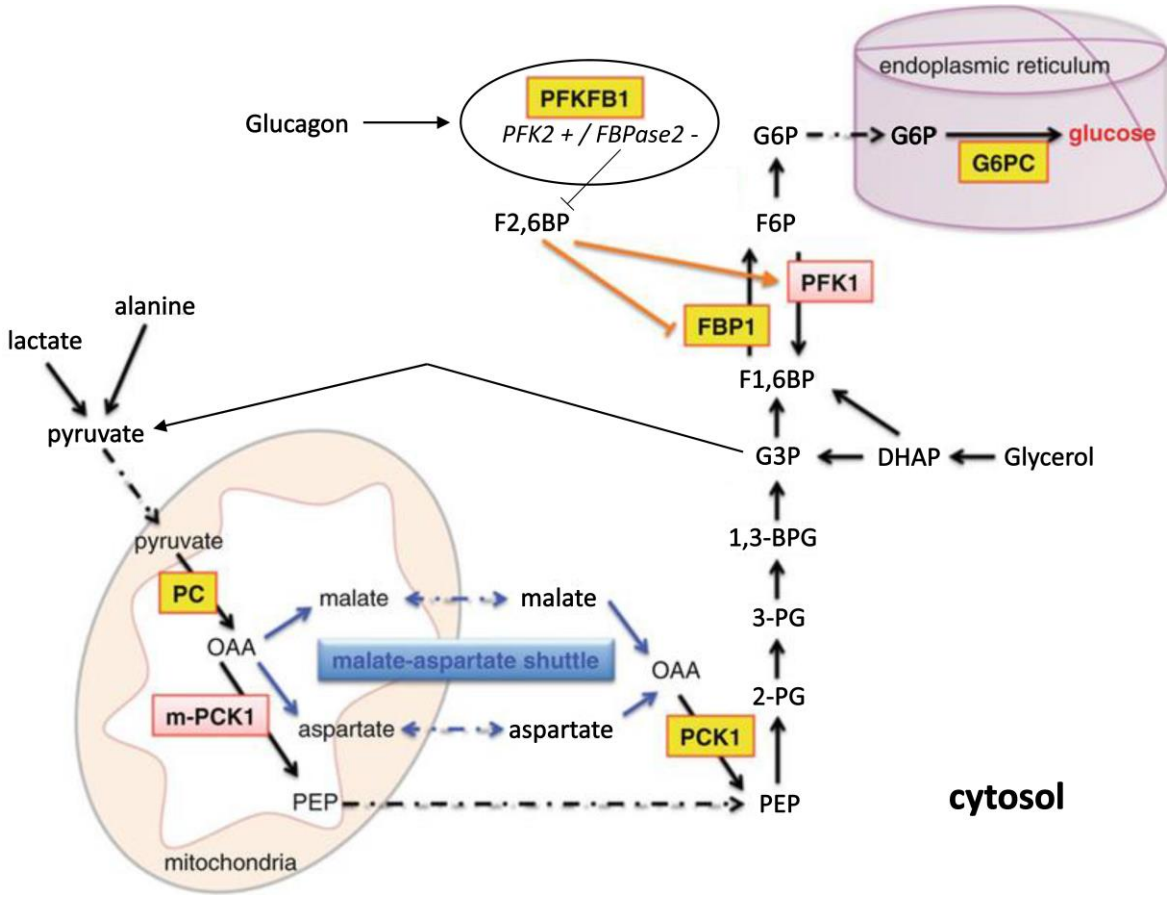

Figure 1.10 The Gluconeogenic pathway.

Within hepatocytes, non-carbohydrate substrates lactate and alanine are converted to pyruvate which is transported into mitochondria and converted by pyruvate carboxylase oxaloacetate (OAA). OAA cannot be transported out of the mitochondria, therefore it is converted into malate or aspartate within the tricarboxylic acid cycle, shuttled out and converted back to cytosolic phosphoenolpyruvate carboxykinase (PCK1) substrate, OAA. Indications have been reported of a PCK1 variant that can convert OAA into phospho-enolpyruvate (PEP) directly within the mitochondria (m-PCK1) before entering the gluconeogenic pathway. Once converted to glyceraldehyde-3-phosphate (G3P) either from metabolism of lactate, alanine or glycerol, G3P can either be metabolised back into lactate or alanine as part of the glycogenolysis pathway, or G3P is converted in fructose-1,6-bisphosphate (F1,6BP), a substrate for fructose-1,6-bisphosphatase 1 (FBP1). However, conversion to fructose-6-phosphate (F6P) is dependent on the bi-directional enzyme phosphofructokinase 2 (PFK2)/ fructose bisphosphatase 2 (FBPase2) (PFKFB1). In the un-phosphorylated state, PFKFB1 favours its intrinsic PFK2 activity which induces phosphofructokinase 1 (PFK1) action via the allosteric activator fructose-2,6-bisphospate (F2,6BP), converting F6P into F1,6BP within the glycogenolysis pathway. In contrast, glucagon signalling phosphorylates PFKBP1, whereupon its intrinsic FBPase2 activity is favoured, inhibiting F26BP activity and increasing FBP1 affinity for F1,6BP and favouring gluconeogenesis.

Hepatocytes can convert the precursor glucose-6-phosphaate (G6P) into glucose within the endoplasmic reticulum by the action of glucose-6-phosphatase catalytic subunit (G6PC) before transport out of the cell and into general blood circulation via the hepatic portal network. Tricarboxylic acid metabolites indicated by blue arrows and GC regulated targets are indicated in yellow. 2-phosphoglycerate (2-PG), 3-phosphoglycerate (3-PG), 1,3-bisphosphoglycerate (1,3-BPG) and dihydroxyacetone phosphate (DHAP) are also indicated. Figure adapted from Kuo et al., 2015.

Focussing on GC regulated targets within the gluconeogenic pathway, PC catalyses the ATP dependent carboxylation of pyruvate into oxaloacetate (OAA) within hepatocyte mitochondria (Utter and Bruce Keech, 1960; Menefee and Zeczycki, 2014). This is an important preliminary step as substrate for the tricarboxylic acid cycle but ultimately as a precursor for the action of PEPCK within gluconeogenesis (Hanson and Garber, 1972; Arinze, Garber and Hansons, 1973; Hansen and Juni, 1974; Méndez-Lucas *et al.*, 2013; Stark *et al.*, 2014). Data regarding direct GC regulation of *PC* transcription however is unclear. Two primary transcripts from alternative splicing events have been identified within rats, regulated by two promoter regions. The proximal promoter is active within gluconeogenic and lipogenic tissues and regulates production of the first transcript, whereas the distal promoter is active within a wide variety of tissues, regulating production of the second transcript (Jitrapakdee and Wallace, 1999). Functional GREs have been identified within the bovine *PC* promoter, but not in rat and human where only indirect GR regulation via CREB, nuclear factor 1 (NF-1) and hepatic nuclear factor 4 α (NHF4α) has been speculated to be the mechanism of PC transcriptional regulation (Jitrapakdee *et al.*, 1997, 2008; White, Koser and Donkin, 2011). Opposing reports however, show either increased or no effect of Dex treatment on PC mRNA levels (Martin, Allan and Titheradge, 1984; Jones, Hothi and Titheradge, 1993; Kuo *et al.*, 2015). Therefore, PC regulation by GCs requires further investigation to determine whether its transcriptional regulation is direct or indirect.

PEPCK expression is increased in a fasting state synergistically by glucagon and GC administration. It is also inhibited by a carbohydrate diet. Both a cytosolic and mitochondrial isoforms of the rate limiting enzyme have been identified, converting OAA into phosphoenolpyruvate (PEP) (Hanson and Garber, 1972; Arinze, Garber and Hansons, 1973; Hansen and Juni, 1974; Méndez-Lucas *et al.*, 2013; Stark *et al.*, 2014). PEPCK is a key target within GC regulated glucose homeostasis, mediated by two promoter GREs within composite glucocorticoid response units (GRUs), identified between -395b to -349b from the TSS within H4IIE rat hepatoma cell lines. The promoter region also contains three other regulatory regions at -451b to -431b (gAF2), -420b to -403b (gAF1), -327b to -321b (gAF3) as well as a cAMP response element (CRE) -93b to -86b from the TSS (Imai *et al.*, 1990, 1993; Scott, Mitchell and Granner, 1996b, 1996a; Vegiopoulos and Herzig, 2007; Kuo *et al.*, 2015; Zhang *et al.*, 2019). These regions are

conserved within human hepatoma (HepG2) cell lines, plus a further two at -933b (dAF1) and -1,365b (dAF2) (Cassuto *et al.*, 2005). PEPCK transcription appears to require synergistic, multi-factorial regulation as reporter gene assays demonstrated that GR binding to individual GREs and AF regions did not confer transactivation alone. GRE affinity for GR was also found to be relatively weak and mutation of either AF1, AF2, GRU or CRE reduced PEPCK transcription by 50-60% whilst a combination completely ablated PEPCK transcription in response to GC stimulation (Imai *et al.*, 1990, 1993; Scott, Mitchell and Granner, 1996a, 1996b; Scott *et al.*, 1998). Composite binding complexes have been demonstrated in vivo between the GRU and CRE. It has been further postulated interactions also include accessory activity of HNF4α and chicken ovalbumin upstream transcription factor (COUP) via gAF1, and hepatic nuclear factor 3 (HNF3) α and β via gAF2 (Imai *et al.*, 1993; Hall, Sladek and Granner, 1995; O'Brien *et al.*, 1995; Scott *et al.*, 1998). Chromatin immunoprecipitation (ChIP) studies have indicated FoxA2, CEBPβ, HNF4α and COUP occupation of the promoter occurs prior to and does not change following GC treatment, indicating a basal state of occupation of these factors is required. GC induced Recruitment of GR transcriptional co-regulators NCOA1, p300, FoxO1, FoxO3 and CREB have been shown to be GC dependent, as is Pol2 recruitment (Hall *et al.*, 2007). The gAF2 element also contains an insulin response element, however, how this confers inhibitory action is not yet fully understood but it has been theorised to have something to do with the loss of histone H3 de-methylation (O'Brien *et al.*, 1990; Hall *et al.*, 2007). Interestingly, PEPCK is inhibited by GCs in WAT by an unknown mechanism (Meisner, Loose and Hanson, 1985; Friedman *et al.*, 1993; Olswang *et al.*, 2003). The PEPCK promoter provides a detailed example of complex co-operative transcription factor binding and co-recruitment that can be required for transcriptional regulation.

During gluconeogenesis, PEP is converted via 5 enzymatic steps to fructose-1,6-bisphosphate (F1,6BP), a pathway which is reversed in glycolysis (Kuo *et al.*, 2015). It is at this point the bi-directional enzyme PFKBP1 regulates the switch between gluconeogenesis and glycolysis pathway directions. PFKBP1 has intrinsic FBPase2 and PFK2 activity, of which the latter is favoured in its de-phosphorylated state. PFK2 induces fructose 2,6-bisphosphatase, an allosteric activator of phospho fructokinase 1 (PFK1) within the glycolytic pathway. However, glucagon signalling pathways induce cAMP and AKT1 phosphorylation of FKB1, favouring its intrinsic FBPase2 activity instead and reducing PFK2 activity and increasing FBP1 affinity for F1,6BP and conversion into fructose-1,6-bisphosphate (F6P) (Hue and Rider, 1987; Marcus *et al.*, 1987; Rider *et al.*, 2004). Dex treatment of ADX rats increases PFKFB1 transcription, presumably via two intronic co-operative GREs identified in HeLa cells, the distal of which has been observed to mediate the greater transactivation (Zimmermann and Rousseau, 1994; McFarlan *et al.*, 1997). As described previously for PEPCK, the PFKFB1 GRU recruits multiple co-factors, including NF1, CEBP, HNF3 and HNF6 within the rat liver (Pierreux *et al.*, 1998).

Within gluconeogenesis, F6P is converted into glucose-6-phosphate by phosphoglucoisomerase, transported to the endoplasmic reticulum where it is converted into glucose by the action of the membrane bound G6PC (De Duve *et al.*, 1949; Hers *et al.*, 1951; El-Maghrabi *et al.*, 1995; Kuo *et al.*, 2015). This is the final GC regulated target known to regulate the gluconeogenic pathway. Its expression is increased after GC administration and decreased in response to insulin (Vander Kooi *et al.*, 2005). Within mouse liver, GR regulation to three identified GREs (-197/-183; -180/-166; -156/-142) appears to be dependent on the recruitment of multiple forkhead transcription factors (FoxO1, FoxO3A) as well as HNF3, HNF4α and CEBP within the GRU of the promoter region (Lin, Morris and Chou, 1998; Schmoll *et al.*, 1999; Vander Kooi *et al.*, 2005). Suggesting similar modes of regulation as previously described for PEPCK. Three GREs have been identified. It should be noted that FoxO1 has been implicated as a necessary factor for full GC mediated transcriptional output of the genes mentioned. Interestingly, FoxO1 has also been shown to be important for insulin's inhibitory effect as FoxO1 liver knockout mice were unable to respond to insulin (Vander Kooi *et al.*, 2005; Onuma *et al.*, 2006; K. Zhang *et al.*, 2012), thus highlighting its potential role within nuclear factor mediated action. Interestingly, G6PC is postulated to be part of a multicomponent enzyme which also includes the transporter protein SLC37A4, which is required for translocation of G6P from the cytoplasm to the endoplasmic reticulum (ER) for conversion by G6PC into glucose within hepatocytes (Narisawa *et al.*, 1978; Van Schaftingen and Gerin, 2002; Kuo *et al.*, 2015).

GCs also interact within glycogen pathways. Even though GC treatment has been reported to increase levels of glycogen within the liver, it has been shown that it also regulates the activity of glycogen synthase. This is mediated by the GC regulated expression of protein phosphatase 1. In the de-phosphorylated state, glycogen synthase will liberate glucose from glycogen stores and therefore increase glucose levels (Kuo *et al.*, 2015).

1.2.8 Fatty acid, triglyceride and lipid regulation by GCs

Fatty acids are mostly dietary in source and transported from the intestine to the liver in chylomicrons due to their lipophobic nature and release non-esterified fatty acids and carbohydrates via the action of lipoprotein lipase for downstream metabolism. A relatively small amount of cholesterol, however, can be synthesized by the liver (Linder *et al.*, 1976; Hellerstein, 1999; Rui, 2014). Briefly, when carbohydrates are in abundance, the glycolytic pathway, metabolises glucose via hydrolyses into pyruvate and metabolised within hepatocyte mitochondria into actetyl coenzymeA (acetyl-CoA) (a product of pyruvate kinase action), converted to the intermediate malonyl-CoA by acetyl-CoA carboxylase (ACC) before conversion to fatty acids by fatty acid synthase (FASN) (Chakravarthy *et al.*, 2005; Rui, 2014).

The two major fat stores within the body are the liver and WAT. Within the liver, fatty acids are esterified with glycerol into triglycerides (TG). This is a more efficient method of storage as TGs contain twice as much energy per gram than glycerol or glucose (Hillgartner, Salati and Goodridge, 1995). Insulin action increases this 'short term' storage of TGs within the liver as they are commonly packaged within lipoproteins and transported to target tissues (predominantly WAT) around the body (Malmström *et al.*, 1997; Gibbons *et al.*, 2004). Non-esterified fatty acid, carbohydrates and glycerol are released into the target metabolic tissues via the hydrolytic action of lipoprotein lipase (LPL), whereupon fatty acids are metabolised or re-esterified for storage within the said tissue. As previously mentioned, WAT is considered to be the major fat depot of the body, however, significant amounts are stored in the liver and muscle (Hillgartner, Salati and Goodridge, 1995; Macfarlane, Forbes and Walker, 2008; de Guia, Rose and Herzig, 2014).

A number of key enzymes within carbohydrate and lipid metabolism are under GC control (Gibbons *et al.*, 2004; de Guia, Rose and Herzig, 2014). Within the liver, carbohydrates are metabolised into lipids for transport around the body within lipoproteins. This process has been shown to be under GC regulation as serum cholesterol in obese and control mice were reduced after hepatic specific GR knockouts, as well as increased TG accumulation in GR knockout hepatocytes *in vivo*. This has been linked to the GR repressive action on hairy enhancer split 1 (HES1) transcription due to the recruitment of HDACs to the promoter (Lemke *et al.*, 2008; Revollo *et al.*, 2013). HES1 is a cAMP inducible repressor, indirectly reducing levels of peroxisome proliferator-activated receptor γ (PPARγ) which has been shown to be a key inducer of lipogenic genes. Presumably, this action occurs within the liver for lipoprotein release (Herzig *et al.*, 2003). There were slight increases in sterol regulatory element binding transcription factor 1 (SREBP-1)c, which has also been implicated within lipogenesis and TG synthesis. However, this finding was not statistically significant and this variant is involved in fatty acid synthesis as opposed to carbohydrate metabolism (Shimomura *et al.*, 1998; Lemke *et al.*, 2008).

Dex induced increases in mRNA have been reported for the key hepatic *de novo* lipid synthesis enzymes ACC and FASN, the latter of which has been shown to be directly GR regulated (Soncini *et al.*, 1995; Xu, Viviano and Rooney, 1995; Lu, Gu and Rooney, 2001; Zhao *et al.*, 2010; Gathercole *et al.*, 2011). Genome wide analysis of Dex treatments in 3T3-L1 cells identified promoter associated GR binding sites for lipid synthesis targets Stearoyl-CoA desaturase 1 & 2 (SCD1) (SCD2), glycerol-3-phosphate acyltransferase 3 & 4 (GPAT3) (GPAT4) and *LPIN1*, as well as the lipolytic factor lipase E and lipid transporters CD36, LDL receptor related protein 1, very low density lipoprotein (VLDL) receptor (VLDLR) and SLC27A2 that facilitate lipid transport. Dex induction of known insulin targets such as the dual specificity phosphatase 1, insulin induced gene 2 and lipocalin 2 (which are all implicated in

insulin resistance), indicated GC induced lipid synthesis and mobilisation (MacDougald *et al.*, 1994; P. Zhang *et al.*, 2008; Yu *et al.*, 2010). It should be noted, however, that most studies have focused on adipocyte function and require further elucidation within hepatic pathways.

Apolipoproteins are synthesized within the liver and have a range of functions which are integral to lipoprotein synthesis, transport and targeted metabolism (Brown and Goldstein, 1983; Werner, Kuipers and Verkade, 2013). In the fasted state, hepatic apolipoprotein synthesis and release into the circulation is increased, transporting TGs, carbohydrates and glycerol to target tissues. However, this process is attenuated by ADX within rodents (van der Sluis *et al.*, 2012). Within the fasted state, the liver will increase synthesis and stability of APOB-100 for VLDL synthesis so as to transport TGs and carbohydrate stores to target tissues around the body. As this synthesis requires carbohydrate substrates, when stores are low, APOB-100 transcription is decreased. Due to the rapid degradation of APOB-100 within the endoplasmic reticulum, the rate of transcription is thought not to be a determinant with regard to VLDL synthesis. However, loss of function of APOB or the rate limiting microsomal triglyceride transfer protein (MTP) which mediates correct folding of APOB, can inhibit the production of VLDL and induce the presentation of the rare conditions familial hypobetalipoproteinemia or abetalipoproteinemia, increasing circulating TG and cholesterol levels (Feingold and Grunfeld, 2000; Tiwari and Siddiqi, 2012; Hooper, Burnett and Watts, 2015). Reduction in LDL receptors within the VLDL (of which APOB contains a similar region), reduces uptake by IDL and reduces the body's capacity to clear VLDLs from the circulation into target tissues for metabolism (Feingold and Grunfeld, 2000).

It has been proposed GCs can induce transcription of apolipoproteins required for assembly and recognition by tissues, however, direct evidence for this in hepatocytes has not been shown, as the majority of research has focussed on adipocyte lipid regulation. For example, apolipoprotein AI (APOAI) and -IV (APOIV) are major constituents of HDLs, some of which are proposed to be transferred from chylomicrons and VLDLs during TG transfer (Lagrost *et al.*, 1989). Transcription of APOAI is dependent on the co-regulatory action of both promoter bound HNF4α and peroxisome proliferator-activated receptor γ coactivator-1α, as is HNF3β for APOAIV transcription. No direct GR regulation of either apolipoprotein has been identified, although HNF3β binding to APOIV promoter region has been postulated to be dependent on GR tethering (Saladin *et al.*, 1996; Taylor *et al.*, 1996; Mooradian, Haas and Wong, 2004; Hanniman *et al.*, 2006; Vegiopoulos and Herzig, 2007). As may be expected, there are tissue specific differences in regulation between liver and adipocytes. For example, APOE is mainly synthesised within the liver and macrophages and is critical to lipoprotein metabolism within the body (Mahley, 1988; Rosenson *et al.*, 2012). However, a recent study of macrophages and

hepatocytes (*in vitro* and *in vivo*) found Dex-induced APOE transcription was increased in macrophages but not hepatocytes, despite a conserved promoter GR binding site identified in humans (-111/-104). The authors postulated phospholipase A2, phospho lipase C and mitogen activated kinase kinase (MEK) pathways mediated inhibition of GR transactivation in hepatocytes (Trusca *et al.*, 2017). Therefore, elucidating liver specific regulation of apolipoproteins and lipoproteins from circulating levels may lead to false discovery. Lack of function clarity is further compounded by studies reporting contradictory data. For example, before TGs are packaged into lipoproteins, they undergo hydrolysis by enzymes such as triacylglycerol hydrolysis. However, Dex has been shown to reduce VLDL synthesis via a reduction in triacylglycerol hydrolysis mRNA levels within hepatocytes (Lehner and Verger, 1997; Dolinsky *et al.*, 2004), whereas other studies have shown Dex increased VLDL production (Mangiapane and Brindley, 1986).

GC regulation of hepatic carbohydrate, fatty acid, lipid synthesis and transport play major roles within homeostasis of tissues around the body. Understanding these mechanisms is highly complex as each study design must control for age, weight, diet and underlying pathology to elucidate mechanisms. Current knowledge of these pathways has been gleaned from adipocyte function studies and is not yet at a level to avoid conflicting reports. Therefore, considerably more hepatic focussed research is required to fully understand the GC role in Fatty acid, triglyceride and lipid regulation (Vegiopoulos and Herzig, 2007; Werner, Kuipers and Verkade, 2013; de Guia, Rose and Herzig, 2014).

1.3 Metabolism and dysregulation of glucocorticoid rhythms

GCs have multi-systemic effects within mammalian systems and their dysregulation can precipitate harmful pathophysiological effects including cognitive and memory acquisition impairment, depression and osteoporosis. Due to their significant role within metabolic homeostasis, dysregulation can also severely impair glucose, lipid, carbohydrate, fatty acid and liver homeostatic control; all of which have been implicated in the ever-increasing prevalence of metabolic syndrome (MetS). MetS describes an array of phenotypes including visceral obesity, hyperglycaemia and hypertension, reduced high density lipoproteins (HDLs) and raised VLDL levels, atherogenic dyslipidaemia, non-alcoholic fatty liver disease (NAFLD) (TG >55mg/g or 5.5% of liver), hepatic steatosis and type II diabetes and can be presented in combination but not all are required for diagnosis (Alberti *et al.*, 2005; Szczepaniak *et al.*, 2005). MetS presents a significant health burden within western societies as the National Health and Nutrition Examination Survey has reported that 23% of the U.S. population have presented MetS criteria (Rochlani *et al.*, 2017). This review will focus on how GC dysregulation has been associated with MetS phenotypes and could play a critical role in its development.

Cushing's Disease and Addison's patients represent the two extremes of GC dysregulation. Cushing's disease is caused by hypercortisolism, 70% of which are due to pituitary adenoma overstimulating GC release from the adrenal glands (Nieman and Ilias, 2005). Patients present with a number of MetS pathology including visceral fat gain and obesity (32-41%), hypertension, impaired glucose tolerance, dyslipidaemia (32-41%) and type II diabetes (20-47%) (Nieman and Ilias, 2005; Stratakis, 2008; Feelders *et al.*, 2012; Buliman *et al.*, 2016). Conversely, Addison's disease is characterised as hypocortisolism, and can be caused by autoimmune hypothyroidism and type I diabetes as well as other rare conditions. Patients present with the opposite symptomology to Cushing's patients with MetS development, as they usually lose weight and suffer from fatigue, anhedonia, hypotension and hypoglycaemia (Chakera and Vaidya, 2010). Whilst both conditions are relatively rare and extreme, the metabolic phenotypes observed provide the 'worst case scenario' example of metabolic adverse effects associated with GC dysregulation and can therefore inform about how dysregulated GC levels affect metabolism and other functions.

1.3.1 Dysregulation of the HPA axis and the molecular 'clock'

Commonly referred to as the 'clock' transcriptome, targets are expressed throughout mammalian central and peripheral tissues, highly interconnected and cyclically transcribed within positive and negative feedback loops and are centrally timed by circadian / ultradian hormonal release, such as GCs (Delaunay and Laudet, 2002; Panda *et al.*, 2002; Staels, 2006; Scott, Carter and Grant, 2008). As up to 9% of transcripts within mouse liver have been shown to be under circadian control, the clock transcriptome represents a highly adaptable and important system (Akhtar *et al.*, 2002). Common targets of investigation include transcription activators such as circadian locomotor output cycles kaput (CLOCK), brain and muscle ARNT-like 1 (BMAL1) as well as the inhibitors period circadian regulator (PER) 1,2 & 3, cryptochrome1, cyrptochrome2 and nuclear receptors REV-ERB and retinoic acid-receptor-related orphan receptors (ROR) (Kume *et al.*, 1999). These targets participate in an oscillating system of core clock processes as CLOCK and BMAL1 (which bind as a heterodimer to promoter elements) induce transcription of PER1 and cryptochrome 1. However, increased levels of PER1 and cryptochrome 1 will negatively feedback and allosterically inhibit CLOCK and BMAL1 binding to DNA (Gekakis *et al.*, 1998; Kume *et al.*, 1999; Shearman *et al.*, 2000; Reppert and Weaver, 2002; Jetten, 2009; Cho *et al.*, 2012).

GC transcriptional regulation for numerous clock targets have been described and importantly, glucose, lipids, carbohydrates, insulin and leptin all exhibit circadian variations in their expression. Therefore, GC dysregulation may mediate its adverse metabolic affects via dysregulation of peripheral clock pathways. Liver specific GR-knockout mice have a faster phase-reset under restricted feeding of

the liver clock than controls. This is potentially mediated by their regulation of Per1 and Per2 (Le Minh *et al.*, 2001). GR has been shown to regulate *PER1* transcription via two GREs ~2kb upstream of the TSS and within intron 1, whilst *PER2* transcription can be induced by BMAL1 dependent GR binding to the proximal promoter region (Conway-Campbell *et al.*, 2010; Reddy *et al.*, 2012; Zani *et al.*, 2013). In a recent study, it was shown the expression of the rate limiting mitochondrial enzymes required for carbohydrate and lipid metabolism accumulated in a diurnal pattern. This was blunted in mice lacking Per1 and Per2 as well as a high fat diet (HFD) (Neufeld-Cohen *et al.*, 2016). Per2 knockouts have reduced fasting glycaemia as well as altered hepatic glycogen accumulation which is postulated to be due to a loss of Per2 direct and indirect induced transcription of glycogen synthase and protein phosphatase-1 (Zani *et al.*, 2013).

The clock transcriptome is highly complex, with a myriad of crosstalk pathways and internally dependent regulation, therefore, it is difficult to identify an individual cause of metabolic phenotypes. For example, CLOCK and REV-ERBα expression is currently understood to not be directly GR regulated, but REV-ERBα has been shown to reduce GR half-life and activity, potentially via HAT activity to the GR (Okabe *et al.*, 2016). CLOCK has been implicated in glycogen metabolism via regulation of glycogen synthase 2 transcription, a rate limiting glycogenic enzyme and REV-ERBα has been shown to directly regulate the expression of gluconeogenic genes PCK and G6PC (Yin *et al.*, 2006; Doi, Oishi and Ishida, 2010). Loss of Clock and REV-ERBα function induces dramatic metabolic changes, developing obesity, hepatic steatosis, hyperglycaemia, hyperleptinemia, hyperlipidaemia, hypoinsulinemia, elevated VLDL and hypercholesteremia. Whereas Rorα knockouts present opposing phenotypes, lowering triglycerides and increasing glucose and apolipoprotein C levels in the blood, however, dysfunction of peripheral clocks may not be the only cause (Raspé *et al.*, 2001, 2002; Turek *et al.*, 2013; Kojetin and Burris, 2014). For example, it was recently shown the restricted feeding attenuated MetS pathology in Cry1:Cry2 and liver specific Rev-erbα/β or Bmal1 knockouts. Even though elements of the clock transcriptome would have been partially intact, the study suggests eating behaviours could be the major influence (Chaix *et al.*, 2019). Therefore, GC dysregulation can drive perturbations in the oscillatory pattern of the peripheral clock transcriptome, but there are clearly numerous other factors that also contribute to the development of MetS.

1.3.2 Feeding and the HPA axis

A myriad of studies has focussed on the loss of synchrony between endogenous circadian patterns (such as GCs) and environmental cues (light/ dark periods), emulating irregular shift work, transmeridian travel and inconsistent sleep patterns and their implication for MetS development. For example, mice left in 20:4hr light:dark cycles significantly gained weight without increasing overall

food intake. This was also associated with increased circulating endocrine hormones leptin and insulin levels as well as aberrant cognitive ability which was associated with a loss in neuronal plasticity (Karatsoreos *et al.*, 2011). These alteration in light:dark periodicity implicate the HPA axis, as even though it is a highly plastic system, adaptions to new light periods are possible, that within humans is thought to be roughly an hour a day per time zone crossed (Eastman *et al.*, 2005; Bullock *et al.*, 2007; Doane *et al.*, 2010). The HPA axis is chiefly regulated by the photoperiod and not activity, therefore individuals with permanent night shift work do not alter diurnal photoperiod endogenous melatonin and cortisol profiles (Roden *et al.*, 1993). Unsurprisingly, night shift workers have a 2-fold higher risk of developing type II diabetes, potentially as consequence of insulin resistant like phenotypes, raising both resting insulin and glucose levels as well as increased oxidized carbohydrates (Gan *et al.*, 2015). Interestingly, these phenotypes were more notable within phase advance as opposed to phase delay conditions (Roden *et al.*, 1993; Scheer *et al.*, 2009; Gonnissen *et al.*, 2012; Gan *et al.*, 2015; Koopman *et al.*, 2017). Similar glucose and insulin insensitivity have been shown in adrenally suppressed patients. Bolus cortisol injections during the natural circadian nadir (17:00) induced significantly elevated post-prandial glucose and insulin levels, compared to those induced by cortisol injections during the natural circadian peak (05:00) (Plat *et al.*, 1999). This finding indicates differences in insulin and glucose sensitivity dependent on the phase of circadian cortisol release and could be particularly pertinent to shift work.

It should be noted that dysregulation of circadian rhythms also affects feeding behaviour which may further contribute to the development of MetS. For example, mice fed a HFD still retain some circadian pattern to their feeding schedule but they consume significantly more during the inactive period without increasing their overall intake (Kohsaka *et al.*, 2007). Indeed, the circadian phase an organism's calorific intake occurs could be very important. Restricting feeding to the inactive period has been shown to induce MetS pathology in mice without altering their activity or calorific intake as well as a loss in synchrony between the SCN (remained intrinsically timed to the photoperiod) and peripheral hepatic molecular clock mRNA levels of Bmal1, Cry1, Cry2, Per1, Per2, Rorα, Pparα, Pparγ and Rev-Erbα, as well as the metabolic targets Pepck, fatty acid binding protein 1 & 4 and fatty acid synthase. Physiologically, these mice developed hypoinsulinemia and raised TG and free fatty acids. As Pparα and Gsk3β are not expressed within the SCN, these targets were identified as key drivers in peripheral misalignment to the central clock, particularly as they are key targets within glucose and lipid metabolism. The adverse metabolic effects were reversed by restricting feeding to the active period and targeted inhibitors, which the authors theorise could have therapeutic implications for shift workers as these inhibitors are already used clinically for mood and anxiety disorders (Kohsaka *et al.*, 2007; Mukherji *et al.*, 2015). These studies indicate metabolic pathways are distinctly integrated

into circadian signalling mechanisms and dysregulation of meal timing relative to circadian cues may be an additionally important factor integrating with GC dysregulation of metabolism.

1.3.3 Maladaptive stress and metabolism

Both physiological and psychological stressors are primary modifiers of the HPA axis. As previously discussed, stress innervation of hypothalamic CRH neurons activates HPA axis release of ACTH, inducing production and secretion of GCs from the adrenal glands. The ultradian regulation of GC levels has implications for the stress response as stress related maximal corticosterone increases are blunted when the stressor is applied during the falling phase of a GC pulse, as was aggression to an unknown male during a self-initiated aggression behavioural task (J. Haller *et al.*, 2000; Sarabdjitsingh *et al.*, 2010). Stress also alters the ultradian interpulse period, indicating modification of endogenous GC pulse frequency (Windle, Wood, Lightman, *et al.*, 1998). Similar perturbations have been recorded in clinically depressed patients who present with increased circulating ACTH and cortisol levels, often with a loss in circadian nadir (Deuschle *et al.*, 1997). Association with the loss of ultradian function has been shown via the blunted response of the HPA axis to secrete ACTH when corticosterone was infused into the circulation constantly as opposed to a hourly pulsatile model (Sarabdjitsingh *et al.*, 2010; Lightman, 2016; Oster *et al.*, 2016).

Stress induced GC release is a natural response that has been postulated to mobilise energy stores from WAT, skeletal muscle and liver. Raising blood glucose levels to provide energy to tissues such as the brain in classic fight or flight responses (Kuo *et al.*, 2015). Under chronic situations, however, these changes can become maladaptive and have been associated with the development of MetS pathology. For example, the likelihood of developing MetS in workers who experience chronic stress (defined as three or more self-determined stressful events a week) were quoted as twice as likely including type II diabetes (Chandola, Brunner and Marmot, 2006; Rod *et al.*, 2009; Edwards *et al.*, 2012). Elevated cortisol levels have been associated with increased weight gain, elevated TGs and fasting glucose levels, and lowered HDL levels in stressed obese individuals when compared to non-stressed obese individuals (Vicennati *et al.*, 2009; Bergmann, Gyntelberg and Faber, 2014; Garbarino and Magnavita, 2015; Ryu *et al.*, 2016). It must be noted that these studies are highly variable as controlling for dietary, circadian activity patterns and general lifestyles are difficult. Increased appetite behaviour in response to stress and GCs has also been reported due to the increased expression of orexigenic genes such as neuropeptide Y (White *et al.*, 1994)

1.3.4 Clinical corticosteroids

As previously mentioned, the discovery of cortisone and its anti-inflammatory affects in rheumatoid arthritic patients in the 1940s garnered huge interest and research (Hench and Kendall, 1949). Soon after, the ability to synthetically produce steroids in large amounts became a rapid and lucrative avenue of research and clinical treatment. Dehydration of the A ring at the 1, 2, position of cortisone or corticosterone, produced prednisone (cortisone derivative) and prednisolone (corticosterone derivative) with increased anti-inflammatory properties and the claim of reduced adverse side-effects. Dex was also created by combining 16α-methylation, 9α-fluorination and 1-dehydrogenation to become the most potent anti-inflammatory of its time (Arth *et al.*, 1958; Hillier, 2007). The desired properties of synthetic glucocorticoids (sGCs) included greater anti-inflammatory action and longer half-lives compared to their endogenous counterparts and before long became the most commonly used anti-inflammatory and immunosuppressive drugs for rheumatic and other inflammatory conditions (Stahn *et al.*, 2007). Their clinical use has become so prolific that pre 2007, in the United States 44.3 million prescriptions were made annually and in the UK, 0.85% of patients >18 years of age were prescribed oral sGCs (0.75% for long time use ≥3 months) over a 20 year period from 1989 (Fardet, Petersen and Nazareth, 2011; Judd *et al.*, 2014).

Due to their structural similarity to adrenal corticosteroids, sGCs will act as ligand for the GR, however, data on ligand half-life's and efficacy are varied and limited. Methylprednisolone circulation has been measured to just over two hours in separate 5 and 8 healthy male cohorts, whilst Dex plasma half-life at just over 3hrs (Al-Habet and Rogers, 1989; Uhl *et al.*, 2002; Nicolaides *et al.*, 2018). An *in vitro* study has shown that Dex treatment can induce GR activation up to 12 hours in AtT20 cells and in the rat pituitary *in vivo* and up to 6hrs in brain regions such as the hippocampus, perirhinal cortex and amygdala (Earl *et al.*, 2017). The reduced activation in brain compared to the periphery is known to be due to Dex extrusion from the brain by the multiple drug resistant P-glycoprotein (Cordon-Cardo *et al.*, 1989; Meijer *et al.*, 1998; Karssen *et al.*, 2001, 2005).

To investigate the effect of sGCs on GR to DNA binding, GR occupancy at the MMTV array within 3617 cells was used in response to 15min exposure and washout to a range of sGCs and the endogenous counterparts cortisol and corticosterone. Acute GR occupancy was similar for all corticosteroids assessed at 15min incubation, but only hydrocortisone, cortisol and corticosterone induced GR occupancy in a transient manner as GR was rapidly lost after hormonal washout. In contrast, the longer half-life engineered sGCs tested induced maximal prolonged GR binding at the MMTV array throughout the wash out period. This experiment was expanded upon using 20min corticosterone or Dex applications followed by 40min washouts repeated over multiple phases. As before, GR was

bound in response to 20min incubation, but only lost in the corticosterone induced data set, whereas Dex induced GR binding in a maximally prolonged manner throughout the wash period. This was repeatedly observed over the experimental timecourse, in addition to changes in RNA PolI2 transcriptional recruitment and DNase hypersensitivity. Together, these data indicate GR binding in response to sGCs can be prolonged to the endogenous corticosterone counterpart and consequently dysregulate postulated ultradian / circadian cyclical gene induction (Stavreva *et al.*, 2009, 2015).

As sGCs can regulate GC responsive targets, loss of circadian / ultradian regulation of GC tissues could have significant effects. Long term administration of a variety of sGCs have been linked to osteoporosis as well as cognitive, memory, learning deficits and depression (Varney, Alexander and MacIndoe, 1984; Wolkowitz, 1994; Manelli and Giustina, 2000; Blalock *et al.*, 2005). Notably for my work, GCs are a principle mediator of metabolic homeostasis, therefore sGCs can induce major adverse side-effects on glucose, fatty acid, lipid and carbohydrate metabolism. Hyperglycaemia is a common side-effect of chronic corticosteroid treatment, most likely due to insulin insensitivity. For example, sGC treatment has been shown to primarily precipitate the development of type 2 diabetes in a cohort of patients with no apparent underlying risk such as family history or obesity (Simmons *et al.*, 2012).

Data on metabolic side effects is highly variable due to differing pharmacological properties of different sGCs, dose, prescription length and underlying pathophysiological condition. For example, high dose prednisolone (30mg) treatment has been shown to be associated with the appearance of insulin resistance urinary markers within 2 days of treatment. A slightly reduced dose of 15mg was associated with the appearance of the same markers by day 16 of treatment (Ellero-Simatos *et al.*, 2012). Similar effects have been reported with doses of 7.5mg, which is also a commonly prescribed dose (van Raalte *et al.*, 2011).

Glucocorticoid	Equivalent dose (mg)	Potency	HPA suppression	Plasma half-life (min)
Short-acting				
Cortisol	20.0	1	1.0	90
Cortisone	25.0	0.8		80-118
Intermediate-acting				
Prednisone	5.0	4.0	4.0	60
Prednisolone	5.0	5.0		115-200
Triamcinolone	4.0	5.0	4.0	30
Methylprednisolone	4.0	5.0	4.0	180
Long-acting				
Dexamethasone	0.75	30	17	200
Betamethasone	0.6	25-40		300

Table 1 Relative dose, potency, HPA suppression and plasma half-life of a selection of endogenous and synthetic glucocorticoids.

Table adapted from Nicolaides et al., 2018 and based from Chrousos, 2005; Stewart and Newell-Price, 2016.

Daily oral Dex treatment over 5 days for paediatric acute lymphoblastic leukaemia, induced raised fasting HDL, LDL, cholesterol, TG, glucose and insulin levels. Glucose was also found to be raised between treatments, even after Dex should have been metabolised and cleared from the patients' systems. Authors used a homeostasis model assessment of insulin resistance and observed increases from 8% to 85% post Dex treatment ('Global IDF/ISPAD Guideline for diabetes in childhood', 2011; Warris *et al.*, 2016). This could be due to inhibition of insulin binding of its complementary receptor which has been observed to be dose dependent, as well as oxidative and non-oxidative glucose disposal (Olefsky *et al.*, 1975; Tappy *et al.*, 1994; van Raalte *et al.*, 2011; Petersons *et al.*, 2013; Pasieka *et al.*, 2016). There are also indications that Dex could directly regulate adipocyte growth. Dex induced reporter gene activity and transcription of VLDLR in adipocyte 3T3-L1 cells via indirect GR regulation. Alterations in transcription could have distinct metabolic affects as increased VLDL expression has been shown to induce differentiation in adipocyte like cells, and VLDL receptor deficient mice have less adipocyte tissue (Ensler *et al.*, 2002).

There is also evidence of ligand specific GR regulation. A recent study in the 3617 MMTV array containing cell line reported a greater proportion of repressed genes with Dex treatment than with

corticosterone treatment (Stavreva *et al.*, 2015). Specific ligand dependent effects on transcription and co-regulator recruitment have also been described for the GC regulated targets GILZ, SLC19A2 and thrombomodulin within A549 cells (Monczor *et al.*, 2019). This data highlights the potential importance of considering which GC ligand is used in experiments for molecular research, especially those related to dynamic GR mediated action, but even more importantly the clinical implications for GC replacement therapy.

1.4 Next generation sequencing technology

1.4.1 Chromatin immunoprecipitation assay next generation sequencing analysis

The ability to identify multiple transcription factor interactions across the genome as well as *de novo* sites represents a highly powerful tool within molecular research and has been available since the turn of the century via utilisation of chromatin immunoprecipitation (ChIP) assays followed by DNA hybridization to a microarray (ChIP-ChIP). However, high density tiling arrays are costly, have a low resolution of local enrichment due to a high minimal fragment size (200b) and are limited by microarray probe capacity (Ren *et al.*, 2000; Iyer *et al.*, 2001).

The next breakthrough in genome mapping came in the form of next generation sequencing (Seq) in 2007 (Johnson *et al.*, 2007; Robertson *et al.*, 2007). Isolated genomic fragments are amplified, aligned to a reference genome and resulting tag profiles computationally modelled into areas of enrichment, the peaks of which associated with protein to DNA points of interaction and height relative to the degree of enrichment. Seq is not restricted by the probe capacity as in ChIP-ChIP but able to process hundreds of millions of fragments in a single run and load smaller DNA concentrations (10-100 ng compared to 2 µg for ChIP-ChIP) and fragment size (~35 b) (Harris *et al.*, 2008). Thus, enhancing spatial resolution of localised protein targets, as is particularly important whilst profiling histone variants, post-translational modification of chromatin, lineage determinant factors and nucleosome positioning (Yuan *et al.*, 2005; Bernstein *et al.*, 2006; Barski *et al.*, 2007; ENCODE Project Consortium, 2007; Lee *et al.*, 2007; Mikkelsen *et al.*, 2007). For these reasons Seq of ChIP'd DNA has been applied to a wide range of transcription factors, histone modifiers and chromatin remodelling complexes in a variety of tissues and organisms (Johnson *et al.*, 2007; Mikkelsen *et al.*, 2007; Visel *et al.*, 2009).

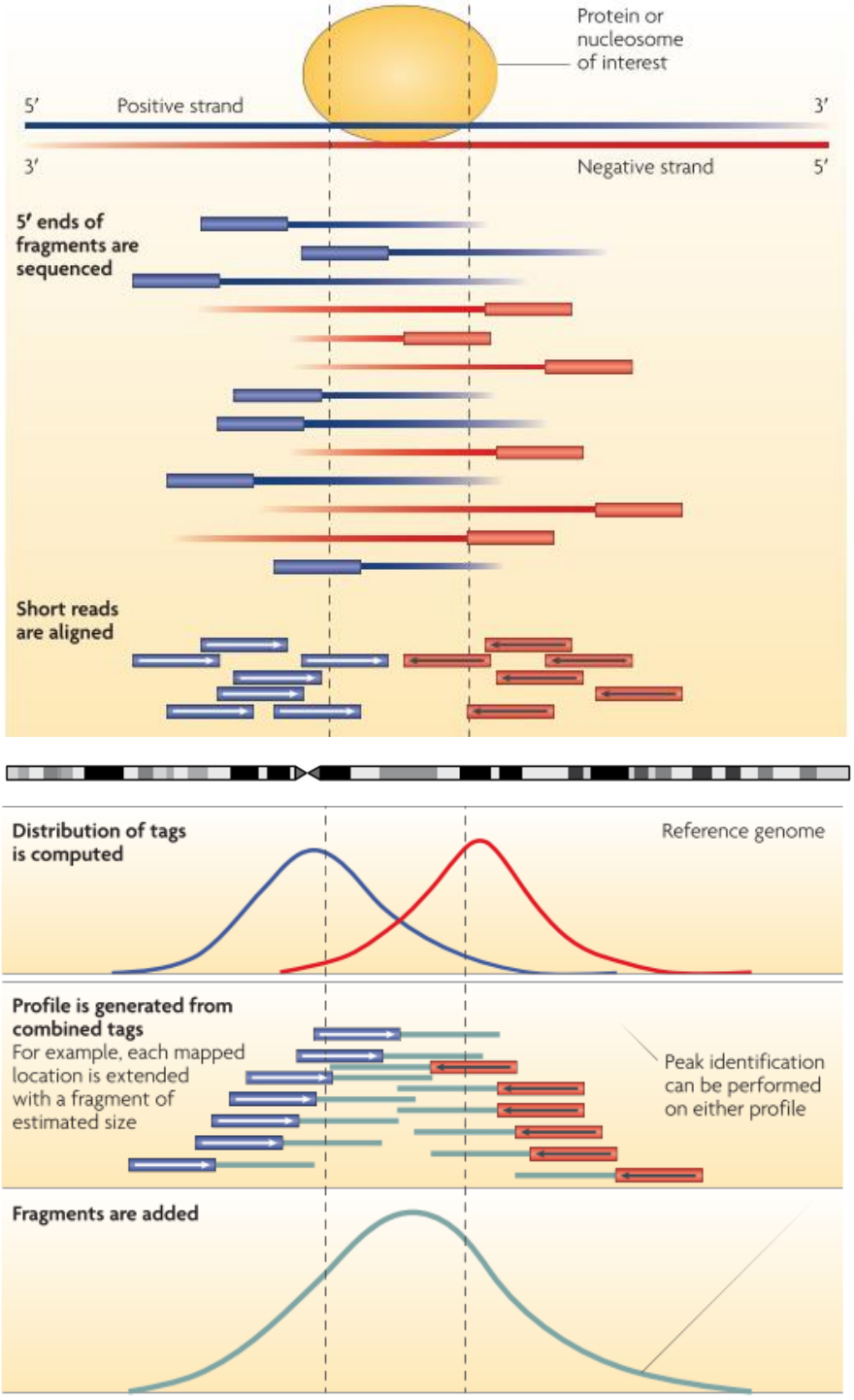

Figure 1.11 Schematic of next generation sequencing methodology.

Genomic DNA is fragmented, sequences bound to proteins of interest are targeted by antibodies and isolated by ChIP assay. Fragments are amplified, 5' end sequenced and aligned to a reference genome and localised tag densities genome wide are computationally analysed to a single peak of enrichments via modelling of forward and reverse fragment densities. Peak zenith denotes localised protein-DNA interaction within a normally binomial distribution of tags. Figure adapted from Park, 2009.

Seq produces large data sets requiring powerful analytical packages to identify significant enrichment regions across the genome. A range of algorithms have been written to identify enriched regions within Seq data. General algorithms include F-Seq and Hotspot (the only algorithms specifically designed to analyse DNase I footprinting data), ZINBA (general peak caller), MACS2 (a model based ChIP-Seq analysis approach) and HOMER (Boyle *et al.*, 2008; Y. Zhang *et al.*, 2008; Park, 2009; Rashid *et al.*, 2011; Baek, Sung and Hager, 2012; Feng *et al.*, 2012; Yang *et al.*, 2014; Heinz *et al.*, 2015).

Briefly, F-Seq measures parametric sequence tag density via implementation and estimated localised tag sequence centre in a smooth Gaussian kernel density estimation (Boyle *et al.*, 2008). This proposedly overcomes histogram bin-boundary interference and introduction of error. This technique is noted for long run time during statistical testing (W. Zhang *et al.*, 2012).

Hotspot identifies regions of enrichment above background and will adjust significance based upon a false discovery rate measured from randomly selected Seq sequences. Therefore, Hotspot is regarded as the only program to apply statistical significance to DNase I hypersensitive site (DHS) peaks (Madrigal and Krajewski, 2012). Hotspot has been widely used by the ENCODE consortium and the latest version implements a “second pass” detection to select relatively small enrichment masked signal bias by areas of enrichment from other localised targets (Baek, Sung and Hager, 2012).

ZINBA identifies genomic regions as background, enriched or zero-inflated using a mixture of regression models without the need for input control. Detected enriched regions within a defined distance are applied to a shape-detection algorithm for sharp signal discovery within broad regions of enrichment. The analysis can also be modified to take into account modelled covariate information (C/G content etc.) to improve low signal-to-noise ratio or complex analysis (Rashid *et al.*, 2011).

HOMER (Hypergeometric Optimization of Motif EnRichment) is a suite of tools designed for *de novo* and known motif discovery, however, a ChIP-Seq enrichment analysis tool is also included. findPeaks identifies enriched clusters of Seq tags across the genome, filtering significant clusters by estimation of a tag threshold according to a Poisson distribution and estimated false discovery rate (FDR). Clusters are then identified as significant based on local and clonal signals within the Seq data as well as fold change to input or IgG control Seq data (Heinz *et al.*, 2010).

MACS empirically models shift size enrichment of sequence reads compared to a background using a poisson distribution model (Pepke, Wold and Mortazavi, 2009; Kim *et al.*, 2011; Rye, Sætrom and Drabløs, 2011).

Koohy, H. et al. reported Hotspot and MACS to be comparatively successful in identifying regions of DHS in DNase-Seq paradigm experimental results but F-seq peak sensitivity was greatest and ZINBA scored the lowest (Koohy *et al.*, 2014).

1.4.2 Motif discovery

Genomic DNA contains short (5 to 20b) biologically significant repeated sequences termed DNA motifs. Transcription factors such as GR bind to GREs within promoter and enhancer sequences of associated targets regulating transcription, and these GREs often have well characterised DNA motifs. Therefore identification of these specific motifs in the ChIP-Seq dataset can provide integral information about binding regulation in a genomic landscape (Rombauts *et al.*, 1999; Das *et al.*, 2007).

Motif analysis detects over represented and conserved motifs from orthologous sequences as a representation of the most likely transcription factor interacting candidates (Das *et al.*, 2007). There are two main types of motif analysis. A word-based (string-based) algorithm enumerates and compares oligonucleotide frequencies, restricting analysis to detect identical short motifs and is used almost exclusively for eukaryotic genomic and optimised data structures (van Helden, André and Collado-Vides, 1998; Sagot, 2009). As transcription factor motif sequences often have longer, weakly constrained positions, these parameters restrict its ability to be applied to prokaryotic genomes and motifs of relatively low fidelity (Vilo *et al.*, 2000). In these instances, a probabilistic sequence model is preferred. Model estimations use a maximum-likelihood principle or Bayesian inference, presenting data in a position weight matrix, where by letter height within a stack of predicted bases is proportional to the occurrence within over represented regions (Hertz, Hartzell and Stormo, 1990). This technique can be particularly sensitive detecting small changes and naturally biologically variable data (Bucher, 1990).

1.5 Research question

Classically, GR interactions are studied within, 'promoter' regions in close proximity to the TSS of regulated genes. Long distance interactions via looping and the functionality of TAD domains, however, are becomingly increasingly recognised for their fundamental biological role, particularly as functional circadian regulated TAD domains have been identified within the mouse liver (Aguilar-Arnal *et al.*, 2013; Zhao *et al.*, 2015; Kim *et al.*, 2018).

These interactions are further complicated by synergistic, GR dependent transcriptional regulation which was first identified for the gene *TAT* and have continued to be documented (Jantzen *et al.*, 1987). Additionally, GR interactions with STAT3, STAT5 and NFκB have been shown to be either transactivatory or transinhibitory; potentially decided by which factor is directly interacting with the

regulatory element within a tethered model of transcriptional control (Stoecklin *et al.*, 1997; Zhang *et al.*, 1997; Aittomäki *et al.*, 2000; Engblom *et al.*, 2007; Langlais *et al.*, 2012). Highlighting the importance of *de novo* identification of GR binding events as well as sequence analysis to identify potential co-regulator response elements.

As cells have multiple intrinsic post-transcriptional mechanisms regulating mRNA and protein production and degradation, as well as the time required for maturity of nascent RNA and translation of proteins, analysis of RNA and protein levels can mislead identification of directly regulated genes. To avoid false negative or false positive results from non-transcription dependent regulation, analysis of both GR binding and RNA Pol2 activity at the level of the genome is paramount to observe direct and indirect transcription factor mediated effects. Therefore, ChIP-ChIP, RT-qPCR and RNA-Seq analysis is not optimal for this investigative paradigm. Currently, the degree of sensitivity required to address and expand basic understanding of direct transcriptional regulation on a genomic scale is only achievable via ChIP-Seq methods.

This has relevance for ultradian dynamics, as oscillations in circulating GCs can range from hourly within the rat to every three hours in the human (Follenius *et al.*, 1987; Veldhuis *et al.*, 1989; Jasper and Engeland, 1991). As these dynamics are so well conserved across mammalian species, it can be postulated oscillations mediate distinct and important regulatory function (Holaday, Martinez and Natelson, 1977; Benton and Yates, 1990; Engler *et al.*, 1990; Carnes *et al.*, 1992; Loudon *et al.*, 1994; Cudd *et al.*, 1995; Windle, Wood, Shanks, *et al.*, 1998; Russell *et al.*, 2010). Particularly as evidence has been published that maximal stress induced circulating corticosterone levels, as well as aggression, can be altered dependent on the phase of the GC pulse the stressor is applied (J Haller *et al.*, 2000; J. Haller *et al.*, 2000; Sarabdjitsingh *et al.*, 2010). It can be postulated, the advantages of an oscillating system is the ability to carry more information for cellular signalling mechanisms than a static profile (Walker, Terry and Lightman, 2010; Walker *et al.*, 2012; Lightman, 2016; Oster *et al.*, 2016).

23% of the united states population were quoted as presenting MetS phenotypes, however, most research highlighting the implications of dysregulated GC rhythms for both cognitive and physiological aberrant metabolic function have focussed on circadian dysregulation. Cushings syndrome as well as chronic stress have been shown to induce raised circulating GC profiles, which effectively dysregulate both circadian and ultradian oscillatory profiles (Deuschle *et al.*, 1997; Nieman and Ilias, 2005; Newell-Price *et al.*, 2006). Despite the fact sGCs are mostly prescribed in a manner that best fits current understanding of endogenous hormone rhythms, patients still over-represent metabolic dysfunction, such as diabetes, compared to other medications (Varney, Alexander and MacIndoe, 1984; Wolkowitz,

1994; Filipsson *et al.*, 2006; Simmons *et al.*, 2012). Therefore, could abolition of ultradian GC oscillations induce these phenotypes, either directly or in a combination with other factors?

Currently, investigation of GR binding dynamics as well as RNA Pol2 activity has only been observed on a genome-wide scale in immortalised cell lines. Additionally, many studies use sGCs as ligand for GR, despite evidence of ligand dependent effects on transcription (Conway-Campbell *et al.*, 2007; Stavreva *et al.*, 2009, 2015; Monczor *et al.*, 2019). Therefore, investigation of corticosterone induced regulation in response to circulating ultradian oscillating levels and the potential repercussions of dysregulation, have distinct and important implications that could be fundamentally important to future circadian research as well as clinical intervention.

1.6 Hypothesis

The ultradian rhythm of the circulating glucocorticoid hormone corticosterone is integral to homeostatic processes, and controls regulation of target gene transcription. We hypothesise that disruption of the pulsatile corticosterone profile will result in dysregulation of GR binding and downstream transcriptional processes involved in regulating key metabolic target genes relevant to metabolic pathology.

1.7 Aims

1) Confirm cell culture evidence of differential regulation of GR binding in the liver during a pulsatile and constant corticosterone treatment, with an *in vivo* rodent model.
2) Characterise genome wide GR binding patterns and RNA polymerase II activity during pulsatile corticosterone infusion compared to a constant delivery.
3) Identify key differentially regulated metabolic gene targets involved in known metabolic syndrome.
4) Develop a chronic infusion model to investigate if the ultradian pulses of corticosterone that underlie the circadian profile alter metabolic responses.

Chapter 2 General methods

2.1 Surgery and husbandry

Adult male Sprague-Dawley rats (250-300g) (Harlan, Bicester, UK) were individually caged in soundproof rooms under standard conditions in 14:10 light/dark cycle (lights on at 05:00hr) with standard chow and water available *ad libitum*. All procedures were carried out in accordance with the UK Home Office animal welfare regulations.

Rats were anaesthetised with a combination of Isoflurane (100% w/w liquid vapour (Merial, UK)) and medical air during bilateral ADX, jugular vein or/ and carotid artery cannulation. The cannula (Smith Medicals, UK) was exteriorised via craniotomy or a vascular access button and attached to a spring and swivel system in individual cages (Figure 2.1). 1mg of Carprofen (Rimadyl, Pfizer, UK) was administered post-operatively for pain relief. 25µg Dex (Sigma, UK) and 2.5ml of glucose (5%)/ saline (0.9%) injected subcutaneously. Up to 5 days of post-surgical recovery was allocated, during which time 0.9% saline drinking water supplemented with 0.15 µg/L of corticosterone (Sigma, UK) was provided *ad libitum* to provide isotonic salt levels and maintenance of HPA axis homeostasis. 16 hours prior to experiment, corticosterone saline drinking water was replaced with saline drinking water to allow an adequate corticosterone washout period prior to the experiment. In some cases, telemetry probes were surgically implanted into the intraparietal space and secured via stitches to the intra-abdominal epidermal layer in intact or ADX rats. Movement and body temperature were recorded via transmitter/ radio receivers (PTD 4000 E-mitter, Starr Life Sciences Corp) placed under the rodent's cage and metal dividers between cages to reduce interference.

Implanted cannula would be 'flushed' daily via withdrawal of blood through the cannula to remove any clots that may have formed and replaced with fresh heparanised saline (1:100) to maintain patency.

2.2 Automated blood sampling

Total corticosterone blood serum samples were taken via an in-house automated blood sampling (ABS) system (Figure 2.1). Briefly, blood is withdrawn via the action of the bi-directional pump from the indwelling cannula towards the pump. Once the required volume has been withdrawn, the pump changes direction and the valve switch system changes the flow direction towards the ABS fraction head for collection. Once the desired volume of blood/ heparinised saline has been collected, the valve/ switch system changes the flow direction back towards the rat. Delivering sterile heparinised saline back into the rat, replacing withdrawn blood volume and maintaining cannula patency. Within this study, 40 µl blood samples were collected every 10 min in 160 µl Heparin: Saline solution (1:100).

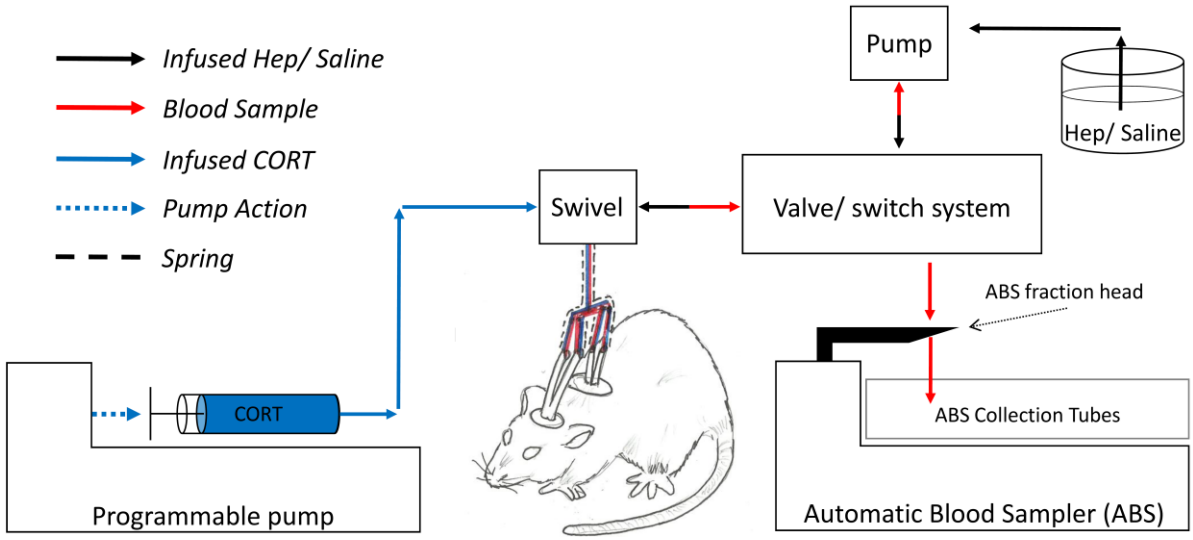

Figure 2.1. Schematic of programmable pump and automated blood sampling system.

Rats implanted with intravenous cannulae, exteriorised either via craniotomy, protected by dental cement "head cap" or a vascular access "button" over the shoulders. Cannulae were protected by spring and attached to a swivel allowing free movement. Programmable pump settings were pre-set to infuse corticosterone solution (blue) at the desired time and rate via intravenous cannula. ABS system withdraws blood (red) from the intravenous cannula through the swivel and valve/ switch system powered by a reversible pump. Once the required volume has been withdrawn, the pump is reversed, and the valves direct the flow to infuse the same volume of heparised saline solution (black) back through the intravenous cannula. The swivel has been designed to incorporate both programmable pump and ABS via two intravenous cannulae if required. Arrows denote direction of travel. Rat was kindly animated by Mr. Martin Flynn.

2.3 Infusion Profiles

To produce *in vivo* 'mock' ultradian pulses (referred to as pulsatile infusion) a programmable pump (PHD Ultra Syringe Pump, Harvard Apparatus, USA) was used to infuse corticosterone solution (solubilised 2-hydroxypropyl-β-cyclodextrin (HBC) complex carrier (Sigma, UK) in 0.9% saline solution) through the jugular vein at a dose of 3.84 µM. Each pulsatile period began with a 20 min infusion at a rate of 1 ml per hour and paused for 40 min and repeated hourly for 3hrs (Figure 2.2). A sustained corticosterone-HBC saline solution (referred to as constant infusion) was infused at a reduced rate of 0.33 ml per hour to match pulsatile corticosterone dose delivered per hour. The constant corticosterone infusion was modified to include an initial increased rate of 1 ml per hour for 10 min before returning to 0.33 ml per hour for the duration of the experiment to ensure no gaps within infusion solution had appeared since charging of cannula and infusion lines. Matched dose was confirmed by area under the curve analysis for both profiles (Figure 2.2).

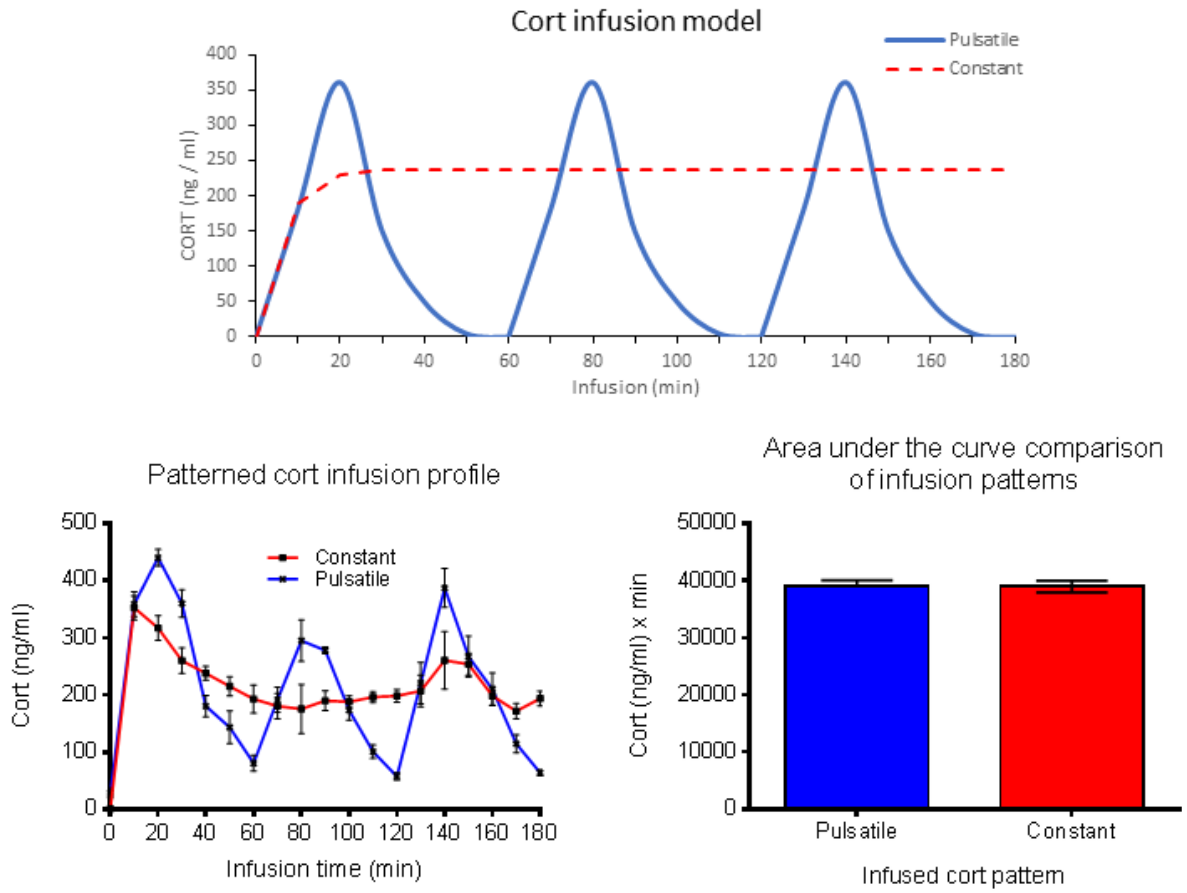

Figure 2.2 Schematic and circulating total blood serum corticosterone levels after pulsatile and constant corticosterone infusions within freely roaming rats.

(A) Pulsatile corticosterone (3.84 µM dose) was infused for 20 min at a rate of 1 ml per hour and paused for 40 min to generate the pulse peak and nadir (blue). A constant infusion of corticosterone was dose matched via reduction of the infusion rate to 0.33ml/hr over 60min (red). The constant infusion profile included an increased infusion rate between 0-10min at 1ml/hr before returning to 0.33ml/hr for the duration of the experiment. Both patterns were repeated for three hours. (B) To confirm infusion model, 10min blood samples from the carotid artery were collected via the ABS over the three-hour corticosterone infusion period. Pulsatile corticosterone infusion total blood serum levels peak at 20, 80 and 140min (374ng/ml ±83), corresponding with the end of hourly 20min corticosterone infusions. corticosterone levels reduced to 68ng/ml ±20 within 40min of each pump cessation. The preliminary increased constant corticosterone infusion rate promotes maximal corticosterone levels at 10min (353ng/ml ±42) before reducing and flattening to 201ng/ml ±51 over a 60-120min period. Between 140-180min corticosterone levels appear to fluctuate between 180-240ng/ml. In response to a pulsatile corticosterone infusion, corticosterone levels were 387ng ±34 and 64ng/ml ±5 at 140min and 180min. Whilst constant infusion induced circulating corticosterone levels

of 261ng/ml ±51 and 194ng/ml ±13. (C) Area under the curve analysis confirmed no difference in circulating total corticosterone between pulsatile and constant corticosterone infusions over the experimental period. Total blood serum corticosterone levels were measured by RIA trunk blood samples. Pulsatile AUC mean= 39,087(ng/ml) x min ±1,025 s.e.m. and constant AUC mean= 38969(ng/ml) x min ±1,007 s.e.m..

A pulsatile HBC complex dissolved in saline solution was used as matched vehicle control infusion (VEH) where indicated. Euthanasia time points corresponded to the third corticosterone pulse zenith and nadir at 140min and 180min infused timepoints respectively. Trunk blood samples were collected for each rat at the point of euthanasia with 40 µl of 0.5M ethylenediaminetetraacetic acid (EDTA) and total blood serum corticosterone levels assessed by radioimmunoassay (RIA).

2.4 Tissue Collection

Liver was dissected and 0.4g was fixed in 1% (v/v) formaldehyde (Sigma, UK), phosphate buffered saline (PBS) (1.37 M NaCl, 2.68 mM KCl, 10.14 mM Na_2HPO_4, pH 7.4) solution for 10 min at room temperature (RT). Formaldehyde cross-linking was quenched with addition of Glycine (final conc. 125 mM) for 5 min and washed three times in ice cold PBS supplemented with 2 mM NaF, 0.2 mM Na Orthovanadate and 1X Complete protease inhibitor (Roche Diagnostics). Fixed liver was stored at -80°C in 0.2g samples in 500 µl of S1 Buffer (10 mM HEPES, pH 7.9, 10 mM KCl, 15 mM $MgCl_2$, 0.1 mM (EDTA), pH 8) supplemented with 0.5 mM Dithiothreitol and 2 mM NaF, 0.2 mM Na Orthovanadate and Complete protease inhibitor.

2.5 Corticosterone radioimmunoassay (RIA)

Plasma was separated from whole blood by centrifugation at 4000 rpm, 4°C. Samples were diluted 1 in 50 with citrate buffer, processed in triplicate and incubated overnight in 50 µl of ^{125}I corticosterone tracer (Oxford BioInnovation DSL Ltd, Oxford, UK) and 50 µl of rabbit anti-rat corticosterone antibody (kindly donated by G. Makara, Hungary). Free/bound separation was performed using charcoal dextran precipitation, centrifuged at 4000 rpm, 4°C and the solution aspirated before the ^{125}I corticosterone tracer in the resulting pellets was read using a gamma counter (Wizard-2470, Perkin Elmer, MA) (Atkinson *et al.*, 2006; Waite *et al.*, 2012). Concentrations of corticosterone in each plasma sample were interpolated from a standard curve. Intra- and inter-assay coefficient of variation of this in house corticosterone assay have been established as 16.65% and 13.30%, respectively (Conway-Campbell *et al.*, 2007).

2.6 Chromatin Fragmentation

Samples were thawed slowly on ice and adjusted to a final volume of 1ml/sample with supplemented S1 buffer, then homogenised on ice using a Dounce homogeniser. The resulting lysate was centrifuged at 4000 rpm at 4°C to collect a crude nuclear pellet, which was then lysed in sodium dodecyl sulphate (SDS) lysis buffer (2% SDS, 10 mM EDTA, 50 mM Tris-HCl (pH8.1) supplemented with NaF and Na orthovanadate and 1X Complete Protease Inhibitor). Chromatin was sonicated using a Branson Sonifier 450 (Branson Ultrasonics, Danbury, CT, USA) to 300-500 bp fragments with multiple 10-sec bursts at 10% output and centrifuged at 13,000 rpm at 4°C to remove cellular debris from the chromatin suspension. Sheared chromatin was stored at -80°C.

2.7 ChIP assay

ChIP buffers were prepared in house, as described in the EZ ChIP kit protocol (Upstate Biotechnology, Lake Placid, NY, USA) with some modifications for use with animal tissue (as described where relevant). Sheared chromatin was removed from -80°C storage and thawed slowly on ice, diluted to desired input concentration in a final volume of 100 µl of SDS lysis buffer, then made up to a final volume of 1 ml with ChIP dilution buffer (0.01% SDS, 1.1% Triton X-100, 1.2 mM EDTA, 16.7 mM Tris-HCl pH8.1, 167 mM NaCl). For the ChIP assay, each input consisted of 50µg of sheared chromatin and individual inputs from each sample were immunoprecipitated against either a GR cocktail (2µg of PA1-510A, 4µl of PA1511A (Thermo Fisher, USA)) (4µg of M-20X sc-1004X (Santa Cruz, USA)) or the serine 2 phosphorylated RNA Pol2 complex (pSer2 Pol2) (2µl ab5095 (Abcam, UK)). Rabbit IgG antibodies were used as negative control (2µg of sc-2027 (Santa Cruz, USA)). All antibodies were incubated overnight at 4°C overnight then incubated with protein A Dynabeads for 4 hours (Sigma-Aldrich, UK). To reduce non-specific binding, the DNA-Antibody-Dynabead slurries were sequentially washed with 150 mM salt buffer (0.1% SDS, 1% Triton X-100, 2 mM EDTA, 20 mM Tris-HCl pH8.1), 500 mM salt buffer (0.1% SDS, 1% Triton X-100, 2 mM EDTA, 20 mM Tris-HCl pH8.1), LiCl buffer (0.25 M LiCl, 1% IGEPAL-CA630, 1% deoxycholic acid sodium salt, 1 mM EDTA, 10 mM Tris-HCl pH8.1) and twice in TE buffer (10 mM Tris-HCl, 1 mM EDTA) (pH 8.0). Complexes were eluted from the Dynabeads in 1% SDS 100 mM NaHCO3. NaCl was added (300mM final concentration) and crosslinks reversed overnight at 65°C in. RNA was removed using RNase treatment (Roche Diagnostics), then protein was digested using proteinase K (Ambion, Huntington, UK) after adjusting each solution with EDTA (1 mM final) and Tris-HCl (4 mM final). DNA was then extracted using 25:24:1 phenol-chloroform-isoamyl alcohol (Sigma, UK) followed by 24:1 chloroform-isoamyl alcohol (Sigma, UK). DNA in the aqueous phase was then precipitated overnight at -20°C with the addition of 2.5 VOL 100% ethanol and 20 µg glycogen (Sigma-Aldrich, UK) before the resulting ChIP DNA was pelleted by centrifugation at 13,000 rpm, 4°C

and washed in 70% Ethanol (13,000 rpm, 4°C), then air dried and suspended in 40 µl nuclease free water (Ambion, Huntington, UK).

2.8 Quantitative Real- Time Polymerase Chain Reaction (RT-qPCR)

Quantitative real-time polymerase chain reaction (RT-qPCR) was used to analyse relative quantities of immunoprecipitated DNA in each ChIP sample at specific sites in and near target genes of interest (Table 1). Primers were designed using the NCBI Primer Design Tool (www.ncbi.nlm.nih.gov/tools/primer-blast/) to selected target regions, as indicated in Table 2. Each reaction was performed in a final volume of 25 µl, with 0.5 µl of template DNA, forward and reverse primers (0.3 mM final concentration) and Fast SYBR Green (Applied Biosystems, Life Technologies, UK) reaction buffer depending on individual assay requirements. Assays were performed on a StepOnePlus™ PCR machine (Applied Biosystems, Life Technologies, UK) using 0.1 ml fast optical 96-well reaction plates (Applied Biosystems, Life Technologies, UK).

Gene of interest	Forward primer sequence	Reverse primer sequence
rn6 Per1 (Intron 16)	CCCGGGTCTTCCTCTGGGCA	CCTGTCCAACGGCCAAGGCC
rn6 Per1 Distal GRE -2500bp from TSS	CCAAGGCTGAGTGCATGTC	GCGGCCAGCGCACTA

Table 2. RT-qPCR primer sequences.

Primer sequences used to test GR and RNA Polymerase II, phospho-Serine 2 binding.

2.9 Infused circulating corticosterone levels of sequenced samples

Total blood serum corticosterone levels from trunk blood samples collected at the point of euthanasia were used to assess circulating corticosterone dynamics in response to either infusion pattern and/ or time point by RIA. Data were assessed using two-way ANOVA followed by Bonferroni's multiple comparisons test adjusted for multiple comparisons. Significant relationships were found in response to infusion pattern, time and interaction ($p<0.0001$). In response to a pulsatile infusion of corticosterone at 140min (pulsatile peak) total blood serum corticosterone levels were raised (670 ±41 ng/ml) to 180min (pulsatile nadir) (64 ±17 ng/ml) ($p<0.0001$). Similarly, 140min and 180min of constant corticosterone infusion produced raised levels of circulating corticosterone compared to pulsatile 180min (625 ±38 ng/ml and 461 ±21 ng/ml respectively) ($p<0.0001$). Pulsatile 180min was unchanged to VEH controls indicating corticosterone levels clear from total blood serum within 40min of corticosterone infusion cessation. There was no difference between pulsatile and constant infusion at 140min, however, there was a reduction in corticosterone by 180min of constant infusion ($p<0.01$). It should be noted that corticosterone level inconsistency from trunk blood samples has been reported

in previous studies (data not shown) likely due to the crude method of collection. Trunk blood sample volumes are not measured whereas ABS samples are accurately diluted 1:5 in heparinized saline, hence ABS data collection is the preferred method modelling circulatory blood total corticosterone dynamics. Nevertheless, trunk blood results are appropriate for confirming opposing infusion pattern paradigms at the point of euthanasia. These data do confirm total blood serum corticosterone levels are increased to VEH in response to 20min and constant corticosterone infusion whereas 40min infusion cessation is appropriate to allow levels to return to VEH control. Thus, producing either a pulsatile or constant corticosterone pattern within the cardiovascular system albeit with indications of fluctuating constant corticosterone infused levels. All bar graphs were plotted using GraphPad Prism v6.07 for Windows (La Jolla California, USA, www.graphpad.com).

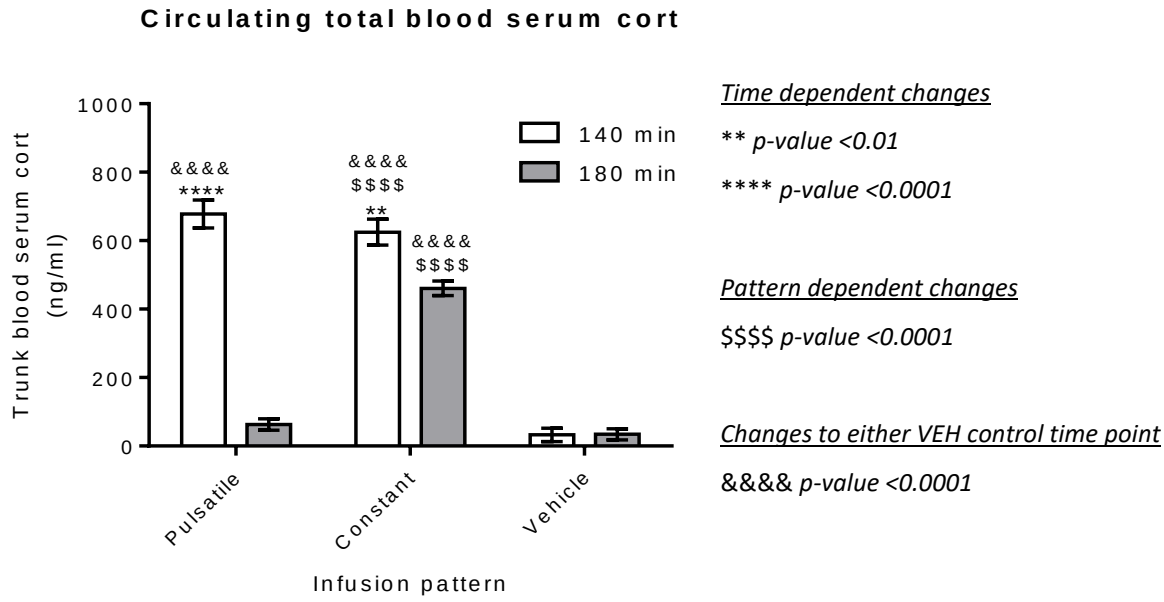

Figure 2.3 Circulating total blood serum corticosterone levels of corticosterone or VEH infused sequenced ChIP samples at the point of euthanasia by RIA.

In response to a third 20min infusion of corticosterone at 140min, circulating corticosterone levels were significantly higher than VEH control (p<0.0001) before significantly dropping after 40min pump cessation (p<0.0001) returning to baseline by 180min. In response to a constant corticosterone infusion, levels were raised at both 140 and 180min to VEH control (p<0.0001). There was a slight but significant reduction from constantly corticosterone infused levels at 140min to 180min by ~150ng/ml (p<0.01) indicating the possibility that corticosterone levels can fluctuate between time points. corticosterone levels after 180min constant corticosterone infusion were also reduced to pulsatile 140min by ~200ng/ml (p<0.05) whereas no difference was detected at 140min constant corticosterone infusion. Changes in corticosterone levels are replicable to ABS data previously

*described. Total blood serum corticosterone levels were measured by RIA from trunk blood samples and analysed by two-way ANOVA with Bonferroni's test adjusted for multiple comparisons. Results after 140min infusion are indicated by white bars whereas 180min by grey bars and data is expressed as mean ±s.e.m.. Pulsatile or constant corticosterone infusion time dependent p-value changes are indicated by **<0.01 and ****<0.0001, 140min and 180min infusion pattern dependent p-value changes are indicated by $$$$<0.0001 and corticosterone infused p-value changes to either VEH control infused time point are indicated by &&&&<0.0001.*

2.10 ChIP-Seq quality control and alignment

ChIP-Seq technical replicates for each corticosterone infusion pattern time point consisted of n=6 biological ChIP repeats, bolstered to n=10 with technical repeats where required in line with the 3Rs guidelines. Biological and technical repeat ChIP samples were selected around the mean based on pSer2Pol2 ChIP assay results to two sites associated with the transcriptionally GR regulated clock gene *Per1* (Figure 3.1 & Figure 4.1). 10 ChIP samples were pooled and concentrated using a UniVapo Vacuum concentrator (Transcriptomics facility, UOB) from approximately 400 µl to 35 µl. Samples were shipped to the National Institute of Health (NIH), Intramural Sequencing Centre (NISC) (Bethesda, MD) on dry ice. Two pooled replicate ChIPs and matched 1% input samples per group underwent library preparation (TrueSeq SBS v3-HS kit (illumina, US)) and sequencing using the Illumina HiSeq2000 platform (Illumina, USA) to 50b at the National Cancer Institute Advanced Technology Center (ATC, Rockville, MD, USA).

Adapters were removed from the sequenced FASTQ files, filtered for a base quality of 33 and sequences of 50b were isolated using Trimmomatic-0.36 (Bolger, Lohse and Usadel, 2014). Trimmed FASTQ files were aligned to the rat genome (UCSC rn6 assembly) using bowtie2 (Langmead and Salzberg, 2012) and duplicate tags removed using SAMtools 1.3.1 (Li *et al.*, 2009). Subsequent analysis was performed using HOMER v4.9 (Heinz *et al.*, 2010).

Counts were normalised to 10 million tags (makeTagDirectory) to allow for cross sample comparisons and visualised using the UCSC genome browser (Kent *et al.*, 2002) (http://genome.ucsc.edu/).

2.11 Identification of GR ChIP-Seq enriched regions

Enrichment of GR tags to 1% input control, were identified (findPeaks) using relaxed settings (-F1 -L1 -P.1 -LP.01 -poisson .1 -style factor). Replicate concordance was assessed using an irreproducible discovery rate (IDR v2.0.3) set to 0.01. Overlapping enrichments between replicates were merged using mergePeaks (HOMER v4.9.1) and filtered according to the IDR estimated confidence threshold. Overlapping confident enrichment regions were merged again (mergePeaks) to create a single list of

enriched GR locations across conditions (Heinz *et al.*, 2015). Visualisation of tag densities, histograms plots and Pearson correlation coefficient calculations were done using EASeq v1.101 (Lerdrup *et al.*, 2016)

2.12 Analysis of differential enrichments

Analyses of pSer2 Pol2 ChIP-Seq enrichment was restricted to genes larger than twice the fragment length (>320b) and transcript coding regions limited to 10Kb from the transcriptional start site (TSS) (Ensemble release Rnor_6.0.92). Raw input ChIP-Seq tag counts were subtracted from both GR and pSer2 Pol enrichment regions (annotatePeaks.pl – HOMER v4.9.1).

Differential GR and pSer2 Pol2 enrichment fold changes were assessed to VEH and between corticosterone infusion time points using getDiffExpression.pl (HOMER v4.9.1) that pipes to DESeq2 (Heinz *et al.*, 2010; Love, Huber and Anders, 2014). For DESeq2 analysis, tags were normalised to tag count within *de novo* binding regions whilst pSer2 Pol2 tag counts were normalised to total sequenced tags across replicates. Differential GR and pSer2 Pol2 enrichments were considered significantly different if fold change >1.5-fold and p-value <0.05 adjusted for multiple measurements and FDR <0.05. Duplicate variant gene Ensemble accession numbers were filtered for the variant reporting the greatest fold change across all conditions and time points. Differential GR enrichments were annotated to the closest pSer2 Pol2 differentially regulated TSS. Fold changes were visualised using heatmap.2 (RStudio 1.0.153).

Distances between TSSs and GR binding regions were assessed using annotatePeaks.pl.

2.13 Motif analysis

Twice the average fragment length (446b) across the centre of GR binding sites were analysed for both *de novo* and known motifs using findMotifsGenome.pl (HOMER v4.9.1). Repeat sequences were masked and optimised for motifs 8, 10 and 12b long. Calculations of motifs per base pair per peaks were calculated using de novo motif matrices within HOMER v4.9.1 and histograms indicate location of the motif relative to the GR binding site centre and plotted using GraphPad Prism v6.07 for Windows (La Jolla California, USA, www.graphpad.com).

nGRE motif sequences were based on published inverted repeat sequences located in the upstream promoter of both the human and mouse thymic stromal lymphopoietin TSS. Motif files were created using seq2profile.pl (HOMER v4.9.1) based in the published sequence $CTCCN_{(0\text{-}2)}GGAGA$ (Surjit *et al.*, 2011; Heinz *et al.*, 2015)

2.14 Pathway analysis

pSer2 Pol2 ChIP-Seq DESeq2 data were analysed via Ingenuity Pathway Analysis ©IPA (Qiagen Inc., https://www.qiagenbioinformatics.com/products/igenuity-pathway-analysis). Enrichment of pathways were identified from genes with fold changes >1.5-fold and adjusted p-value <0.05 to VEH control and z-score predictions assessed from liver tissue and HepG3, hepatoma, hepatocyte cell lines as well as mice, rat and human published data. Positive and negative z-scores represent either predicted activation or inhibition respectively based upon the fraction of genes known to regulate the pathway and degree of fold change and significance. The greater the predictive confidence, the greater the z-score. Documentation indicates a z-score >2 (or <-2) represents a significant prediction. Z-score values were plotted using GraphPad Prism v6.07 for Windows (La Jolla California, USA, www.graphpad.com).

Chapter 3 Genome wide binding of the glucocorticoid receptor in the liver during ultradian or constant corticosterone replacement in ADX rats.

3.1 Background

The GR is a member of the nuclear receptor superfamily and is a transcription factor with ligand dependent activity ('A Unified Nomenclature System for the Nuclear receptor superfamily', 1999; Bledsoe *et al.*, 2002). The adrenal GC hormone is the endogenous ligand for the GR, which upon activation will translocate into the nucleus, where it can bind to GREs, recruit co-factors and regulate transcription of target genes (Meijsing *et al.*, 2007; Oakley and Cidlowski, 2013; Ratman *et al.*, 2013).

Adrenal GC secretion is under HPA axis control and is conserved across mammalian species. Synchronised to the photoperiod, the SCN regulates HPA axis activity which in turn induces maximal GC secretion from the adrenal glands into the circulatory system prior to the active period and gradually decreasing towards the onset of the inactive period. Thus, a 'circadian' profile of GC release is produced and due to the lipophilic molecular structure, GCs will readily diffuse across into nearly all cells within the body. Oscillations in circulating levels have also been recorded in the hippocampus and subcutaneous tissue within the rat (Jasper and Engeland, 1991; Droste *et al.*, 2008, 2009; Qian *et al.*, 2012). However, studies with more frequent blood sampling have shown an underlying oscillating rhythm of GC pulses, termed the 'ultradian' profile (Windle, Wood, Shanks, *et al.*, 1998; Lightman and Conway-Campbell, 2010). Recent studies have shown that intrinsic delays within both the positive feed forward and negative feedback arms of the HPA axis naturally produce oscillations in GC secretion, which result in discrete pulses measured in circulating blood serum and some tissues (Droste *et al.*, 2008; Walker, Terry and Lightman, 2010; Qian *et al.*, 2012; Walker *et al.*, 2012). It is the amplitude of these pulses that is under circadian control.

The predominant GC in rodents is corticosterone whereas cortisol is predominant in humans. This has implications for the ultradian pulse frequency as corticosterone has a shorter half-life than cortisol, at 8-9min and 62-97min respectively (Weitzman, 1976; Veldhuis *et al.*, 1989; Windle, Wood, Lightman, *et al.*, 1998). Presumably, the differing half-lives contribute to a different pulse frequency, as corticosterone pulses occur at intervals of 56-60min whereas cortisol pulses in humans occur at intervals of 95-180min (Follenius *et al.*, 1987; Veldhuis *et al.*, 1989; Jasper and Engeland, 1991).

Genome wide ChIP-Seq investigation of GR binding in mouse liver found ~11,000-13,000 binding sites in response to Dex treatment and a comparative analysis to other cell types indicated 83% of the

binding sites were tissue specific (Grøntved *et al.*, 2013; Lim *et al.*, 2015). This was associated with a change in RNA Pol2 occupancy at ~400 genes, indicating significant transcriptional change, presumably in response to Dex induced GR binding (Grøntved *et al.*, 2013).

Recent studies modelling ultradian corticosterone replacement within the rat, have indicated the GR binds at characterised GREs known to regulate the GC target gene *Per1*, in the liver and hippocampus during the rise (maximal at the peak) of a corticosterone pulse before fully dissociating after corticosterone clearance from the circulation within 40min (Conway-Campbell *et al.*, 2010, 2012). This mock ultradian model of corticosterone replacement, synchronises binding and loss of GR from the DNA template, which can be repeated over a series of pulses, inducing pulsatile transcriptional occupancy as well as hnRNA production (Stavreva *et al.*, 2009; Conway-Campbell *et al.*, 2010, 2011; George *et al.*, 2017). Additionally, a genome wide GR ChIP-Seq study within derived murine mammary adenocarcinoma epithelial cells (3617) confirmed 'slow cycling' of GR binding, synchronised to the ultradian corticosterone rhythm at a large number of GC target sites which was markedly altered by constant corticosterone treatment (Stavreva *et al.*, 2015). Regardless of this very compelling data, the question remains whether similar genome wide regulation occurs in a more physiologically relevant cell type or tissue?

To date, *in vivo* investigation of GR binding dynamics during ultradian pulses have only been investigated at a small selection of target sites and genomic studies have utilised artificial constructs within cell lines. It is therefore not presently known whether ultradian GR recruitment occurs across all GR binding sites and if dynamics can be altered by dysregulated GC exposure *in vivo*, for example by constant corticosterone treatment. Within this chapter, I plan to assess genome-wide GR binding profiles in the liver in response to infused mock 'ultradian' pulses of corticosterone within ADX rats. These results will be used to confirm whether the observed *in vivo* pulsatile recruitment to the *Per1* hypersensitive GRE in hippocampal and liver tissue also occurs across all GR binding sites or whether it is selective to a subset. Further, it will be determined whether a constant corticosterone infusion disrupts any observed dynamics.

3.2 Hypothesis

Within the liver, GR recruitment to the DNA is differentially regulated in a pattern dependent manner by a pulsatile or constant corticosterone infusion into the circulation of ADX rats.

3.3 Aims

1. Identify GR recruitment at the peak and nadir of a mock 'ultradian' GC infused pulse.

2. Assess, if any, changes in recruitment dynamics in response to a matched constant GC infusion.
3. Characterise GR binding within the liver

3.4 Method

All methods of GR ChIP-Seq analysis were done according to general methods discussed within Chapter 2.

Briefly, FASTQ files were assessed and trimmed to desired settings using Trimmomatic-0.36 (Bolger, Lohse and Usadel, 2014) and aligned to the Rn6 genome using Bowtie2 (Langmead and Salzberg, 2012).

De novo GR binding sites were identified within each replicate against corresponding 1% input controls using findPeaks (HOMER v4.9.1) with relaxed settings (Heinz *et al.*, 2010). Confident and concordant GR enrichments across replicates were identified using an irreproducible discovery rate (IDR v2.0.3) analysis. All concordant binding regions were analysed and any that overlapped were merged into a single region by mergePeaks (HOMER v4.9.1) (Heinz *et al.*, 2010).

Tag density and distribution across GR binding regions were visualised using EASeq (Lerdrup *et al.*, 2016) and the UCSC genome browser (Kent *et al.*, 2002) (https://genome.ucsc.edu/).

Enriched sequenced tag densities at every *de novo* GR binding region in response to a corticosterone infused time point was assessed against pooled VEH controls as well as between corticosterone infused time points by DESeq2 analysis, normalised to total tag count within identified enriched regions. Comparisons were filtered for significance by a fold change >0.585 (log2) and p-value <0.05 adjusted for multiple measurements. All other results were assigned the value 0. Results were visualised using heatmap.2 (RStudio 1.0.153) and eulerr (Larsson *et al.*, 2019).

Overrepresented palindromic sequences, masked for repeating sequences, were identified within 446b region at the centre of corticosterone regulated GR binding sites using findMotifsGenome.pl (HOMER v4.9.1). Histograms indicate location of the motif relative to the centre.

All histograms were plotted using HOMER and GraphPad Prism v6.07 for Windows (La Jolla California, USA, www.graphpad.com) and are reported as mean ±s.e.m..

3.5 Results

3.5.1 ChIP assay validation

ChIP-Seq samples were aligned to the Rn6 genome and normalised to 10million tags for comparison and visualisation using the UCSC genome browser. Prior to Seq, single aliquots of each ChIP assay were analysed for GR binding at the known GC regulated target, the clock gene *Per1*. A GRE containing region, 2.5kb upstream of the TSS has previously been characterised as a GR binding site in liver as well as other cell and tissue types (Stavreva *et al.*, 2009; Conway-Campbell *et al.*, 2011; Reddy *et al.*, 2012). No GR binding, to our knowledge, has been described for an intragenic region between intron 16 and 17, therefore, primers were designed for both regions to respectively act as positive and negative controls for GR binding in RT-qPCR analysis.

In response to three hourly 20min pulses of corticosterone infusion, GR binding was assessed at the characterised GRE containing GR binding site, at time points corresponding to the peak (140min) and nadir (180min) of the third pulse of the pulsatile corticosterone infusion as well as matched constantly infused time points. Two-way ANOVA indicated a significant effect of time ($p=0.0156$), infusion pattern ($p<0.0001$) as well as a significant interaction ($p=0.0312$) between the two. Post-hoc analysis revealed GR binding was significantly increased ~3 fold ($p<0.01$) at the corticosterone pulse peak (140min) compared to nadir (180min) (1.24 ±0.19 and 0.47 ±0.05 respectively) (Figure 3.1 A). GR binding in response to the constant corticosterone infusion were raised and not significantly different between 140min and 180min infused time points (1.33 ±0.15 and 1.20 ±0.14 respectively). Results indicate prolonged GR binding, as no change was detected between the pulse peak of the pulsatile corticosterone infusion and the matched constant infused time point. There was a significant ~3 fold increase ($p<0.01$) in GR binding after 180min of constantly infused corticosterone compared to pulse nadir (180min). GR binding in response to the VEH infusion was unchanged between 140min and 180min and significantly lower than all corticosterone infused time points (0.26 ±0.13 and 0.19 ±0.08 respectively).

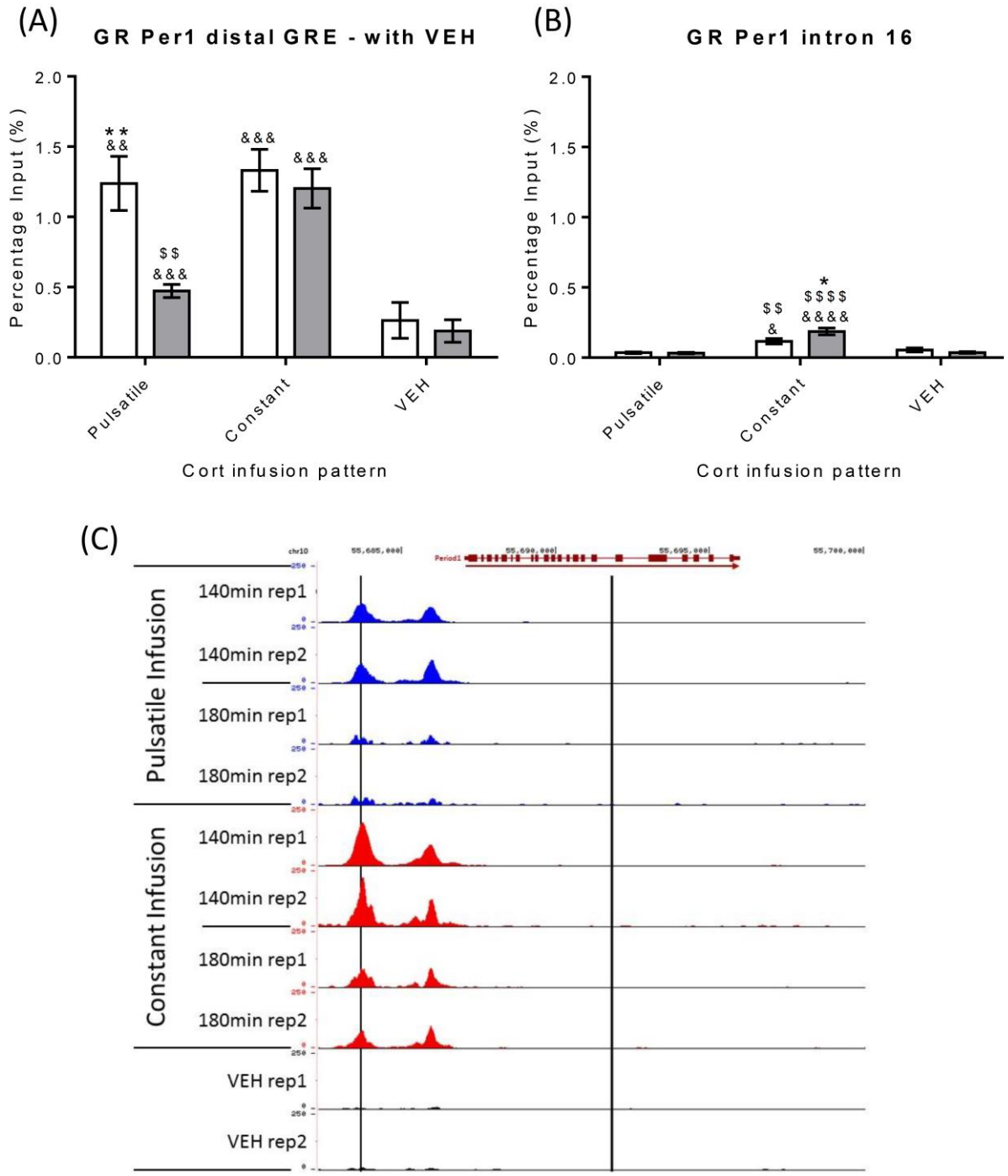

Figure 3.1 Assessment of positive and negative control sites for GR binding in the clock gene *Per1*. *ChIP assay samples used in the next generation sequencing analysis, was evaluated by RT-qPCR to the distal GRE 2.5kb upstream of the clock gene Per1 (A). For GR binding at the distal GRE site, significant effects of time (p=0.0156), infusion pattern (p<0.0001) and interaction (p=0.0312) were detected by two-way ANOVA. (B) At the Intron16 site, a highly significant effect of infusion pattern (p<0.0001) and a significant effect of time and interaction (p<0.05) were detected by two-way ANOVA. All significant differences detected by Bonferroni multiple comparison post-hoc tests are shown on the graphs, with comparisons between cort infused and* VEH *infused matched time point represented by & symbols,*

*comparisons between cort infused time points (within infusion pattern) represented by * and comparisons between infusion pattern (at the same timepoint) represented by $ symbols. Significance values are $^{*,\$,\&}p<0.05$, $^{**,\$\$,\&\&}p<0.01$, $^{***,\$\$\$,\&\&\&}p<0.001$, $^{****,\$\$\$\$,\&\&\&\&}p<0.0001$. All data are expressed as mean ± s.e.m. (C) GR binding was visualised using the UCSC genome browser for ChIP-Seq tag density enrichment in the vicinity of the Per1 gene (maroon track at top of figure) on chromosome 10 (chr10:55,682,284-55,700,077). The site of the distal GRE is indicated by the left black line and intron16 by the right black line. Increased tag density was observed at the Per1 distal GRE site in response to the pulsatile corticosterone infusion (blue) at 140min. Reduced tag density was observed at this site in the pulsatile corticosterone infusion (blue) at 180min. With constant corticosterone infusion, further increased tag density (red) was observed at the distal Per1 site for both time points. No visible peak in tag densities was seen at Per1 intron16 (black line to the right) for any of the treatment and/or time conditions. Genome browser shots describe Per1 as transcribed from the anti-sense strand (left to right) and intron/ exon coding region (exons represented as maroon blocks in gene track) locations from Ensembl rn6 co-ordinates. Data normalised to 10million tags and y-axis 0-250.*

Within the negative control, intronic region, two-way ANOVA indicated a significant effect of time ($p=0.0001$) as well as infusion pattern and interaction between the two ($p<0.05$) (Figure 3.1 B). Post-hoc analysis revealed GR binding was low at both pulsatile infused time points and not significantly changed between 140min and 180min (0.04 ±0.01 and 0.03 ±0.01 respectively). VEH infusion resulted in similarly low GR binding levels at both time points (0.05 ±0.01 and 0.04 ±0.01 respectively), however, in response to a constant corticosterone infusion, relative levels of GR were increased by ~1.5-fold ($p<0.05$) at the 180min compared to the 140min infused time point (0.19 ±0.02 and 0.12 ±0.02 respectively). Both time points were significantly raised to VEH infusion by 2- ($p<0.05$) and 5-fold ($p<0.0001$) respectively. As a significant elevated result at this intronic site was unexpected, UCSC genome browser shots plotting normalised tag density of aligned tags across the *Per1* coding region and primer sites have been included (Figure 3.1 C). At the positive (GRE containing) control primer site, relative increases in tag density are consistent with RT-qPCR results. Interestingly, the distal GR binding site corresponding to the positive control primer set has been previously described as a 'hypersensitive' site (Reddy *et al.*, 2012). In our data, we can observe a slightly increased tag density compared to the site most proximal to the TSS. In contrast, within the negative (intronic region) control primer site, no discrete peaks are observable, indicating this region does not contain a GR binding site and is potentially due to RT-qPCR sensitivity.

Together these data indicate that pulsatile corticosterone infusion induces GR binding at the pulse peak, which is lost to a significant degree within the nadir. In response to constant infusion, GR is bound to a similar level as pulsatile peak and remains at this high level after 180min, consistent with previous *in vivo* data (Stavreva *et al.*, 2009; Conway-Campbell *et al.*, 2011).

3.5.2 GR ChIP-Seq replicate concordance

Pearson correlation coefficient analysis was used to assess the degree of concordance between enriched GR binding regions across replicates at each corticosterone and VEH infused time point. In response to a VEH infusion, 118 enrichments were detected with a Pearson correlation coefficient of 0.797 (Figure 3.2C). The number of enrichments was unexpected, as GR was expected to be unbound in ADX rats without corticosterone ligand exposure, however, the Pearson correlation coefficient value did indicate positive, strong association and concordance between replicate tag densities and was therefore considered to be confident.

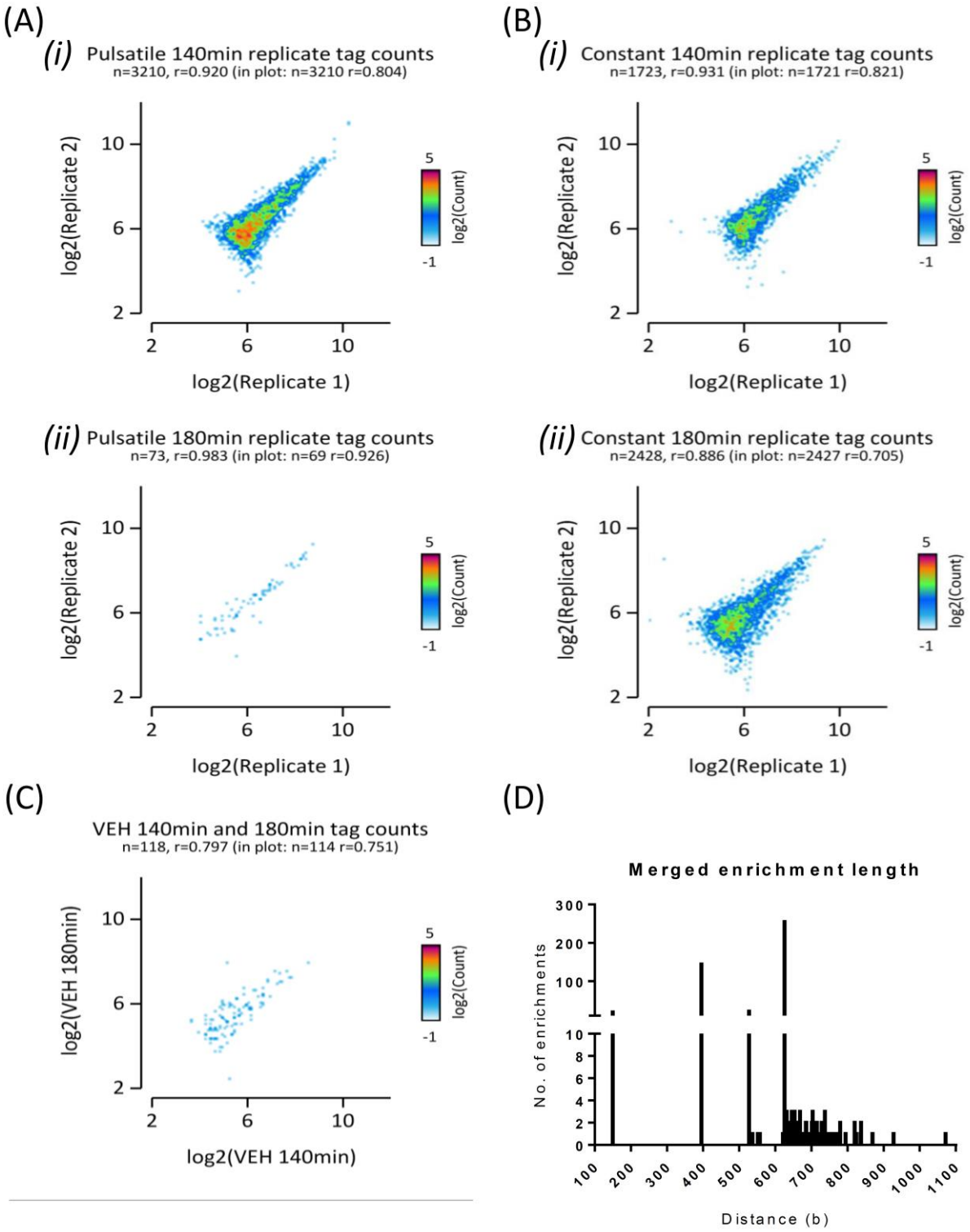

Figure 3.2 Replicate concordance and GR enrichment length

2D histogram of concordant enrichment tag counts (log2) identified by IDR for each replicate in response to either pulsatile (A) or constant corticosterone (B) at infusion time points 140min (i) and 180min (ii) compared to VEH *(C). Pearson correlation coefficient analysis indicated acceptable concordance between replicates (r>0.88 (A and B) and (r=0.797 (C)). Tag counts were normalised to 10 million and both axes segmented into 100 bins. Normalised tag count (log2) within each bin is*

colour coded according to the heatmap. Images produced from EASeq (Lerdrup et al., 2016). (D) Histogram plotting the distribution of total GR binding region lengths after overlapping regions between infused time points were merged. Minimum =149b, 25th percentile =395b, median =625b, 75th percentile = 625b, Mean =558b and maximum =1,071b.

In response to pulsatile corticosterone infusion, 3,210 enrichments were detected at the pulse peak, but only 73 were detected at the pulse nadir (Figure 3.2 A). Pearson correlation coefficient values were 0.92 and 0.98 respectively, indicating a positive, strong association and concordance between replicates. In response to 140min constant corticosterone infusion, the total number of identified enrichments was reduced in comparison to the pulsatile peak to 1,721. Enrichment numbers were slightly increased by 180min of constant corticosterone infusion to 2,428 compared to 140min but still less than corticosterone pulse peak. A slight drop in Pearson correlation coefficient values to 0.93 and 0.886 respectively were recorded but are still considered strong inter-replicate concordance values. Taken together, we concluded that both corticosterone and VEH infused time point replicates were concordant for use in downstream analysis. Overlapping enrichments between all conditions were merged into a single list of 3,980 GR binding sites for comparative analysis (Figure 3.2 D).

3.5.3 GR tag density and distribution at merged enrichment regions

Assessment of raw tags at merged enrichments and across conditions indicated increased tag intensity in response to the pulsatile corticosterone peak as well as at both constantly infused time points (Figure 3.3). All conditions associated with raised circulating corticosterone levels (Figure 2.2). Intensity was decreased in response to the pulsatile nadir and either VEH time point; conditions associated with negligible circulatory corticosterone levels. Pulsatile nadir tag intensity appeared slightly raised to VEH, however this was purely based on qualitative assessment at this stage.

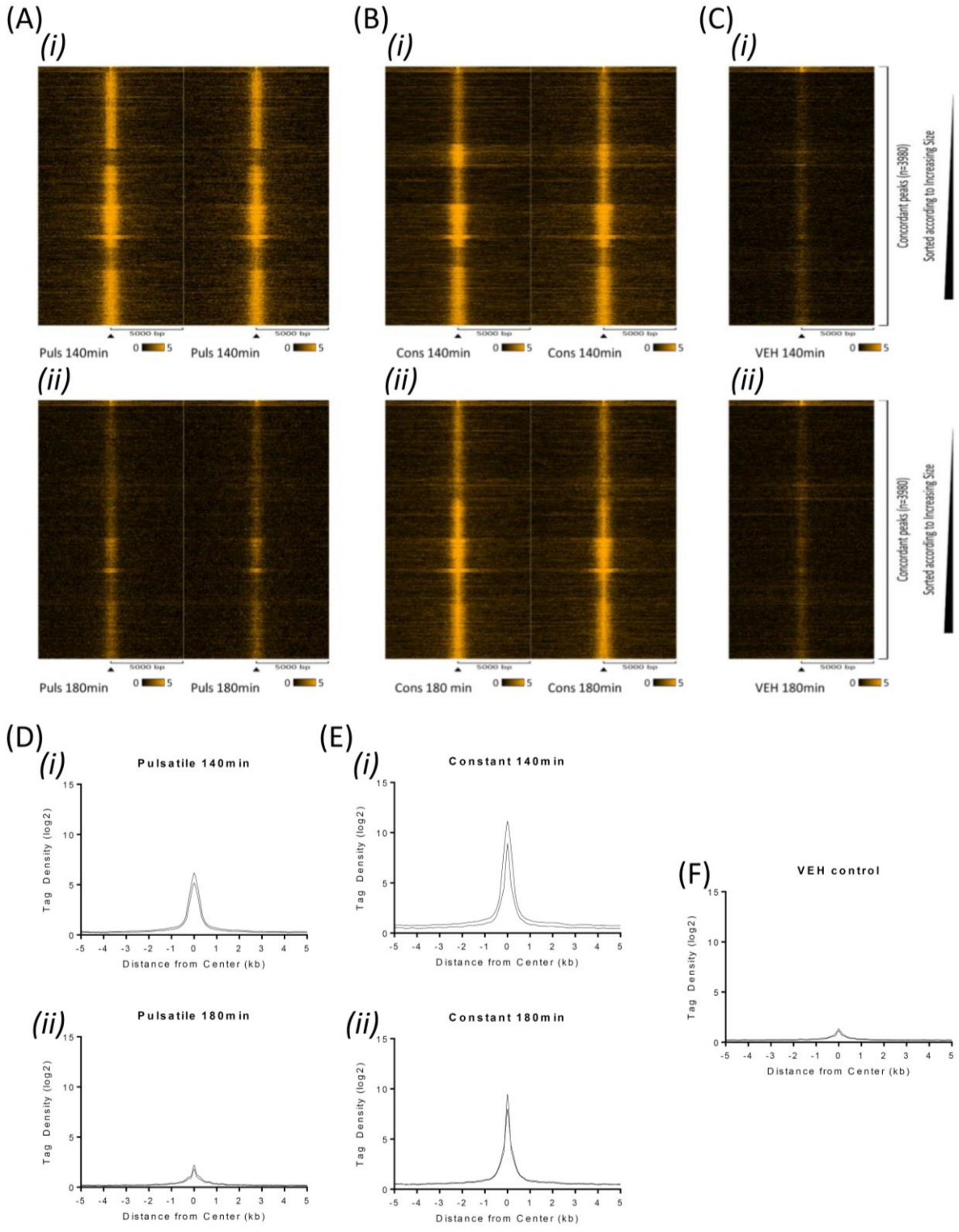

Figure 3.3 GR tag density and distribution between replicates.

Heatmap plots visualise changes in tag intensity at merged enrichment regions within each replicate in response to either pulsatile corticosterone (A), constant corticosterone (B) or VEH *(C) at infusion time points 140min (i) and 180min (ii). Tag intensity across enrichment regions were increased at 140min pulsatile corticosterone (Ai) and at both constant time points (Bi and Bii) to a similar degree across regions, relative to* VEH *(Ci and Cii). At 180min pulsatile corticosterone (Aii) tag intensity across*

enrichment regions was reduced to similar levels as those observed in the VEH *infusion groups (Ci and Cii). Tag count intensity normalised to 1million reads per 1kb is plotted on the x-axis, with 5kb in either direction from the centre segmented into 200 bins. The degree of intensity is indicated by heatmap, according to the 0-5 scale bar. Graphs were plotted using EASeq* (Lerdrup *et al.*, 2016)*. Histograms of tag distribution 5kb in either direction of the merged enrichment centre was plotted for pulsatile corticosterone (D), constant corticosterone (E) or* VEH *(F) at infusion times 140min (i) and 180min (ii). In all cases, peaks in tag density were observed at enrichment centre and reduced to negligible levels within 1kb in either direction. High tag density levels were seen in pulsatile corticosterone at 140min (Di) compared to low tag density levels seen in pulsatile corticosterone at 180min (Dii) and* VEH *at both time points (Fi and Fii). Relatively high tag density levels were seen in constant corticosterone at both time points (Ei) (Eii). Raw tags (log2) were segmented in 5b bins, spanning 5kb in each direction from enrichment centre. Graphs were plotted using GraphPad Prism 6 for windows.*

Histograms of raw tag distribution was maximal at the centre of de novo enrichment regions and was reduced in either direction to negligible counts within 1kb, indicating GR binding locations were most likely at the enrichment centre. Pulsatile corticosterone peak appeared to induce a much larger tag pile up than pulsatile corticosterone nadir (Figure 3.3 D) and VEH (Figure 3.3 F). Taken together, these data indicated high levels of GR recruitment at the pulse peak were rapidly returned to baseline within the pulse nadir. In response to constant corticosterone infusion, tag intensity was concentrated at the centre of enrichments and increased to similar levels as pulsatile peak, across both time points (Figure 3.3 E).

3.5.4 Filtering significant induction of GR binding

Prior to any differential analysis, VEH replicates were analysed across binding regions by DESeq2 and no significant differences in tag density were detected (data not shown); therefore, both VEH replicates were pooled.

To investigate statistically relevant corticosterone induced changes in GR binding relative to VEH control, normalised raw tag counts within binding regions were analysed by DESeq2. In response to a pulsatile corticosterone peak, increases in enrichment were detected at 2,658 sites, whilst a loss was detected at 50 sites (Figure 3.4 A). No enrichments passed significance thresholds at the pulsatile nadir (Figure 3.4 B). In response to a constant corticosterone infusion, gains in GR enrichment were detected at 1,263 and 1,953 sites after 140min (Figure 3.4 C) and 180min (Figure 3.4 D) infused time points as well as losses at 10 and 9 sites respectively. Results corroborate previous intensity and histogram data (Figure 3.3); GR binding is increased at the pulse peak (140min) of the pulsatile infusion and at both

140 and 180min time points during constant infusion. Interestingly, pulsatile peak was more effective at inducing changes in enrichment than either constant corticosterone time point.

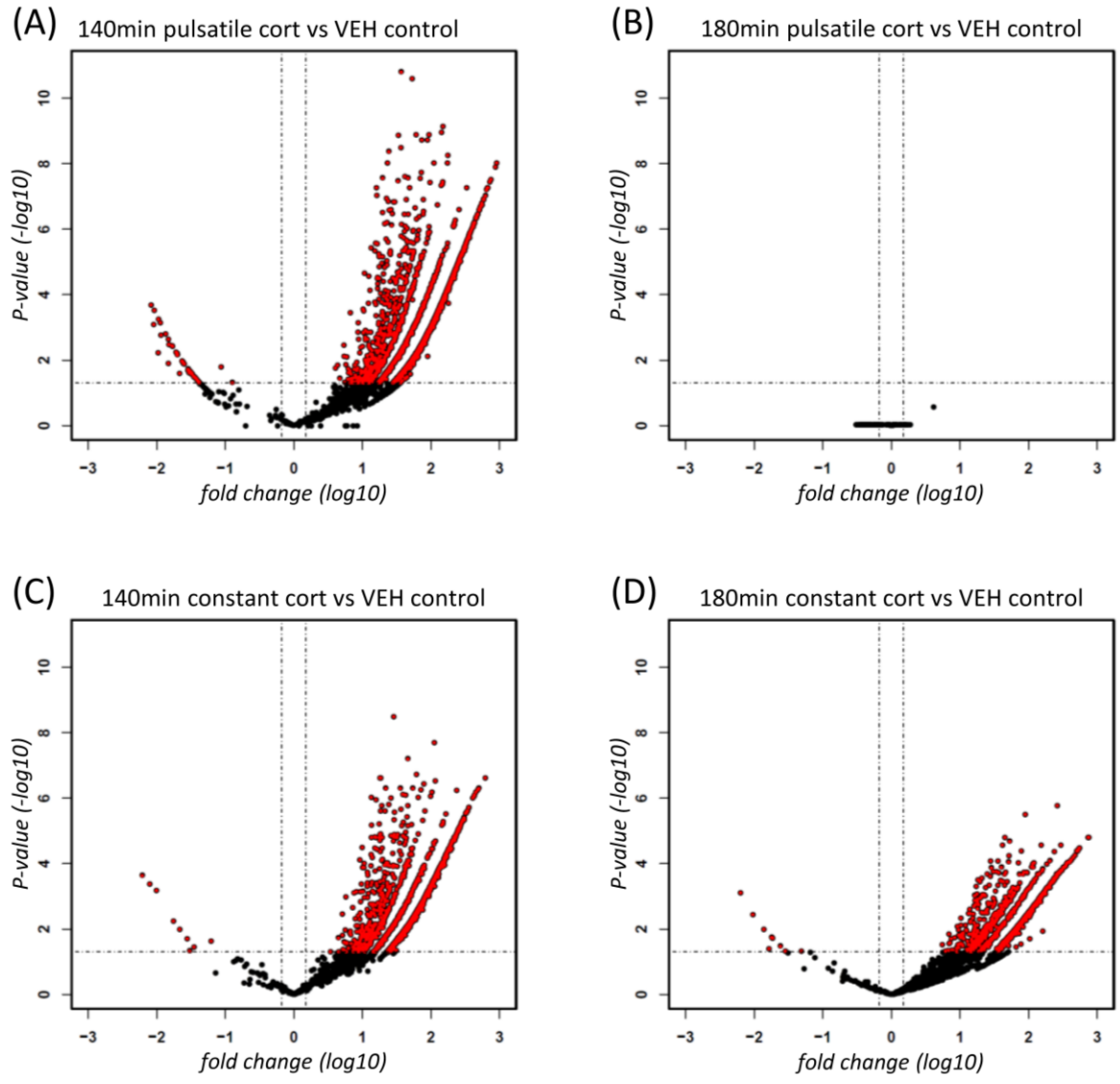

(E)

		Up-regulated	Down-regulated
Pulsatile	140min	2,658	50
	180min	0	0
Constant	140min	1,263	10
	180min	1,953	9

Figure 3.4 Differential GR binding over time during pulsatile or constant corticosterone infusion. *Volcano plots showing GR enrichment fold change (log10) and adjusted p-value (-log10) relative to* VEH *control for pulsatile corticosterone infusion at 140min (A) and 180min (B) as well as constant*

corticosterone infusion at 140min (C) and 180min (D). Enrichments were filtered for significant changes (red). (E) Table reports the number of differentially regulated enrichments and direction of change by either pulsatile or constant corticosterone infusion at 140 and 180min time points, relative to VEH *control. Tags were normalised to total tags within enrichments and fold change >0.176 or <-0.176 (log10) (latitudinal lines), p-value adjusted for multiple comparisons <0.05 (-log10) (longitudinal lines) and FDR<0.05 are plotted in red on volcano plots. All other values are plotted in black.*

3.5.5 GR binding dynamics during pulsatile versus constant corticosterone infusion

Fold changes in enrichment at identified GR binding sites were hierarchically clustered and visualised within the heatmap (Figure 3.5 A). The corticosterone pulse peak induced significant GR binding at 68% of identified sites; 24% of which were unique to this condition as shown in the Venn diagram (Figure 3.5 B). Constant corticosterone infusion induced GR binding at a reduced 32% of total sites, at the 140min time point matched to pulse peak. However, in contrast to the pulsatile nadir's lack of detectable GR binding; constant corticosterone infusion was able to induce GR binding at 49% of total sites at the matched infused timepoint (180min).

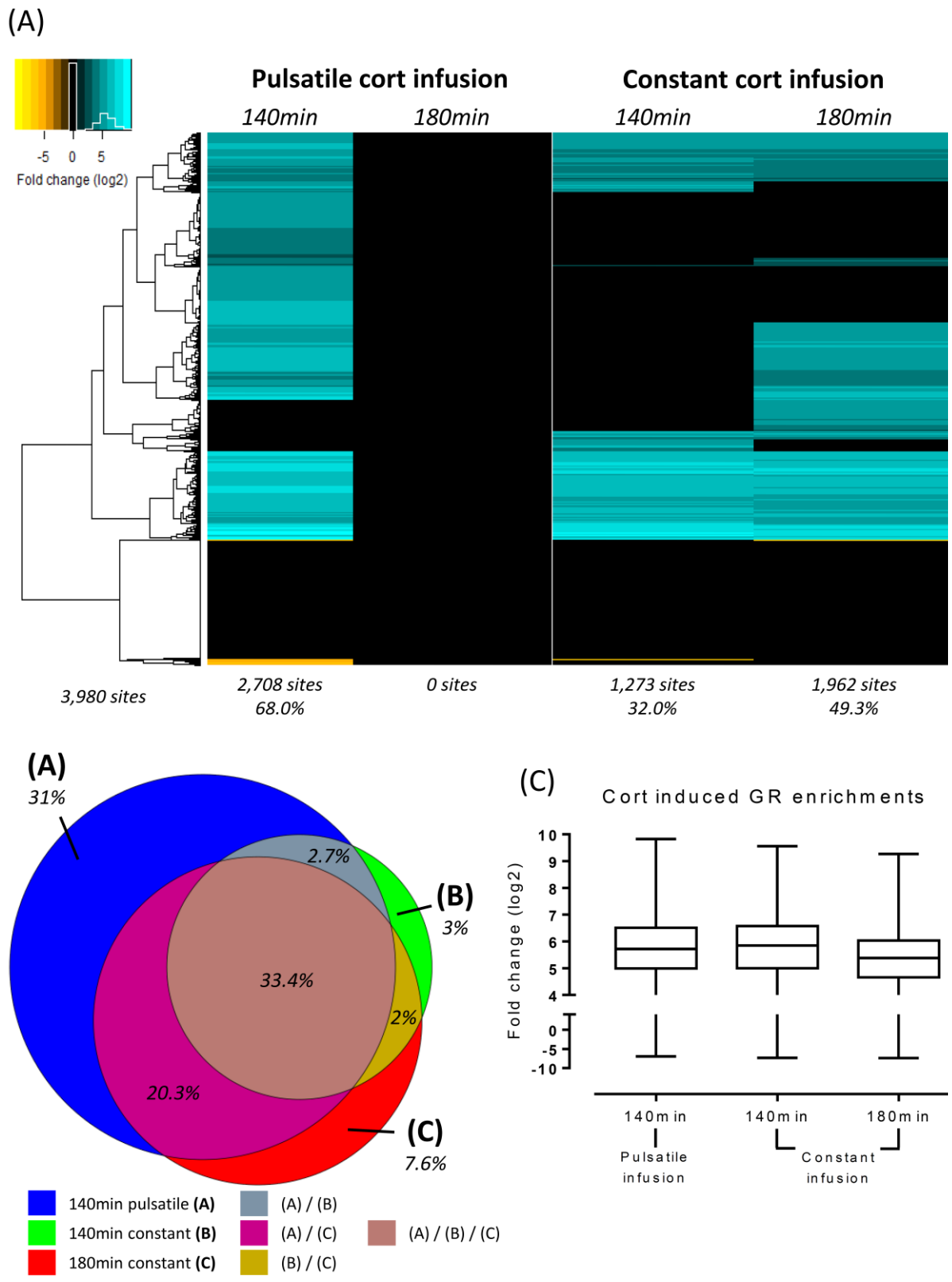

Figure 3.5 GR binding sites inducible by infused patterned corticosterone time points (PCTs).

(A) Visualisation of differentially regulated GR binding in response to either pulsatile or constant corticosterone infusion at times 140 and 180min. GR binding regions were hierarchically clustered according to amplitude of fold changes in response to each corticosterone infused time point, relative

to VEH*. Heatmap colour intensity indicates degree of fold change (log2) as shown within the legend (top left) as well as distribution (white trace). Tags were normalised to total tag count within merged GR binding regions and filtered for log2 fold changes >0.585 or <-0.585, p-value adjusted for multiple comparisons <0.05 and FDR <0.05 to* VEH *control are plotted. All other enrichments were given the value 0. (B) VENN diagram of the number of differentially enriched regions to* VEH *control in response to 140min pulsatile and 140min and 180min constant corticosterone infused time points were plotted using eulerr* (Larsson *et al.*, 2019)*. (C) Little difference in distribution of corticosterone infused time points induced fold change to* VEH *control was found. Percentiles of corticosterone infused time points fold change to* VEH *control min: -6.9, -7.3, -7.3; 25th percentile: 5.0, 5.0, 4.7; Median: 5.7, 5.8, 5.3; 75th percentile: 6.5, 6.6, 6.0; max: 9.8, 9.6, 9.3 values for 140min pulsatile, 140min and 180min constant corticosterone infusions respectively. Y-axis is split into -10 to 4 and 4 to 10 segments of fold change (log2).*

GR binding events that were unique to either 140min or 180min constant corticosterone infusion occurred at just 2% and 5% of sites respectively, and a further 1.6% were present at both time points (Figure 3.5 B). However, 33.4% of GR binding events were common to pulsatile peak and both constant corticosterone time points, indicating GR binding across all corticosterone regulated sites are distinctly phasic in response to pulsatile corticosterone infusion. Of those, a proportion that are bound at the corticosterone pulse peak are subjected to prolonged GR occupancy over time during constant corticosterone infusion, however, pulsatile infusion at the corticosterone pulse peak was further capable of inducing a large proportion of GR binding not induced by any other corticosterone infused time point. Only a relatively small subset of GR binding events was constant corticosterone responsive only. The data further shows a greater number of GR binding events in common after the 180min constant infused time point (16%) than the 140min infused time point (2%) when compared to the corticosterone pulse peak, potentially suggesting constant corticosterone infusion induced gradual increases in GR binding over time.

As previously mentioned, a number of sites reported significantly reduced tag densities relative to VEH control. Despite these representing just 1.4% of total binding sites, these reductions were unexpected as we hypothesised we would only detect GR binding in response to corticosterone ligand exposure. Interrogation of these sites indicated the majority were decreased by pulsatile peak only (1%), which returned to VEH levels in the nadir, indicating a transient loss of GR from these sites. Only a relatively small number of sites were reduced in response to 140min and 180min constant corticosterone infused time points (0.05% and 0.08% respectively), the rest were shared in combination and only one

site reported a loss in enrichment in response to each corticosterone infused time point (0.03%). No increases were recorded at these sites to VEH control.

During the analysis of these sites, I referred to the concordant GR binding region results (findPeaks and IDR analysis of Seq replicates) for each corticosterone and VEH infused time point. 38 of the 56 sites reduced by corticosterone infusion were within VEH identified GR binding regions, 19 of which were specifically found in response to the VEH infusion and no corticosterone infused time point. Plus, the presence of a GRE within 15 of the 56 sites suggest at least a proportion could be classical GR binding events, despite the opposing effect of corticosterone exposure. Additionally, analysis of tag density distribution around the centre of these enrichments (Figure 3.6) reports a distinct loss of tag density in response to 140min pulsatile corticosterone infusion compared to all other conditions. Indicating not only transient corticosterone exposure is more effective at reducing tag density within these regions, but also any loss is recoverable within the pulse nadir after 180min. Taken together and as pearson correlation coefficient analysis and differential analysis by DESeq2 indicated non-significant change between VEH 140min and 180min samples, we have no reason to disregard these sites as false positives.

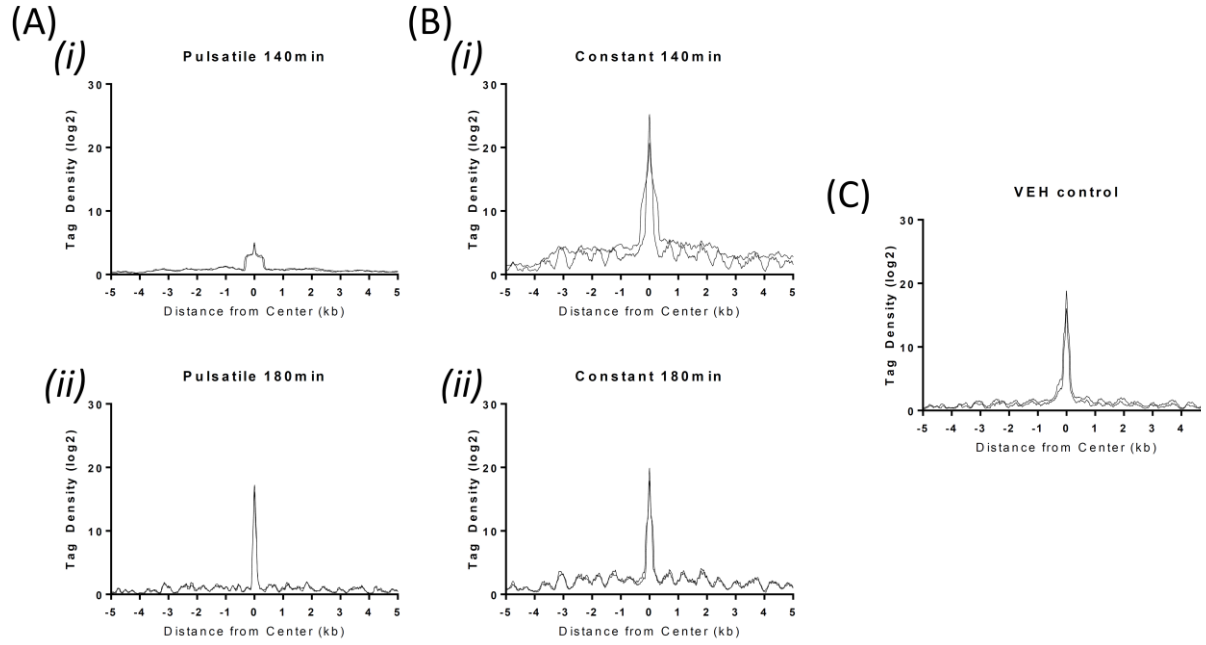

Figure 3.6 Tag density histograms of regions that report a CORT dependent loss in enrichment compared to VEH control.

Histograms of tag distribution 5kb in either direction of the merged enrichment centre was plotted for pulsatile corticosterone (A), constant corticosterone (B) or VEH *(C) at infusion times 140min (i) and 180min (ii). In all cases, peaks in tag density were observed at enrichment centre and reduced to negligible levels within 1kb in either direction. Tag density levels remain relatively unchanged between*

pulsatile corticosterone after 180min and either constant infusion (Bi) (Bii) compared to VEH control (C). 140min of pulsatile corticosterone did report a marked loss in tag density compared to all other conditions (Ai). Raw tags (log2) were segmented in 5b bins, spanning 5kb in each direction from enrichment centre. Graphs were plotted using GraphPad Prism 6 for windows.

3.5.6 Time and pattern dependent GR binding

As a pulsatile corticosterone infusion induced a cohort of GR binding events that was not significantly detected in response to a constant corticosterone infusion compared to VEH control, it raises the question about time and pattern corticosterone dependent differences. Therefore, out of the 3,098 GR binding regions that were induced to VEH control, time dependent and pattern dependent changes in GR enrichment were investigated between corticosterone infused time points.

In response to a pulsatile infusion, 50.7% of corticosterone inducible sites were regulated in a time dependent manner, with 50.6% significantly increased by the pulse peak compared to nadir (Figure 3.7). In contrast, constant infusion only significantly regulated 2.5% of GR binding events in a time dependent manner; 2.2% of which were increased at the 140min constantly infused time point.

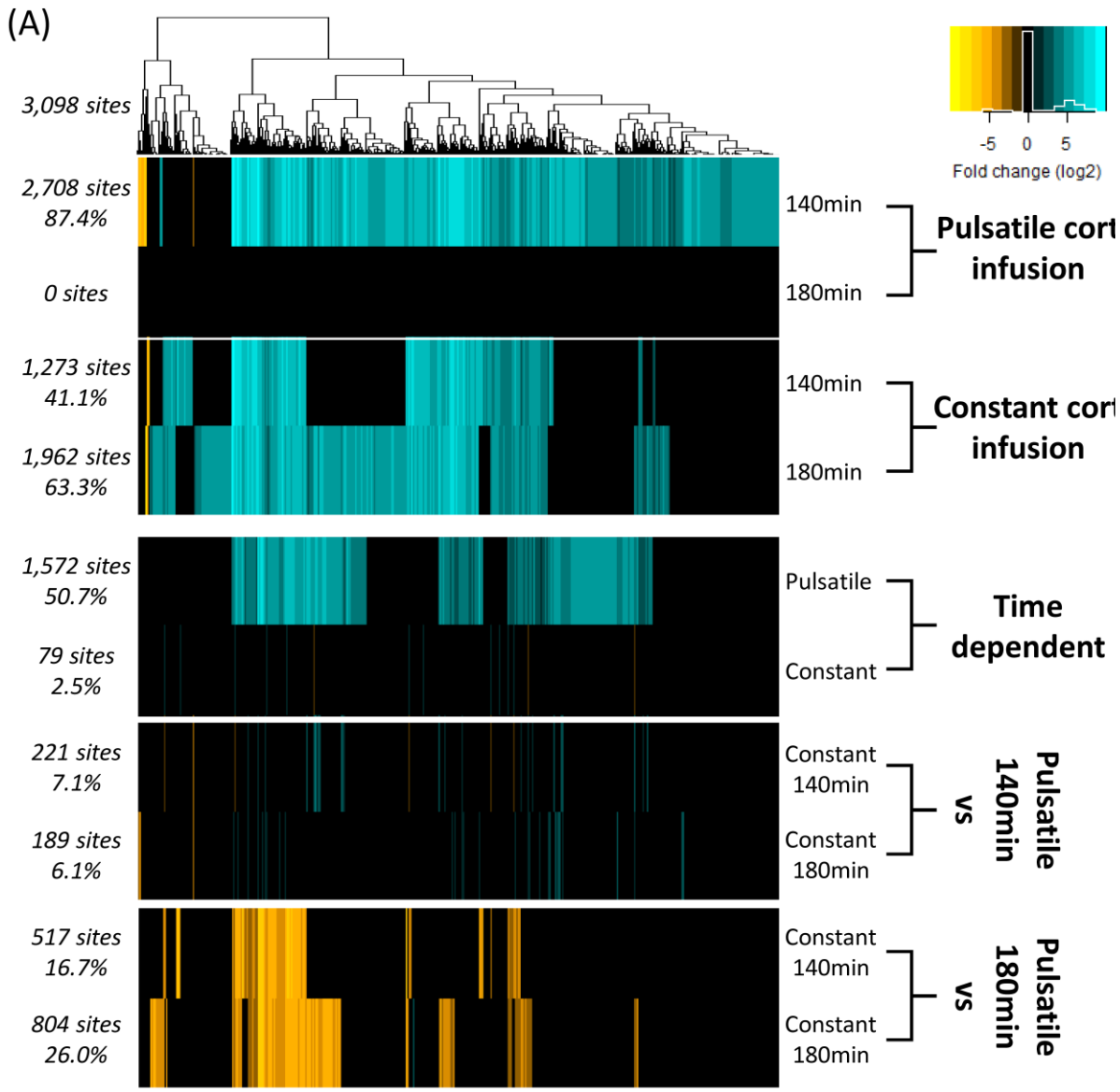

Figure 3.7 Time and pattern dependent changes in GR binding.

Heatmap visualisation of regions that were differentially enriched to VEH *in response to corticosterone infused time point, compared to another corticosterone infused time point. Enrichments of log2 fold change were hierarchically clustered according to amplitude of change in response to each pattern of infusion. First four rows indicate fold change in GR enrichment in response to a corticosterone infused time point against* VEH*. Time dependent rows represent 140min vs 180min pulsatile and then constant corticosterone infusion. Subsequent double rows represent 140min and then 180min corticosterone infusion time points vs either constant infused time points. Heatmap colour intensity indicates degree of fold change as shown within the legend (top right) as well as distribution (white trace). Tags were normalised to total tag count within merged enriched regions and fold change >0.585 or <-0.585, p-value adjusted for multiple comparisons <0.05 and FDR<0.05 are plotted. All other enrichments were given the value 0.*

Changes in enrichment, between inducible sites in response to pulsatile peak and to either 140min and 180min constant corticosterone infusion time points, were 7.1% and 6.1% respectively. Of these, 6.2% and 5.5% respectively were enriched by the pulsatile peak, indicating pulsatile peak was more effective at inducing GR binding at these sites. Comparison of the corticosterone pulse nadir to either constant infused time point reported 16.7% and 30.0% of sites were down regulated at the pulse nadir. Indicating an increase in GR binding across both constantly infused time points to nadir.

3.5.7 Motif analysis of GR binding sites

GR binding to the genome can be directed to regulatory elements such as the GRE, however, the GR can also interact with binding sites via response elements complimentary to other nuclear factors either as a composite or tethered co-factor complex (Biddie *et al.*, 2011; Grøntved *et al.*, 2013; Uhlenhaut *et al.*, 2013). *De novo* motif analysis of sequences from GR binding regions differentially enriched to VEH control (total of 3,098 regions) indicated the most significant over-represented homologous palindromic sequence resembled a GRE motif (0.92 score) within 39% of target sequences (Table 3). However, out of the top 6 most significant motifs (including the GRE), the most abundant resembled a forkhead box M1 (FOXM1) transcription factor motif (0.92 score) within 43% of binding regions. Despite this increased abundance, significance of representation in target sequences compared to background was greatly reduced from a p-value of 1e-458 to 1e-95. Sequences resembling known GR co-regulator motifs for HNF4α (0.94 score) and AR half-sites (0.76 score) were identified in 31.2% and 24.1% of target sequences respectively (Biddie *et al.*, 2011; Biddie, Conway-campbell and Lightman, 2012; Grøntved *et al.*, 2013). Other over-represented motifs resembled CCAAT enhancer binding protein alpha (CEBPA) (0.95 score) and the STAT5 (0.97 score) motifs (0.76 score).

	Target sequences (%)	Background sequences (%)	Score	P-value	Motif logo
GRE	39.1	8.0	0.92	1e-458	
CEBPA	35.7	15.2	0.95	1e-160	
HNF4a	31.2	12.2	0.94	1e-155	
STAT5	17.9	5.5	0.97	1e-120	
FOXM1	43.2	25.2	0.92	1e-95	
AR half-site	24.1	11.9	0.76	1e-71	

Table 3 De novo motif analysis of GR binding site sequences.

Table reports, identification and occurrence of the top 6 significantly over-represented sequences within corticosterone regulated GR binding sites to VEH *control and restricted to an area of 233b in either direction of the centre. P-value represents significance of identified sequence to randomly selected background DNA sequences, score is equal to the degree of similarity between de novo and known motif sequence, motif base logo indicates specific probability (s.p.) of base occurrence.*

All top 6 significant de novo motifs identified were located around the centre of the GR binding region, but GREs reported a greater occurrence to other motifs (Figure 3.8 A). Motif occurrence within regions that were induced by pulsatile peak or 140min and 180min constant corticosterone infusion time points were investigated separately but little difference was observed. Finally, the occurrence of potentially co-operative motif sequences within GRE containing regions were investigated. HNF4α and STAT5 were the most abundant (55.8% and 54.2% respectively) followed closely by AR half-sites (45.4%); representing the most likely to co-operatively direct GR binding to the genome (Figure 3.8 B). FOXM1 was relatively quite low compared to other motif occurrences.

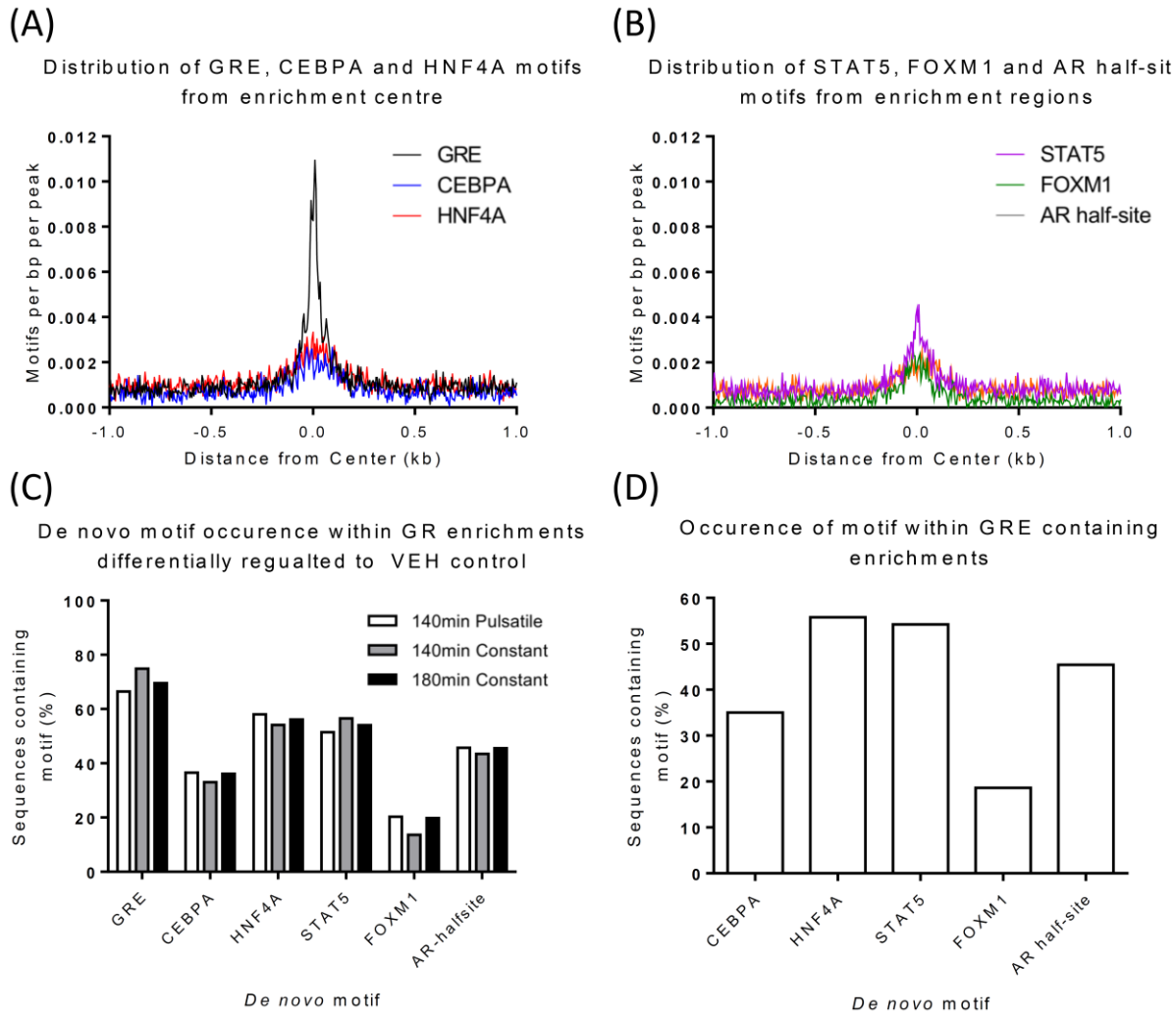

Figure 3.8 Distribution and percentage of discovered motifs within PCT induced GR binding regions. *3,098 corticosterone regulated binding regions differentially enriched to* VEH *control in response to either pulsatile or constant corticosterone infusion after 140min and 180min were assessed identified de novo motif sequences. (A)(B) Of the top six significant motifs identified, GREs reported the largest occurrence at the centre of the enriched regions. CEBPA, HNF4A, STAT5, FOXM1 and AR half-sites were similarly distributed but occurrence was distinctly reduced. (C) GR binding regions were separated into the 2,708 regions differentially enriched by 140min pulsatile, 1,273 by 140min constant and 1,962 by 180min constant and motif occurrence was plotted. De novo motif distribution of GREs was the most prevalent at 66-74% of enrichments whilst FOXM1 was the least at 14-20%. However, there was no distinct difference in percentages of motif occurrence in response to a PCT corticosterone over another. (D) The presence of one of the top six most significant motifs was investigated within GRE containing enrichments significantly changed to* VEH *control by patterned corticosterone infusion. HNF4A was present in the most GRE containing sequences (56%) with STAT5 (54%) and AR half-sites (45%) slightly reduced. The two lowest were CEBPB and FOXM1 which were only present in 35% and*

19% of GRE containing enrichments. De novo motifs were identified within 233b regions in either direction from the centre.

GR enrichment regions were further investigated for the presence of a nGRE like sequence as identified by Surjit et al., within the upstream promoter of both the human and mouse thymic stromal lymphopoietin TSS. Of the 3,098 sites, just 2.23% regions contained a nGRE related sequence. Only two of these regions (0.06%) report a loss in GR enrichment.

3.6 Discussion

GR binding at the peak of the third corticosterone infused pulse via the jugular vein, can induce phasic genome-wide GR binding within the ADX rat liver. Interestingly, this phenomenon is not limited to a subset of sites but is observed at the vast majority (~90%) of our identified corticosterone regulated GR binding sites. Furthermore, bound GR was reported to dissociate from all binding sites, returning to baseline levels within the corticosterone pulse nadir. This phasic GR recruitment was not an intrinsic rhythm, as a constant corticosterone infusion prolonged GR binding. 26% of sites were induced by both corticosterone pulse peak and the matched constant corticosterone infused time point (140min) whilst only a small subset were induced by constant corticosterone infusion uniquely (~12%). Despite these subsets, GR binding was more effectively induced by the corticosterone pulse peak than any single corticosterone infused time point. Together, these observations indicate GR recruitment to the genome is highly corticosterone regulated and synchronised to hourly ultradian pulses.

As several sites were significantly bound at the pulse peak and no other corticosterone infused time point, it was theorised these could represent dose dependent sites. To match the dose delivered between 20min pulsatile and 60min constant corticosterone infusion, a lower rate was used which induced a slightly lowered circulating corticosterone measurement (Figure 2.3). Levels at the infused pulsatile peak (140min) were at 387ng/ml ±34, whereas constant infused corticosterone levels were reduced at 261ng/ml ±51 at the matched time point. Therefore, this subset of GR bound at the pulsatile peak only are either exclusively responsive to a transient, rising phase of corticosterone or are dose dependent.

Phasic GR binding in response to the pulsatile corticosterone infusion was dysregulated and prolonged by a constant corticosterone infusion. Additionally, there were indications that not all sites were maximally bound, as an increase in the number of significant binding sites over time was detected by 180min of infusion compared to 140min. Perhaps indicating constant corticosterone infusion was gradually increasing GR binding levels over time (Figure 3.5).

This study discovered 3,980 binding sites after merging all *de novo* GR binding regions from all corticosterone and VEH infused time points, however, I present evidence that several sites were either not significantly regulated by corticosterone infusion or significantly decreased relative to VEH control. Whether the non-inducible sites are bound but at very low levels or represent corticosterone ligand-independent/ VEH induced GR binding is unclear without further investigation. Disregarding potential Seq error, extra-adrenal *de novo* GC synthesis has been identified within intestine, skin, brain and lymphoid tissue within rodents and therefore presents the possibility of GR activation irrespective of adrenalectomy and independent of the corticosterone infusion (Vacchio, Papadopoulos and Ashwell, 1994; Taves, Gomez-Sanchez and Soma, 2011). There is further evidence GR can be bound by a selection of co-factors in the absence of ligand. Perhaps this is an example of an active co-factor with the capacity to recruit GR to the genome within a tethered model of binding (Pfaff and Fletterick, 2010; Monczor *et al.*, 2019). This model may require a loss of corticosterone induced inhibition. Furthermore, non-liganded GR translocation into the nucleus has also been reported in response to shear stress, abnormal pH and temperatures as well as activation by tumour necrosis factor (TNF)α in COS-1 cells, but I would consider inductions by these methods unlikely and does not adequately explain the return of GR enrichment within the nadir of the pulsatile corticosterone infusion to VEH control levels (Ji, Jing and Diamond, 2003; Verhoog *et al.*, 2011; Scheschowitsch, Leite and Assreuy, 2017). If we consider these are real binding events via mechanisms not controlled for, I would hypothesise losses in response to corticosterone are most likely due to chromatin re-organisation in response to the large number of infused corticosterone induced GR binding across the genome. Multiple studies have shown GR binding induces re-organisation of the chromatin architecture and we could be observing increasing chromatin density and 'closing' at these sites, dis-placing GR (John *et al.*, 2008, 2011; Grøntved *et al.*, 2013; Kuznetsova *et al.*, 2015; Stavreva *et al.*, 2015). This would explain why there is a recovery of enrichment within the nadir of the pulsatile corticosterone infused time point (180min). However, this would require much further study, primarily to validate extra-adrenal stimulation of GR that is bound to these select sites and chromatin accessibility.

The number of potential GR binding sites discovered is lower than two recent studies within the mouse liver (11,000 sites). The first study used Dex treatment and a GR enrichment detection algorithm called hotspot to identify bound sites, so discrepancy may be due to differences in affinity, half-life and efficacy between ligands as well as the analysis algorithm (Baek, Sung and Hager, 2012; Grøntved *et al.*, 2013). The second study however, was conducted within adrenally intact mice and found endogenous circadian variation in corticosterone induced GR binding at 11,000 sites despite similar HOMER detection methods. It should be noted, peak identification thresholds would be highly varied compared to mine, nor was any subsequent IDR analysis applied to identify concordant enrichments

between replicates (Heinz *et al.*, 2010; Lim *et al.*, 2015). I hypothesise discrepancies between GR enrichment detection and stringency limits for statistically significant GR binding regions reduced the number of GR binding sites to other studies, however, determination of this hypothesis could only be completed upon parallel analysis of published sequenced data. As I have successfully identified robust changes in GR binding, I would conclude analysis parameters were suited to my research question.

Similar to other published studies, characterisation of inducible GR binding sites revealed not only GRE motifs, but other known co-factor motifs (Grøntved *et al.*, 2013; Lim *et al.*, 2015; Sasse *et al.*, 2015; Hemmer *et al.*, 2019). Comparison between studies of the relative occurrence of motifs within GR binding regions is difficult to ascertain from the literature due to tissue and cell type variability as well as analytical methods applied which were not always detailed within methods. For example, the two previously mentioned mouse liver studies quote a wide range of GRE occurrence within GR binding sites of 60% to 12% respectively, therefore, rates found within this study are difficult to compare (Grøntved *et al.*, 2013; Lim *et al.*, 2015). However, select motifs were identified that have been previously characterised as co-regulators for the GR and within the liver, such as STAT5, HNF4α and CEBP. Potentially indicating co-operatively directed binding and regulation of GRs (Hemmer *et al.*, 2019). Examination of the GR enrichment sequences revealed little evidence of nGRE like sequences (2.21% of regions). It has been postulated that as binding affinity to these sequences is reduced compared to classic GRE sequences and could therefore make detection of these sites difficult. Additionally, nGRE sequences have been characterised within macrophages and as GC action is to suppress the immune response, perhaps nGRE sequences are mostly relevant within that cell type (Uhlenhaut *et al.*, 2013; Jubb *et al.*, 2016). Either way, this study did not find robust evidence for a potential interaction between the GR and nGRE like sequences.

In conclusion, this data presents strong, robust evidence that GR binding to the genome within an ultradian modelled system occurs in a phasic manner, synchronised to the rising and falling levels of corticosterone. GR dynamics can be dysregulated in a prolonged manner by alteration to a constant level of corticosterone, without changing the overall dose delivered and identifies potential GR co-regulator motifs characterised within other *in vivo* liver studies. These data highlight the distinct regulatory role, ultradian like oscillations can have on GR recruitment at all regulated sites.

Chapter 4 Genome-wide RNA polymerase II binding in liver during ultradian or constant corticosterone replacement in adrenalectomised rats.

4.1 Background

Transcription of genes is dependent on the recruitment of the pre-Pol complex to regions typically 30b upstream of the TSS. This is usually directed by interactions between the TATA box binding protein subunit of the pre-Pol complex and TATA sequences within the DNA as well as other initiator sequences (Wang, Carey and Gralla, 1992; Wiley, Kraus and Mertz, 1992; Ponjavic *et al.*, 2006; Sandelin *et al.*, 2007). The pre-Pol complex can then direct RNA Pol2 to the core promoter as well as unwind DNA via the action of the helicase XPB subunit of the pre-Pol complex prior to active synthesis of complimentary RNA sequences (Wang, Carey and Gralla, 1992; Tirode *et al.*, 1999; Hahn, 2004; Luse, 2014).

The phosphorylation of specific carboxy-terminal domain residues within RNA Pol2 directs multiple RNA processing factors. Investigation of residues within this region has identified phosphorylation of Ser5 (pSer5 Pol2) by Kin28 occurs predominantly within the promoter region and has been observed to be lost within the elongation phase of RNA synthesis (~200 nucleotides) (Corden, 1990; Hengartner *et al.*, 1998; Komarnitsky, Cho and Buratowski, 2000). In contrast, phosphorylation of Ser2 by the carboxy terminal domain kinase 1 (Cdk1) occurs during the transcriptional elongation phase. Enrichment of Ser2 phosphorylated RNA Pol2 complexes (pSer2 Pol2) has been reported to increase towards the 3' end of actively transcribing genes and may be important for the efficient recruitment of 3' polyadenylation factors (Cho *et al.*, 2001). Importantly, phosphorylation of Ser2 is associated with actively transcribing RNA Pol2 and hence provides a valuable tool for assessing dynamic changes in transcription (Ahn, Kim and Buratowski, 2004).

Using specific antibodies for either phosphorylated state, occupation of RNA Pol2 at intragenic regions can be investigated using ChIP-Seq methods. However, identification of *de novo* enrichment and downstream analysis of RNA Pol2 occupied regions presents systematic challenges different to transcription factor ChIP-Seq analysis. These challenges include the identification of *de novo* enriched sites relative to background controls, such as with the GR analysis presented in Chapter 3. Algorithms of this type have been primarily designed to identify localised, discrete regions of enrichment as transcription factors (such as GR) bind to short specific recognition elements (Harmanci, Rozowsky and Gerstein, 2014). For example, the GR data presented previously, was sequenced from average

chromatin fragments of ~300b and identified enriched regions were on average 558b long, with the centre of the enrichment indicating the site of GR binding. Similar discrete enriched regions are not commonly observed in RNA Pol2 ChIP-Seq analysis. Creation of disulphide bonds during the fixing of tissue will trap RNA Pol2 as it actively transcribes through the gene's coding region, which will vary greatly. Further, RNA Pol2 sequenced tag heights are highly stochastic throughout broad enrichment regions as low mappability and repeat regions do not sequence as efficiently as others. This is a problem for *de novo* identification as algorithms will identify sharp rises or falls within broad enriched regions as multiple single regions, fragmenting enrichments throughout the broad coding region (Lee and Schatz, 2012; Harmanci, Rozowsky and Gerstein, 2014). Some commonly used ChIP-Seq analysis tools have been designed to identify these RNA Pol2 enrichment traces via local thresholding and merging of proximal enriched region methods, but very few algorithms (such as PeakSeq and MUSIC) have been designed to specifically analyse RNA Pol2 enrichments (Y. Zhang *et al.*, 2008; Rozowsky *et al.*, 2009; Heinz *et al.*, 2010; Harmanci, Rozowsky and Gerstein, 2014). Alternatively, Bayesian change-point, local island identification and clustering methods have also been used, but ChIP-Seq analysis of RNA Pol2 occupancy still appears to be a relatively underexplored area of research with regard to analytical provision (Zang *et al.*, 2009; Xing *et al.*, 2012; Harmanci, Rozowsky and Gerstein, 2014).

Despite analytical challenges, pSer2 Pol2 ChIP-Seq can provide important information regarding dynamics of active transcription, particularly relevant to my work investigating rhythmic GR regulation over a short time frame. Previous *in vivo* studies investigating the effects of corticosterone induced, transient binding of GR to the regulatory GRE of the *Per1* gene in rat liver identified slightly delayed but phasic increases and decreases in nascent Per1 transcript production synchronised to corticosterone/ GR binding dynamics that are repeatable. Similar RNA Pol2 phasic dynamics of occupancy were reported within promoters across the MMTV array within 3134 cells in a series of photobleaching experiments. These changes were validated as transcriptionally active by phasic hnRNA production at a selection of targets. As previously shown with the GR, these phasic dynamics are not intrinsic and are dysregulated in a sustained manner by the sGC Dex, which has a prolonged half-life compared to corticosterone (Stavreva *et al.*, 2009). Cell line work was expanded upon using ChIP-Seq analysis of pSer5 Pol2 occupation within MMTV array promoters, reporting similar phasic increases that were dysregulated and remained increased throughout corticosterone exposure over 60min at majority of targets, as opposed to a 20min increase that returned to basal levels within 40min hormone washout (Stavreva *et al.*, 2015).

In Chapter 3, I demonstrated that genome-wide GR recruitment to corticosterone regulated binding sites within the liver is highly infusion pattern dependent. Therefore, in this chapter I expand upon

these findings by investigating whether resultant RNA Pol2 occupancy can be synchronised in a similarly dynamic manner by pulsatile or constant corticosterone replacement in ADX rats. As phosphorylation of the Ser2 residue wtihin the RNA Pol2 complex is associated with the actively transcribing RNA Pol2 complex, the liver pSer2 Pol2 ChIP-Seq data will be considered a proxy for active transcription, so that we can begin to understand how the ultradian profile, as well as its dysregulation, regulates overall transcriptional output within this key metabolic target organ.

4.2 Aims

1. Identify pSer2 Pol2 recruitment at the peak and nadir of a mock 'ultradian' GC infused pulse.
2. Assess, if there are any changes in recruitment dynamics in response to a dose-matched constant GC infusion.

4.3 Method

All methods of pSer2 Pol2 ChIP-Seq analysis were done according to general methods discussed within Chapter 2.

Briefly, ChIP-Seq quality control and alignment to the genome was handled in parallel to GR Seq analysis up to identification of *de novo* enrichment regions. Instead, regions for differential enrichment analysis were defined from gene transcript loci according to the Ensembl Rn6 genome build (Rnor_6.0.92). To mitigate bias of micro RNAs and increased significance to extremely long genes, coding regions smaller than twice the fragment length (<320b) were removed and regions were restricted to a maximum length of 10kb from the TSS.

Histograms of pSer2 Pol2 tag density were restricted to transcripts that exceeded a 10kb coding region length and transcribed from the sense strand. This was to keep the TSS aligned across transcript regions for accurate assessment.

All other analysis settings were used in parallel to GR ChIP-Seq methods except for the DESeq2 analysis. Raw tag counts were normalised to total sequenced tags within replicates to avoid individual tags being counted multiple times and biasing the normalisation. These were based on methods previously published (Stavreva *et al.*, 2015).

4.4 Results

4.4.1 ChIP assay validation

ChIP-Seq samples were aligned to the Rn6 genome and normalised to 10million tags for comparison and visualisation using the UCSC genome browser. Prior to Seq, aliquots of each ChIP assay were

analysed for pSer2 Pol2 enrichment at the known GR regulated target, the clock gene *Per1*. Previously, increased Per1 nascent RNA production has been reported to be synchronised to rising and falling corticosterone levels, which were also associated to phasic GR binding at the distal upstream regulatory GRE (-2.5kb from the *Per1* TSS) (Stavreva *et al.*, 2009; Conway-Campbell *et al.*, 2011). RT-qPCR primers designed as positive and negative controls for GR binding at the distal GRE and an intronic region (intron 16) (Table 2) respectively, can still be used to investigate pSer2 Pol2 occupancy, but as recruitment is expected to be confined to within coding regions, the intronic primer becomes the positive control whilst the intergenic, distal GRE site would act as negative control.

Two-way ANOVA of pSer2 Pol2 occupation of the distal GRE site indicated an effect of infusion pattern ($p<0.0001$) but not of time ($p=0.2137$), however, there was a significant interaction between the two ($p=0018$). Post-hoc analysis revealed a lack of significant differences in pSer2 Pol2 enrichment between the corticosterone pulse peak (140min) and nadir (180min) (0.72 ±0.11 and 0.41 ±0.04 respectively) and neither was significantly different to VEH control at either 140min or 180min infused time points (0.46 ±0.06 and 0.48 ±0.06 respectively) (Figure 4.1 A). Therefore, no change in pSer2 Pol2 was detected at the upstream GRE in response to a pulsatile infusion of corticosterone as expected at an intergenic site. In contrast, constant infusion resulted in ~2-3 fold increase in pSer2 Pol2 enrichment at both 140min and 180min infused time points, which were significantly raised to matched VEH and pulsatile corticosterone infused time points ($p<0.001$ and $p<0.0001$ respectively). Despite two-way ANOVA indicating a significant interaction between time and infusion pattern, there was no significant difference of RNA Pol2 enrichment detected between 140min and 180min of constantly infused corticosterone (1.36 ±0.16 and 1.46 ±0.1 respectively). I postulate the observed significant interaction is due to the non-significant trend of increased pSer2 Pol2 enrichment at the corticosterone pulse peak in response to a pulsatile infusion.

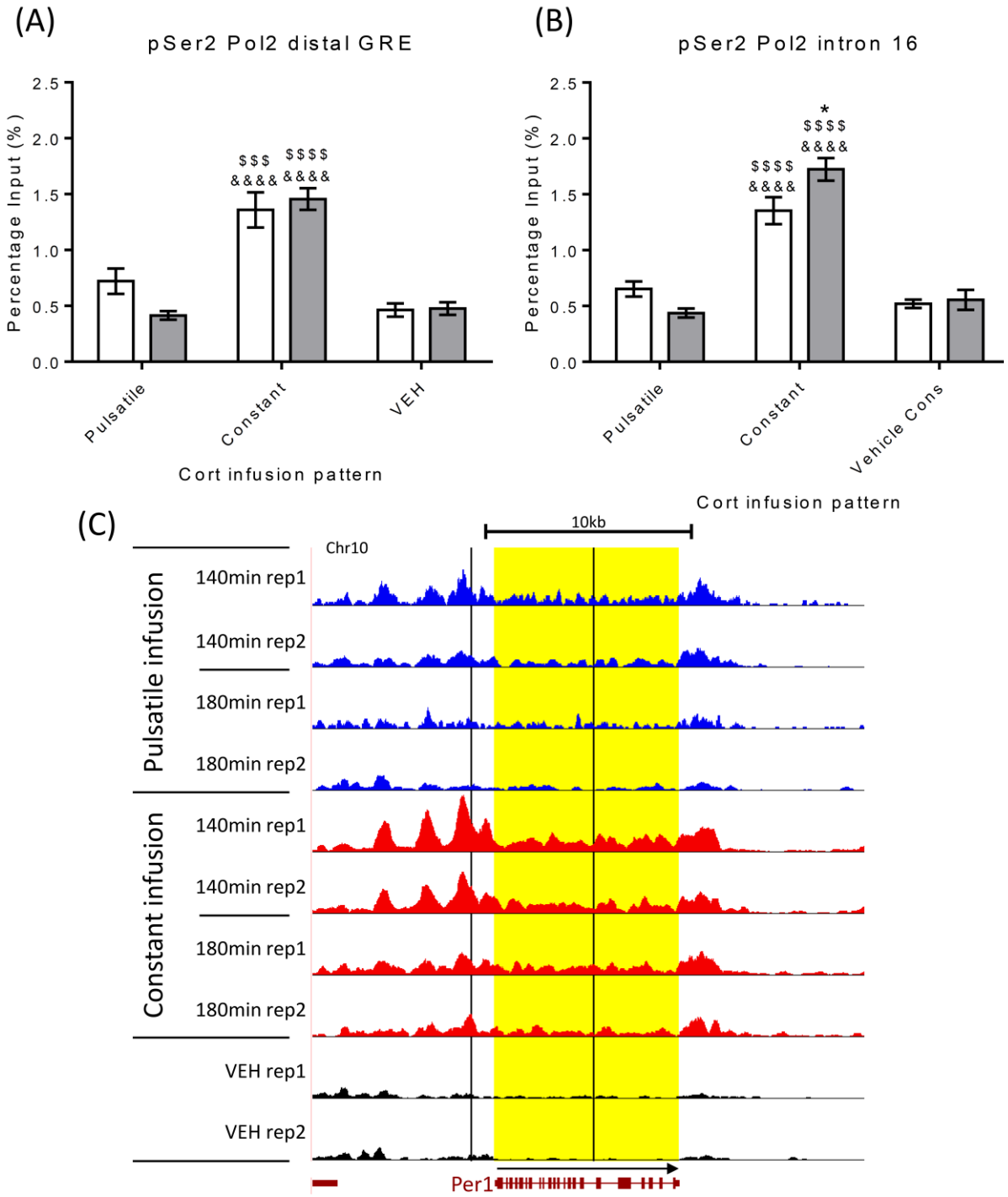

Figure 4.1 Assessment of positive and negative control sites for pSer2 Pol2 occupation to the clock gene Per1.

ChIP assay samples used in the Seq analysis, were evaluated by RT-qPCR to the distal GRE 2.5kb upstream of the clock gene Per1 (A). For pSer2 Pol2 enrichment at the Per1 distal GRE, two-way ANOVA detected a highly significant effect of corticosterone infusion pattern (p<0.0001), no significant effect of time (p=0.2137), but a significant interaction between pattern and time (p=0018). (B) At the Intron16 site, two-way ANOVA detected a highly significant effect of infusion pattern

*(p<0.0001), no significant effect of time (p=0.3786), but a highly significant interaction between pattern and time (p<0.0001). All significant differences detected by Bonferroni multiple comparison post-tests are shown on the graphs, with comparisons between corticosterone infused and VEH infused controls represented by & symbols, comparisons between time points (within infusion pattern) represented by * symbols, and comparisons between infusion pattern (at the same timepoint) represented by $ symbols. All data are expressed as mean ± s.e.m. Significance values are *,$,&p<0.05, **,$$,&&p<0.01, ***,$$$,&&&p<0.001, ****,$$$$,&&&&p<0.0001. (C) GR binding was visualised using the UCSC genome browser ChIP-Seq tag density pile around the Per1 coding region (bottom maroon track) of chromosome 10 (chr10:55,682,284-55,700,077). The site of the distal GRE is indicated by the left black line and intron16 by the right black line. Replicate traces for pulsatile (blue) and constant (red) corticosterone infusions at 140 and 180min timepoints are shown relative to VEH (black). pSer2-RNA Pol2 tag density traces within the Per1 gene coding region boundaries (highlighted in yellow), as well as upstream and downstream of Per1 coding region boundaries, are visibly and markedly increased for all corticosterone infused groups relative to VEH infused control groups. Chromosome number as well as 10kb scale bar indicated at the top of the genome browser shots. At the bottom, Per1 is transcribed from the anti-sense strand (left to right) and intron/ exon coding region (exon within intragenic maroon blocks) locations from Ensembl rn6 co-ordinates are indicated. Data normalised to 10million tags and y-axis 0-40.*

Despite the surprising enrichment of pSer2 Pol2 at the intergenic GRE region, occupancy was investigated at the Per1 intronic site. Two-way ANOVA analysis indicated an effect of infusion pattern ($p<0.0001$) but not of time ($p=0.3786$), however, a significant interaction was observed ($p<0.0001$). Post hoc analysis reported no significant difference in enrichment between pulsatile peak and nadir (0.65 ±0.07 and 0.44 ±0.04 respectively) or to either VEH infused time point (0.52 ±0.04 and 0.56 ±0.09 respectively). However, in response to a constant corticosterone infusion, both 140min and 180min time points (1.4 ±0.12 and 1.72 ±0.1 respectively) were significantly raised ~2-3 fold to time-matched pulsatile corticosterone and VEH time points ($p<0.0001$) (Figure 4.1 B).

Interestingly, the pattern of pSer2 Pol2 binding in response to the different patterned corticosterone and VEH infused time points were relatively similar at both sites (inter- and intra-genic). Therefore, as before, we visually inspected tag enrichment of aligned Seq data using the UCSC genome browser over a 17.5kb region encompassing and extending the *Per1* TSS and 3' end (Kent *et al.*, 2002). Subjective assessment of the distal primer site indicated tag density in response to pulsatile corticosterone infusion was marginally increased at the pulse peak compared to both corticosterone nadir and VEH UCSC tracks. Increased tag density was observed at 140min of constantly infused corticosterone

compared to all other patterned corticosterone and VEH infused time points, whilst the tag density after 180min of constantly infused corticosterone was more similar to the corticosterone pulse peak.

Subjective assessment of the UCSC tracks at the position of the intron 16 RT-qPCR primer site, indicated overall pSer2 Pol2 tag density levels were much lower compared to the distal GRE site across all conditions. However, when comparing between conditions at both distal and intronic sites, pSer2 Pol2 tag densities appeared to differ in a pattern dependent manner. pSer2 Pol2 occupancy was increased at the corticosterone pulse peak (140min) compared to nadir (180min), whereas constant corticosterone infusion induced increased occupancy across both matched time points. All of which were raised to VEH control. Due to the relatively low tag density at the intronic site however, the results observed in the RT-qPCR data are not easily visible. Furthermore, tag density was not concentrated within the *Per1* coding boundaries and extended well past the distal GRE site. Together, data visualised within the UCSC genome browser tracks strongly indicated regions chosen for our initial RT-qPCR assessment were far from ideally positioned and not suitable as positive or negative controls.

Unlike at *Per1*, it was discovered upon further inspection of UCSC genome browser tracks other known GC regulated targets such as serine dehydratase (*Sds*), *Tat* and *Gilz*; increased pSer2 Pol2 tag density was distributed in a defined manner to distal intergenic region densities, that was within annotated gene boundaries (TSS and 3' boundaries of intergenic regions) but often extended marginally into the 5' and 3' UTR of select genes (Figure 4.2) (Jantzen *et al.*, 1987; Su and Pitot, 1992; Wang *et al.*, 2004).

In response to a pulsatile corticosterone infusion, pSer2 Pol2 occupancy across all three targets appeared to be increased at the pulse peak compared to the nadir, indicating phasic, corticosterone synchronised increases in occupation. Interestingly, there was negligible pSer2 Pol2 tag density in the VEH control for *Sds* and *Gilz* (Figure 4.2). In contrast however, pSer2 Pol2 density within the *Tat* coding region, was visibly enriched in response to the VEH controls. In response to a pulsatile corticosterone infusion, tag density was marginally increased at the pulse peak (140min), but noticeably reduced by the nadir (180min) in comparison to the raised VEH levels. Indicating modulation of basal active transcription.

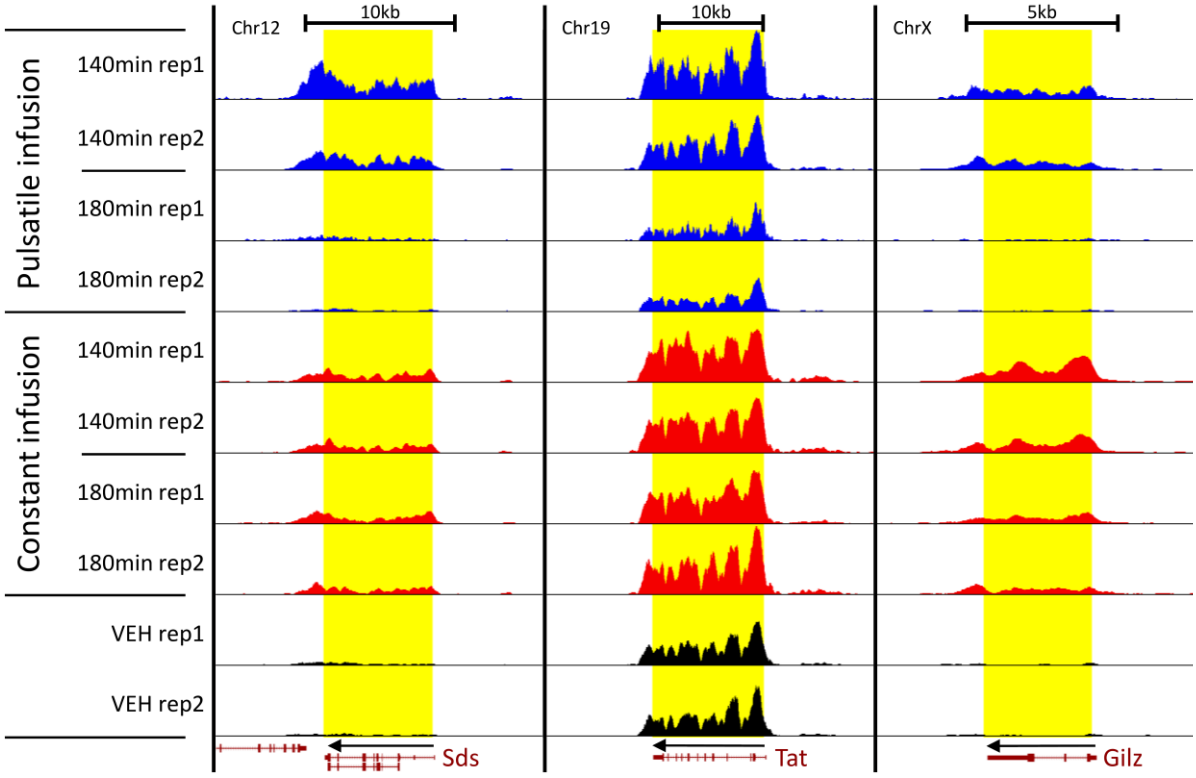

Figure 4.2 pSer2 Pol2 tag distribution over intragenic GC regulated gene regions.

Sequenced tag distribution of pSer2 Pol2 replicates in response to pulsatile, constant and VEH infusion after 140min and 180min was visualised using the UCSC genome browser within and extending from the TSS and 3' end of the GC regulated targets Sds (41,613,118-41,635,053b), Tat (41,665,082-41,696,752b) and Gilz (111,880,663-111,891,528b). pSer2 Pol2 occupation in response to a corticosterone or VEH infused time point is concentrated throughout intragenic, coded regions (highlighted in yellow) but often extends from the 5' and 3' end before returning to negligible levels. Chromosome number as well as 10kb and 5kb scale bars are indicated at the top of the genome browser shots. At the bottom, Sds, Tat and Gilz intron/ exon coding region (exon within intragenic maroon blocks) locations from Ensembl rn6 co-ordinates are indicated as transcribed from the anti-sense strand (right to left). Data normalised to 10million tags and y-axis 0-230.

In response to a constant corticosterone infusion, pSer2 Pol2 tag density (whilst variable between genes) was similar across time points for each respective gene. Compared to corticosterone pulse peak, constant corticosterone induced half maximal pSer2 Pol2 tag density within the Sds intragenic region, whilst *Tat* and *Gilz* were similar at both 140min and 180min infused time points. Subjectively, results indicate pSer2 Pol2 occupancy can be altered by infused corticosterone patterns in a similarly dynamic manner to previously reported GR recruitment profiles (Chapter 3). Additionally, I present evidence of gene specific basal pSer2 Pol2 occupancy in response to a VEH infusion at GC regulated genes within the liver of ADX rats.

In reference to the suitability of the *Per1* primer sites tested as positive and negative controls for pSer2 Pol2 occupancy; inspection of UCSC track data indicated *Per1* was far less ideal for measuring robust changes in pSer2 Pol2 occupancy compared to other candidate GC target genes. Intra- and intergenic associated tag density levels were very low as the track height was set to 40 for Per1 whereas other GC targets were set to 140. Further, tag densities were not defined between coded (intragenic) and non-coded (intergenic) regions in comparison to *Sds*, *Tat* and *Gilz* coded regions (Figure 4.1 & Figure 4.2). Therefore, *Per1* primers were determined to be ineffective negative and positive controls for pSer2 Pol2 analysis, but as visual inspection of other GC regulated targets indicated patterned corticosterone effects, analysis was continued across the genome.

4.4.2 pSer2 Pol2 tag enrichment detection

De novo pSer2 Pol2 enrichments were analysed using MUSIC, MACS2, findPeaks and hotspot peak detection algorithms. Upon visual inspection, enrichment regions were highly fragmented throughout key GC targets due to highly stochastic pSer2 Pol2 broad enrichments, as observed within Figure 4.1 and Figure 4.2 (Lee and Schatz, 2012; Harmanci, Rozowsky and Gerstein, 2014). Efforts to merge regions within suitable distances proved inaccurate, particularly when genes were within proximity to other 3' and 5' ends of other genes. Therefore, based on previously published methods (Stavreva *et al.*, 2015), pSer2 Pol2 enrichment was assessed according to the 5' and 3' loci of coding regions from the Ensembl genome (Rn6). Transcript regions smaller than twice the sequenced fragment lengths were removed, and regions restricted to 10kb if the transcript was longer.

4.4.3 pSer2 Pol2 assessment of replicate concordance

Pearson correlation coefficient analysis was applied for each corticosterone and VEH infused time point between replicates. Results indicated a large positive strength of association and concordance between replicates (>0.91) (Figure 4.3). As the same number of regions were investigated for all replicates, no indications can be made of the ability of a patterned corticosterone or VEH infused time point to induce changes between conditions. It should be noted, that even though strong Pearson correlation coefficients were reported, as a large number of regions are plotted (>11,000), non-concordant data could potentially be masked. Furthermore, gene variant genomic co-ordinates overlap, duplicating sequenced reads within the data, potentially biasing results.

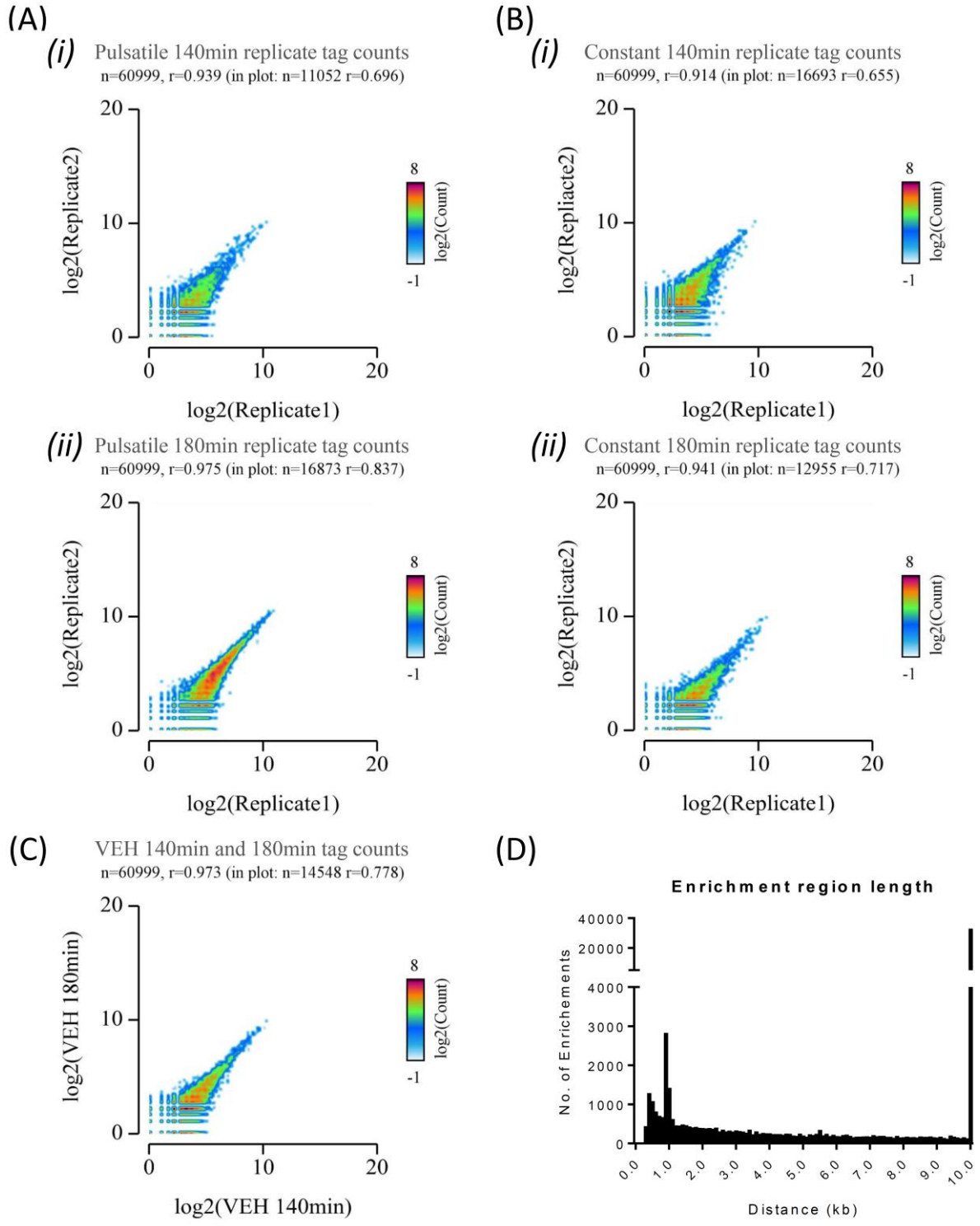

Figure 4.3 Characterisation of replicate concordance and distribution of intragenic region lengths investigated.

2D histograms of concordant enrichment tag counts (log2) within Ensembl coded regions for each replicate in response to either pulsatile (A) or constant corticosterone infusion (B) as well as VEH infusion (C) at 140min (i) and 180min (ii) time points. Pearson correlation coefficient analysis indicated strong replicate concordance (r>0.9) for all datasets. (D) Distribution of Intragenic regions lengths that

were >620b and limited to 10kb were plotted within the histogram. Percentiles reported minimum = 321b, 25th percentile = 2,606b, median =10kb, 75th percentile = 10kb, Mean = 10kb and maximum =10kb. 2D histograms plot normalised tag counts to 10 million with x and y-axis segmented into 100 bins; the number of regions within each bin is indicated by legend (log2) and images were produced by EASeq (Lerdrup et al., 2016).

4.4.4 pSer2 Pol2 tag density and distribution from the TSS

To investigate concordance between replicates, distribution of pSer2 Pol2 sequenced normalised tags upstream and downstream of the TSS was assessed for all conditions within 10kb coded regions on the sense strand only, to avoid plot misalignment of the TSS within histograms. Across corticosterone and VEH infused time points, maximal enrichment of sequenced tags was concentrated at +62.5b ±5.39 s.e.m. from the TSS (Figure 4.4 C). As the histograms plot a well-defined peak for all conditions and replicates, data indicates an increased concentration of pSer2 Pol2 occupancy just downstream of the TSS that is maximally variable between infused time points. Greatest tag density was observed in response to a constant corticosterone infusion replicates at 140min (4.6 and 3.99 per base per region) (Figure 4.2 Bi). The second highest density was observed in a single replicate (2.63 per base per region) in response to a pulsatile corticosterone infusion at the pulse peak (140min). In comparison, reduced tag density was reported for the second replicate (1.99 per base per region) (Figure 4.2 Ai) which was within the range of other corticosterone and VEH infused maximal tag densities.

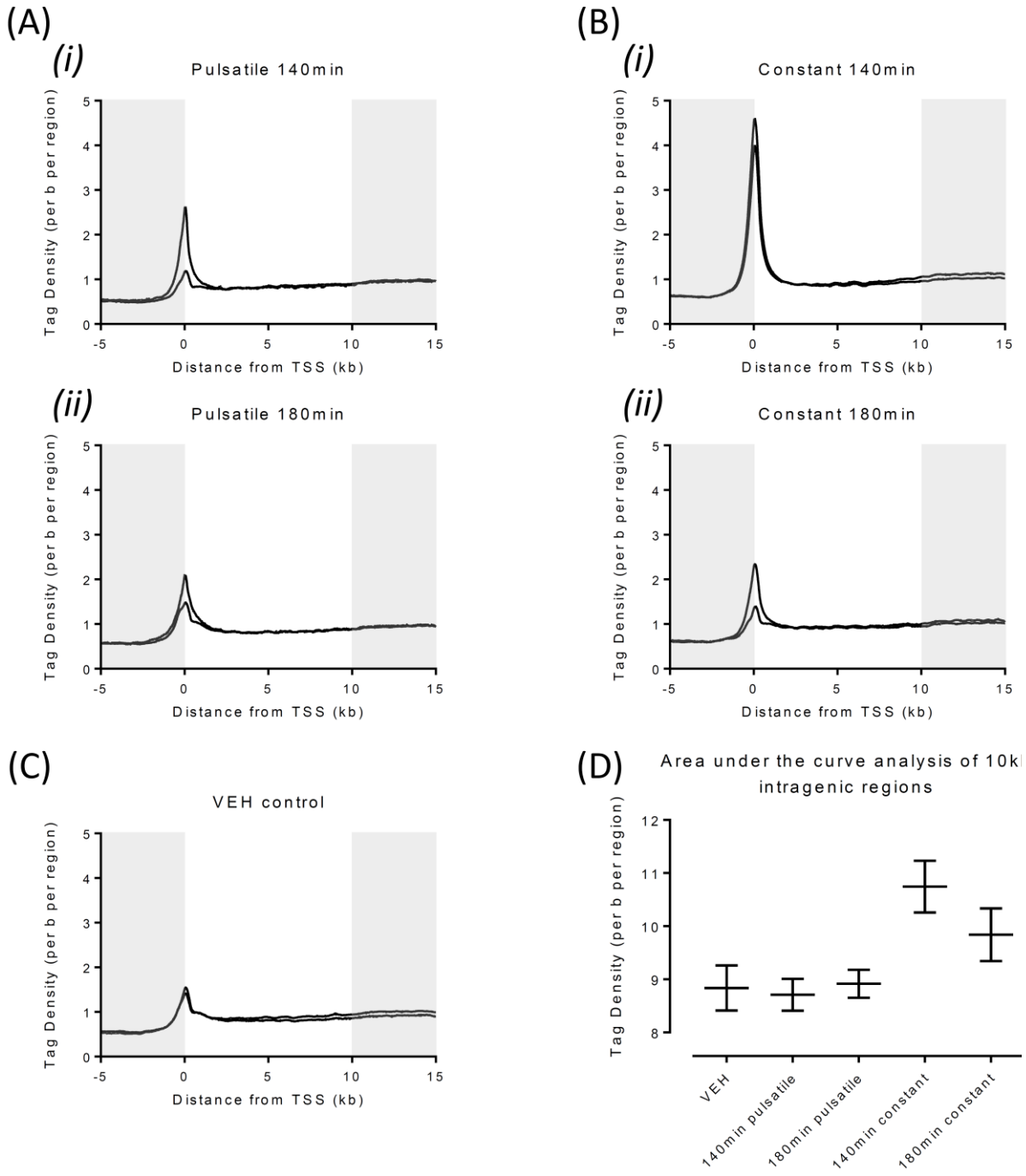

Figure 4.4 Replicate pSer2 Pol2 tag density, distribution and distance from TSS.

Tag density regions were restricted to coding regions equal to 10kb from the TSS and coded on the sense strand. Within these regions, tag density changes within -5kb to +15kb of the TSS were plotted using histograms in overlay for each replicate within each group, including pulsatile (A) or constant corticosterone (B) infusion at times 140min (i) and 180min (ii), compared to VEH (C) infusion. Some variation in replicate tag density and distribution can be visualised in these plots. Therefore, area under the curve analysis (D) was used to assess overall changes within a 0-10kb region from the TSS. Tags were normalised to 10 million and segmented in 5b bins, spanning -5kb and +15kb in each

direction from TSS. Tag density area under the curve was analysed between 0kb to +10kb of the TSS (un-shaded area).

Despite the reported changes in maximal tag densities, differential analysis assesses tag enrichment across the coding region to a maximal length of 10kb. Therefore, area under the curve analysis was used to assess potential changes in enrichment. Similarly to maximal tag density values, the greatest value was recorded in response to the constant corticosterone infusion after 140min (11.09 and 10.4 per base per region x kb) which was reduced by 180min (10.19 and 9.49 per base per region x kb) (Figure 4.2 D). Area under the curve results were lowered in response to both VEH (9.14 and 8.54 per base per region x kb respectively) and pulsatile corticosterone at 140min (8.92 and 8.50 per base per region x kb) and 180min (9.10 and 8.73 per base per region x kb) infused time points. Observations of median values indicated a slight drop in response to the corticosterone pulse peak (140min) compared to nadir (180min) and VEH infusions, however, as standard deviation between these conditions overlapped it is difficult to interpret.

Together these data indicate that tag density between replicates is similar when viewed across a 10kb intragenic region and patterned corticosterone infusion induces alterations in pSer2 Pol2 occupancy.

4.4.5 Detection of significant changes in pSer2 Pol2 occupancy

Prior to any differential analysis, VEH replicates were analysed at all binding regions by DESeq2 and no significant differences in tag density were detected (data not shown); therefore, both VEH replicates were pooled.

To investigate statistically relevant corticosterone induced changes in pSer2 Pol2 occupancy relative to VEH control, total Seq raw tag counts were normalised and analysed by DESeq2. In response to a pulsatile corticosterone infusion, a greater number of regions were differentially enriched (relative to VEH control) for pSer2 Pol2 at the corticosterone pulse peak (140min) (Figure 4.5 A) compared to nadir (180min) (Figure 4.5 B). Volcano plots also indicate data is skewed towards a loss in pSer2 Pol2 occupancy at both pulsatile infused time points.

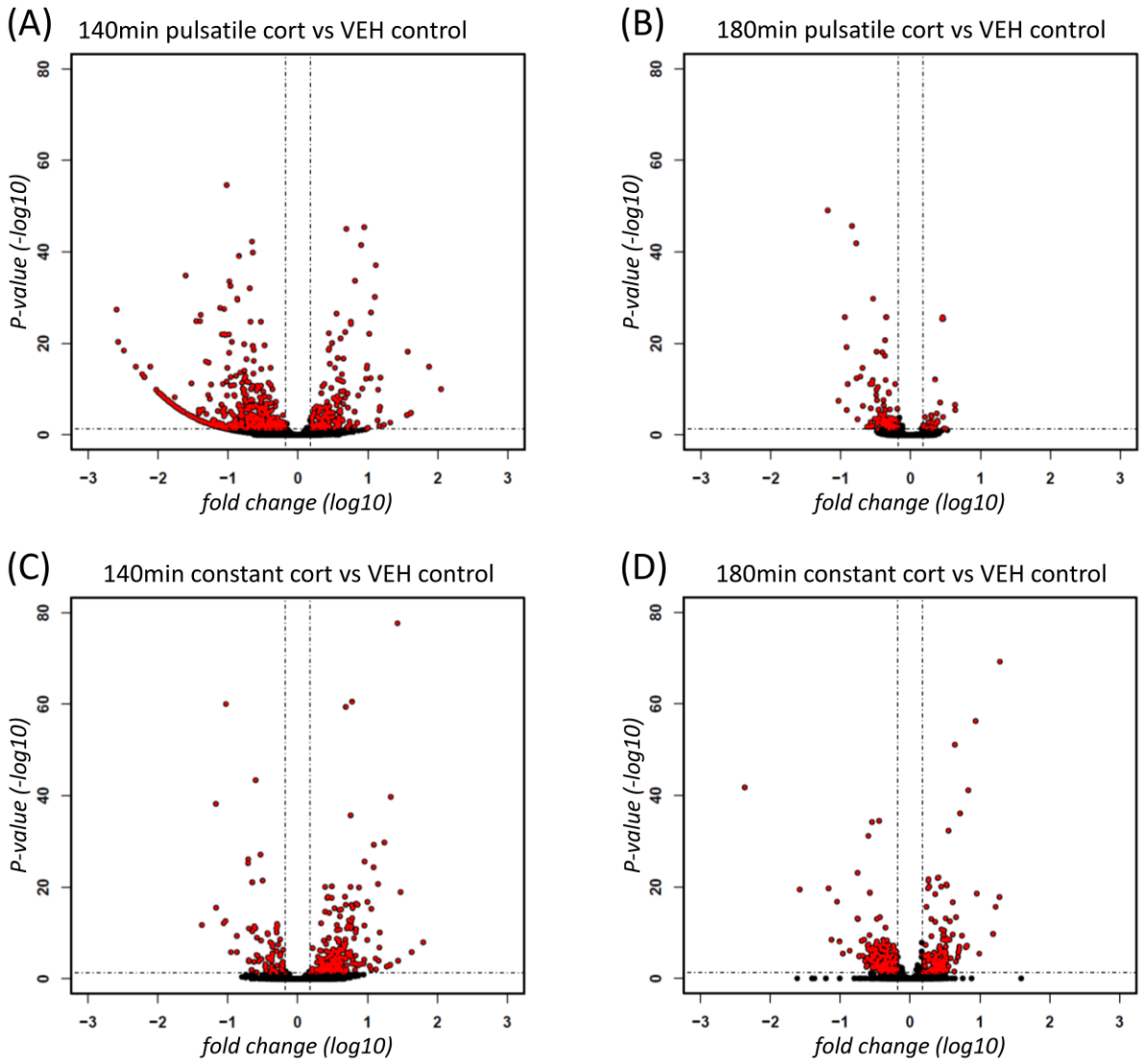

Figure 4.5 Modulation of pSer2 Pol2 enrichment over time during pulsatile and constant corticosterone infusion.

Volcano plots showing changes in pSer2 Pol2 tag density enrichment in response to pulsatile corticosterone infusion at 140min (corticosterone pulse peak) (A) and at 180min (corticosterone pulse nadir) (B) as well as constant corticosterone infusion at 140min (C) and 180min (D) relative to VEH control. Significant changes in pSer2 Pol2 enrichment within Ensembl gene coding regions (indicated in red) appeared to be greatest in the 140min pulsatile corticosterone dataset, which was markedly reduced in the 180min pulsatile corticosterone dataset. In contrast, number of intragenic regions subject to significant increased or decreased pSer2 Pol2 enrichment appeared similar between the constantly infused corticosterone time points. X-axis indicates fold change (log10) and y-axis the adjusted p-value (-log10).

Subjectively, little difference was observed between the distribution of significantly gained or lost pSer2 Pol2 occupied targets after 140min and 180min constant corticosterone infused time points

(Figure 4.5 C & D). However, the number of differentially regulated regions appeared to be reduced to corticosterone pulse peak but raised to corticosterone pulse nadir with no obvious bias for gain or loss in pSer2 Pol2 occupancy. Interestingly, there were no indications within the DESeq2 analysis of the increased enrichment of pSer2 Pol2 as indicated by area under the curve data in response to constant corticosterone infusion (Figure 4.4 D). This is potentially due to the normalisation of tag counts within the DESeq2 analysis.

With reference to the clock gene *Per1* investigated previously (Figure 4.1), DESeq2 analysis indicated pSer2 Pol2 enrichment fold change to VEH was greater than significance thresholds. However, the adjusted p-value did not pass significance threshold (>0.433) (data not shown). Therefore, this study could not identify *Per1* as a robust, pattered corticosterone regulated targets within these conditions and analyses.

4.4.6 pSer Pol2 dynamics

Out of all the regions assessed for pSer2 Pol2 occupancy, only individual Ensembl gene IDs were kept for downstream analysis. If multiple variants were significantly regulated, the region with the greatest cumulative fold change across corticosterone infused time points was kept. All other regions, as well as those with no significant change in response to corticosterone were removed, revealing a total of 715 targets as differentially regulated by a single, or combination of, pattern corticosterone infused time points relative to VEH control (Figure 4.6).

In response to a pulsatile corticosterone infusion, 77.3% of regulated targets had significantly altered pSer2 Pol2 enrichment relative to VEH control at the pulse peak (140min) which was reduced to 14.5% of targets within the nadir (Figure 4.6). At both time points, the majority (~3/4) had significantly decreased pSer2 Pol2 enrichment relative to VEH control, albeit more distinct within the pulse peak due to the greater number of targets. Taken together, these data report that pulsatile corticosterone infusion can induce phasic and synchronised changes in pSer2 Pol2 occupation to the corticosterone pulse peak over specific genes, which was decreased across the majority of targets. Indicating a down-regulation of transcription that would be more distinct at the pulse peak than nadir.

(A)

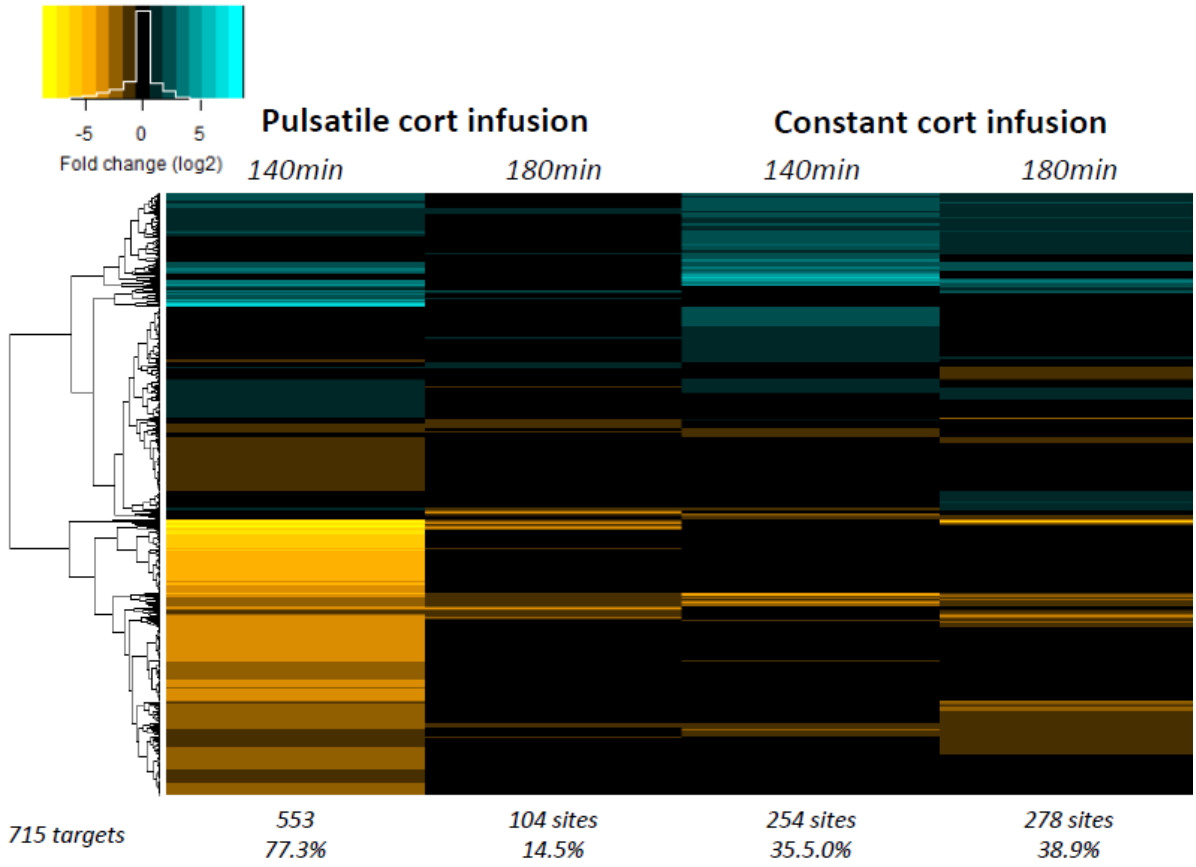

(B)

		Up-regulated	Down-regulated
Pulsatile	140min	147	406
	180min	24	80
Constant	140min	196	58
	180min	138	140

716 cort regulated sites

Figure 4.6 Pattern and time dependent pSer2 Pol2 genome-wide enrichment profiles.

pSer2 Pol2 tags were normalised to total sequenced tag counts and significant fold changes were defined as >0.585 or <-0.585 (log2), p-value <0.05 adjusted for multiple comparisons and FDR <0.05 from VEH control. Only the greatest cumulative fold change for each target variant is reported. (A) pSer2 Pol2 differentially increased (cyan) or decreased (yellow) enriched regions were hierarchically clustered according to amplitude of fold changes in response to each corticosterone infused time point. Heatmap colour intensity indicates degree of fold change (log2) as shown within the legend (top left) as well as distribution (white trace). (B) Table reports the number of pSer2 Pol2 differentially

intragenic regions and direction of change by either pulsatile or constant corticosterone infusion at 140 and 180min time points, relative to VEH control.

In response to 140min constantly infused corticosterone, 35.5% of regions were differentially enriched for pSer2 Pol2, which was marginally increased to 38.9% by 180min. Contrary to the pulsatile corticosterone infusion effects, ~3/4 regions reported an increased pSer2 Pol2 enrichment at the constantly infused matched time point for the corticosterone pulse peak. This was not observed by 180min, as the total numbers of increased or decreased pSer2 Pol2 enriched regions were equally distributed.

Together, these data indicate that changes in pSer2 Pol2 occupation are synchronised to oscillating corticosterone levels and GR binding dynamics at select genes, which became dysregulated by a constant corticosterone infusion. I also report distinct differences in transcription between infusion patterns, as pulsatile corticosterone exposure was more effective at inducing repression whilst constant exposure was more effective at activation of the majority of genes.

To investigate if an individual corticosterone infused time points was more effective at inducing changes in pSer2 Pol2 occupation, the distribution of fold change values to VEH was investigated. Time dependent differences in response to either infusion pattern indicated percentile values for both increased and decreased pSer2 Pol2 occupancy fold change were greatest at 140min compared to 180min (Figure 4.7 B).

Comparison of percentile values between infusion patterns, indicated losses of pSer2 Pol2 occupancy were greater at the pulsatile infused, corticosterone peak (140min) compared to either constant infused time point, whilst 140min of constantly infused corticosterone induced the greater percentiles of fold change for increases in pSer2 Pol2 enrichment. Corticosterone pulse peak nadir (180min) had the lowest percentile fold change values whether pSer2 Pol2 enrichment was increased or lost. These results validate previous observations within Figure 4.6.

(A)

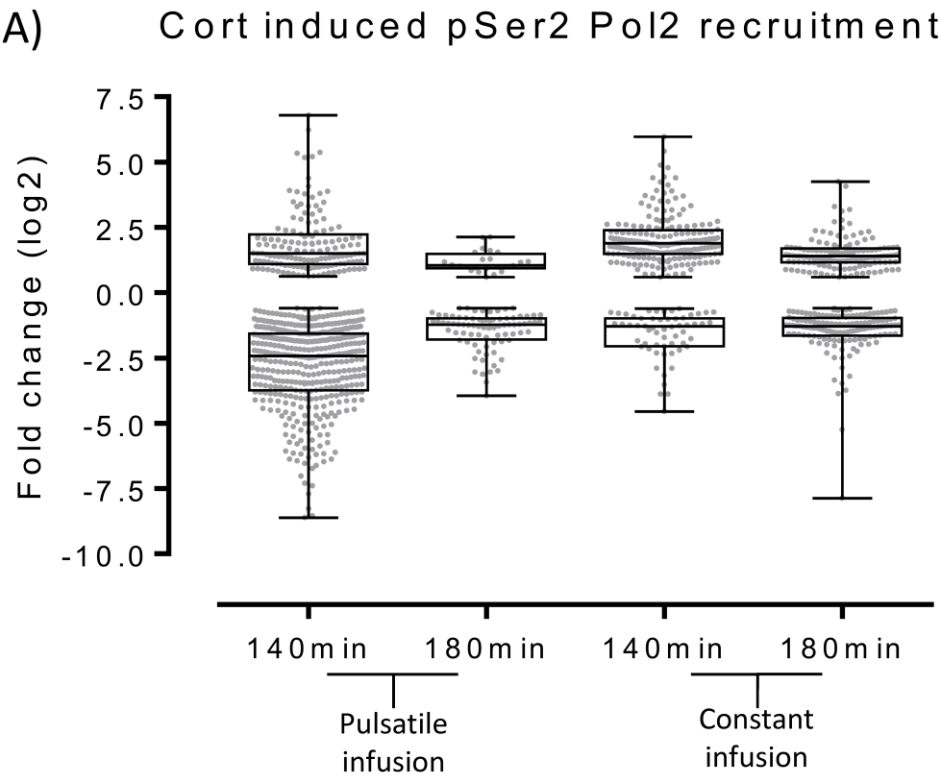

(B)

	Cort infusion	Min	25th percentile	Median	75th percentile	Max
Fold change increase to VEH control (log2)	140min pulsatile	0.63 | -0.59	1.09 | -1.56	1.50 | -2.42	2.23 | -3.74	6.79 | -8.62
	180min pulsatile	0.59 | -0.59	0.92 | -0.99	1.04 | -1.23	1.48 | -1.79	2.13 | -3.94
	140min constant	0.59 | -0.59	1.48 | -0.98	1.89 | -1.29	2.40 | -2.06	5.97 | -4.55
	180min constant	0.60 | -0.60	1.15 | -0.96	1.40 | -1.29	1.70 | -1.65	4.26 | -7.87

Figure 4.7 Distribution of fold change and p-values of differentially regulated pSer2 Pol2 intragenic regions.

(A) Distribution of fold increased or decreased (log2) pSer2 Pol2 enrichments within intragenic regions against respective p-values were plotted in response to corticosterone infused time points compared to VEH control were plotted. (B) Table reports quartile values for both gained and lost fold changes (log2) in pSer2 Pol2 enrichment in response to each corticosterone infused time point compared to VEH control. pSer2 Pol2 tags were normalised to total sequenced tag counts and regions filtered for enrichment fold changes >0.585 or <-0.585 (log2), p-value adjusted for multiple comparisons <0.05 and FDR<0.05 from VEH control. Only the greatest cumulative fold change for each target variant is reported.

I then investigated if a combination of patterned corticosterone infused time points were more effective at inducing changes in pSer2 Pol2 enrichment within the same region. Results report pulsatile corticosterone infusion at the pulse peak (140min) alone induced changes in the greatest number of regions, regulating 297 genes (Figure 4.8). Interestingly, the next largest number of regions were regulated by a combination of 140min constant only (77 genes), 140min pulsatile/ 180min constant (73 genes) or 140min pulsatile/ 140min constant/ 180min constant (78 genes) corticosterone infused time points. This is of interest as these combinations of time points are all associated with raised circulating corticosterone levels (Figure 2.3), unlike the negligible levels found at the pulsatile corticosterone nadir (180min). Indicating a strong correlation between raised circulating corticosterone and inducible changes in pSer2 Pol2 occupation.

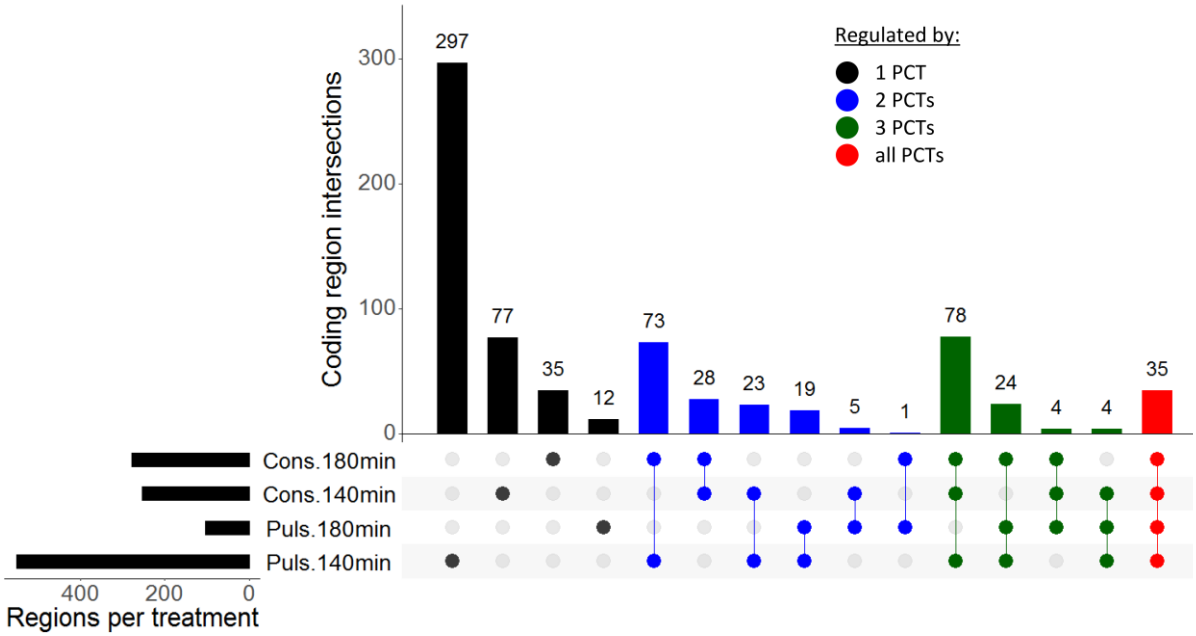

Figure 4.8 Number of pSer2 Pol2 enrichments regulated by one or multiple corticosterone pattern infused time points.

Intragenic regions were investigated for differential pSer2 Pol2 recruitment, relative to VEH control in response to corticosterone infused time points. Regions were plotted according to whether a single or multiple corticosterone infused time point induced changes in occupancy. The largest number of regions were regulated by 140min pulsatile corticosterone infusion only, equal to 42% of all corticosterone regulated regions. The next largest number of regions were regulated by three combinations of infused time points including 140min constant only; 140min pulsatile and 180min constant; 140min pulsatile, 140min constant and 180min constant corticosterone infusion. These represent 10-11% of all regulated regions. Total number of differentially pSer2 Pol2 recruited intragenic regions by each corticosterone infused time point is indicated by the bottom left horizontal

bar chart. Regulation by a single or multiple infused time point are indicated by spots and the number directly above the corresponding bar. Colour indicates whether a single (black), two (blue), three (green) or all four (red) infused time points differentially regulated pSer2 Pol2 occupancy and were plotted using UpSetR (Conway, Lex and Gehlenborg, 2017).

4.4.7 Time and pattern dependent pSer2 Pol2 occupancy

Similar to previous GR ChIP-Seq data; because pulsatile corticosterone infusion regulated distinct changes in pSer2 Pol2 occupation compared to constantly infused time points, time and pattern dependent differences between corticosterone infused time points were investigated by DESeq2 analysis.

Significant time dependent changes in pSer2 Pol2 enrichment between the corticosterone pulse peak (140min) and nadir (180min) were detected at 60.3% of regions in response to a pulsatile corticosterone infusion. This indicated robust phasic changes in pSer2 Pol2 occupation (Figure 4.9), whereas, in response to the constant corticosterone infusion, just 14.1% of sites were regulated.

Significant pattern dependent changes were investigated at either corticosterone pulse peak (140min) or at the nadir (180min) and compared to both 140min and 180min of constantly infused corticosterone. Pulsatile corticosterone peak induced differential enrichment in 35.4% of regions, which was reduced to 15.9% in response to 140min and 180min constant infused time points respectively. Though a greater degree of differentially regulated regions were identified between the pulsatile corticosterone nadir and either constant infused time point (27.7% and 24.1% respectively).

Together, these data indicate robust, pulsatile corticosterone synchronised pSer2 Pol2 occupancy across majority of targets is dysregulated by a constant corticosterone infusion. Interestingly, unlike the GR ChIP-Seq data, there were more differences at 140min between the pulsatile and constant infusions compared to the 180min time point, most likely due to the differing induction of inhibition and activation by the two patterns. Particularly as these data indicate pro-longed corticosterone induced transcription which was also reported for GR binding in response to a constant infusion.

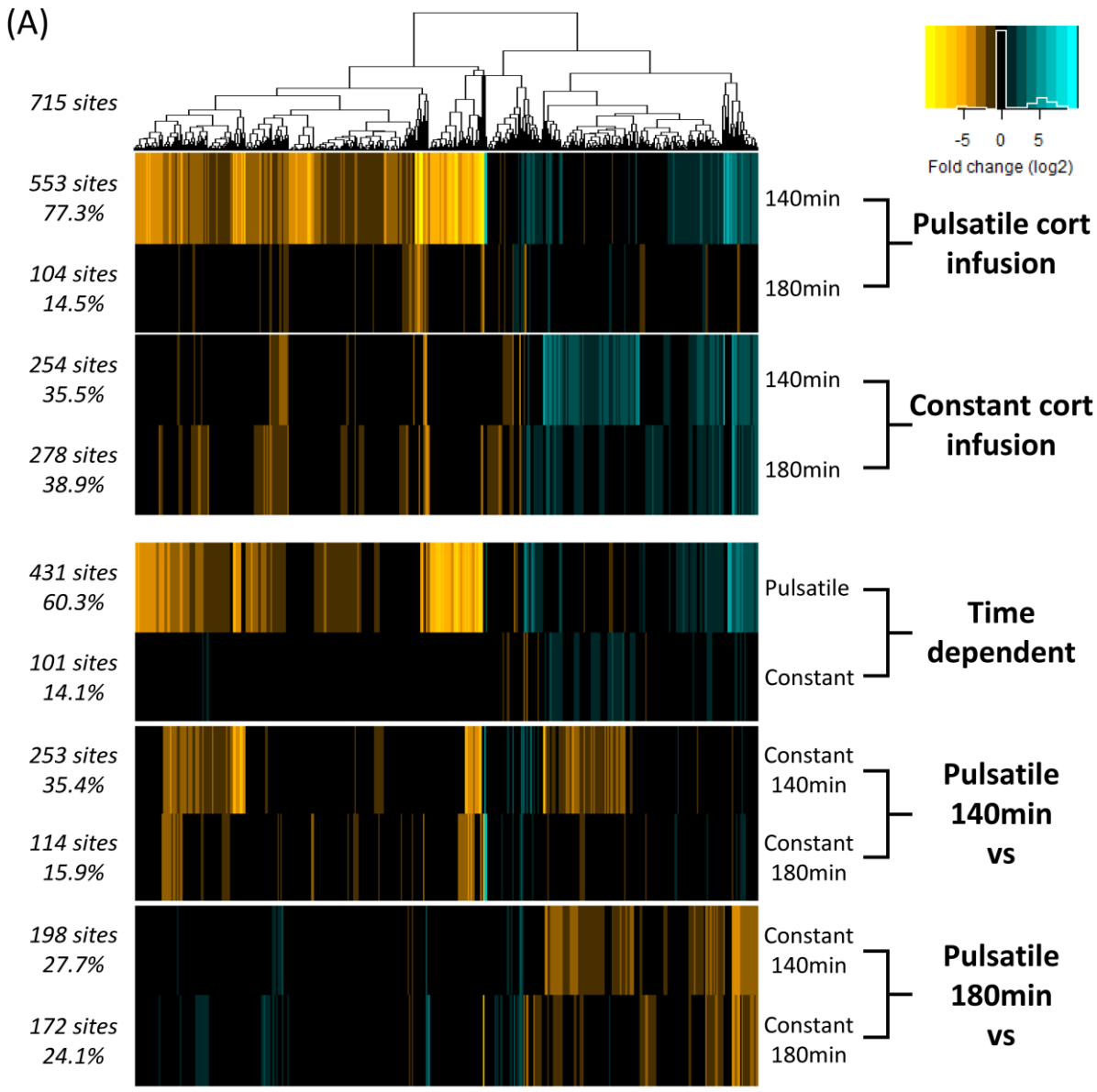

Figure 4.9 Changes in pSer2 Pol2 occupancy in response to infused patterned corticosterone time points.

Heatmap visualisation of pSer2 Pol2 differentially increased (cyan) or decreased (yellow) enriched regions, hierarchically clustered according to amplitude of fold change in response to each corticosterone infused time point. First four rows indicate fold change (log2) of corticosterone infused time points against VEH control. The next two rows below represent time dependent changes between 140min and 180min infused time points in response to a pulsatile infusion and then constant corticosterone infusion. The next double rows represent comparisons between 140min pulsatile corticosterone (corticosterone pulse peak) against either 140min or 180min constant corticosterone infusion. Final two rows represent comparisons between 180min pulsatile corticosterone infusion (corticosterone pulse nadir) against either 140min or 180min constant corticosterone infusions. pSer2 Pol2 tags were normalised to total sequenced tag counts and regions filtered for enrichment fold

changes >0.585 or <-0.585 (log2), p-value <0.05 adjusted for multiple comparisons and FDR<0.05 from VEH control. Only the greatest cumulative fold change for each target variant is reported and heatmap colour intensity indicates degree of fold change (log2) as shown within the legend (top right) as well as distribution (white trace).

4.5 Discussion

pSer2 Pol2 enrichment at a selection of targets within the liver has been shown to be highly phasic in response to mock ultradian pulses of corticosterone delivered into the circulation of adrenalectomised rats that are not intrinsic as dynamics become dysregulated in response to a matched constant corticosterone infusion. I therefore report, within the liver, both GR binding as well as transcriptional regulation is robustly regulated by ultradian corticosterone rhythms and their dysregulation.

Interestingly, as with the induction of GR binding, pulsatile corticosterone infusion at the pulse peak (140min) induced changes in pSer2 Pol2 occupancy within the greatest number of genes compared to any other corticosterone infused time point (Figure 4.6). Further, I report differing patterns of corticosterone exposure can opposingly regulate transcriptional activity, as 3 out of 4 differentially occupied targets reported a loss in pSer2 Pol2, indicating a repressive transcriptional effect of pulsatile corticosterone exposure. In contrast at the matched time point, constantly infused corticosterone induced the opposite in 36% of regulated genes, indicating overall activation of transcription. Together, these data report differing patterns of corticosterone exposure *in vivo* can have distinct and opposing transcriptional effects within the rat liver. A previous study using Affymetrix GeneChip technology to investigate the effects of a 20min 100nM corticosterone administration on nerve growth factor-differentiated catecholaminergic (PC12) cells, found only downregulation of GC responsive genes within 1hr of hormone washout. However, upregulation of genes was detected much later, at the 3hr timepoint (Morsink *et al.*, 2006). This is of interest as my data within the liver indicates a predominantly repressive action of transcription in response to acute, transient pulsatile corticosterone exposure, but the opposite during constant corticosterone infusion. In contrast, a genome-wide study assessing dynamic pSer5 Pol2 occupancy in mouse mammary adenocarcinoma cells at the MMTV array found mostly increased pSer5 Pol2 occupancy in response to both a pulsatile and constant corticosterone treatment over 60min (Stavreva *et al.*, 2015). Despite similarities in analyses methods, there were a number of different conditions; my study investigated occupancy of a different phosphorylated forms of RNA Pol2, within an animal model as opposed to an artificial construct in a cell line, doses of corticosterone cannot be matched and widely differing time points were analysed. Therefore, it is difficult to compare confidently across studies other than identifying both show differing patterns of corticosterone exposure modulates transcriptional activity. Similar

issues arise when comparing other *in vivo* studies. hnRNA microarray or pSer5 Pol2 ChIP-Seq analysis within adrenalectomised rat livers revealed the proportion of differentially occupied targets was slightly skewed towards repression after 6hr or 1hr Dex administration respectively (Duma *et al.*, 2010; Grøntved *et al.*, 2013). But, ligand specific effects cannot be discounted, as the study by Stavreva., et al. (2015) reported an overall loss of RNA Pol2 occupation in response to Dex, whereas corticosterone was inducive (Stavreva *et al.*, 2015). Together, these data highlight the importance of physiologically relevant, dynamic GC regulation of transcription as well as the need for clarity in response to differing patterns as well as differing GC ligands within *in vivo* models of biological systems as opposed to artificial constructs such as the MMTV array.

An intriguing density profile was discovered during the interrogation of pSer2 Pol2 tag distribution around the TSS. Distinct peaks of sequenced tags were consistently observed in response to any corticosterone and VEH infused time point between +35b to +95b from the TSS, which could be explained by a promoter-pausing model of transcription (Figure 4.4). When RNA Pol2 is recruited to the promoter, the complex can enter the elongation phase and transcribe a short nucleotide sequence (about +50b in mammalian cells) prior to pausing that would explain the increased presence of RNA Pol2 at these positions (Rougvie and Lis, 1988; Muse *et al.*, 2007; Core, Waterfall and Lis, 2008; Rahl *et al.*, 2010; Quinodoz *et al.*, 2014). This process has been described as a common bimodal model of RNA Pol2 occupancy and transcription within mammalian cells and to my knowledge has not been shown in this manner (Quinodoz *et al.*, 2014).

The investigation undertaken within this study identified a total of 715 corticosterone regulated genes to VEH control (Figure 4.6). This is a relatively restricted list when one considers the total number of genes within the Ensembl rat genome build. Whether my analysis was too restrictive or suitably sensitive is difficult to ascertain as a major analytical limitation was the inability to perform *de novo* identification of enriched pSer2 Pol2 occupied regions to background. Detection algorithms fragmented broad stochastic enrichments that were not overcome via merging of proximal regions and was further compounded when analysis was compared across corticosterone and VEH infused time points for differential analyses. Therefore, a method was adopted from a previous study by defining enrichment regions according to Ensembl (Rn6) genomic co-ordinates (Stavreva *et al.*, 2015). It became evident during preliminary analysis via inspection of UCSC genome browser tag density traces, that broad pSer2 Pol2 enrichments often did not align with gene intragenic boundaries loci, indicating that despite improvements from previous iterations and genomic loci within the rat genome may not be suitably accurate for this type of analyses. As loci are based heavily on RNA Seq data, inaccurate intragenic boundary loci can be reported. Together, this can introduce a large degree of

error as indicated by UCSC genome browser screenshots for the GC regulated, metabolic target *Lpin1* (Figure 4.10). If the analysis included only the larger single variant, the pSer2 Pol2 enriched region would be missed. Due to the same tags being counted within overlapping variants and genes, tag bias could also be introduced to the DESeq2 normalisation. Despite these limitations, the method used in this study was the best available for this data, and whilst not perfect, still reports a selection of statistically significant and robust changes in hepatic transcriptional regulation *in vivo*. Satisfying the original aims of the research.

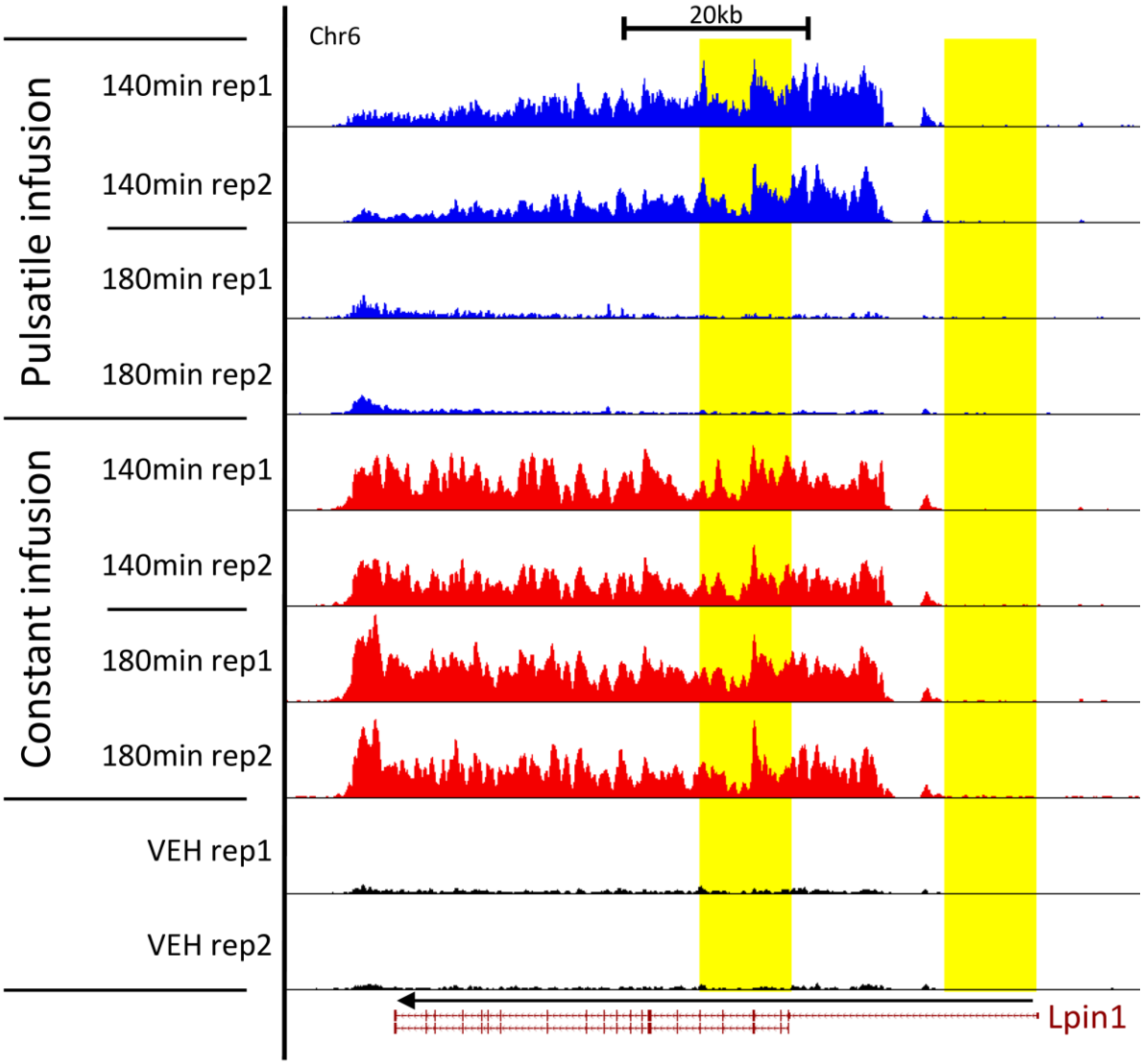

Figure 4.10 Lpin1 variants and regions of pSer2 Pol2 enrichment analysed.

Sequenced tag distribution of pSer2 Pol2 replicates in response to pulsatile, constant and VEH infusion after 140min and 180min were visualised using the UCSC genome browser within and extending from the TSS and 3' end of the GC regulated target Lpin1 (41,788,031-41,881,762b). pSer2 Pol2 occupation in response to a corticosterone or VEH infusion is concentrated within the intragenic region for both variants. However, pSer2 Pol2 enrichment begins ~15kb downstream from the larger of the two

variants and upstream of the smaller variant TSS. Raised levels continue throughout and marginally past the 3' end of both. As analysis was restricted to a 10kb region from the TSS (highlighted in yellow) only analysis of the smaller variant would incorporate increased pSer2 Pol2 tag densities. Chromosome number as well as 10kb and 5kb scale bars are indicated at the top of the genome browser shots. At the bottom, Lpin1 intron/ exon coding region (exon within intragenic maroon blocks) locations from Ensembl rn6 co-ordinates are indicated as transcribed from the anti-sense strand (right to left). Data normalised to 10million tags and y-axis 0-230.

In conclusion, this data presents evidence that pSer2 Pol2 recruitment to a select number of targets within an ultradian corticosterone replacement paradigm, is strongly phasic and synchronised to rising and falling levels of circulating corticosterone and reported dynamic GR binding to the genome. My data further demonstrates that this well-regulated relationship, between ligand, receptor and transcriptional outcome becomes dysregulated when exposed to constant circulating corticosterone, with marked changes in transcriptional regulation of GC target genes over time. My study highlights the potential impact patterned GC exposure can have on a metabolically important target organ such as the liver.

Chapter 5 Characterisation of GR binding and RNA Pol2 occupancy and pathway analysis reveals potential mechanisms for glucocorticoid dysregulated pathologies.

5.1 Background

Over the last two chapters, I have shown how ultradian GC pulses induce synchronised phasic GR and RNA Pol2 binding across the genome. I report in Chapter 3 that of the 2,708 binding events induced at the pulse peak, all were lost by the nadir in response to a pulsatile corticosterone infusion. Similarly, but to a reduced degree, I report in Chapter 4 that 553 genes were differentially occupied at the pulse peak compared to just 104 by the nadir. Together, these data indicate robust phasic and synchronised GR binding as well as transcriptional activity by oscillating corticosterone levels. Interestingly, decreased pSer2 Pol2 occupancy was detected within majority of targets at both corticosterone peak and nadir; indicating an overall inhibitory effect. These dynamics were dysregulated in response to a dose-matched constant corticosterone infusion, as GR binding was no longer phasic but maintained in a prolonged manner and pSer2 Pol2 occupancy was also dysregulated. Interestingly, at the matched time point for the corticosterone pulse peak, constant infusion increased occupancy for majority of genes. Indicating phasic dynamics are distinctly dysregulated by a constant corticosterone infusion and I provide evidence that these changes induce opposing transcriptional activity.

Within this chapter I will investigate the relationship between pattern dependent GR binding and pSer2 Pol2 occupancy of GC target genes. Additionally, using pSer2 Pol2 occupancy as a proxy for active transcription, I will perform functional pathway analysis on my identified set of pattern dependent differentially regulated genes to determine whether changes are associated with metabolic dysfunction or other disease states.

5.2 Aims

1) Investigate potential GR mediated effects of pSer2 Pol2 occupancy in response to patterned corticosterone.
2) Assess pSer2 Pol2 changes in occupancy and their potential effect on metabolic downstream pathways.
3) Identify key pathways and gene targets that are differentially regulated by different corticosterone patterned infusion, with particular focus on any that may play a significant role within metabolic dysregulation.

5.3 Methods

All methods of analysis were done according to general methods discussed within Chapter 2.

Briefly, GR binding sites as well as pSer2 Pol2 occupied sites that were significantly regulated by patterned corticosterone infusion compared to VEH control were used in all downstream analysis.

Genic locations of GR binding sites as well as measurements of distance from the closest GR binding site to the TSS of a differentially pSer2 Pol2 occupied target was calculated using annotatePeaks.pl (HOMER) (Heinz *et al.*, 2010) and graphs plotted using Prism v6.07 for Windows (La Jolla California, USA, www.graphpad.com).

For the pathway analysis pSer2 Pol2 ChIP-Seq DESeq2 data were analysed via the Ingenuity Pathway Analysis package ©IPA (Qiagen Inc., https://www.qiagenbioinformatics.com/products/igenuity-pathway-analysis). Enrichment of pathways were identified from genes with fold changes >1.5-fold and adjusted p-value <0.05 to VEH control and z-score predictions assessed from liver tissue and HepG3, hepatoma, hepatocyte cell lines as well as mice, rat and human published data. Positive and negative z-scores represent either predicted activation or inhibition respectively based upon the fraction of genes known to regulate the particular pathway and degree of fold change and significance. The greater the predictive confidence, the greater the z-score. Documentation indicates a z-score >2 (or <-2) represents a significant prediction. Z-score values were plotted using GraphPad Prism v6.07 for Windows (La Jolla California, USA, www.graphpad.com).

5.4 Results

5.4.1 Induction of GR binding and pSer2 Pol2 occupancy at select GC regulated targets

The GC regulated targets *Per1*, *Sds*, *Tat*, *Gilz* and *Lpin1* were visually inspected using the UCSC genome browser for validation of GR binding sites characterised within the literature as well as pSer2 Pol2 regulated occupation. Previously, two transcriptionally regulating GR binding sites have been characterised for *Per1*, the distal of which has been described as 'hypersensitive' for GR binding (Reddy *et al.*, 2012). In the human alveolar epithelial A549 cell line, these two GRE containing GR binding sites were identified 2kb upstream of the TSS and within intron1 according to the hg19 version of the human genome (Reddy *et al.*, 2012). Whereas in the mouse liver, as well different cell lines, both GR binding sites were found within the first intron. It should be noted, the genome build was not indicated by the authors, making it difficult to make comparisons between studies (Grøntved *et al.*, 2013). Together this data indicates two GR binding sites are conserved between mammals and genome builds, but variable in location to the TSS. In my data, two corticosterone regulated GR binding sites

were discovered at ~-1kb (chr10:55,685,633-55,686,257) and ~-3.5kb (chr10:55,683,482-55,684,046) upstream of the TSS. Both were bound by GR at all corticosterone infused time points except for pulse nadir (180min) (Figure 5.1). However, investigation of significant corticosterone time and pattern dependent changes were highly variable. Despite a 16- and 17-fold induction of GR binding at the ~-1kb and ~-3.5kb binding sites respectively in response to the corticosterone pulse peak (140min), no significant changes were reported to the corticosterone pulse nadir (180min) at either site. Indeed, no significant changes were detected between corticosterone infused time points at the proximal ~-1kb site. Whereas, at the distal site (which has been described as 'hypersensitive'), a 2.4-fold time dependent induction of GR binding was detected at 140min compared to 180min constant corticosterone infusion. This increase at 140min of constantly infused corticosterone was also significantly pattern dependent, as GR binding was ~2.2 fold increased at the corticosterone pulse peak (140min). No significant changes in pSer2 Pol2 occupation of *Per1*, however, were detected in response to any infused corticosterone condition compared to VEH control.

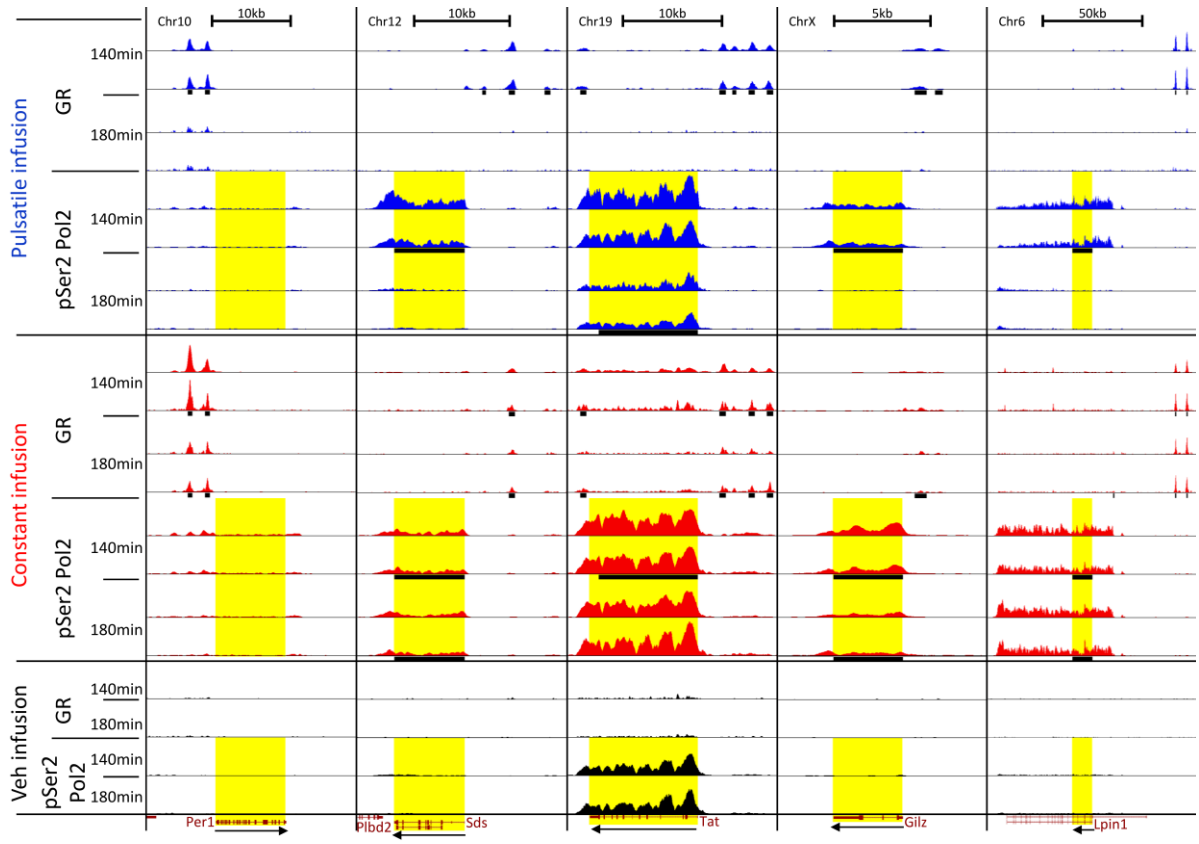

Figure 5.1 GR and pSer2 Pol2 sequenced tag density profiles across the glucocorticoid target genes *Per1*, *Sds*, *Tat*, *Gilz* and *Lpin1*.

GR and pSer2 Pol2 replicate sequenced tag density distribution in response to pulsatile, constant and VEH infusion at 140min and 180min was visualised using the UCSC genome browser. Chromosomal loci shown are chr10 55,678,227-55,704,917b (Per1), chr12 41,616,490-41,638,425b (Sds), chr19

41,673,112-41,694,225b (Tat), chrX 111,881427-111,892,292b (Gilz) and chr6 41,790,201-41,895,649b (Lpin1). Regions analysed for differential pSer2 Pol2 enrichment are indicated in yellow. Any GR and pSer2 Pol2 tag densities reported as significantly differentially enriched to VEH control are indicated by black boxes underneath replicate traces. Chromosome number as well as 10kb and 50kb scale bars are indicated at the top of the genome browser shots. At the left, Per1 is transcribed from the sense strand (left to right) whereas Sds, Tat, Gilz and Lpin1 are transcribed from the antisense strand (right to left) as indicated by arrows. The reference gene track at base of figure shows the Intron/ exon coding region (exon within intragenic maroon blocks) locations from Ensembl rn6 co-ordinates . Data normalised to 10million tags and y-axis was set to-0-250.

Sds is an enzyme that catalyses the deamination of serine (derived from glycine) into pyruvate within gluconeogenesis and changes in mRNA levels have been shown to be robustly circadian and Dex responsive (Sandoval and Sols, 1974; Kanamoto, Su and Pitot, 1991; Ogawa and Ansai, 1995; Ogawa *et al.*, 2002). Two synergistic GR binding sites were identified in rat hepatoma (7AD-7) cells >5kb upstream of the TSS, of which the distal was reported to confer the greater transactivator effect (Su and Pitot, 1992). In my data, three corticosterone induced GR binding sites were identified ~-2kb (chr12:41,629,565-41,629,959), ~-5kb (chr12:41,632,348-41,632,972) and ~-8.5kb (chr12:41,636,073-41,636,697) upstream of the larger coding variant TSS. The previously characterised GR binding sites are most likely the two most distal sites in our data (Su and Pitot, 1992). Interestingly, both the proximal and distal GR binding sites were bound in response to a corticosterone pulse peak (140min), whereas the central GR binding site was responsive to all corticosterone infused timepoints apart from pulse nadir (180min). The most proximal and central GR binding sites were induced in a significantly phasic, time dependent manner 42- and 24-fold respectively, by the corticosterone pulse peak (140min) compared to nadir (180min). None were differentially regulated between constant corticosterone timepoints, despite a 4.8-fold enrichment to VEH control at the central binding site. Only the central site reported a significant pattern dependent difference with a 10-fold decrease at the pulse nadir (180min) compared to constant infusion (180min). pSer2 Pol2 occupation was induced in a phasic manner by a pulsatile corticosterone infusion, with occupancy increased 3.3-fold at the corticosterone pulse peak (140min) compared to nadir (180min). No changes were detected across constantly infused timepoints despite the 5.9-fold enrichment to VEH control. There were significant pattern dependent differences in pSer2 Pol2 enrichment, with a 1.9-fold increase at pulse peak relative to constant infusion at 140min and a 3.3-fold decrease at pulse nadir relative to constant infusion at 180min. This data indicates robust and synchronised corticosterone pattern dependent changes in both GR binding and pSer2 Pol2 occupation of *Sds*. Further, the central GR binding site may

confer the greatest regulatory action, whilst the other two sites may act synergistically to confer patterned corticosterone regulation of pSer2 Pol2 occupation.

Tat is a rate limiting enzyme involved within catabolism of tyrosine into ketogenic and gluconeogenic substrates in hepatic mitochondria (Granner and Hargrove, 1983). Transcription of this gluconeogenic target was one of the first to be identified as dependent on dual regulatory GR binding regions upstream of the TSS (Jantzen *et al.*, 1987). Within our data, four corticosterone inducible GR binding regions were identified ~-2.5kb (chr19:41,688,403-41,689,032), ~-3.5kb (chr19:41,689,712-41,690,106), ~-5.5kb (chr19:41,691,352-41,691,976) and ~-7kb (chr19:41,693,173-41,693,832) upstream of the TSS (Figure 5.1). There was also a 3' GR binding site, ~+11.5kb (chr19:41,674,388-41,675,013) downstream from the TSS. GR binding, at all sites except for the ~-3.5kb site, was induced at the corticosterone pulse peak and both constantly infused timepoints. Whilst, at the ~-3.5kb site GR was only bound at the corticosterone pulse peak. All GR binding sites were time dependently induced by a pulsatile infusion; increased at the pulse peak as opposed to nadir (+11.5kb: 9.7-fold; -2.5kb: 170-fold; ~-5.5kb: 9.0-fold; ~-7kb: 36.8-fold) but were unchanged across constant corticosterone timepoints despite their enrichment above VEH control. Except for the ~3.5kb GR binding site, which was not significantly changed by patterned corticosterone or indeed any other comparison. Only the upstream sites -2.5kb, -5.5kb and -7kb were pattern dependent with 100-fold, 6-fold and 25-fold decreases respectivly in response to the pulse nadir (180min) compared to the constantly infused matched time point. The 3' +11.5kb site was not significantly regulated in a pattern dependent manner. Interestingly, there were indications of increased pSer2 Pol2 Seq tags in response to both corticosterone pulse peak as well as VEH infused controls, which was not significantly different, indicating no change in basally active transcription. There was a significant, 2.5-fold reduction in pSer2 Pol2 occupation at the pulse nadir compared to VEH control. Despite an increased pSer2 Pol2 enrichment detected in response to 140min of constantly infused corticosterone and not 180min, relative to VEH control, there was no significant difference in enrichment between constant corticosterone timepoints. Finally, there was a 2.4-fold pattern dependent decrease in pSer2 Pol2 enrichment in the corticosterone pulse nadir, when compared to the constant corticosterone matched timepoint of 180min. This data indicates that GR binding at all sites, except for the ~3.5kb site, were robustly regulated by infused corticosterone patterns. However, pattern dependent transcriptional change was more complicated, with decreased pSer2 Pol2 enrichment at the corticosterone pulse nadir and increased enrichment during constant corticosterone infusion.

Gilz inhibits NFκB and the activation of monocytes and macrophages within anti-inflammatory pathways (D'Adamio *et al.*, 1997; Hamdi *et al.*, 2007). mRNA expression has been shown to fluctuate

in a circadian manner in adipose tissue and Dex has been observed to induce mRNA expression within the liver (Ayyar *et al.*, 2015). Presumably via the two GRE regions identified within a +2.5kb region of the TSS in lung adenocarcinoma (A549) cells, but observations within these cells of endogenous mRNA profiles were highly variable and not robustly circadian (Wang *et al.*, 2004; van der Laan *et al.*, 2008; Monczor *et al.*, 2019). Similarly, pulsatile GC replacement was shown by George et al., 2017 to be unable to induce pulsatile expression of Gilz nascent transcript in the prefrontal cortex of the rat (George *et al.*, 2017). In my data, two inducible GR binding sites were discovered ~-1kb (chrX:111,888,508-111,889,132) and ~-2kb (chrX:111,889,568-111,889,962) upstream of the *Gilz* TSS. Both sites were bound at the corticosterone pulse peak but only the ~-1kb site was bound in response to constant corticosterone infusion at the 180min timepoint. Upon further analysis however, neither site was significantly changed in a time or pattern dependent manner, even though sites were significantly induced to VEH control, the differences in enrichment were not robust enough to confidently identify robust pattern or time dependent effects for GR binding. Despite the lack of observable corticosterone pattern induced GR binding events, pSer2 Pol2 enrichment was significantly regulated in both a pattern and time dependent manner. Increased pSer2 Pol2 was observed in response to all infused time points except corticosterone pulse nadir (180min). A significant time-dependent 9.2-fold increase was found at the corticosterone pulse peak (140min) compared to nadir (180min) and a similar but reduced 2.2-fold increase was observed in the same comparison but in response to the constant infusion. The increased pSer2 Pol2 occupation at 140min was unchanged despite whether a pulsatile or constant corticosterone infusion was used, but there was a significant 6.7-fold reduction at the 180min time point in response to a pulsatile corticosterone infusion, relative to the constant corticosterone infusion. My data indicates that, despite a lack of pattern and time dependent GR binding at proximal GR binding sites, pSer2 Pol2 occupation within the *Gilz* gene was significantly modified in a corticosterone pattern and time dependent manner. This may indicate that the proximal GR binding sites are not directly regulating dynamic changes in Gilz expression in liver, consistent with reports that Gilz can also be regulated by dynamic long-range interactions (Stavreva et al 2015).

LPIN1 is an important PPARα co-factor oxidising fatty acids within the liver as well as inducing adipocyte differentiation (Finck *et al.*, 2006). Further, transcriptional regulation has been reported to be dependent on GR binding at a GRE upstream of the TSS in mouse liver hepatoma (hepa 1-6) and pre-adipogenic mouse embryonic fibroblast (3T3-L1) cells (P. Zhang *et al.*, 2008). In my data, two inducible GR binding sites were identified ~-42kb (chr6:41,884,401-41,885,025) and ~-48kb (chr6:41,890,043-41,890667) upstream of the TSS of the shorter variant (Figure 5.1). GR binding as well as pSer2 Pol2 occupancy was induced in response to all corticosterone infused timepoints except

the pulse nadir (180min). In response to pulsatile corticosterone infusion, GR binding was significantly time dependent, with 23-fold increased binding at the ~-42kb site and 16-fold increased binding at the ~-48kb binding site, at the pulse peak (140min) compared to nadir (180min). No significant time dependent differences were reported in response to a constant infusion, despite increased GR binding of 350-fold (140min) and 418-fold (180min) compared to VEH control. Similarly, no significant pattern dependent changes in GR binding were detected between pulsatile and constant corticosterone infusion at 140min. There was however, a ~17 fold and ~11 fold pattern dependent decrease in GR binding at the 180min timepoint in pulsatile compared to constant corticosterone infusion. Similar dynamics were reported for pSer2 Pol2 intragenic occupation as phasic, 15-fold increases were detected at the corticosterone pulse peak, compared to pulse nadir. No significant time dependent changes in *Lpin1* pSer2 Pol2 enrichment were reported for constant infusion, despite 13-fold and 10-fold increased occupation at both 140min and 180min infused time points respectively, relative to VEH. No significant pattern dependent differences were reported between pulsatile and constant corticosterone infusion at 140min, but there was at 180min with 25-fold decreased RNA Pol2 enrichment in response to pulsatile compared to constant corticosterone infusion. Together, these data indicate robustly corticosterone pattern dependent regulation of both proximal GR binding and pSer2 Pol2 intragenic occupation.

5.4.2 GR binding site distribution is unchanged by patterned corticosterone timepoint

Genome-wide GR binding locations are highly dependent on cell-specific chromatin organisation. As transcriptional control was reported to be modified by infused corticosterone timepoints, GR binding site location within intergenic and intragenic regions was investigated for the presence of any differences between the different patterned corticosterone treatments and timepoints.

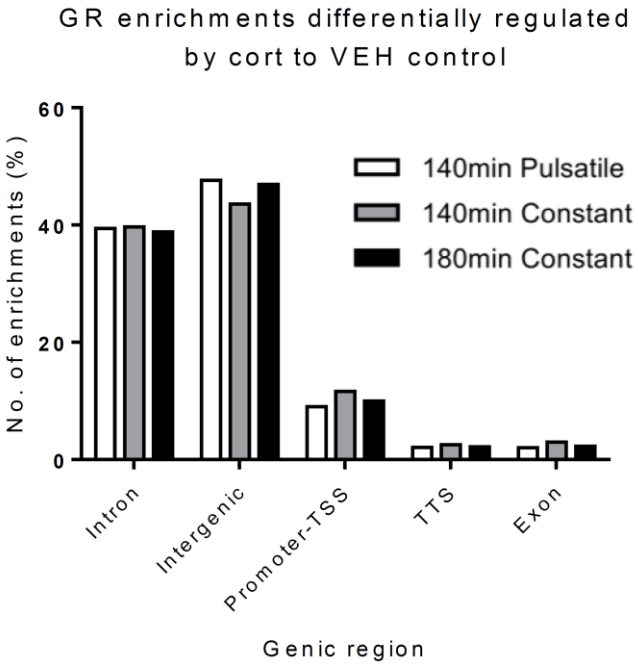

Figure 5.2 Distribution of GR binding sites within genic regions across the genome.

The distribution of GR binding sites by intragenic region in response to either pulsatile corticosterone pulse peak (140min) (white bar) or constant corticosterone infusion at 140min (grey bar) and 180min (black bar). GR binding sites were split into TSS proximal promoter regions (-2.5kb to +0.1kb of the TSS) and intragenic binding sites were split into intronic and exonic regions as well as transcription termination sites (TTS). All other non-coding regions were classed as intergenic.

The majority of patterned corticosterone inducible binding sites were found within intergenic regions, irrespective of whether they were induced by the corticosterone pulse peak (140min) or either 140min and 180min constantly infused timepoints (47.6, 43.6 and 46.9% respectively) (Figure 5.2). The second greatest number of sites were induced within intragenic regions, specifically at intronic sites (39.4%, 39.7% and 38.8% respectively). Exonic sites (2.0%, 3.0% and 2.3% respectively) and transcriptional termination sites (TTS) (2.1%, 2.5% and 2.2% respectively) made up only a small percentage of these. Interestingly, a concentration of sites was found within promoter regions (9.0%, 11.6% and 10.0%) defined as -2.5kb to +0.1kb of the TSS relative to their overall genomic coverage. No obvious differences were observed in overall distribution in response to a single or combination of corticosterone condition and timepoint.

5.4.3 Distance to the proximal GR binding site is predictive of pSer2 Pol2 occupancy changes

GR has been found to exert transcriptional effects over long distances. Within my data, we investigated any potential relationship between changes in pSer2 Pol2 occupancy within a gene, and its distance from the closest corticosterone regulated GR binding site(s). All GR ChIP-Seq datasets were

interrogated in this way, except for pulsatile corticosterone nadir as no GR binding was detected in analysis relative to VEH control (Figure 3.5).

Interestingly, genes with GR binding sites in closer proximity were more likely to be transcriptionally upregulated during the corticosterone pulse peak, i.e. increased pSer2 Pol2 occupancy. Typical examples of GR proximal associated increased transcription include the targets *Per1* (RT-qPCR only), *Gilz* and *Lpin1* as shown above. In contrast, genes without GR binding sites in proximity were more likely to be transcriptionally repressed during the corticosterone pulse peak, i.e. have decreased pSer2 Pol2 occupancy. For example, 25% of gene targets with a GR binding site <860b from the TSS exhibited increased pSer2 Pol2 enrichment (Figure 5.3), whereas 25% of gene targets with a GR binding site >0.86kb and <20.3kb from the TSS exhibited decreased pSer2 Pol2 enrichment during the corticosterone pulse peak. This represents a difference of ~19.5kb (from GR binding site and gene TSS) between the two groups. The same phenomenon was observed throughout 50%, 75% and 100% percentiles with differences of 83.2kb, 357.6kb and 9,646.5kb respectively.

Similar distributions were observed in response to either matched constant corticosterone infused timepoint to varying degrees. After 140min of constant corticosterone infusion the difference was less pronounced at 25%, 50% and 75% percentiles (a difference of 5.6kb, 22.7kb and 221.6kb respectively) and relative distances from the TSS were on average double the distance to the most proximal induced GR binding site compared to the pulsatile infused matched timepoint (corticosterone pulse peak). However, at the 100% percentile the difference in distance was unchanged.

Similar distributions were observed in response to 180min of constantly infused corticosterone between increased or decreased pSer2 Pol2 occupation and the closest GR binding site, however, differences between percentiles was increased in comparison to any other corticosterone infused time point (a difference of 118kb, 415kb, 1,215.7kb and 22,111.3kb at 25%, 50%, 75% and 100% respectively).

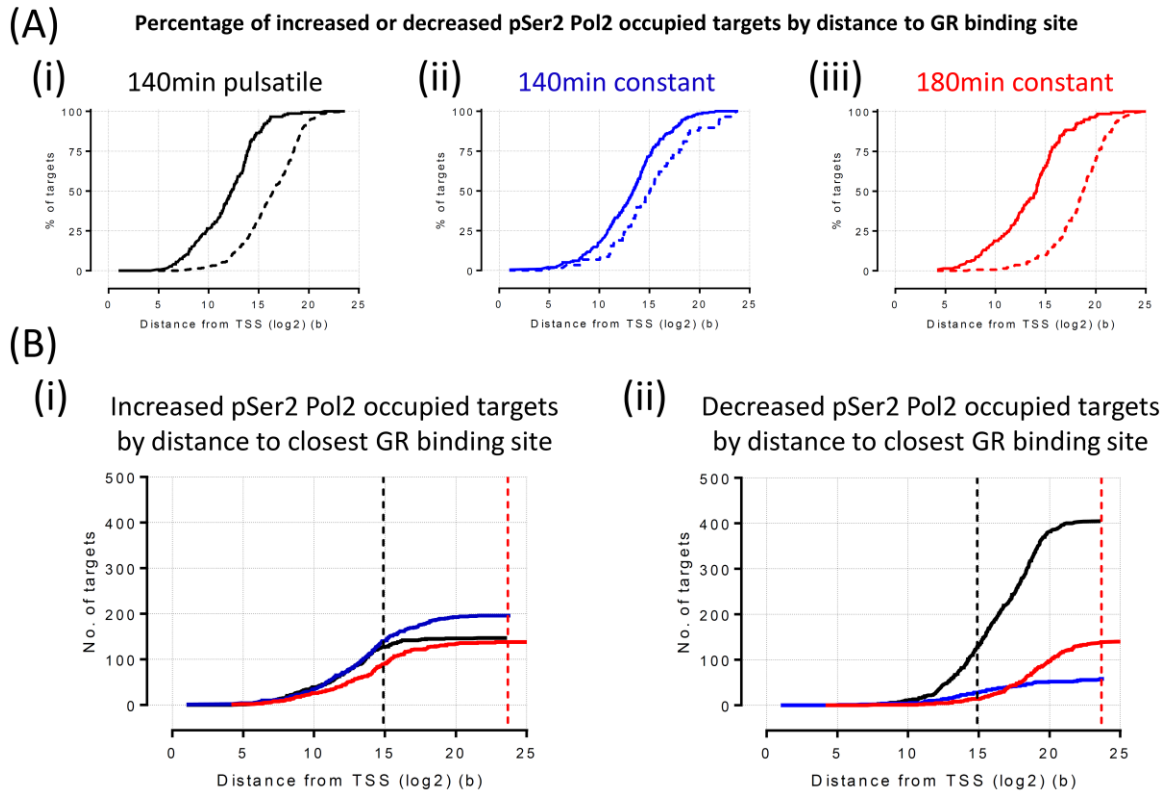

Figure 5.3 Distance between GR binding site and the TSS of the closest regulated gene relates to probability of pSer2 Pol2 gain or loss in occupancy.

(A) The percentage of either increased (solid line) or decreased (dotted line) pSer2 Pol2 occupied targets was plotted against the distance (log2) to the most proximal induced GR binding site by corticosterone to VEH control in response to the pulsatile infusion at the pulse peak (140min) (black) (i) and either 140min (blue) (ii) or 180min (red) (iii) matched constant corticosterone infused timepoints. (B) The same comparison was plotted but with total numbers of either increased (i) or decreased (ii) pSer2 Pol2 occupied targets to VEH control. Dotted lines indicate at what distance the total number of targets that reported a loss in pSer2 Pol2 occupancy was greater than the total number of targets that reported a gain in response to the pulsatile corticosterone pulse peak (14.9kb) (black) and 180min constant (23.6kb) (red) corticosterone infusion. At no point was this observed in response to 140min constantly infused corticosterone. Pulsatile corticosterone pulse nadir (180min) was not plotted as no GR binding sites were differentially induced to VEH control. Changes in Pser2 Pol2 occupancy were analysed in regions >620b and limited to intragenic regions <10kb from the TSS according to Ensembl (Rn6) co-ordinates and filtered for unique gene transcripts. Log2 distances were measured from differentially regulated target TSSs to the most proximal GR binding site in response to a corticosterone infused timepoint. Both pSer2 Pol2 and GR data were normalised to total enrichment or total sequenced tags respectively and differential analysis filtered results by fold change

>1.5, FDR<0.05 and p-value <0.05 adjusted for multiple comparisons compared to VEH infused control by DESeq2.

There were further differences observed between corticosterone infused timepoints when total numbers of targets were plotted for either increased or decreased pSer2 Pol2 occupied targets. In response to a pulsatile corticosterone peak (140min) the number of targets that reported a decrease in pSer2 Pol2 occupation was only greater within targets that had an induced proximal GR binding site >29.9kb away. Whereas, in response to 180min constant corticosterone infusion, this was reported for targets that had an induced proximal GR binding site >12,803,190kb away, a distinct difference in GR distribution. Interestingly, the total number of regions with decreased pSer2 Pol2 occupancy in response to 140min constantly infused corticosterone was at no point greater than targets with an increased occupancy, when sorted by distance to the proximal inducible GR binding site.

I investigated whether observed effects could be explained via the distribution of nGRE related motifs within GR binding regions. Of the GR enrichments closest to the TSS of GC regulated genes, only just 2.23% of GC regulated targets contained a nGRE related sequence.

Investigation of the closest identified GR binding site reports just 1.4% of GC regulated targets contained a nGRE related sequence. The instances of enriched GR binding in response to a corticosterone infused time point did not match up between the GR and pSer2 Pol2 differential results i.e. whilst enrichment of a GR binding site occurred at the same infused time point as a change in pSer2 Pol2 occupation, there were occurrences where GR was enriched and had no effect on pSer2 Pol2 occupation. Additionally, no trend was observed between distance of nGRE like motif containing GR enrichment and pSer2 Pol2 occupation.Together, these data present evidence that increasing distance of GR binding site to a TSS is associated with an increased likelihood of decreased RNA Pol2 occupancy and hence transcription does not appear to be dependent on the presence of a nGRE associated sequence. Observed differences are more likely dependent on distance of GR binding sites as well as corticosterone pattern and time of infusion.

5.4.4 Functional pathway analysis

As described previously, phosphorylation of the Ser2 residue within the carboxy-terminal domain of the RNA Pol2 is associated with the actively transcribing RNA Pol2 complex as it progresses through the coding region (Cho *et al.*, 2001; Ahn, Kim and Buratowski, 2004). Therefore, I have interpreted changes in pSer2 pol2 occupancy as changes in gene transcription, hence, fold changes in pSer2 Pol2 occupancy and associated p-values were analysed using the Ingenuity Pathway Analysis software (Qiagen, Inc.) (Krämer *et al.*, 2014). A feature of the analysis is to predict either an activatory or

inhibitory 'direction' according to published literature. This, z-score, is calculated by the ratio of either activating or inhibiting effects by the number of targets characterised within a downstream pathway and significance is assessed within a binomial model. The IPA analysis recommends any positive (predictive activation) or negative (predictive inhibition) z-score >2 is a significant observation.

5.4.5 Patterned corticosterone regulation of the inflammatory pathway.

GCs have potent anti-inflammatory properties. Consistent with this, pathway analysis of targets regulated by patterned corticosterone predicted inhibition of the inflammatory pathway at both 140min and 180min infused constant corticosterone timepoints (z-score of -1-15 and -0.59 respectively) (Figure 5.4 A). Inhibition of the inflammatory pathway was also predicted at the corticosterone pulse peak (140min) (z-score of -0.18) but no prediction was made for the pulse nadir (180min). As previously described within section 5.3, analysis documentation outlines z-scores >2 (or <-2) as a significant prediction, therefore all observations reported are trends of inhibition that may facilitate a greater anti-inflammatory effect in response to a constant corticosterone exposure.

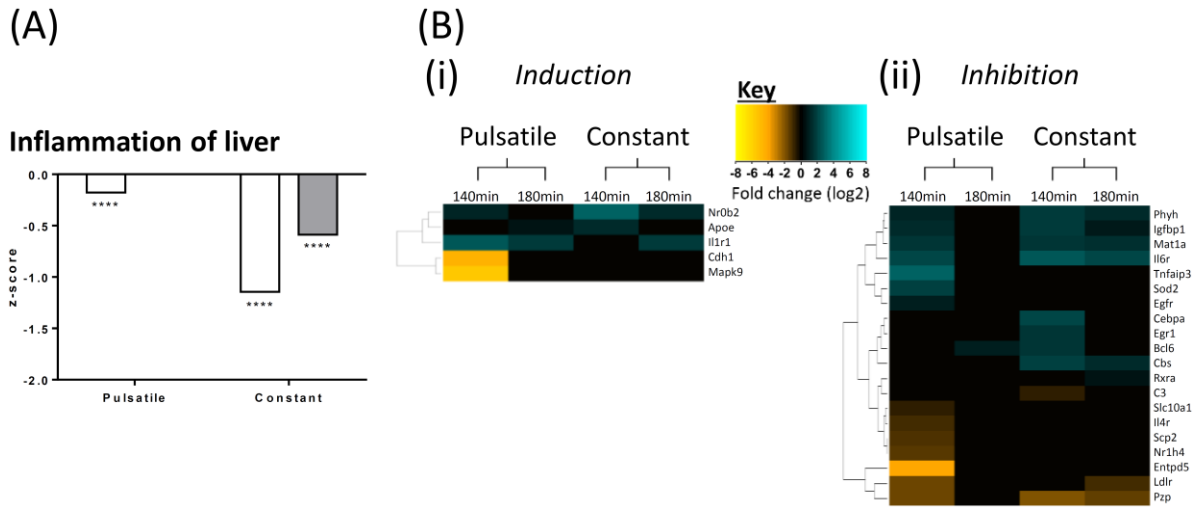

Figure 5.4 Predicted modulation of the inflammatory pathway by patterned corticosterone infusion timepoints.

(A) Analysis of pSer2 Pol2 occupied targets in the hepatic inflammatory pathway in response to both pulsatile and matched constant corticosterone infusion at 140min (white bars) and 180min (grey bars). Fold changes >1.5 from VEH infused control and p-values <0.05 adjusted for multiple comparisons were analysed by IPA software. Positive and negative z-scores >2 indicate significant predicted activation or inhibition respectively. (B) Differential occupancy of pSer2 Pol2 was hierarchically clustered by fold change values and plotted within heatmaps to the centre and right. Results were separated into factors known to activate (i) or inhibit (ii) inflammation. Degree of increased (cyan) or decreased (yellow) log2 fold change is indicated by colour intensity, as shown

*within the key towards the top of the figure. Changes in pSer2 Pol2 occupancy to VEH control were analysed in regions >620b and limited to intragenic regions <10kb from the TSS according to Ensembl (Rn6) co-ordinates and filtered for unique gene transcripts. Z-score p-values are indicated by ****<0.0001.*

Within the regulated inflammatory genes identified within the analysis, *Cdh1* and *Mapk9* could represent a couple of interesting targets for further study, as they are labelled as activators of inflammation, but transcription (pSer2 Pol2 occupancy) is transiently decreased in response to the pulsatile corticosterone infusion. Whereas, transcription of several inhibitory targets is increased across time points in response to constant corticosterone exposure, including *Phyh*, *Mat1a*, *Il6r* and *Cbs*. These genes could be responsible for the increased predictive trend of anti-inflammatory action.

5.4.6 Canonical pathways

Focusing on the canonical metabolic pathways, analysis predicted activation/ inhibition of key pathways in a patterned corticosterone dependent manner. In the liver, cholesterol synthesis and its metabolism is a primary function, however the liver metabolises a wide range of substrates such as melatonin, serotonin and methionine. For example, up to 90% of circulating melatonin is metabolised within a single pass through the hepatic portal circulation (Lane and Moss, 1985; Chojnacki *et al.*, 2012).

Inhibition of cholesterol biosynthesis was predicted for pulsatile corticosterone, with a trend observed at pulse peak (z-score of -1.89), which was significant within the nadir (z-score of -2) (Figure 5.5 Ai). However, in response to constant infusion, no change was predicted at 140min, and a trend of inhibition reported at 180min (z-score of -1). Data indicates overall inhibition of cholesterol biosynthesis in response to pulsatile compared to constant infusion, possibly increasing cholesterol biosynthesis during constant corticosterone exposure.

Out of the genes that were differentially regulated by patterned corticosterone, just *Dhcr24* reported transiently increased transcription during pulsatile infusion, which was prolonged with constant corticosterone infusion (Figure 5.5 Bi). Transcription at most targets was decreased however, in response to the corticosterone pulse peak only, of which *Cyp51*, *Dhcr7* and *LSS* were distinct.

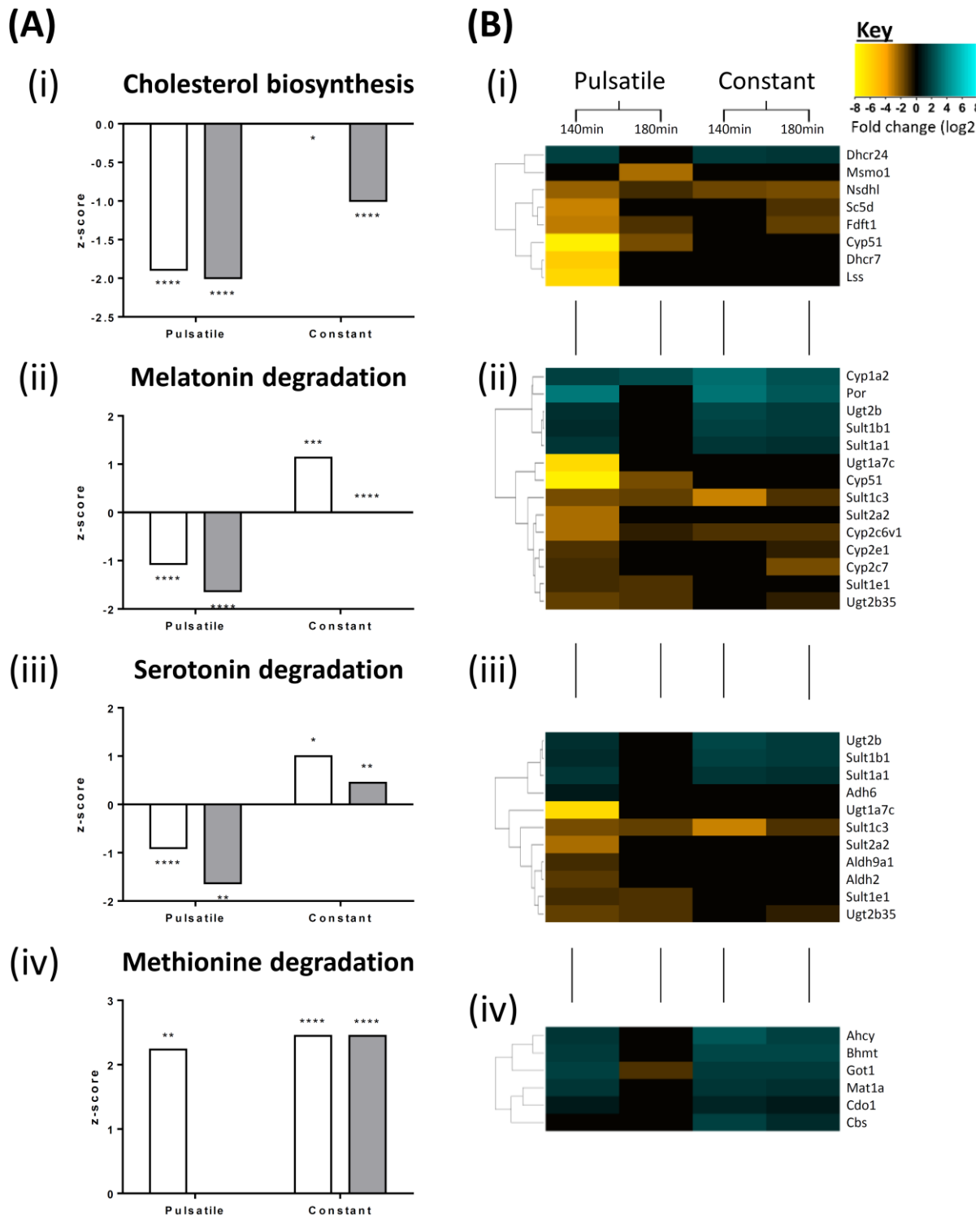

Figure 5.5 Canonical pathways regulated by patterned corticosterone infusion timepoints.

Canonical pathway analysis of pSer2 Pol2 occupancy changes in response to both pulsatile and matched constant corticosterone infusion at 140min (white bars) and 180min (grey bars). Fold changes >1.5 from VEH infused control and p-values <0.05 adjusted for multiple comparisons were analysed by IPA software. Positive and negative z-scores >2 indicate significant predicted activation or inhibition respectively. Differential occupancy of pSer2 Pol2 was hierarchically clustered by fold

*change values and plotted within heatmaps to the right. Degree of increased (cyan) or decreased (yellow) log2 fold change is indicated by the colour intensity as shown within the key towards the top of the figure. Canonical pathway analysis indicated changes in cholesterol biosynthesis I, II (via 24,25-dihydrolanosterol) and III (via Desmosterol), superpathway of melatonin degradation 1 and methionine degradation as well as serotonin degradation. Changes in Pser2 Pol2 occupancy to VEH control were analysed in regions >620b and limited to intragenic regions <10kb from the TSS according to Ensembl (Rn6) co-ordinates and filtered for unique gene transcripts. Z-score p-values are indicated by *<0.05, **<0.01, ***<0.001 and ****<0.0001.*

Similar trends were observed within degrative pathways of melatonin and serotonin. In response to a pulsatile corticosterone infusion, a trend of inhibition was predicted at the corticosterone pulse peak (140min), and nadir (180min) for both melatonin (z-scores of -1.07 and -1.63 respectively) (Figure 5.5 Aii) and serotonin (z-scores of -0.91 and -1.63 respectively) (Figure 5.5 Aiii). In response to constantly infused corticosterone, trends of activation were predicted for both pathways at 140min (z-score of 1.13 and 1.00 respectively) but only at 180min for serotonin (z-score of 0.45). Together, this data indicates the potential for increases circulating melatonin and serotonin in response to a pulsatile corticosterone infusion.

pSer2 Pol2 occupation of several genes was increased in response to patterned corticosterone infusion including *Por*, *Ugt2b*, *Sult1b1* and *Sult1a1*; all of which were also enriched within serotonin degradation apart from *Por*. Occupation of all other 9 regulated genes was decreased in a transient manner to pulsatile corticosterone infusion, with indication of dysregulation in response to constant infusion. This was more evident with occupation of genes involved in the serotonin pathway, as *Ugt1a7c*, *Sult2a2*, *Aldh9a1* and *Aldh2* were significantly lost to VEH control at the corticosterone pulse peak only.

Significant predicted activations of the methionine degrative pathway were reported in response to the corticosterone pulse peak (140min) (z-score of 2.24), as well as in response to 140min and 180min constantly infused timepoints (z-score of 2.45 for both) (Figure 5.5 Aiv). No prediction was made for the corticosterone pulse nadir (180min). Therefore, this data strongly indicates a prolonged methionine degradation in response to a constant corticosterone infusion, as opposed to a transient activation that is synchronised to a corticosterone pulse peak, presumably reducing circulating methionine.

Predicted activation of methionine degradation was significant at the corticosterone pulse peak and either constant corticosterone timepoints. Out of the six differentially occupied pSer2 Pol2 targets, *Ahcy*, *Bhmt* and *Mat1a* reported similar increases in pSer2 Pol2 occupation (Figure 5.5 Biv).

Interestingly, *Got1* was similarly increased but also reported a decrease in occupation at the corticosterone pulse nadir to VEH control whilst *Cbs/Cbsl* was only increasingly occupied in response to a constantly infused corticosterone. These targets present prime candidates for further corticosterone dynamically regulated research.

5.4.7 Patterned corticosterone regulation of glucose homeostatic pathways.

Within the liver, dysregulation of glucose homeostasis is an important risk factor in the development of MetS phenotypes. Specifically, high glucose and insulin levels are indicators of insulin resistance and can lead to obesity and type II diabetes (Vegiopoulos and Herzig, 2007; de Guia, Rose and Herzig, 2014).

Pathway analysis reported activatory trends of glycogen quantity in response to pulsatile corticosterone at the pulse peak (140min) (z-score 1.67), but not at the nadir (180min) (Figure 5.6 Ai). In response to constant corticosterone, trends of activation were predicted at both corticosterone infused timepoints (z-score of 0.71 for both), indicating constant corticosterone exposure could increase glycogen quantities compared to pulsatile corticosterone induced, transient activation.

Three corticosterone regulated genes known to activate this pathway, reported increased transcription in response to raised circulating corticosterone of *Pfkfb1* was highly induced to VEH control. It should be noted, transcription of *Pfkfb1* has bene characterised as a GC responsive and the enzyme is bi-directional, favouring either favoured glycolytic or gluconeogenic pathways within hepatocytes which is mostly dependent on glucagon signalling (Hue and Rider, 1987; Marcus *et al.*, 1987; Rider *et al.*, 2004). Therefore, despite it being quoted as increasing glycogen, it has multi-regulatory roles. The other two genes were *H6pd* and *Myc*. *Dusp1* also reported similar dynamics, but too a much lesser degree.

The observed increased confidence predicted at the corticosterone pulse peak is probably due to the loss of *Jun* and *Gjb1* transcription at this time point. Together, these represent key genes within this pathway that are corticosterone regulated.

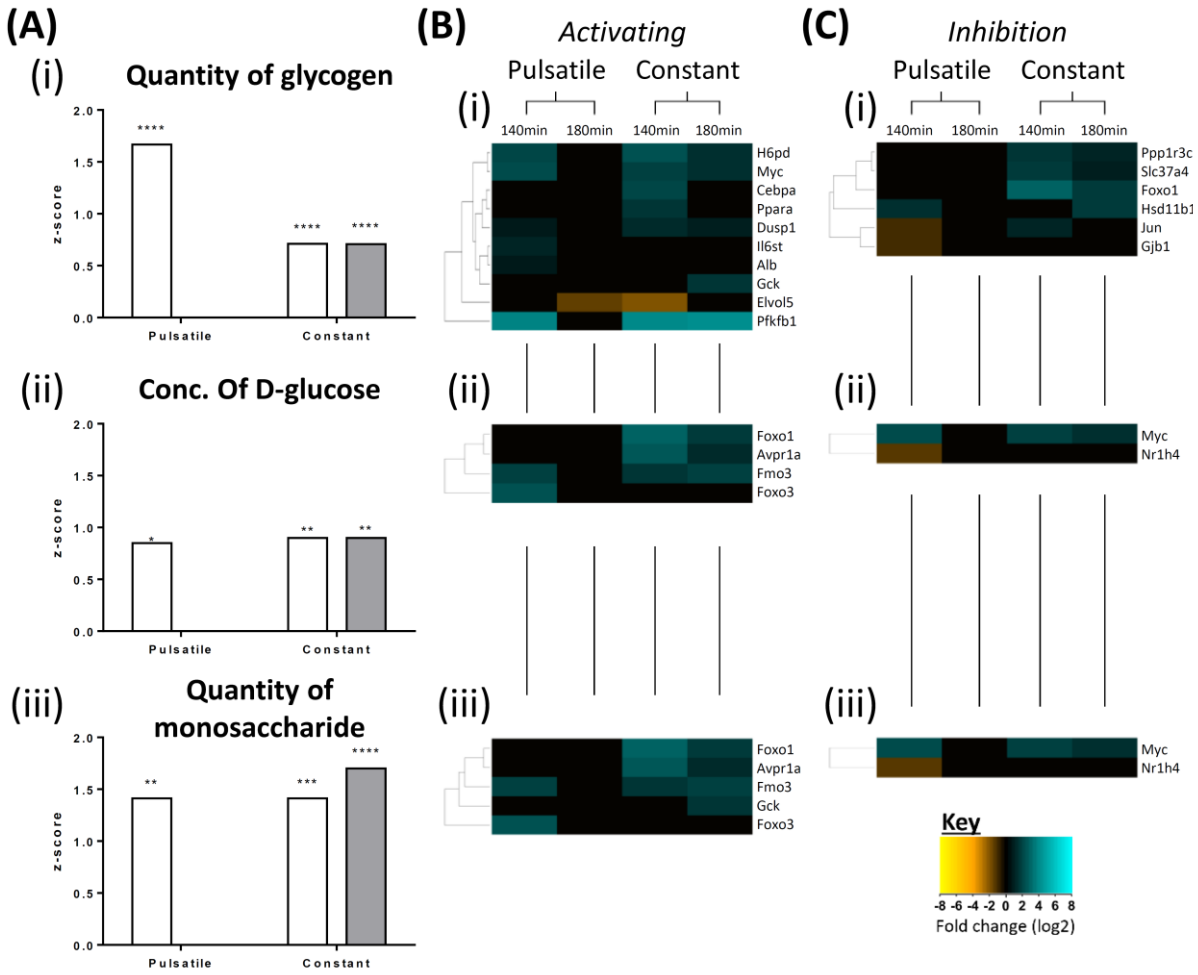

Figure 5.6 Predicted modulation of glucose metabolic pathways by patterned corticosterone infusion timepoints.

*(A) Predicted activation or inhibition was based upon analysis of pSer2 Pol2 occupied targets involved in glucose homeostatic pathways in response to both pulsatile and matched constant corticosterone infusion at 140min (white bars) and 180min (grey bars). Fold changes >1.5 from VEH infused control and p-values <0.05 adjusted for multiple comparisons were analysed by IPA software. Positive and negative z-scores >2 indicate significant predicted activation or inhibition respectively. Differential occupancy of pSer2 Pol2 was hierarchically clustered by fold change values and plotted within heatmaps to the centre and right. Results were separated into factors known to activate (B) or inhibit (C). Degree of increased (cyan) or decreased (yellow) log2 fold change is indicated by colour intensity, as shown within the key towards the bottom of the figure. Results indicated quantity of Glycogen (i), concentration of D-glucose (ii) and quantity of monosaccharide (iii) were modulated by corticosterone infused timepoints. Changes in pSer2 Pol2 occupancy to VEH control were analysed in regions >620b and limited to intragenic regions <10kb from the TSS according to Ensembl (Rn6) co-ordinates and filtered for unique gene transcripts. Z-score p-values are indicated by *<0.05, **<0.01, ***<0.001 and ****<0.0001.*

Similar predictive dynamics were observed for concentrations of dietary D-glucose and monosaccharide pathways. Trends of activation were reported in response to the pulsatile corticosterone infusion at the pulse peak (140min) as well as both 140min and 180min constantly infused timepoints for D-glucose (z-scores of 0.85, 0.90 and 0.90 respectively) (Figure 5.6 Aii) as well as for the quantity of monosaccharides (z-scores of 1.41, 1.41 and 1.70 respectively) (Figure 5.6 Aiii). Whereas, no prediction was reported at the corticosterone pulse nadir (180min) for either. In a similar way to glycogen; constant corticosterone exposure could increase both glucose and monosaccharide levels.

Interestingly, differentially occupied targets within the monosaccharide pathway were also activatory within the D-glucose pathway (Figure 5.6 Bii & Biii). Only *Gck* (also within the glycogen pathway) was exclusive to the monosaccharide pathway. Increased transcription of *Foxo1* and *Avpr1a* was reported in response to a constant corticosterone infusion only, whereas *Fmo3* was also transiently increased in response to a pulsatile exposure. All these were activatory of these pathways, whereas corticosterone pattern regulated increases in transcription of the gene *Myc* (which was activatory for glycogen) was inhibitory.

Together, this data indicates trends of prolonged increases in glycogen, D-glucose and monosaccharides in response to constantly infused corticosterone as opposed to transient increases synchronised to the corticosterone pulse peak during pulsatile infusion.

5.4.8 pSer2 Pol2 occupancy predicts modulation of growth and necrotic pathways in response to patterned corticosterone infusion.

Growth hormones and GCs play a distinct synergistic role within energy homeostasis via targeted activation of nuclear factors such as STAT5 and GR respectively. STAT5 has been shown to mediate cell proliferation, differentiation and survival in a post-natal mouse model that required co-regulator interactions with the GR in a composite manner (Stoecklin *et al.*, 1997; Tronche *et al.*, 2004; Engblom *et al.*, 2007). Impairment of this interaction can dysregulate lipid metabolism and induce hepatic steatosis (Friedbichler *et al.*, 2012; Mueller *et al.*, 2012).

Analysis of corticosterone regulated genes indicated trends of liver growth in response to the constant corticosterone infusion at 140min (z-score of 1.70) and 180min (z-score of 1.77) but not in response to the pulsatile corticosterone infusion (Figure 5.7 Ai). Similar trends in response to the constant corticosterone infusion were predicted for the proliferation of liver cells (z-score of 1.60 and 1.76 respectively) (Figure 5.7 Aii), as well as a transient trend of activation predicted in response to the pulsatile infusion at the corticosterone pulse peak (140min) (z-score of 0.98). Together these data

suggest transient (if any) activation is prolonged upon the loss of corticosterone oscillations, which may increase growth and proliferation within the liver.

Increased transcription of *Nr1i2*, *Pik3r1*, *Myc*, *Nfkbia* and *Il6r* identified in response to the pulse peak but not nadir, were prolonged by constant corticosterone exposure, presumably inducing both growth and proliferative pathways in corticosterone pattern dependent manner. Whereas, transcription of *Jun*, *Il4r*, *Inhba*, *Raf1* and *Pml* was decreased at the corticosterone pulse peak only and would have been responsible for the reduced confidence of prediction at this time point. Out of the inhibitory genes, transcription of *Entpd5*, *Nr1h4*, *Dlc1* and *Cbp2* was similarly regulated by corticosterone, but in a reduced transcriptional capacity. Interestingly the activatory gene *Agt* (robustly corticosterone pattern increased transcription) and inhibitory *Igf1* (decreased transcription at the pulse nadir and constant corticosterone) were the only genes not enriched in both pathways.

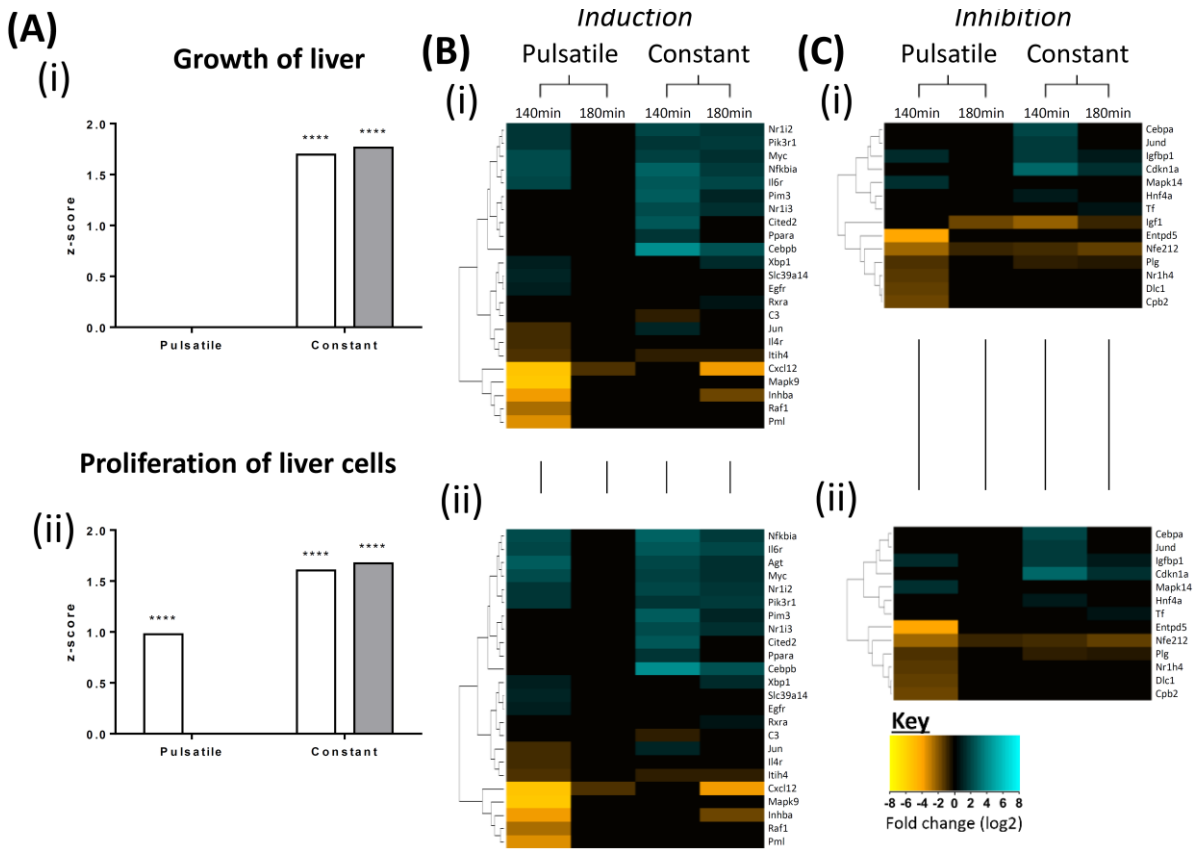

Figure 5.7 Predicted modulation of growth and proliferative pathways by patterned corticosterone infusion timepoints.

(A) Predicted activation or inhibition was based upon analysis of pSer2 Pol2 occupied targets regulating growth and proliferation in response to both pulsatile and matched constant corticosterone infusion at 140min (white bars) and 180min (grey bars). Fold changes >1.5 from VEH infused control

*and p-values <0.05 adjusted for multiple comparisons were analysed by IPA software. Positive and negative z-scores >2 indicate significant predicted activation or inhibition respectively. Differential occupancy of pSer2 Pol2 was hierarchically clustered by fold change values and plotted within heatmaps to the centre and right. Results were separated into factors known to activate (B) or inhibit (C). Degree of increased (cyan) or decreased (yellow) log2 fold change is indicated by colour intensity, as shown within the key towards the bottom of the figure. Results indicated growth of liver (i) and proliferation of liver cells (ii) modulated by corticosterone infused timepoints. Changes in Pser2 Pol2 occupancy to VEH control were analysed in regions >620b and limited to intragenic regions <10kb from the TSS according to Ensembl (Rn6) co-ordinates and filtered for unique gene transcripts. Z-score p-values are indicated by ****<0.0001.*

Interestingly, opposing necrotic and cell death pathways reported similar trends predicted for proliferation, in response to the corticosterone pulse peak (140min) (z-scores of 1.24 and 1.15 respectively) (Figure 5.8 Ai) and at both constant corticosterone timepoints of 140min (z-scores of 1.65 and 1.90) and 180min (z-scores of 1.34 and 1.10). Together this data indicates transient activation of necrotic and cell death pathways in response to pulsatile corticosterone infusion, could be dysregulated and prolonged in response to constant corticosterone infusion.

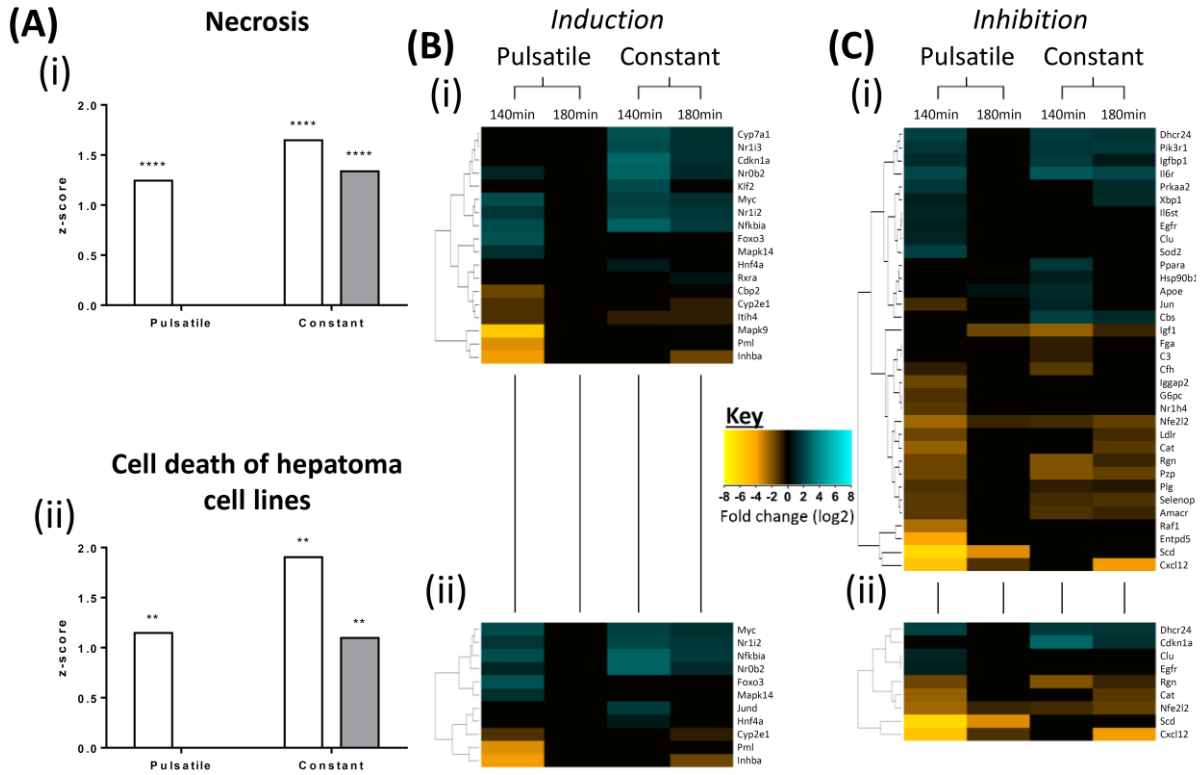

Figure 5.8 Predicted modulation of necrotic and cell death of hepatoma cell line pathways by patterned corticosterone infusion timepoints.

*(A) Predicted activation or inhibition was based upon analysis of pSer2 Pol2 occupied targets regulating both necrotic and cell death pathways in response to pulsatile and matched constant corticosterone infusion at 140min (white bars) and 180min (grey bars). Fold changes >1.5 from VEH infused control and p-values <0.05 adjusted for multiple comparisons were analysed by IPA software. Positive and negative z-scores >2 indicate significant predicted activation or inhibition respectively. Differential occupancy of pSer2 Pol2 was hierarchically clustered by fold change values and plotted within heatmaps to the centre and right. Results were separated into factors known to activate (B) or inhibit (C). Degree of increased (cyan) or decreased (yellow) log2 fold change is indicated by colour intensity, as shown within the key in the middle of the figure. Results indicate necrotic (i) and cell death of hepatoma cell lines (ii) modulated by corticosterone infused timepoints. Changes in Pser2 Pol2 occupancy to VEH control were analysed in regions >620b and limited to intragenic regions <10kb from the TSS according to Ensembl (Rn6) co-ordinates and filtered for unique gene transcripts. Z-score p-values are indicated by *<0.05, **<0.01 and ****<0.0001.*

Most corticosterone regulated targets that were regulatory of the hepatoma cell death pathway were also enriched within the necrotic pathway. Except for the activatory and inhibitory targets, *Jund* and *Cdkn1a*, which were only regulatory of the cell death pathway. Activatory targets reporting corticosterone pattern increased transcription were *Nr0b2*, *Myc*, *Nr1i2* and *Nfκbiα* (Figure 5.8 B), whilst a loss was reported at the inhibitory targets *Rgn*, *Pzp*, *Plg*, *Selenop* and *Amacr* (Figure 5.8 C).

It is also worthy of note, a proportion of genes were identified as either activatory or inhibitory, for growth/ proliferative as well as necrotic/ cell death pathways. This indicates a high level of crosstalk between the pathways identified as well as bi-functional responses of genes. Or it could simply be a lack of clarity regarding direct target effects within pathways. Together, this data does indicate a pulsatile corticosterone exposure, could transiently affect hepatocyte turnover within the liver, which upon constant corticosterone exposure would become dysregulated and potentially increased.

5.4.9 pSer2 Pol2 occupancy predicts modulation of carbohydrate pathways and factors involved in lipid homeostasis in response to patterned corticosterone infusion.

Carbohydrate, fatty acid and lipid metabolism as well as lipoprotein synthesis and packaging for distribution around the body (predominantly WAT) is highly dependent on hepatic function (Vegiopoulos and Herzig, 2007; Werner, Kuipers and Verkade, 2013; de Guia, Rose and Herzig, 2014). Dysregulation of these homeostatic processes can induce raised circulating VLDLs and reduced HDLs, dyslipidaemia and NAFLD. All phenotypes associated with MetS (Alberti *et al.*, 2005; Szczepaniak *et al.*, 2005).

Pathway analysis of differentially corticosterone regulated genes that regulate the metabolism of carbohydrates, predicted trends of inhibition in response to the corticosterone pulse peak (140min) (z-score -1.68) and none by the nadir (Figure 5.9 Ai). In response to a constant corticosterone infusion, very weak confidence of inhibition and activation were predicted at 140min and 180min infused time points (z-score of -0.04 and 0.12 respectively) indicating a loss of transient inhibition and dysregulation by constant corticosterone exposure, which could increase metabolism of carbohydrates within the liver.

Reduced transcription of genes known to activate carbohydrate synthesis was identified in *Nr1h4*, *Gpam* and *Aqp9* in response to the corticosterone pulse peak only and down-regulation of *Scd* was greater at the same time point compared to nadir. Furthermore, *Dusp6* transcription was transiently reduced in a similar manner but also in response to constant corticosterone exposure. Whilst, increased transcription of *PPP1r3c*, *Slc37a4* (translocation protein for G6pc) and *Ppp1r3b* was in response to constant corticosterone only (de Guia, Rose and Herzig, 2014; Kuo *et al.*, 2015). A reduced number of inhibitory genes were corticosterone pattern regulated, with *H6pd* and *Nr0b2* transcription increased in response to raised circulating corticosterone time points and *Avpr1a* and *Nr1i3* transcription increased in response to constant corticosterone infusion only.

Analysis of corticosterone regulated genes that affect carbohydrate quantities, predicted trends of activation in a transient manner at the pulse peak (z-score 1.84) but not by the nadir in response to a pulsatile corticosterone infusion (Figure 5.9 Aii). In response to a constant infusion, trends of activation were predicted in a pro-longed manner across 140min and 180min time points (z-score 1.53 and 1.64 respectively) Together, analysis indicates trends of transient activation of carbohydrate quantity, were dysregulated in a prolonged manner, potentially increasing carbohydrates in response to constant corticosterone exposure within the liver.

Transcription of genes associated with the quantity of carbohydrates that were increased in response to raised circulating infused corticosterone included *Bhmt*, *Fmo3* and *H6pd*, whilst *Ppp1r3c*, *Foxo1* and *Avpr1a* were constant corticosterone dependent only. Transcription of the inhibitory genes *Gjb1* and *Scp2* were decreased in response to the corticosterone pulse peak only.

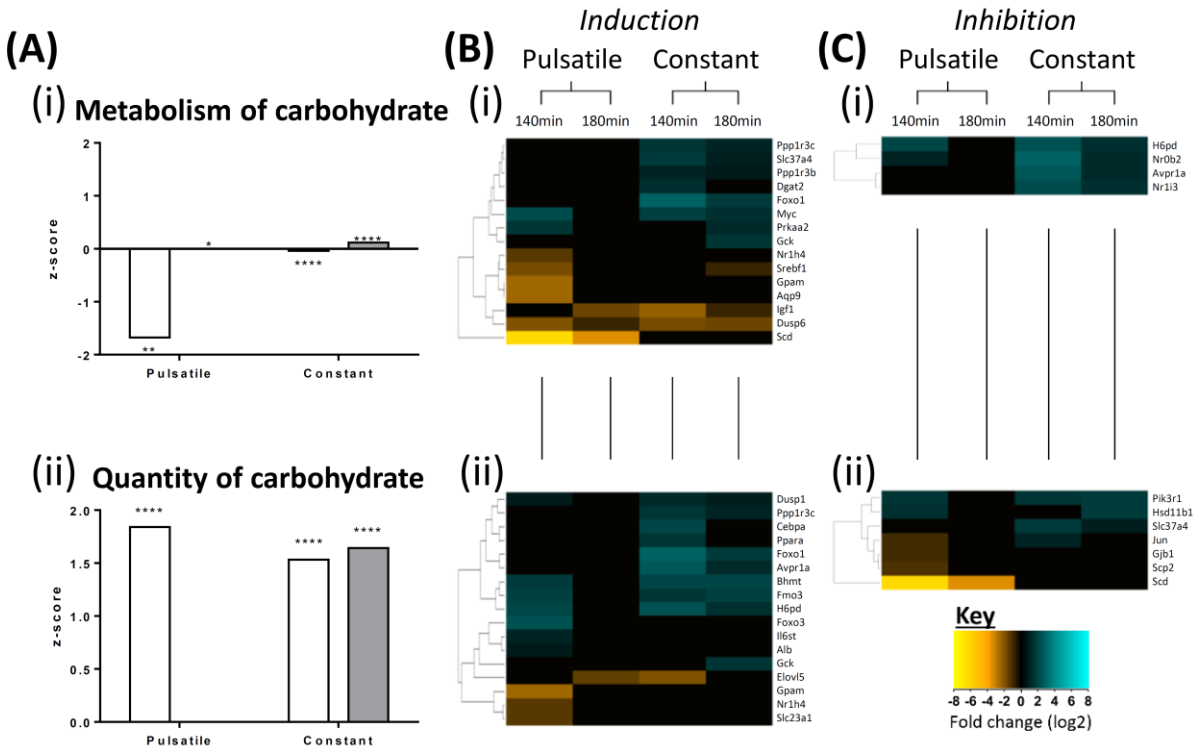

Figure 5.9 Predicted modulation of carbohydrate metabolic pathways by patterned corticosterone infusion timepoints.

*(A) Predicted activation or inhibition was based upon analysis of pSer2 Pol2 occupied targets regulating carbohydrate metabolism in response to pulsatile and matched constant corticosterone infusion at 140min (white bars) and 180min (grey bars). Fold changes >1.5 from VEH infused control and p-values <0.05 adjusted for multiple comparisons were analysed by IPA software. Positive and negative z-scores >2 indicate significant predicted activation or inhibition respectively. Differential occupancy of pSer2 Pol2 was hierarchically clustered by fold change values and plotted within heatmaps to the right. Results were separated into factors known to activate (B) or inhibit (C). Degree of increased (cyan) or decreased (yellow) log2 fold change is indicated by colour intensity, as shown within the key. Results indicated metabolism of carbohydrate (i) and quantity of carbohydrate (ii) were modulated by corticosterone infused timepoints. Changes in pSer2 Pol2 occupancy to VEH control were analysed in regions >620b and limited to intragenic regions <10kb from the TSS according to Ensembl (Rn6) co-ordinates and filtered for unique gene transcripts. Z-score p-values are indicated by *<0.05, **<0.01 and ****<0.0001.*

Despite multiple studies highlighting the significant role of GCs within TG, fatty acid and lipid metabolism, interpretation of patterned corticosterone regulation was difficult due to limited numbers of differentially regulated targets. In response to the pulsatile infusion, trends of inhibition were predicted at the corticosterone pulse peak for the concentration of triacylglycerol (Figure 5.1 Ai) and lipids (Figure 5.10 Aii) (z-score of -1.08 and -1.13 respectively) whilst predicted activation for fatty

acid concentration (Figure 5.10 Aiii) (z-score of 0.60). Similar but inverted trends were predicted by the pulse nadir (z-scores of 0.10, 0.60 and -1.31 respectively) indicating transient regulation. In response to constant corticosterone infusion, analysis reported trends of inhibition for TGs (z-score of -0.34 and -0.41), fatty acids (z-scores -1.15 and -0.51) and lipids (z-scores of -1.12 and -0.54). These data indicate that transient, pulsatile regulation of these pathways which are dysregulated by constant corticosterone exposure in a pro-longed and inhibitory action is possible, however, confidence of predictions was low.

Analysis of corticosterone regulated genes reported enrichment of a number of genes with shared regulatory function in hyperlipidaemia and dyslipidaemia pathways as shown in Figure 5.10 B, except for *Srebf1*, *Hsd11b1*, *Nr0b2*, *Apoe* and *Fasn*, but with low confidence predictive trends (data not shown). Interrogation of individual corticosterone regulated genes within pathways, indicated increased transcription of *Lpin1* and to a lesser degree *Nr0b2*, was induced by raised corticosterone infused time points except for pulse nadir. Similar trends but inhibitive, were observed for *Apob*. Transcription of *Fasn* was inhibited at both pulsatile corticosterone time points, but to a greater degree at the pulse peak and *Foxo1* transcription was increased in response to a constant corticosterone exposure only.

Together, despite the literature indicating dysregulating GCs can induce raised TG, fatty acid and lipid levels, my data indicated loss of transient transcription was potentially inhibitive of these pathways. Under further interrogation, I have identified key corticosterone regulated targets that present ideal candidates for further study.

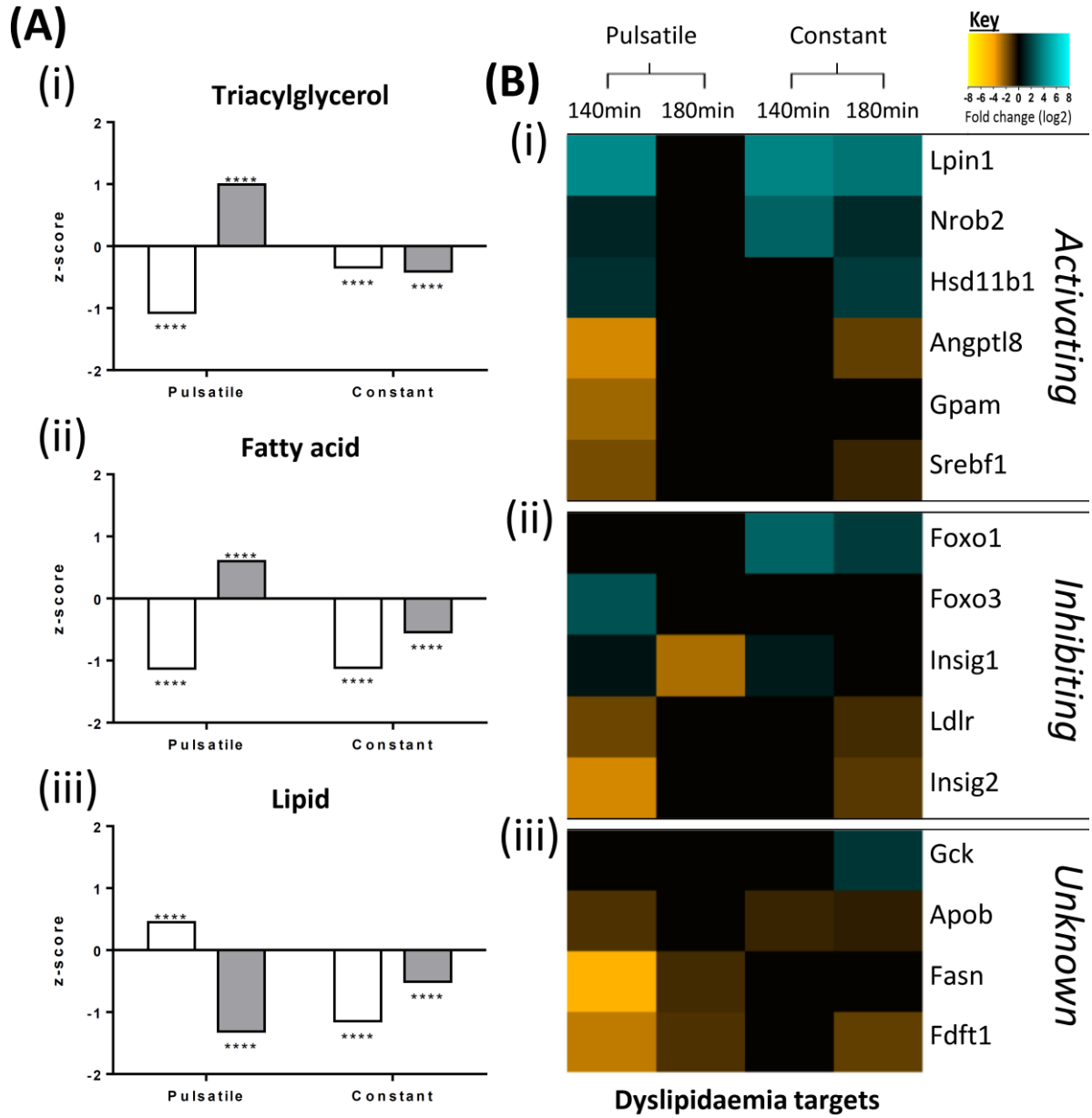

Figure 5.10 Predicted pathway activation or inhibition of lipid, triglyceride and fatty acid metabolism.

Predicted activation or inhibition was based upon analysis of pSer2 Pol2 occupied targets regulating the concentration of triacylglycerols (A), fatty acids (B) and lipids (C) in response to pulsatile and matched constant corticosterone infusion at 140min (white bars) and 180min (grey bars). Differential occupancy of pSer2 Pol2 targets within the hyperlipidaemic and dyslipidaemia pathways were hierarchically clustered by fold change values and plotted within heatmaps to the right. Results were separated into factors known to activate, inhibit or unknown effects on pathways. Targets apart from Lpin1, Angptl8, Insig2, Fdft1 and Fasn are involved in at least one of the three triacylglycerol, fatty acid and lipid pathways. Degree of increased (cyan) or decreased (yellow) log2 fold change is indicated by colour intensity, as shown within the key towards the top of the figure. Fold changes >1.5 from VEH

*infused control and p-values <0.05 adjusted for multiple comparisons were analysed by IPA software. Positive and negative z-scores >2 indicate significant predicted activation or inhibition respectively. Pser2 Pol2 occupancy to VEH control were analysed in regions >620b and limited to intragenic regions <10kb from the TSS according to Ensembl (Rn6) co-ordinates and filtered for unique gene transcripts. Z-score p-values are indicated by ***<0.001 and ****<0.0001.*

5.5 Discussion

Multiple studies have demonstrated that GRs are not required to bind within close proximity to a TSS or within the 'promoter' region to exert transcriptional regulation (Ratman *et al.*, 2013). Indeed, further genomic studies have indicated up to ~7% of binding sites were within regions varying from 2.5kb to 20kb regions of the TSS and that the largest proportion of GR binding sites were within intergenic regions (43.6-57.6%) as presented within this thesis (Figure 5.2) (John *et al.*, 2011; Rao *et al.*, 2011; Uhlenhaut *et al.*, 2013). An interesting correlation was found within the data when genes were sorted into either increased or decreased corticosterone dependent transcription (increased or decreased pSer2 Pol2 occupancy) and plotted against the distance from the TSS to closest corticosterone induced GR binding event. It was observed that transcriptionally up-regulated genes were more likely to have a relatively closer GR binding site than those that were down-regulated (Figure 5.3). A similar relationship has been identified with mRNA abundancy in response to Dex administration within human alveolar epithelial (A549) cells (Reddy, Pauli and Sprouse, 2009). Due to such a limited number of nGRE associated sequence containing GR enrichment regions, no association could be made between the observed inhibitive effect of GR binding to nGRE motifs. Particularly when one considers just 2.23% of enriched GR regions contained a nGRE like sequence and approx. 75% of genes were inhibited by patterned corticosterone infusion. Exact mechanisms, therefore, are yet to be elucidated; however, it does provide an intriguing observation of distanced GR transcriptional control as well as further evidence that use of pSer2 Pol2 occupancy as a proxy of transcription is appropriate.

Pathway analysis of corticosterone regulated targets reported non-significant predictions for all pathways except cholesterol biosynthesis at the pulse nadir (Figure 5.5 Ai) and methionine degradation in response to raised circulating corticosterone time points (pulse peak and both constant corticosterone infused time points) (Figure 5.5 Aiii). The lack of confident predictions is most likely due to the limited number of regulated genes, as this analysis is primarily designed for RNA-Seq data. Despite the lack of significance, trends of transient corticosterone regulation of key metabolic pathways were predicted for the quantity of glycogen, monosaccharide and carbohydrate, proliferation of liver cells, cell death and necrosis as well as the significant result for cholesterol and

to a limited extent lipids. Whereas, TGs, fatty acids and metabolism of carbohydrates were inhibited in a similar manner, synchronised to the pulse peak of pulsatile corticosterone infusion. Interestingly, in response to a constant corticosterone infusion, dysregulation of pathway transient activation/ repression was predicted for all pathways.

Dysregulation of these pathways could induce aberrant metabolic function as found with MetS phenotypes. Loss of inhibitory cholesterol synthesis by the constant corticosterone infusion could increase cholesterol levels, which have been associated with hypertension and obesity, as well as liver fibrosis, steatohepatitis and steatosis (Ioannou *et al.*, 2009; Van Rooyen *et al.*, 2011; Ichimura *et al.*, 2015). Similarly, prolonged activation of methionine degradation could reduce methionine levels and potentially increase methionine metabolites within the liver, which are associated with fatty liver development and NAFLD (Mato, Martínez-Chantar and Lu, 2008; Kharbanda, 2009). Prolonged increases of glucose and its derivatives has long been associated with insulin resistance, hyperglycaemia and diabetes (de Guia, Rose and Herzig, 2014; Kuo *et al.*, 2015; Zhou *et al.*, 2016; Yaribeygi *et al.*, 2019), whilst dysregulated growth and apoptotic pathways are associated with non-alcoholic steatohepatitis (NASH) and fibrosis (Feldstein *et al.*, 2003; Argo *et al.*, 2009; Luedde, Kaplowitz and Schwabe, 2014).

Despite the inability of the pathway analysis to predict significant activation or inhibition, I have highlighted corticosterone targets known to regulate these pathways that would be interesting to characterise in future studies. For example, *Got*, *Slc37a4*, *G6pc* and *Pfkfb1* dysregulation of transient transcriptional control could have distinct effects for glucose whilst *Scd*, *Lpin1*, *Apob* and *Fasn* for TG, fatty acid and lipid homeostasis. Particularly as 28 genes enriched within the pathways highlighted within this thesis, were identified as robustly corticosterone regulated i.e. significant and transient increased or decreased regulation in response to a pulsatile corticosterone infusion, whilst constant corticosterone exposure dysregulated this profile and indicated prolonged levels of increased transcription across time points (Figure 5.11 A).

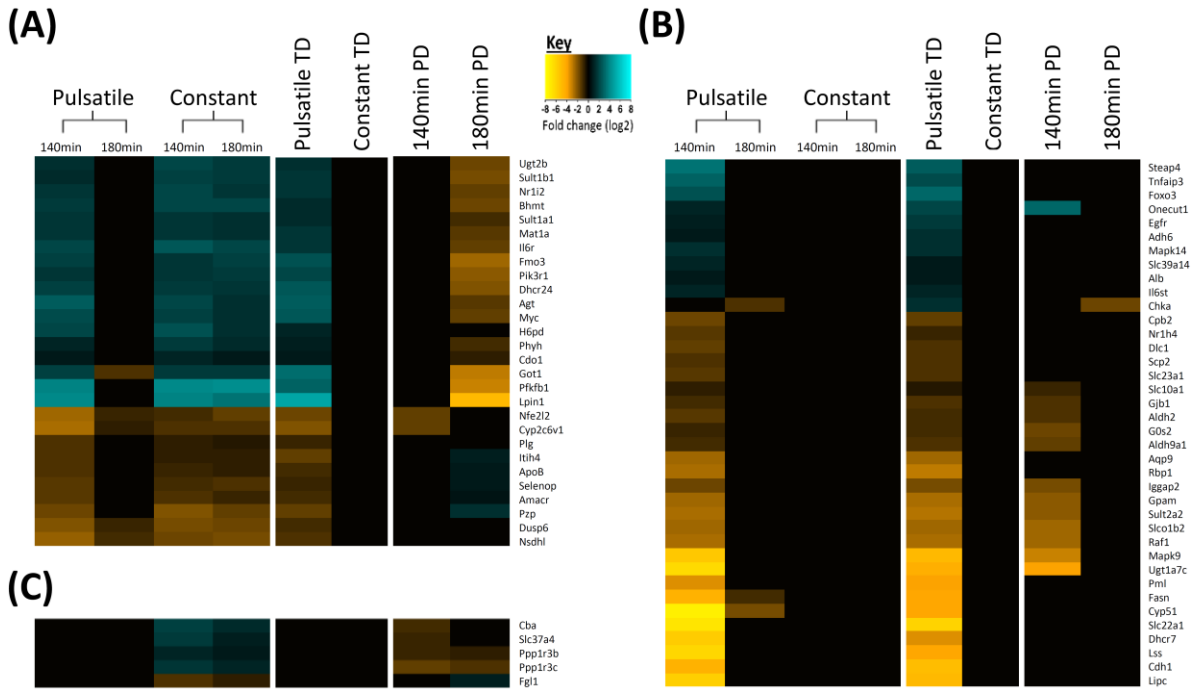

Figure 5.11 Corticosterone pattern regulated targets involved in pathway regulation.

Analysis of differentially pSer2 Pol2 occupied genes identified key targets known to regulate inflammatory, glycogen, glucose, monosaccharide, growth and proliferative, necrotic and cell death, carbohydrate fatty acid, triglyceride lipid, dyslipidemic as well as canonical melatonin, serotonin and methionine degradative and cholesterol biosynthesis pathways. These were split into distinct dynamic changes in occupation. First, targets which significantly time dependent (TD) in response to pulsatile infusion only but enriched to VEH control at both constant corticosterone timepoints were defined as corticosterone pattern dependent (A). Secondly, targets similarly TD in response to a pulsatile infusion but not enriched to VEH by a constant corticosterone infusion were defined as pulsatile responsive only (B). Finally, targets that were not TD in response pulsatile corticosterone infusion but were enriched to VEH in response to constant corticosterone infusion only and not TD were defined as constant responsive (C). Degree of increased (cyan) or decreased (yellow) log2 fold change is indicated by colour intensity, as shown within the key towards the top of the figure. Fold changes >1.5 from VEH infused control and p-values <0.05 adjusted for multiple comparisons were analysed by IPA software. Pser2 Pol2 occupancy to VEH control were analysed in regions >620b and limited to intragenic regions <10kb from the TSS according to Ensembl (Rn6) co-ordinates and filtered for unique gene transcripts. pSer2 Pol2 differentially occupied targets which were pattern dependent (PD) at 140min and 180min timepoints were also indicated.

In conclusion, analyses of the functional effects of GR and pSer2 Pol2 corticosterone pattern regulation provides two main findings. First, corticosterone regulated increases in transcription are more likely to occur within targets where the distance between the TSS and an inducible GR binding site are

relatively short, and transcription is more likely to be decreased with an increasing distance to bound GR sites. Secondly, analysis of corticosterone regulated genes predicts a number of pathways in energy and liver growth/ death could be transiently regulated by ultradian oscillations of corticosterone, which are dysregulated by constant corticosterone exposure within a relatively short experimental time scale. These data indicate dysregulation of GCs could be a key factor in the development of associated pathologies such as insulin resistance, diabetes, dyslipidaemia, hyperlipidaemia, fibrosis, NASH and NAFLD MetS phenotypes.

Chapter 6 Modelling the 24hour artificial 'ultradian' Corticosterone infusion pattern

6.1 Background

The GR and pSer2 Pol2 ChIP-Seq data revealed dynamic GR binding and transcriptional regulation synchronised to peak and nadir of corticosterone pulses. Interpretation of the resulting effects, using functional pathway analysis, highlighted how key metabolic pathways were also dynamically regulated during pulsatile corticosterone exposure. Notably, pulsatile infusion induced phasic activation or inhibition of pathways known to be important for metabolic processes within the liver, including inflammatory regulation, glucose homeostasis, carbohydrate, lipid and fatty acid metabolism. Phasic activation of the cellular proliferation pathway was seemingly counterbalanced with phasic activation of cellular apoptotic pathways during pulsatile corticosterone infusion.

In contrast, constant infusion of a matched corticosterone dose significantly dysregulated the characteristic ultradian dynamics of GR binding and RNA Pol2 enrichment within GC target genes. These pattern dependent effects were found to impact upon important metabolic functional pathways, with notable differences in the predicted trends for pathways mentioned previously. Dysregulation of these pathways is known to be associated with phenotypes of MetS such as insulin resistance, diabetes, dyslipidaemia, liver fibrosis and NASH and NAFLD. My data now contributes to our understanding about how altered GC rhythms, via dysregulated action of GR and aberrant transcriptional regulation of GC target genes in the liver, may directly induce the early stages of development of these conditions.

Despite how rapid and robust observed transcriptional changes were in response to the two GC patterns over the 3hr timescale in my experiments, we expect that physiological changes would take far longer to become apparent. In fact, development of MetS as a result of GC dysfunction and the pathways highlighted within this study may even take years to develop fully, therefore, a more chronic experimental model is needed to test whether we can start to see measurable physiological changes (Jia *et al.*, 2018).

Within this chapter, I have modelled the 24hr endogenous ultradian GC profile, based upon data I collected from adrenally intact rats and have designed a corticosterone replacement protocol that delivers hourly 20min pulses of different amplitudes into in ADX rats, to recapitulate the circadian and ultradian corticosterone profile.

6.2 Aims

- Model the endogenous ultradian circulating total blood serum corticosterone profiles within the rat.
- Design a corticosterone infusion replacement profile with both circadian and ultradian characteristics.

6.3 Methods

All methods of analysis were done according to general methods discussed within Chapter 2.

Briefly, adult male Sprague-Dawley rats (250-300g) (Harlan, Bicester, UK) were housed under standard conditions, 12:12 light/ dark cycle (lights on at 06:00h) with food and water available *ad libitum*.

Surgical bilateral ADX or sham, I.P. telemetry probe implantation as well as jugular vein and carotid artery cannulation were performed under anaesthesia. ADX rats were provided with 0.15µg/L of corticosterone in 0.9% saline drinking water whilst sham operated control rats were provided with plain water. Both groups had access to normal chow, ad libitum during the 5-day post-surgical recovery period. All cannulae were flushed daily with 1% heparinised saline (0.9M) to maintain patency every 24hrs. Telemetry recordings of activity and temperature were collected every 10mins throughout.

In ADX rats, 16 hrs prior to corticosterone infusions, corticosterone supplemented saline was replaced with 0.9% saline for drinking, to allow adequate washout period within the circulation.

Blood samples were collected every 10mins from either the carotid artery or jugular vein using the ABS system over a 28hr period and total blood serum corticosterone was measured via in-house RIA.

Within ADX rats, 3.84µM corticosterone-HBC conjugate was infused in 20min periods at variable rates hourly over a total 28hr period via the jugular vein.

6.4 Results

To accurately model circulating endogenous ultradian corticosterone oscillations over 24hrs, blood samples were collected from sham ADX rats every 10mins as well as activity and core body temperature (°C) data.

Assessment of individual total blood serum corticosterone profiles revealed evidence of ultradian hourly pulses within the circadian active period (data not shown). When the data was averaged across rodents, the circadian rhythm was still clearly seen but the distinct ultradian pulses were no longer evident as pulses are not synchronised to a suitable degree between biological replicates (Figure 6.1

A). The circadian corticosterone rise began at ~Zt7 (5hrs before lights off) and does not return to basal levels until ~Zt22 (2hrs before lights on) consistent with previously published data (Windle, Wood, Lightman, *et al.*, 1998; Windle, Wood, Shanks, *et al.*, 1998; Waite *et al.*, 2012; Walker *et al.*, 2014). Maximal corticosterone (146ng/ml ±26) was detected at Zt12:40.

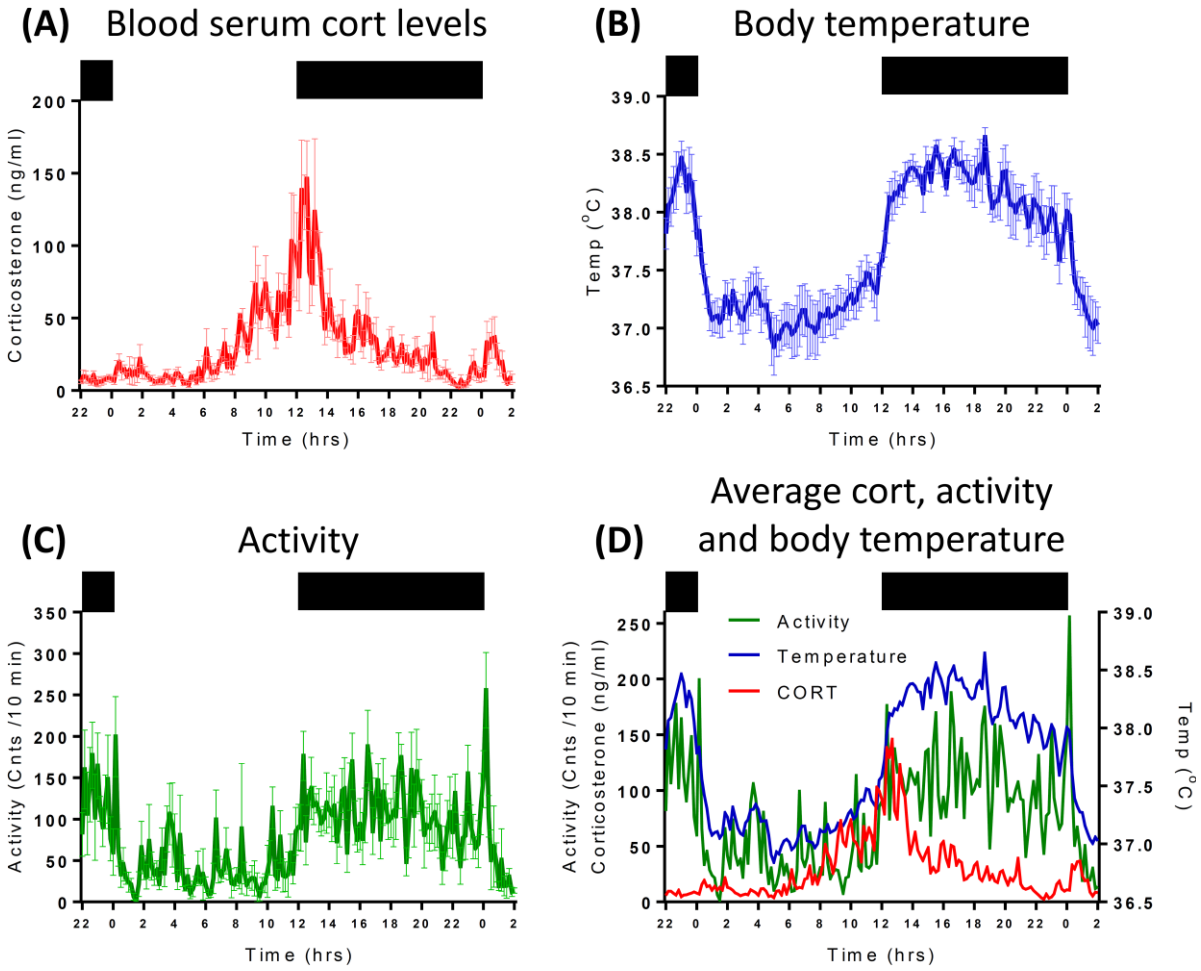

Figure 6.1 Circulating corticosterone, body temperature and activity profiles in sham adrenalectomised rats.

Jugular vein blood samples were taken at 10min intervals over 28hrs and total blood serum corticosterone levels were assessed using an in-house RIA (red). Analysis identified corticosterone peak at Zt12:40 (A). Telemetry probes were also implanted into the intraperitoneal space recording body temperature (blue) (B) and activity (green) (C) and data binned into 10min segments. Robust circadian profiles were observed in all three metrics (D). Rats (N=6) were sham adrenalectomised and housed in standard conditions under a 12:12 light schedule (dark bar indicates lights off), error bars represent mean ± s.e.m..

Analysis of average activity and body temperature data indicated a high degree of similarity to corticosterone changes. A distinct rise in body temperature was recorded between Zt12-14 and

maintained until ~Zt20-22 before returning to basal levels, of which Zt4:50 recorded the minimum temperature (36.8°C ±0.25) (Figure 6.1 B). Activity profiles followed a similar pattern to body temperature (Figure 6.1 C). Interestingly, maximal corticosterone levels coincided with the onset of increased body temperature and activity, however, both body temperature and activity remained elevated whilst corticosterone levels gradually retuned to nadir within the period ~Zt20-22.

As my acute corticosterone replacement infusion model was 3hrs, the 24hr period was segmented into eight 3hr blocks. Zt11-14 was allocated as the circadian corticosterone peak period, based on maximal endogenous corticosterone level having been detected at Zt12:40 (Figure 6.2 A). Over this 3hr period, the maximal rate of 1ml/hr over 20min every hour was used.

To introduce the appropriate circadian amplitude variations into the infused corticosterone pulses, endogenous corticosterone data was analysed over each 3hr period by area under the curve. Fold decrease relative to circadian peak (Zt11-14) was calculated for each 3hr period, and infusion rates were appropriately reduced from the maximal rate of 1ml/hr by the calculated factor (Figure 6.2 B&C). Analysis and subsequent infusion profile design predicted a similar profile of relative change to endogenous profiles, particularly across a similar time segment (Zt2-5) as observed within endogenous corticosterone profiles (Figure 6.2 D).

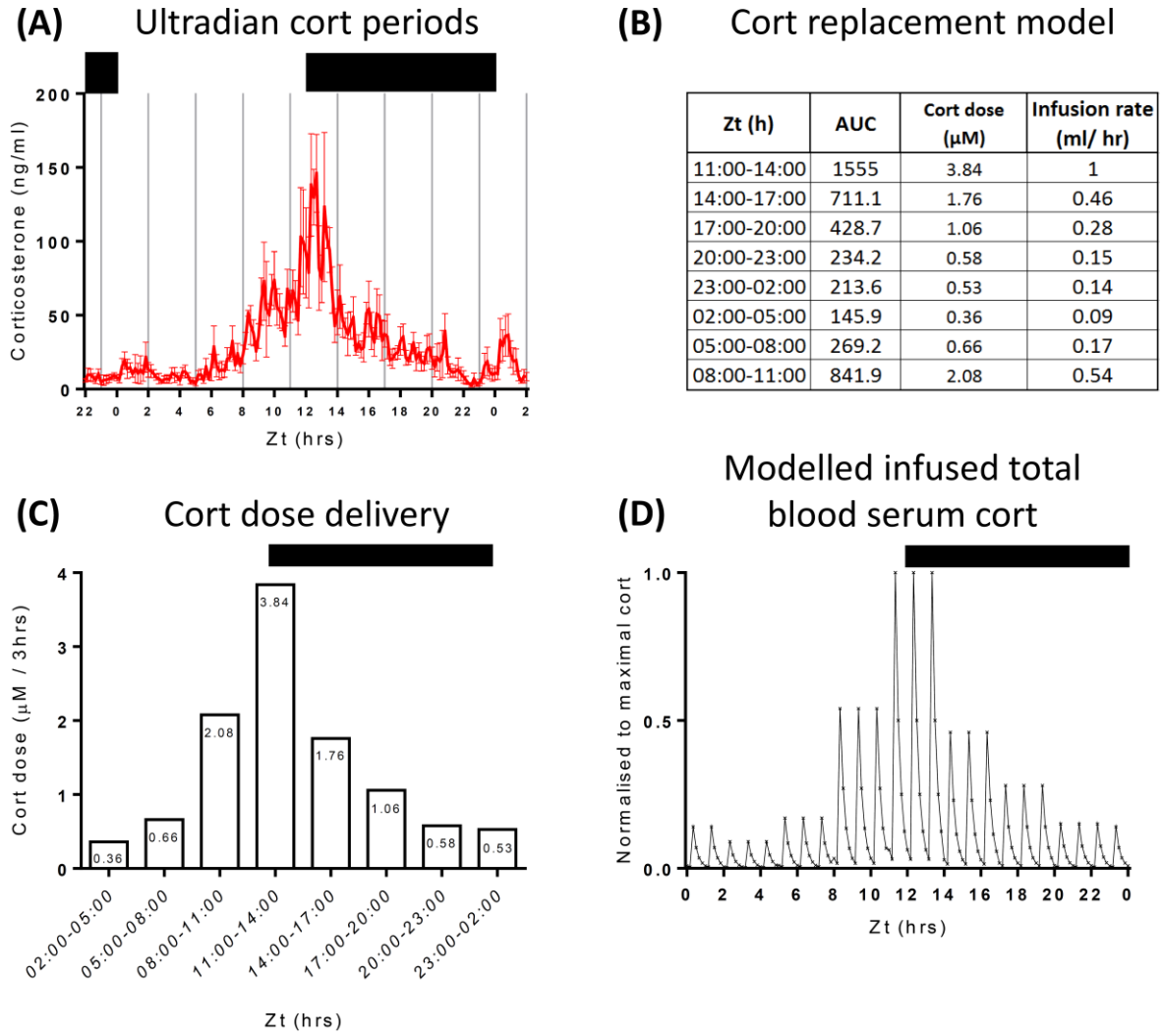

Zt (h)	AUC	Cort dose (µM)	Infusion rate (ml/ hr)
11:00-14:00	1555	3.84	1
14:00-17:00	711.1	1.76	0.46
17:00-20:00	428.7	1.06	0.28
20:00-23:00	234.2	0.58	0.15
23:00-02:00	213.6	0.53	0.14
02:00-05:00	145.9	0.36	0.09
05:00-08:00	269.2	0.66	0.17
08:00-11:00	841.9	2.08	0.54

Figure 6.2 Modelling the 24hr 'ultradian' corticosterone profile.

The period between Zt11-14 was allocated as circadian peak according to 10min profiling of total circulating corticosterone. The rest of the 24hr period was segmented accordingly (A). Rats (N=6) were sham adrenalectomised and housed in standard conditions under a 12:12 light schedule (dark bar indicates lights off), error bars represent mean ± s.e.m.. Each 3hr section was assessed using an area under the curve analysis. Factor changes in results to circadian peak (Zt11-14) were used to calculate changes to the infused corticosterone dose, using 3.84µM for the maximal delivered dose, as used in the acute model (B). Modelled changes in doses within 3hr sections (C) as well as a hypothetical circulating corticosterone levels (normalised to circadian peak) (D) over 24hrs resembled endogenous ultradian profiles.

To validate the modelled ultradian infusion model, corticosterone was infused into adrenalectomised rats over a 28hr period via the jugular vein, whilst simultaneous blood samples were collected from the carotid artery every 10mins throughout. Differing vessels were chosen so as to collect data on

corticosterone levels that had passed through the circulation network. Telemetry probes were also implanted I.P. to confirm intact circadian activity and body temperature profiles.

Within the infusion model, an initial increased rate for 2min 30sec was used to prime the infusion line and cannula with corticosterone-HBC saline prior to the modelled infusion. Due to an error in initial programming of the infusion pump, 5 pulses of corticosterone-HBC saline were erroneously infused at this rate between Zt22-3. This was corrected for the remainder of the modelled infusion (Figure 6.3 B).

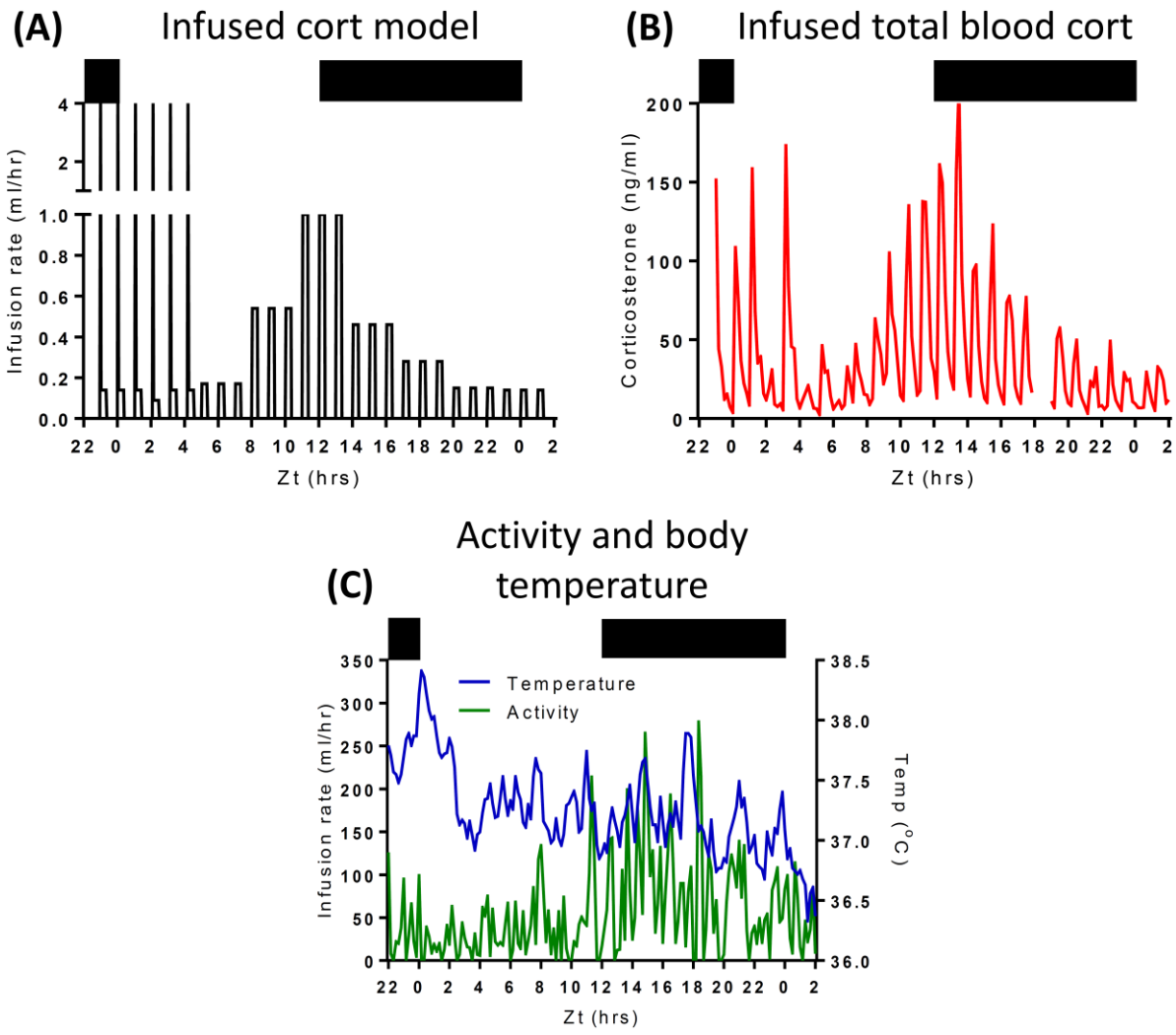

Figure 6.3 Validation of the mock 'ultradian' corticosterone infusion.

28hr corticosterone-HBC saline infusion profiles, modelled to mimic a typical endogenous ultradian corticosterone profile, were infused via jugular implanted canulae during simultaneous blood sampling from the carotid artery of an adrenalectomised rat. Infusion rates were modelled over a 28hr period (A) and total blood corticosterone levels were assessed via RIA (B). Body temperature and activity data was also collected over the infusion and sampling period (C). Light schedule was 12:12 (black bar indicates lights off) and n=1.

From an initial total of 8 rats, only four were successfully dual cannulated due to the high degree of difficulty cannulating the carotid artery which. One of the four blocked prior to experimental testing and two of the three remaining suffered adverse effects and were terminated prior to infusion completion. A full 28hr profile of corticosterone, body temperature and activity data were collected from a single rat. Rapid increases in circulating total corticosterone were recorded during each 20min infusion of corticosterone, which was rapidly cleared within 40min of each infusion, returning to basal levels before the next pulse (Figure 6.3 B). The amplitude of the delivered pulses varied as expected over the 28hr period, recapitulating previously characterised endogenous measurements. Overall, corticosterone increased from Zt6 to a maximal corticosterone level at Zt13:30 (209ng/ml) in response to the maximal infused dose of corticosterone (Figure 6.3 A). Pulse amplitude gradually decreased throughout the following period until reaching minimal levels at Zt23:20 (29ng/ml). Corresponding well with endogenous circadian nadir data. Despite the methodological error that occurred between Zt22-3, corticosterone data indicates the infusion model can replace circulating corticosterone in an adrenalectomised rat with both ultradian and circadian components.

Analysis of telemetry data during corticosterone replacement, indicated that whilst increases in activity were associated with lights off similar to adrenally intact controls, body temperature did not and gradually decreased throughout the infusion period from ~38°C to 36.5°C (Figure 6.3 C). This is most likely an adverse effect associated with the dual cannulation method, as examination of telemetry data prior to infusion, reported drops in body temperature were associated with flushing of cannula to maintain patency. To fully remove any blood clots that may form within the cannula, heparinised saline is withdrawn until a small amount of blood (approx. 100µL) is drawn from the cannula. Whereupon fresh sterile heparinised saline (approx. 100µL) is infused back, clearing the cannula of blood and pushing a small amount into the circulation. Despite this method being used multiple times and no previous adverse effects observed in previous double cannulation experiments (Figure 2.2), these flushes may have induced a slight drop in blood pressure and thus core temperature.

6.5 Discussion

To my knowledge, GC replacement with both ultradian and circadian characteristics for use in a chronic model has not been shown before within the ADX rat. Within this pilot study, I have presented data showing that my model can deliver a physiologically realistic, hourly pulsatile corticosterone infusion via the jugular vein with circadian variations of amplitude across a 24hr period.

As this characterisation has been successful in only one male ADX rat, due to adverse reactions associated with the double cannulation combination of jugular and carotid vessels, further refinement

of the procedure (followed by validation) is required. To avoid adverse reactions found with the combination of carotid and jugular cannulation used in this study, two cannulas will be inserted into a single jugular vein, as previously used in our group.

Within this thesis, I have presented data showing that a 3hr pulsatile corticosterone infusion model will regulate synchronised, transient GR recruitment across regulated targets throughout the genome, which will induce similar profiles of up-regulated or down-regulated transcription of select genes important for regulation of metabolic pathways within the liver. I further report, loss of oscillating corticosterone, dysregulates both GR and transcriptional dynamics, in a manner that could modulate pathways integral to the development of MetS phenotypes. Despite these indications, I have not investigated any changes in circulating metabolic markers, nor would I expect to find any within a 3hr timescale as measurable physiological changes will take longer to develop. Additionally, the 3hr model was specifically designed to avoid having to account for circadian changes, therefore, to fully investigate the development of aberrant metabolic function that could be translationally significant for clinical studies, the infusion model has to be extended.

Primarily, the model was designed to investigate whether metabolic action could be differentially regulated by a pulsatile ultradian or non-oscillatory, constant circadian pattern of circulating corticosterone. Therefore, I have also designed a novel matched constant circadian infusion model using similar methods. This constant circadian corticosterone replacement model, infuses over a 60min period but at a reduced rate, matching the dose delivered over the 1hr to the 20min pulsatile infusion (Figure 6.4).

(A)

Zt (hr)	AUC	Cort dose (μM)	Pulsatile infusion rate (ml/hr)	Constant infusion rate (ml/hr)
11:00 - 14:00	1,555	3.84	1	0.33
14:00 - 17:00	711.1	1.76	0.46	0.15
17:00 - 20:00	428.7	1.06	0.28	0.09
20:00 - 23:00	234.2	0.58	0.15	0.05
23:00 - 02:00	213.6	0.53	0.14	0.05
02:00 - 05:00	145.9	0.36	0.09	0.03
05:00 - 08:00	269.2	0.66	0.17	0.06
08:00 - 11:00	841.9	2.08	0.54	0.18

(B) Models of ultradian and circadian cort replacement

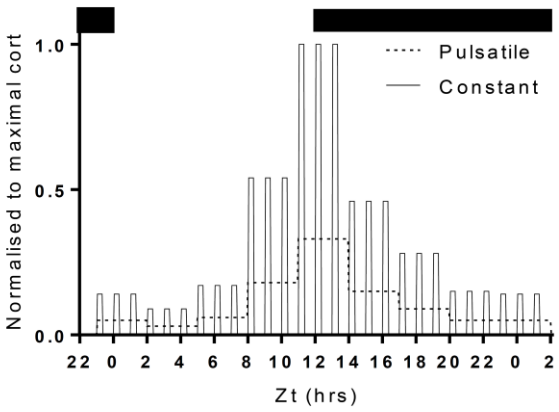

Figure 6.4 Schematic of a matched modelled loss of pulsatile corticosterone infusion.

Table describes the dose of corticosterone infusion delivered every 3hrs over a 24hr period as well as the rates used for either infusion pattern (A). To induce a pulsatile infusion pattern (dashed line),

corticosterone would be infused over a 20min period followed by a 40min pause and repeated hourly according to the table. Whereas, to induce a constant infusion pattern (solid line), corticosterone would be infused over the full 60min period every hour, but at a reduced rate to the pulsatile infusion, therefore matching total dose delivered every hour between infused patterns (B).

Based on my experience of duration of canula patency, an experimental infusion period can be extended up to a 5-day chronic model. This may potentially be long enough to induce changes within metabolic homeostatic processes and detect measurable differences in circulating fatty acid, TG and lipid levels. The model can also be used to investigate GC phase shifts to the photoperiod, as found with transmeridian travel (a.k.a. jet lag) as well as an alteration of feeding behaviour as found with variable shift work. This model will also be useful for investigation of other GR regulated physiological process, and to assess effects on other important GC target tissues such as the brain, as corticosterone replacement is conducted in unstressed conditions and freely behaving conscious rats.

Chapter 7 General Discussion

7.1 Summary of findings

In this thesis, I report novel *in vivo* data showing how ultradian corticosterone replacement in ADX rats synchronises liver GR binding to the corticosterone pulse peak, at ~ 3,000 binding sites across the genome. GR binding was found to be phasic in 100% of cases, with complete dissociation from all binding sites within the corticosterone pulse nadir, hence, ultradian GR binding dynamics are tightly regulated by the pulsatile corticosterone pattern. Dysregulation of the ultradian rhythm via a dose matched constant infusion induced prolonged GR binding at the majority of these binding sites, indicating that pulsatile GR dynamics are extremely sensitive to disruption when circulating corticosterone rhythms are dysregulated. I report that genome-wide RNA Pol2 access to the chromatin template is also dynamically regulated, with precise timing synchronised by pulsatile corticosterone. I report the first evidence for a functional consequence of dysregulated ultradian corticosterone exposure in liver, as constant infusion resulted in distinct and opposing transcriptional outcomes to pulsatile infusion. While pulsatile corticosterone predominantly induced gene repression in the majority of cases, constant corticosterone predominantly induced gene transactivation in the majority of cases at 140min. The differentially regulated genes were found to be enriched within key metabolic pathways known to induce insulin resistance, diabetes, obesity, dyslipidaemia, fatty liver disease and hepatic steatosis within dysregulated GC pathology. Taken together, my data highlights the importance of maintaining the ultradian GC profile for homeostatic metabolic function via tightly controlled regulation of GR dependent transcriptional dynamics. This is the first evidence directly linking dysregulated ultradian GC rhythms with early transcriptional changes in known metabolic risk factors for the development of MetS. Finally, I have designed a novel 24hr corticosterone replacement model that will be used in future research to determine how these early changes manifest into metabolic changes over a longer timeframe.

My research and findings of underlying metabolic mechanisms is extremely relevant to current public and government interests in tackling metabolic phenotypes that have risen in parallel with rhythm disrupting lifestyles, chronic stress, and prevalence of long-acting synthetic steroid treatments. Targets found to be sensitive to rhythm disrupting GC exposure in this study will inform translational approaches, in particular the identification of druggable candidates for therapeutic intervention in GC pathology and its associated metabolic dysregulation.

7.2 Overview of corticosterone patterned regulation

The main focus of my work has been to investigate the biological significance of the ultradian GC rhythm. Adrenal circadian GC release is synchronised to the photoperiod via the HPA axis (Weitzman, 1976; Lightman and Conway-Campbell, 2010). Due to intrinsic delayed positive feed forward and negative feedback mechanisms regulating adrenal GC secretion, combined with its short half-life upon entering the circulation, circulating GC levels oscillate in an ultradian rhythm within the circadian rhythm. The majority of research investigating the importance of GC rhythms focussed on the circadian rhythm, with 6-12hr intervals between data collection which misses the underlying ultradian dynamics, despite their highly conserved nature within mammalian biology (Krieger *et al.*, 1971; Holaday, Martinez and Natelson, 1977; Benton and Yates, 1990; Engler *et al.*, 1990; Carnes *et al.*, 1992; Loudon *et al.*, 1994; Cudd *et al.*, 1995; Windle, Wood, Shanks, *et al.*, 1998) and have been demonstrated to play important roles in a diverse range of physiological functions (Windle, Wood, Lightman, *et al.*, 1998; Conway-Campbell *et al.*, 2010; Sarabdjitsingh *et al.*, 2010, 2014, 2016; Kalafatakis *et al.*, 2018). It therefore seems short sighted to ignore their potential role in metabolic regulatory functions, as this is a major function ascribed to GCs (Kyrou, Chrousos and Tsigos, 2006; de Guia, Rose and Herzig, 2014; Kuo *et al.*, 2015)

7.2.1 Mock 'ultradian' corticosterone pulses direct robust glucocorticoid receptor binding and synchronised transcription

Within Chapter 3, I present novel *in vivo* data, showing that physiological pulsatile corticosterone infusion into ADX rats, induced GR binding at 87.4% of corticosterone regulated sites across the genome exclusively at the peak of the pulse which was lost within the pulse nadir (Figure 3.7). To my knowledge, similar GR dynamics *in vivo* have only been reported for the well characterised *Per1* GRE ~2.5kb upstream from the TSS. Authors reported that three bolus 100µg corticosterone injections were associated with maximal GR binding at the peak of each corticosterone pulse and dissociated to basal levels within the corticosterone pulse nadir after 40min. They also reported phasic hnRNA production of Per1 that was slightly delayed to both corticosterone and increased GR levels (Figure 1.9) (Stavreva *et al.*, 2009). My work validates that not only are these dynamics replicable using a corticosterone replacement infusion model via the jugular vein, but also that ultradian corticosterone dynamics can direct GR binding across all accessible binding sites across the genome which is not restricted to select targets.

As previously mentioned, the GR is an oxosteroid nuclear transcription factor, mediating transcriptional regulation via recruitment of co-factors for its intrinsic transactivator/ transinhibitory mechanisms (Oakley and Cidlowski, 2013; Ratman *et al.*, 2013). Previously it has been shown that

oscillating GR binding to the regulatory GRE of Per1 induced phasic hnRNA production in rat liver (Stavreva *et al.*, 2009). In chapter 4, I expanded upon my GR binding data to present novel RNA Pol2 ChIP-Seq data that indicated transcriptional regulation (gain of RNA Pol2 occupancy) of 77.3% of the liver corticosterone regulated genes identified in this study were similarly pulsatile. While there were many cases of increased transcription, gene repression (loss of RNA Pol2 occupancy) was found in the majority of cases (73.4%), synchronised to the corticosterone pulse peak. Irrespective of the direction of change, there was a return to basal levels within the pulse nadir for the vast majority (85.1%) of cases (Figure 4.6) and just 14.5% of genes were differentially enriched relative to VEH control within the pulse nadir. These data strongly support a model whereby pulsatile GC exposure induces transient liver specific GR binding across the genome to mediate robust phasic transcriptional regulation of GC target genes in liver.

My data in rat liver is consistent with findings from an *in vitro* model of GR binding and RNA Pol2 occupancy within a mouse mammary carcinoma (3617) cell line. A series of real time live cell imaging experiments showed that GR recruitment to the artificial MMTV array was synchronised to pulses of 15min corticosterone exposure, that fully dissociated within 45min of hormone withdrawal and was repeatable over multiple cycles of stimulation in the same cells (Stavreva *et al.*, 2009). The authors expanded upon these findings using similar ChIP-Seq methods to those used in this thesis and reported RNA Pol2 occupancy was similarly synchronised. Their data, however, indicated corticosterone administration increased transcription at the majority of gene targets in response to a single 20min (followed by 40min washout) and 60min corticosterone administration (Stavreva *et al.*, 2015). Interestingly, Affymetrix GeneChIP data analysis of nerve growth factor-determined catecholaminergic (PC12) cells after a 20min 100nM corticosterone pulse, indicated that the predominant effect was a reduction in mRNA levels at 1hr while increased mRNA levels were detected at a much later time of 3hrs after the corticosterone pulse (Morsink *et al.*, 2006). The data I have presented here may indicate that repeated transient GR binding cycles are required to maintain repressive transcriptional effects as observed at the 1hr time point in PC12 cells. It is also possible that the delayed effects on mRNA upregulation in the Morsink study could be due to a timing delay in RNA processing, required to produce the mature transcript, or other post-transcriptional mechanisms. Alternatively, taken together with my findings, these data may highlight a potentially distinct regulatory role for dynamic regulation of transcriptional mechanisms over varying timescales.

7.2.2 Constant corticosterone exposure can induce prolonged GR binding and dysregulate synchronised transcriptional regulation

Expanding upon these results, I presented novel *in vivo* data that shows how replacing ultradian pulses with dose matched constant infusion robustly dysregulated both GR and RNA Pol2 dynamics. Of all the GR binding sites identified as distinctly corticosterone regulated in this study, 87.4% were bound at the peak (140min) compared to 0% at the nadir (180min). GR binding in response to the dose matched constant corticosterone infusion whereas, was found at fewer sites than with pulsatile peak, with 32.0% of sites bound at 140min and 49.3% at 180min.

A differential analysis for time dependent effects (within each pattern) confirmed the extent of dysregulation of phasic GR binding during constant corticosterone exposure as significant time dependent differences in GR binding was found for 50.7% of sites during pulsatile infusion but only 2.5% of sites during constant infusion (Figure 3.7).

In Chapter 4, I reported that pulsatile infusion resulted in a highly defined temporal regulation of transcription for GC target genes. At the corticosterone pulse peak, 77.3% of target genes were found to have significant changes in Pol2 occupancy, whereas, only 14.5% of genes were at the nadir to VEH control. This indicates a dynamic regulation of transcription coinciding predominantly with the pulse peak. Constant infusion markedly impacted upon the dynamics of phasic RNA Pol2 activity over time, with 35.5% and 38.9% of target genes found to have significant changes in Pol2 occupancy at 140min and 180min respectively, relative to VEH control (Figure 4.6).

Similar to GR dynamics, differential analysis for time dependent effects (within each pattern) confirmed the extent of dysregulation of phasic transcriptional regulation during constant corticosterone exposure. Here, significant time dependent differences in relative RNA Pol2 enrichment were found for 60.3% of sites during pulsatile infusion but just 14.1% of sites during constant infusion (Figure 4.6).

As described in the previous section (4.4.6) pulsatile corticosterone was found to be more effective at inducing transcriptional repression of the majority of regulated targets, with reduced pSer2 Pol2 occupancy detected at 73.4% of regulated genes at the pulse peak. In contrast, constant corticosterone was found to be much more effective at inducing upregulation, with increased pSer2 Pol2 occupancy detected at 77.2% and 49.6% of total regulated genes at 140min and 180min respectively (Figure 4.6).

The opposing outcome of pulsatile versus constant corticosterone treatment for GC regulation of the liver transcriptome was not supported by the data from the only other genome-wide study of this type

(Stavreva *et al.*, 2015). The Stavreva study was performed in a mouse mammary carcinoma cell line, where no pattern dependent differential repressing or transactivating regulation was noted (Stavreva *et al.*, 2015). As previously mentioned, mRNA production within PC12 cells was decreased post 1hr of corticosterone exposure, which was increased by 3hrs (Morsink *et al.*, 2006). As only the Morsink et al. 2006 study used a similar time point to mine, one could conclude rapid, transient corticosterone and ultimately GR binding is required to induce inhibitory transcription. More research is required to confirm these dynamics, as well as clarify the discrepancies between different cell types, and *in vitro* versus *in vivo* observations.

My data also highlights that constant corticosterone infusion was less effective than the corticosterone pulse peak at inducing GR binding, as well as regulating RNA Pol2 access to the chromatin template. Of the sites inducible by corticosterone, 47% were exclusively pulse peak dependent, whereas only 8.6% were exclusively induced by constant corticosterone (Figure 3.5). For the remaining 44.1% of binding sites, GR binding was commonly responsive to at least two of the three conditions with raised circulating corticosterone. Similar dynamics were observed in transcriptional regulation, as differential RNA Pol2 occupation was detected in 41.5% of regulated genes at the corticosterone pulse peak only, which reduced greatly to just 10.9% of regulated genes commonly responsive to all three conditions with raised circulating corticosterone (Figure 4.8).

Dysregulation of RNA Pol2 dynamics during constant corticosterone exposure was more complicated than the simple prolonged duration effect observed with GR. There was also strong evidence for opposing overall transcriptional effects between pulsatile and constant corticosterone exposure as well as many gene specific differences evident within the data, which will be discussed in more detail in section 7.3.

7.2.3 Dose-dependent effects

To match the infused corticosterone doses between the two patterned infusion groups, the constant infusion rate was lower. The same dose was delivered over 60min in the constant group but over 20min in the pulsatile group, therefore, circulating corticosterone concentration was highest at the pulse peak compared to any other condition and time point (Figure 2.2). Previously published data has indicated GR binding within the hippocampus of male ADX rats was induced at many of the same sites by two differing doses, however, a sub-group of sites were induced in response to the high dose only (Polman, de Kloet and Datson, 2013). As the data indicated distinct and opposing transcriptional induction by either patterned corticosterone exposure, I would hypothesise the peak dependent sites are more likely to be dose dependent. Despite this, I would not conclude observed transcriptional differences between infusion patterns are mostly dose dependent, as the loss of transient GR binding

is distinctly robust and cannot be discounted as a primary and synergistic factor for transcriptional dysregulation.

7.3 Observations between transcriptional activity and proximal or distal GR binding

In this study I found a relationship in the data that an increased distance, between the TSS and the closest regulated GR binding site, increased the likelihood of transcriptional inhibition of the gene which I cannot identify as nGRE mediated (Figure 5.2). To my knowledge, this phenomenon has only been reported *in vitro* in response to Dex administration in A549 cells with differential mRNA expression analysed by RNA-Seq (Reddy, Pauli and Sprouse, 2009). As this is observed in both RNA Pol2 occupancy as well as mRNA production, the data in part justifies the use of RNA Pol2 occupancy as a proxy for transcription, as well as indicating that this may represent a novel mode of GR mediated transcriptional regulation.

Regulation of GR responsive genes has been observed over long distances and via TAD domains that rely on chromatin reorganisation to either 'open' or 'close' sites to transcription factors and their complexes as well as the transcriptional machinery (Ito *et al.*, 2006; Kuznetsova *et al.*, 2015; Kim *et al.*, 2018). This suggests the mechanisms of chromatin reorganisation needed for transcriptional regulation may depend on the proximity of a GR binding event (Grøntved *et al.*, 2015; Stavreva *et al.*, 2015; Jubb *et al.*, 2017; Stubbs, Flynn and Conway-Campbell, 2018). Although the majority of GR binding sites are located in pre-accessible 'open' chromatin, several sites can also be found in highly compacted 'closed' chromatin that is non-permissive for RNA Pol2 access to the TSS and gene bodies within these regions (Archer *et al.*, 1991; John *et al.*, 2008, 2011; Reddy, Pauli and Sprouse, 2009; Jubb *et al.*, 2017). However, GR binding can initiate local chromatin opening via recruitment of co-factors such as the HATs CBP and P300 as well as chromatin remodelling factors such as the SWI/SNF complex, which slide nucleosomes open to increase accessibility for RNA Pol2 and the transcriptional machinery (Chakravarti *et al.*, 1996; Gerritsen *et al.*, 1997; Koh *et al.*, 2001; Belandia *et al.*, 2002). Even sites thought to be pre-accessible can also be opened further for gene regulation following glucocorticoid treatment (John *et al.*, 2008; Burd *et al.*, 2012).

Despite these potential mechanisms, the role of chromatin remodelling in GR transcriptional inhibition is not well understood and so far, a greater role of SWI/SNF in transcriptional activation and induction of genes has been identified (John *et al.*, 2008). Other chromatin reorganisation mechanisms may be required for long distance transcriptional inhibition such as chromatin looping, bringing a distant GR binding site into closer proximity with the TSS (Hakim *et al.*, 2009; McDowell *et al.*, 2018). For this study the degree of pre and post chromatin accessibility within regions of inducible GR binding were not investigated. So, no conclusions can be made as to whether binding sites induced by the

corticosterone treatment are located within 'open' or 'closed' chromatin or whether decompaction occurs. Further studies are needed to explore regulation of transcriptional inhibition and why a larger distance may frequently be found. New techniques that could help answer this question include Hi-C to detect chromatin interactions, DNA-FISH to assess chromatin decompaction and DNase1-Seq or ATAC-Seq to assess chromatin accessibility (Buenrostro *et al.*, 2013; Jubb *et al.*, 2017). I would suggest further studies using some of these techniques would be important to explore mechanisms of not only GR mediated transactivation or transrepression but also in relation to pulsatile and constant corticosterone exposure.

7.4 Homeostatic metabolic implications

Within my thesis, I present the key metabolic pathways affected by differential pattern dependent corticosterone treatment. Some of these were predicted to be significantly activated or inhibited in response to an infused corticosterone condition and/or time point, many others were only trending. Together this data indicates key pathways can be synchronised to ultradian corticosterone oscillations within the liver, the dysregulation of which could potentially lead to the development of aberrant metabolic phenotypes associated with GC dysfunction and the development of MetS.

The HPA axis is a highly plastic system, with the ability to adapt natural oscillations of GC release from the adrenal glands in response to a range of physical and psychological stimuli, the degree of which can be dependent on the self-perceived degree of a stressor (Pariante and Lightman, 2008; Lightman and Conway-Campbell, 2010; Sarabdjitsingh *et al.*, 2010). These processes can become maladaptive, as clinically depressed patients present with flattened circadian rhythmicity as well as raised circulating ACTH and cortisol (Deuschle *et al.*, 1997). Most research into endocrine rhythms has mainly focussed on dysregulation of circadian dynamics, whilst ultradian GC dysregulation remains a relatively underexplored but potentially important area. For example, the application of a stressor not only increases the interpulse period, but the degree of the physiological, neural and behavioural response to stress is dependent on the pulse phase (Windle, Wood, Lightman, *et al.*, 1998; J. Haller *et al.*, 2000; Sarabdjitsingh *et al.*, 2010). Additionally, stress responsiveness, emotional processing and memory are blunted by constant corticosterone infusion (Sarabdjitsingh *et al.*, 2010; Kalafatakis *et al.*, 2018).

GCs are well known to either directly or synergistically regulate key targets within metabolic pathways of glucose, lipid, carbohydrate and cholesterol homeostasis within the liver; therefore dysregulation could have serious consequences (Kyrou, Chrousos and Tsigos, 2006). It has been demonstrated that workers who suffer chronic stress (defined as three events a week) were twice as likely to develop type II diabetes (Chandola, Brunner and Marmot, 2006). Cushing's Disease is characterised by

hypercortisolism and there is an over representation of metabolic dysfunction including the development of significant visceral fat deposits and obesity (32-41%), dyslipidaemia (32-41%) and type II diabetes (20-47%) in these patients (Nieman and Ilias, 2005; Stratakis, 2008; Feelders *et al.*, 2012; Buliman *et al.*, 2016). Loss of HPA axis synchrony to the photoperiod is associated with increased weight gain and risk of diabetes without increasing overall food intake in rodents, which may be an important mechanism underlying the cause of a twofold increased risk of developing diabetes as observed within human studies of variable shift workers (De Bacquer *et al.*, 2009; Karatsoreos *et al.*, 2011).

As my data has indicated distinctly pulsatile GR binding and transcription in the liver, which becomes significantly dysregulated during constant infusion, what impact might this have for metabolic pathology?

7.4.1 Glucose homeostasis

Trends of activation within pathways regulating glycogen, monosaccharides and dietary glucose were predicted at the corticosterone pulse peak but not within the nadir, indicating transient activation which becomes prolonged in response to constant corticosterone exposure. The functional impact of this may include the potential for prolonged elevations in circulating glucose levels.

Transcriptional regulation of the gluconeogenic targets *Pfkfb1*, *G6pc* and *Slc37a4* were significantly pattern dependent and GR binding was found with varying proximity to the TSS of each of these genes. *Pffkb1* is a bi-directional, rate limiting enzyme that is regulated in part by glucagon, switching the direction of glucose metabolism within hepatocytes favouring either gluconeogenesis or glycolysis. Within my data, I report a GR binding site (6kb upstream) that is robustly regulated and synchronised to circulating corticosterone infused patterns. Interestingly, RNA Pol2 was robustly increased at the pulse peak as well as prolonged in response to the constant infusion, indicating dysregulation of ultradian oscillations increases *Pfkfb1* expression. As *Pfkfb1* was enriched within the pathway for increasing quantity of glycogen, the functional impact of ultradian dysregulation may be to increase glycogen within the liver as shown in Dex treated fasted, ADX mice and rats (Mersmann and Segal, 1969; Exton *et al.*, 1976; de Guia, Rose and Herzig, 2014).Due to its glucagon regulated bi-directional effects however, it is difficult to predict the glucose regulated effects due to variable transcription rates.

GC pathology is often associated with increased glucose production and mobilisation, and the inability to reduce glucose levels, leading to insulin resistance. *G6pc* and the associated carrier protein *Slc37a4*, are both rate limiting, converting glucose-6-phosphate into glucose. Deficiency of which is associated

with glycogen storage disease and a hypoglycaemic states (de Guia, Rose and Herzig, 2014; Kishnani *et al.*, 2014; Kuo *et al.*, 2015; Bali *et al.*, 2016). *G6pc* was transcriptionally repressed at the corticosterone pulse peak only, whilst *Slc37a4* was significantly upregulated by constant corticosterone infusion in a prolonged manner, with significantly increased expression relative to both pulsatile infusion and veh control. Two robustly pattern dependent GR binding sites (6kb and 12kb) upstream of *G6pc* TSS, and a single robustly pattern dependent GR binding site (0.1kb) upstream of *Slc37a4* TSS were found.

The impact of constant corticosterone exposure, via the combined changes in expression of these two genes, may therefore be an increased glucose production within hepatocytes. Additionally, overexpression of G6pc and presumably its carrier protein Slc37a4 has also been shown to precipitate hyperinsulinemia, decreased glycogen storage in the liver, and TG storage in peripheral tissues (Massillon *et al.*, 1996; Trinh *et al.*, 1998; Massillon, 2001; Gautier-Stein *et al.*, 2012). Therefore, together these two targets are prime candidates for a causal role in inducing aberrant glucose metabolism during ultradian corticosterone rhythm dysregulation.

Despite the lack of a significant prediction for the insulin resistance pathway, one of the key targets within the pathway, insulin like growth factor 1 (*Igf1*), was found to be highly pattern dependent in its regulation. RNA Pol2 occupancy in the *Igf1* gene was reduced at the corticosterone pulse peak and at both constant corticosterone time points, indicating a prolonged decrease in transcription during constant corticosterone exposure. Significantly pattern dependent GR binding was identified 34.5kb downstream of the TSS. Igf1 mRNA has been reported previously to be reduced by Dex treatment in human KLE endometrial-like cells (Lembessis, Kalariti and Koutsilieris, 2004). There is also evidence for a link associating Igf1 hormone levels (either very low or very high levels) with an increased risk for insulin resistance and diabetes (Lembessis, Kalariti and Koutsilieris, 2004; Schneider *et al.*, 2011; Friedrich *et al.*, 2012).

Together, this data highlights *G6pc*, *Slc37a4* and *Igf1* as ultradian regulated genes that could be key targets for further study regarding dysregulated GC pathology as well as corticosterone mediated insulin resistance.

7.4.2 Fatty acid, TG, lipid and apolipoprotein metabolism

Within this thesis, I present statistically significant pathway predictions of inhibited cholesterol production at the corticosterone pulse nadir as well as a selection of novel ultradian targets that, upon dysregulation by a constant corticosterone infusion, may play a role increasing storage of cholesterol, TG and lipids within the liver. Risk factors associated with the MetS phenotypes, NASH and NAFLD.

Pathway analysis of corticosterone regulated targets predicted a significant inhibition in the quantity of cholesterol at the pulse nadir in response to pulsatile infusion indicating dysregulation of ultradian rhythms could increase levels within the liver (Figure 5.5). Corticosterone synchronised trends of increased carbohydrates were also predicted at the pulse peak, but prolonged in response to a constant infusion (Figure 5.9), indicating a potential accumulation within the liver. Similar trends were not predicted for TG, fatty acid and lipid pathways, as despite evidence of synchronised ultradian regulation, prolonged trends of inhibition were predicted in response to a constant corticosterone infusion. This was disappointing as there are many studies that show an association with dysregulated GCs and hyperlipidaemia (Vegiopoulos and Herzig, 2007; Lemke *et al.*, 2008; Lu *et al.*, 2012; Kuo *et al.*, 2015). Upon further examination, key metabolic targets enriched within these pathways' present ideal candidates for future research and potentially indicate a more chronic model of GC dysregulation is required for phenotypic development.

Fasn converts the intermediate metabolite malonyl coenzymeA into fatty acids in a rate limiting reaction within de novo lipogenesis (Chakravarthy *et al.*, 2005; de Guia, Rose and Herzig, 2014; Rui, 2014). Within my data, *Fasn* and *Scd* (another factor involved in de novo lipogenesis) reported corticosterone synchronised losses of RNA Pol2 in response to the pulsatile infusion but not in response to a constant corticosterone infusion as well as corticosterone regulated binding sites 78kb upstream and 13kb downstream of the *Fasn* and *Scd* TSS respectively. Together, this data could indicate GR mediated increases in expression in response to disruption of ultradian oscillations, which could be important when one considers increased Scd mRNA levels are reported within obese and lipoatrophic diabetic mice as well as hepatic steatosis (Cohen *et al.*, 2002; Asilmaz *et al.*, 2004). Similar raised levels have been reported within NAFLD patients as well as TG accumulation within the liver indicating increased de novo lipogenesis could be significant with regard to aberrant metabolic function (Kotronen *et al.*, 2009). Although studies within leptin-deficient (ob/ob) mice indicate just 11% ±1 of TG within the liver originate from de novo synthesis, therefore despite indication of synthesis, effects could be minimal (Iizuka, Miller and Uyeda, 2006; Jensen-Urstad and Semenkovich, 2012).

Similarly, RNA Pol2 occupation of *Lpin1* was increased in a prolonged manner by constant corticosterone infusion (Figure 4.2 and Figure 4.10). Pathway analysis indicated a regulatory role within hyperlipidaemia and dyslipidaemia pathways and similarly, over expression has been associated with increase adipocyte TG uptake and obesity, however, direct observations within the liver and its role with other Lpin variants remains to be fully elucidated (Phan and Reue, 2005; Finck *et al.*, 2006; Reue and Dwyer, 2009).

Interestingly, my data also reported losses of RNA Pol2 at the apolipoprotein gene, *Apob*, were synchronised to the corticosterone pulse but prolonged in response to a constant infusion as well as a corticosterone regulated GR binding site 26kb upstream of the TSS. APOB is required for VLDL synthesis and function, facilitating lipid accumulation within the lipoprotein as well as endocytosis by intermediate density lipoproteins, lowering VLDL levels within the circulation (Powell *et al.*, 1987; Atzel and Wetterau, 1993). As VLDL synthesis and function are integral to the livers ability to transport TG, lipids and other metabolites out of the liver and into the circulation which is a known risk factor of NAFLD and NASH, any dysregulation of synthesis could have significant effects over a prolonged period (Wetterau *et al.*, 1992; Linton, Fame and Young, 1993; Ozcan *et al.*, 2004; Ota, Gayet and Ginsberg, 2008; Jiang, Robson and Yao, 2013; Welty, 2014).

I therefore hypothesise, dysregulation of ultradian oscillations by raised, non-oscillating GC exposure could increase the transcription of specific genes increasing deposition of TG, cholesterol and carbohydrates within the liver. Coupled with a loss in VLDL synthesis over a prolonged period could develop NAFLD and NASH phenotypes. Further research is required over a chronic model of GC replacement for confirmation and assessment.

7.4.3 Serotonin and melatonin metabolism

Trends of increased melatonin and serotonin degradation were predicted in a phasic manner, synchronized to corticosterone pulse peak and prolonged in response to the constant corticosterone infusion, indicating pattern dependence.

In vivo microdialysis measurement of both serotonin and melatonin have reported diurnal variations within the pineal gland, however, 95% of circulating serotonin is produced within the duodenum of the gut which also reports a degree of circadian rhythmicity (Sun *et al.*, 2002; Ebert-Zavos *et al.*, 2013). Melatonin is produced from serotonin within the pineal gland and is also secreted in an inverted circadian profile to GCs (Lane and Moss, 1985; Chojnacki *et al.*, 2012). As the liver metabolises up to 90% of circulating melatonin within a single pass through the hepatic portal circulation, alteration in degradative pathways could have a large impact (Lane and Moss, 1985; Chojnacki *et al.*, 2012).

Increased serotonin uptake and metabolism within the liver is associated with increased mitochondrial reactive oxygen species and lipid peroxides. Risk factors associated with NASH and potentially loss of ultradian oscillations as trends indicated a prolonged increase in degradation. Patients with liver cirrhosis have raised melatonin levels compared to controls, potentially due to a loss of clearance within the liver (Iguchi, Kato and Inayashi, 1982; Nocito *et al.*, 2007). Additionally, single nucleotide polymorphism (SNP) within the melatonin receptor 1B reported increased glucose

and insulin secretion and was predictive of type 2 diabetes (Lyssenko *et al.*, 2009). Therefore, constant corticosterone induction of melatonin degradation could be protective.

In conclusion, prolonged activation of serotonin and melatonin degradation could have opposing effects regarding liver damage but present interesting candidates for future research considering their well-documented role within circadian biology.

7.4.4 Hepatocyte turnover

Seemingly opposing pathways for growth and proliferation, and necrosis and cell death were similarly enriched with pattern dependent targets, potentially indicating that hepatic cell turnover rate is sensitive to GC rhythm disruption. This may have implications for increased risk of the development of liver cancer, fibrosis and NASH (Feldstein *et al.*, 2003; Argo *et al.*, 2009; Luedde, Kaplowitz and Schwabe, 2014).

Pathway analysis of differentially occupied RNA Pol2 genes, indicated predictive trends of increased proliferation and liver growth synchronised to the corticosterone pulse peak, were prolonged during constant corticosterone infusion. Interestingly, analysis predicted similar trends of activation for necrotic and cell death pathways. Within the liver, hepatocyte turnover is relatively low as a study in male Wistar rat liver demonstrated just 0.05% of hepatocytes were in an apoptotic state at any one time (Columbano *et al.*, 1985; Luedde, Kaplowitz and Schwabe, 2014). Despite this, the liver has a relatively rapid and specialised capacity for regeneration after lobectomy of up to 3 of its 5 lobes (2/3 total mass) (Higgins and Anderson, 1931). Regeneration due to partial hepatectomy is a tightly regulated process, with two rounds of DNA synthesis and proliferation followed by apoptosis that is thought to correct for any over proliferation (Sakamoto *et al.*, 1999). Considering this capacity and ability for liver growth or cell death, any perturbation in cellular pathways could potentially have serious implications.

Motif analysis showed that 54% of GR binding regions, which contained a GRE, also contained an over-expressed sequence that resembled a STAT5 motif, indicating a co-regulation between GR and STAT5 at these sites (Table 3). STAT5 is activated by a signalling cascade initiated by growth hormone, which regulates gene expression in the liver via the membrane bound growth hormone receptor. Activated STAT5 and GR form a potent transactivation complex to induce transcription of growth factors in the liver (Engblom *et al.*, 2007; Hennighausen and Robinson, 2008). Interestingly, loss of STAT5B can reduce IGF1 expression that has been linked to reduced overall body growth as well as fatty liver, hepatic steatosis and impaired cell proliferation, as has GR liver specific knockouts (Tronche *et al.*, 2004; Cui *et al.*, 2007; Engblom *et al.*, 2007). Within the necrosis pathway, *Igf1* was identified as

inhibitory and transient losses of RNA Pol2 occupancy were found in response to pulsatile but prolonged by constant corticosterone exposure.

Unfortunately, there is a lack of clarity within the data, as similarly activatory or inhibitory genes enriched within growth/ proliferative pathways were also identified in necrotic/ cell death pathways. This is most probably due to multiple pleiotropic transcription factors within each pathway. For example, analysis listed the MYC proto-oncogene, BHLH transcription factor gene (*Myc*) as activatory of all four pathways (Zheng, Cubero and Nevzorova, 2017). c-Myc transcription can be induced via growth factor activation and has been identified as an immediate early gene, whose expression is increased by 30min post-lobectomy and reaching maximal levels twice at 2hr and 3hr time points (Ohgaki *et al.*, 1996; Thorgeirsson and Santouni-Rugiu, 2003; Zheng, Cubero and Nevzorova, 2017). As c-MYC is a key transcription factor driving transition of hepatocytes from G_0/G_1 to S phase, these peaks in expression are associated with hepatocyte proliferation as mentioned previously (Thompson *et al.*, 1986). It has been shown that c-MYC sensitizes a cell to apoptosis via indirect inhibition of p53 proteasomal degradation (Zindy *et al.*, 1998). Hence, loss of c-MYC transcriptional control has long been associated with hepatic carcinoma and has been replicated within a hepatocyte specific Myc overexpressing mouse model (alb-Cre^{+}/$cMYC^{tg}$). Tumours developed in 40% of these mice at 45 weeks old, and 80% by 65 weeks (Evan and Littlewood, 1993; Hoffman and Liebermann, 2008; Freimuth *et al.*, 2010). Increased collagen deposits leading to fibrogenesis and damage are also associated with this mutant mouse line. Increased collagen deposits have also been observed clinically and are postulated to further progress to hepatocellular carcinoma (Nevzorova *et al.*, 2013; Zheng, Cubero and Nevzorova, 2017). Interestingly however, co-expression of c-MYC and hepatocyte growth factor inhibits proliferation and tumour growth (Thorgeirsson and Santouni-Rugiu, 2003). MYC function is not reserved just to hepatocyte proliferative and apoptotic pathways, as my analysis also listed *Myc* as activatory within the glycogen quantity pathway. This is unsurprising as evidence has shown Myc could be protective against HFD induced insulin resistance, obesity and hyperglycaemia due to its involvement in hepatic glucose accumulation and carbohydrate metabolism (Valera *et al.*, 1995; Riu *et al.*, 2003; Zheng, Cubero and Nevzorova, 2017).

Analysis also listed *Igbp1* as inhibitory of growth and proliferative pathways, despite a recent study indicating knockout reduced the capacity for liver regeneration after lobectomy (Leu *et al.*, 2003). Within a tethered, complimentary co-factor complex, opposing or synergistic transcriptional effects can be dependent upon whichever co-regulator is bound to the DNA as described for NFκB or STAT transcription factor complexes with GR (Jonat *et al.*, 1990; Ray and Prefontaine, 1994; Stoecklin *et al.*, 1997; Aittomäki *et al.*, 2000; Rao *et al.*, 2011; Ratman *et al.*, 2013). A mechanism of this type could

explain opposing observations, nevertheless, it is reasonable to conclude that targets highlighted within these pathways have complex interactions that are yet to be fully elucidated. Whilst this data does not define an overall increase or decrease in hepatocytes, it does indicate a potential for dysregulation of turnover rates. The outcome of this dysregulation would need to be assessed over a longer timeframe using my chronic infusion protocol, particularly because proliferation, cell death and necrosis pathways have been associated with an increased risk of cancer, fibrosis and NASH (Feldstein *et al.*, 2003; Argo *et al.*, 2009; Luedde, Kaplowitz and Schwabe, 2014).

7.4.5 Chronic model

Within this thesis, I have highlighted that MetS may take years to develop, therefore, detection of such robust, early changes within the first 3hrs of GC rhythm dysregulation is quite remarkable (Edwards *et al.*, 2012; Medina-Santillán *et al.*, 2013; Bergmann, Gyntelberg and Faber, 2014; Kaur, 2014). The ability to detect and observe how these changes affect metabolism over an extended period with a chronic treatment protocol would represent an important and fascinating tool for future research into dysregulated ultradian and circadian GC rhythms.

Circulating metabolites such as TGs, lipids, free fatty acids, carbohydrates and VLDLs are known to fluctuate in a circadian manner and aberrant regulation has long been associated with dysregulated GCs (Kalsbeek, la Fleur and Fliers, 2014; Poggiogalle, Jamshed and Peterson, 2018). Furthermore, despite numerous studies investigating manipulation of the photoperiod or characterisation within sustained hyper- or hypocortisolism states (as found within Cushing's and Addison patients), no-one has investigated the relative contribution of the ultradian versus the circadian GC profile in maintaining 'healthy' metabolic function.

To answer these fundamental questions, I present a novel, hourly pulsed ultradian model of GC replacement within the ADX rat, that incorporates circadian variation in pulse amplitude over a 24hr period. Here, I have presented the first evidence that dynamic oscillations in circulating corticosterone can be delivered via a programmable infusion pump in a manner that models both circadian and ultradian endogenous corticosterone rhythms, albeit only in a pilot study (n=1) so far (Figure 6.3). To my knowledge, this is the first physiologically realistic ultradian corticosterone replacement infusion model, *in vivo*. I expanded upon this model to also design a replacement infusion that incorporated a circadian aspect, but without the ultradian pulsatile rhythm.

This infusion protocol has great potential for use over a chronic timeframe to assess functional changes arising from circadian and/or ultradian dysregulation. Applications extend beyond assessment of liver function, as multiple GC targets including adipose tissue, muscle, and the brain

could be affected by chronically dysregulated GCs. In particular, cognitive impairment and depression have been reportedly associated with dysregulated GCs (Deuschle *et al.*, 1997; Michaud, Forget and Cohen, 2009; Guo *et al.*, 2018). Stress related aggressive behaviour, as well as appetite and weight loss, are not only mediated by the self-perceived degree of a stressful event, but also at what point within a circadian and ultradian profile it is applied (Akabayashi *et al.*, 1994; Martí, Martí and Armario, 1994; Rybkin *et al.*, 1997; Windle, Wood, Lightman, *et al.*, 1998; J Haller *et al.*, 2000; J. Haller *et al.*, 2000; Shimizu *et al.*, 2010; Ciriaco *et al.*, 2013; Simic *et al.*, 2013). Therefore, the ability to accurately interrogate system / tissue / cellular function in response to an acute or more chronic GC disruption paradigm within a specific circadian and/ or ultradian GC phase will be exceptionally informative about the processes of dynamic physiological regulation.

7.4.6 Clinical importance

Hypercortisolism, most commonly associated with Cushing's disease, is associated with a myriad of aberrant metabolic effects such as obesity, insulin resistance, diabetes mellitus and dyslipidaemia (Nieman and Ilias, 2005). Interestingly, other cohorts of patients including those suffering with chronic depressive disorder, chronic stress conditions and chronic inflammatory disease have also been reported to exhibit hypercortisolism and poor metabolic profiles, albeit to a lesser extent than Cushing's patients (Deuschle *et al.*, 1997; Young, Carlson and Brown, 2001; Pariante, 2006; Pariante and Lightman, 2008; Lightman and Conway-Campbell, 2010; Almadi, Cathers and Chow, 2013). A particularly interesting and well characterised cohort of patients suffering from the chronic condition of obstructive sleep apnoea have been extensively assessed for associations between their hypercortisolism and poor metabolic profile. Analysis of 24hr blood profiling and metabolic assessments undertaken before and after treatment reported elevated ACTH and cortisol secretion along with increased incidence of metabolic syndrome pathology were mitigated by successful treatment with continuous positive airway pressure therapy (David E. Henley, Buchanan, *et al.*, 2009; David E. Henley, Russell, *et al.*, 2009).

How do these clinical associations relate to my findings of altered metabolic gene regulation during constant GC infusion? It is first important to understand that hypercortisolism does not induce constant adrenal cortisol secretion. Ultradian pulsatility is still maintained, although in a significantly dysregulated form. Therefore, the clinical cases described above are not exposed to completely steady state GC levels, as experienced by the rats in my experimental protocol. It is, however, important to note that one of the defining features of hypercortisolism is elevated GC levels during the ultradian nadir (in most cases) and during the circadian nadir (in some cases). My data has demonstrated that it is the loss of the ultradian nadir during constant GC infusion that is the most significant factor for

inducing profound dysregulation of genes enriched within pathways known to induce MetS phenotypes. Overtime, chronic elevation in nadir GC levels may lead to the more severe manifestation of metabolic phenotypes observed in patients suffering with hypercortisolism.

In contrast, hypocortisolism is adrenal insufficiency (such as found in Addison disease patients) and is commonly treated with a GC replacement therapy regime of two to three oral hydrocortisone pills per day. Clinicians are already aware of the importance of the circadian rhythm of GC secretion and attempt to artificially reinstate the circadian component of endogenous GC release as the first of three doses is to be taken within the morning and is equivalent to 2/3 of the total dose taken within 24hrs (Charmandari, Nicolaides and Chrousos, 2014). Despite this 'optimal' replacement regime, patients suffer from a range of metabolic side effects that are directly related to GC replacement dose and pattern (Filipsson *et al.*, 2006). This is potentially relevant to my premise as delivery via oral dosing produces a smooth rise of GCs in the circulation which is prolonged over many hours. But perhaps, to mitigate these observed side effects, preservation of ultradian GC dynamics is required rather than simply the right dose in a general circadian manner. Based upon the dynamics of the intracellular GR and transcriptional machinery that have been explained in my data, it is likely that the prolonged hydrocortisone exposure in these patients will similarly induce prolonged GR activation and aberrant transcriptional regulation of many of the same metabolic pathway targets identified in my study. Therefore, again, the lack of pulsatile GC dynamics in these patients may be a root cause of their poor metabolic profiles.

Due to their powerful anti-inflammatory properties, sGCs have become a cornerstone in the treatment of a wide range of inflammatory conditions; with 0.85% of patients >18years of age prescribed oral sGCs within the UK (Fardet, Petersen and Nazareth, 2011). sGCs have been rationally designed with structural similarity to the endogenous GCs, however, they are not metabolised in the body as rapidly. The half-lives of sGCs are significantly prolonged compared to their endogenous counterparts as the circulating prednisolone half-life has been reported at just over 2 hrs and Dex at 3hrs. The biological half-life has however been described to be considerably longer. Recent evidence has indicated that methylprednisolone and Dex can induce GR binding in peripheral GC targets such as the pituitary for over 6hrs and 12hrs respectively, and in the brain for over 3hrs and 6hrs respectively (Al-Habet and Rogers, 1989; Uhl *et al.*, 2002; Earl *et al.*, 2017; Nicolaides *et al.*, 2018). Disregarding potential ligand specific effects, clinical corticosteroid treatment was shown to primarily precipitate the development of type II diabetes in a cohort of patients that did not present underlying risk factors (Simmons *et al.*, 2012). Similarly, 5 days of oral Dex treatment within paediatric acute lymphoblastic leukaemia induced prolonged raised HDL, LDL, cholesterol, TG, glucose and insulin

levels despite complete metabolism of Dex (Warris *et al.*, 2016). Finally, a recent meta study concluded prescription of the sGC Dex and prednisolone were significant risk factors for development of insulin resistance within individuals with no underlying pathology (Zhou *et al.*, 2016).

In all the clinical cases described in this section, it is apparent that there are some common elements. First, prolonged and/or dysregulated GC dynamics with the potential for inducing prolonged and/or dysregulated GR dynamics are common factors. Most importantly, in all cases loss of pulsatile nadir GC levels appears to be the defining feature for increased risk of MetS development. My data provides a potential mechanism whereby phasic GR recruitment and dissociation from the DNA is needed to optimally regulate metabolic homeostatic pathways in the liver.

Together, these data emphasise the clinical importance of strategies aimed at reinstating HPA axis rhythms and adrenal GC secretory dynamics in conditions such as chronic stress, depression and inflammatory diseases. For GC replacement therapy in adrenal insufficiency and GC treatment in a broad range of inflammatory conditions, more consideration should be given to understanding and recapitulating endogenous rhythms of hormones and their intracellular systems when developing treatment strategies and mitigation of steroid associated side effects.

Chapter 8 References

'A Unified Nomenclature System for the Nuclear receptor superfamily' (1999) *Cell*, 97(2), pp. 161–163. Available at: http://www.ens-lyon.fr/LBMC/LAUDET/nomenc. (Accessed: 21 March 2019).

Agarwal, A. K. *et al.* (1994) 'NAD(+)-dependent isoform of 11 beta-hydroxysteroid dehydrogenase. Cloning and characterization of cDNA from sheep kidney.', *The Journal of biological chemistry*, 269(42), pp. 25959–62. Available at: http://www.ncbi.nlm.nih.gov/pubmed/7929304 (Accessed: 20 April 2019).

Aguilar-Arnal, L. *et al.* (2013) 'Cycles in spatial and temporal chromosomal organization driven by the circadian clock', *Nature Structural & Molecular Biology*, 20(10), pp. 1206–1213. doi: 10.1038/nsmb.2667.

Aguilar-Arnal, L. and Sassone-Corsi, P. (2015) 'Chromatin landscape and circadian dynamics: Spatial and temporal organization of clock transcription.', *Proceedings of the National Academy of Sciences of the United States of America*. National Academy of Sciences, 112(22), pp. 6863–70. doi: 10.1073/pnas.1411264111.

Ahn, S. H., Kim, M. and Buratowski, S. (2004) 'Phosphorylation of Serine 2 within the RNA Polymerase II C-Terminal Domain Couples Transcription and 3' End Processing', *Molecular Cell*. Cell Press, 13(1), pp. 67–76. doi: 10.1016/S1097-2765(03)00492-1.

Aittomäki, S. *et al.* (2000) 'Cooperation among Stat1, glucocorticoid receptor, and PU.1 in transcriptional activation of the high-affinity Fc gamma receptor I in monocytes.', *Journal of immunology (Baltimore, Md. : 1950)*. American Association of Immunologists, 164(11), pp. 5689–97. doi: 10.4049/JIMMUNOL.164.11.5689.

Akabayashi, A. *et al.* (1994) 'Hypothalamic neuropeptide Y, its gene expression and receptor activity: relation to circulating corticosterone in adrenalectomized rats.', *Brain research*, 665(2), pp. 201–12. Available at: http://www.ncbi.nlm.nih.gov/pubmed/7895055 (Accessed: 26 May 2019).

Akhtar, R. A. *et al.* (2002) 'Circadian cycling of the mouse liver transcriptome, as revealed by cDNA microarray, is driven by the suprachiasmatic nucleus.', *Current biology : CB*, 12(7), pp. 540–50. Available at: http://www.ncbi.nlm.nih.gov/pubmed/11937022 (Accessed: 20 May 2019).

Al-Habet, S. M. and Rogers, H. J. (1989) 'Methylprednisolone pharmacokinetics after intravenous and oral administration.', *British Journal of Clinical Pharmacology*. Wiley-Blackwell, 27(3), p. 285. Available at: https://www.ncbi.nlm.nih.gov/pmc/articles/PMC1379824/ (Accessed: 30 March 2019).

Alberti, K. G. M. M. *et al.* (2005) 'The metabolic syndrome--a new worldwide definition.', *Lancet (London, England)*. Elsevier, 366(9491), pp. 1059–62. doi: 10.1016/S0140-6736(05)67402-8.

Almadi, T., Cathers, I. and Chow, C. M. (2013) 'Associations among work-related stress,

cortisol, inflammation, and metabolic syndrome', *Psychophysiology*. John Wiley & Sons, Ltd (10.1111), 50(9), pp. 821–830. doi: 10.1111/psyp.12069.

Almlöf, T. *et al.* (1998) 'Role of Important Hydrophobic Amino Acids in the Interaction between the Glucocorticoid Receptor τ1-Core Activation Domain and Target Factors †', *Biochemistry*, 37(26), pp. 9586–9594. doi: 10.1021/bi973029x.

Amelung, D. *et al.* (1953) 'Conversion of cortisone to compound F', *The Journal of Clinical Endocrinology & Metabolism*. Narnia, 13(9), pp. 1125–1126. doi: 10.1210/jcem-13-9-1125.

Archer, T. K. *et al.* (1991) 'Transcription factor access is mediated by accurately positioned nucleosomes on the mouse mammary tumor virus promoter.', *Molecular and cellular biology*, 11(2), pp. 688–98. Available at: http://www.ncbi.nlm.nih.gov/pubmed/1846670 (Accessed: 28 March 2019).

Archer, T. K. and Lee, H.-L. (1997) 'Visualization of Multicomponent Transcription Factor Complexes on Chromatin and Nonnucleosomal Templatesin Vivo', *Methods*. Academic Press, 11(2), pp. 235–245. doi: 10.1006/METH.1996.0410.

Argo, C. K. *et al.* (2009) 'Systematic review of risk factors for fibrosis progression in non-alcoholic steatohepatitis', *Journal of Hepatology*. Elsevier, 51(2), pp. 371–379. doi: 10.1016/J.JHEP.2009.03.019.

Arinze, I. J., Garber, A. J. and Hansons, R. W. (1973) *The Regulation of Gluconeogenesis in Mammalian Liver THE ROLE OF lLIITOCHONDRIAL PHOSPHOENOLPYRUVATE CARBOXYKINASE**. Available at: http://www.jbc.org/ (Accessed: 6 April 2019).

Arth, G. E. *et al.* (1958) '16-METHYLATED STEROIDS. I. 16α-METHYLATED ANALOGS OF CORTISONE, A NEW GROUP OF ANTI-INFLAMMATORY STEROIDS', *Journal of the American Chemical Society*. American Chemical Society, 80(12), pp. 3160–3161. doi: 10.1021/ja01545a061.

Aschoff, J. (1965) 'CIRCADIAN RHYTHMS IN MAN.', *Science (New York, N.Y.)*. American Association for the Advancement of Science, 148(3676), pp. 1427–32. doi: 10.1126/SCIENCE.148.3676.1427.

Asilmaz, E. *et al.* (2004) 'Site and mechanism of leptin action in a rodent form of congenital lipodystrophy.', *The Journal of clinical investigation*. American Society for Clinical Investigation, 113(3), pp. 414–24. doi: 10.1172/JCI19511.

Atkinson, H. C. *et al.* (2006) 'Diurnal variation in the responsiveness of the hypothalamic-pituitary-adrenal axis of the male rat to noise stress.', *Journal of neuroendocrinology*, 18(7), pp. 526–33. doi: 10.1111/j.1365-2826.2006.01444.x.

Atzel, A. and Wetterau, J. R. (1993) 'Mechanism of microsomal triglyceride transfer protein catalyzed lipid transport.', *Biochemistry*, 32(39), pp. 10444–50. Available at: http://www.ncbi.nlm.nih.gov/pubmed/8399189 (Accessed: 14 May 2019).

Ayyar, V. S. *et al.* (2015) 'Quantitative tissue-specific dynamics of in vivo GILZ mRNA expression and regulation by endogenous and exogenous glucocorticoids', *Physiological Reports*, 3(6), p. e12382. doi: 10.14814/phy2.12382.

De Bacquer, D. *et al.* (2009) 'Rotating shift work and the metabolic syndrome: a prospective study', *International Journal of Epidemiology*. Oxford University Press, 38(3), pp. 848–854. doi: 10.1093/ije/dyn360.

Baek, S., Sung, M.-H. and Hager, G. L. (2012) 'Quantitative Analysis of Genome-Wide Chromatin Remodelling', *Methods in Molecular Biology*, 833, pp. 433–441. doi: 10.1007/978-1-61779-477-3_26.

La Baer, J. and Yamamoto, K. R. (1994) 'Analysis of the DNA-binding affinity, Sequence Specificity and Context Dependence of the Glucocorticoid Receptor Zinc Finger Region', *Journal of Molecular Biology*. Academic Press, 239(5), pp. 664–688. doi: 10.1006/JMBI.1994.1405.

Bali, D. S. *et al.* (2016) *Glycogen Storage Disease Type I*, *GeneReviews®*. University of Washington, Seattle. Available at: http://www.ncbi.nlm.nih.gov/pubmed/20301489 (Accessed: 28 May 2019).

Ballard, P. L. *et al.* (1975) 'A Radioreceptor Assay for Evaluation of the Plasma Glucocorticoid Activity of Natural and Synthetic Steroids in Man1', *The Journal of Clinical Endocrinology & Metabolism*. Narnia, 41(2), pp. 290–304. doi: 10.1210/jcem-41-2-290.

Ballinger, C. A. *et al.* (1999) 'Identification of CHIP, a novel tetratricopeptide repeat-containing protein that interacts with heat shock proteins and negatively regulates chaperone functions.', *Molecular and cellular biology*, 19(6), pp. 4535–45. doi: 10.1128/mcb.19.6.4535.

Bamberger, C. M. *et al.* (1995) 'Glucocorticoid receptor beta, a potential endogenous inhibitor of glucocorticoid action in humans.', *The Journal of clinical investigation*. American Society for Clinical Investigation, 95(6), pp. 2435–41. doi: 10.1172/JCI117943.

Bannister, A. J. and Kouzarides, T. (2011) 'Regulation of chromatin by histone modifications.', *Cell research*. Nature Publishing Group, 21(3), pp. 381–95. doi: 10.1038/cr.2011.22.

Barski, A. *et al.* (2007) 'High-Resolution Profiling of Histone Methylations in the Human Genome', *Cell*, 129(4), pp. 823–837. doi: 10.1016/j.cell.2007.05.009.

Beato, M. *et al.* (1989) 'DNA regulatory elements for steroid hormones.', *Journal of steroid biochemistry*, 32(5), pp. 737–47. Available at: http://www.ncbi.nlm.nih.gov/pubmed/2661921 (Accessed: 25 March 2019).

Bednar, J. *et al.* (1998) 'Nucleosomes, linker DNA, and linker histone form a unique structural motif that directs the higher-order folding and compaction of chromatin.', *Proceedings of the National Academy of Sciences of the United States of America*. National Academy of Sciences, 95(24), pp.

14173–8. doi: 10.1073/PNAS.95.24.14173.

Belandia, B. *et al.* (2002) 'Targeting of SWI/SNF chromatin remodelling complexes to estrogen-responsive genes.', *The EMBO journal*, 21(15), pp. 4094–103. Available at: http://www.ncbi.nlm.nih.gov/pubmed/12145209 (Accessed: 12 April 2019).

Benton, L. A. and Yates, F. E. (1990) 'Ultradian adrenocortical and circulatory oscillations in conscious dogs', *https://doi.org/10.1152/ajpregu.1990.258.3.R578*. American Physiological Society Bethesda, MD . doi: 10.1152/AJPREGU.1990.258.3.R578.

Bergmann, N., Gyntelberg, F. and Faber, J. (2014) 'The appraisal of chronic stress and the development of the metabolic syndrome: a systematic review of prospective cohort studies.', *Endocrine connections*. Bioscientifica Ltd., 3(2), pp. R55-80. doi: 10.1530/EC-14-0031.

Berk, M. L. and Finkelstein, J. A. (1981) 'Afferent projections to the preoptic area and hypothalamic regions in the rat brain', *Neuroscience*. Pergamon, 6(8), pp. 1601–1624. doi: 10.1016/0306-4522(81)90227-X.

Bernstein, B. E. *et al.* (2006) 'A Bivalent Chromatin Structure Marks Key Developmental Genes in Embryonic Stem Cells', *Cell*, 125(2), pp. 315–326. doi: 10.1016/j.cell.2006.02.041.

Biddie, S. C. *et al.* (2011) 'Transcription Factor AP1 Potentiates Chromatin Accessibility and Glucocorticoid Receptor Binding', *Molecular Cell*, 43(1), pp. 145–155. doi: 10.1016/j.molcel.2011.06.016.

Biddie, S. C., Conway-campbell, B. L. and Lightman, S. L. (2012) 'Dynamic regulation of glucocorticoid signalling in health and disease', *Rheumatology*, 51(3), pp. 403–412. doi: 10.1093/rheumatology/ker215.

Blalock, S. J. *et al.* (2005) 'Patient knowledge, beliefs, and behavior concerning the prevention and treatment of glucocorticoid-induced osteoporosis', *Arthritis Care and Research*, 53(5), pp. 732–739. doi: 10.1002/art.21446.

Bledsoe, R. K. *et al.* (2002) 'Crystal structure of the glucocorticoid receptor ligand binding domain reveals a novel mode of receptor dimerization and coactivator recognition.', *Cell*. Elsevier, 110(1), pp. 93–105. doi: 10.1016/S0092-8674(02)00817-6.

Blind, R. D. and Garabedian, M. J. (2008) 'Differential recruitment of glucocorticoid receptor phospho-isoforms to glucocorticoid-induced genes', *The Journal of Steroid Biochemistry and Molecular Biology*. Pergamon, 109(1–2), pp. 150–157. doi: 10.1016/J.JSBMB.2008.01.002.

Bodwell, J. E. *et al.* (1991) *Identification of Phosphorylated Sites in the Mouse*, *Journal of Biological Chemistry*. Available at: http://www.jbc.org/content/266/12/7549.full.pdf (Accessed: 25 March 2019).

Bolger, A. M., Lohse, M. and Usadel, B. (2014) 'Trimmomatic: a flexible trimmer for Illumina

sequence data.', *Bioinformatics (Oxford, England)*. Oxford University Press, 30(15), pp. 2114–20. doi: 10.1093/bioinformatics/btu170.

De Bosscher, K. *et al.* (2000) 'Glucocorticoids repress NF-kappaB-driven genes by disturbing the interaction of p65 with the basal transcription machinery, irrespective of coactivator levels in the cell.', *Proceedings of the National Academy of Sciences of the United States of America*. National Academy of Sciences, 97(8), pp. 3919–24. Available at: http://www.ncbi.nlm.nih.gov/pubmed/10760263 (Accessed: 12 April 2019).

Bourguet, W. *et al.* (1995) 'Crystal structure of the ligand-binding domain of the human nuclear receptor RXR-α', *Nature*. Nature Publishing Group, 375(6530), pp. 377–382. doi: 10.1038/375377a0.

Boyle, A. P. *et al.* (2008) 'F-Seq: A feature density estimator for high-throughput sequence tags', *Bioinformatics*, 24(21), pp. 2537–2538. doi: 10.1093/bioinformatics/btn480.

Bresnick, E. H. *et al.* (1989) *THE JOURNAL OF BIOLOGICAL CHEMISTRY Evidence That the 90-kDa Heat Shock Protein Is Necessary for the Steroid Binding Conformation of the L Cell Glucocorticoid Receptor**. Available at: http://www.jbc.org/content/264/9/4992.full.pdf (Accessed: 21 March 2019).

Brown, M. S. and Goldstein, J. L. (1983) 'PERSPECTIVES Lipoprotein Receptors in the Liver - Control signals for plasma cholesterol traffic', *The journal of clinical investigational of clinical investigation*, 72(3), pp. 743–747. Available at: https://www.ncbi.nlm.nih.gov/pmc/articles/PMC1129238/pdf/jcinvest00769-0002.pdf (Accessed: 10 April 2019).

Bucher, P. (1990) 'Weight matrix descriptions of four eukaryotic RNA polymerase II promoter elements derived from 502 unrelated promoter sequences', *Journal of Molecular Biology*, 212(4), pp. 563–578. doi: 10.1016/0022-2836(90)90223-9.

Buenrostro, J. D. *et al.* (2013) 'Transposition of native chromatin for fast and sensitive epigenomic profiling of open chromatin, DNA-binding proteins and nucleosome position', *Nature Methods*. Nature Research, 10(12), pp. 1213–1218. doi: 10.1038/nmeth.2688.

Buliman, A. *et al.* (2016) 'Cushing's disease: a multidisciplinary overview of the clinical features, diagnosis, and treatment.', *Journal of medicine and life*. Carol Davila - University Press, 9(1), pp. 12–18. Available at: http://www.ncbi.nlm.nih.gov/pubmed/27974908 (Accessed: 14 April 2019).

Bullock, N. *et al.* (2007) 'Effect of long haul travel on maximal sprint performance and diurnal variations in elite skeleton athletes', *British Journal of Sports Medicine*, 41(9), pp. 569–573. doi: 10.1136/bjsm.2006.033233.

Burd, C. J. *et al.* (2012) 'Analysis of Chromatin Dynamics during Glucocorticoid Receptor Activation', *Molecular and Cellular Biology*. American Society for Microbiology (ASM), 32(10), p. 1805.

doi: 10.1128/MCB.06206-11.

Carnes, M. *et al.* (1989) 'Plasma Adrenocorticotropic Hormone in the Rat Demonstrates Three Different Rhythms within 24 h', *Neuroendocrinology*. Karger Publishers, 50(1), pp. 17–25. doi: 10.1159/000125197.

Carnes, M. *et al.* (1990) 'Effects of Immunoneutralization of Corticotropin-Releasing Hormone on Ultradian Rhythms of Plasma Adrenocorticotropin*', *Endocrinology*. Narnia, 126(4), pp. 1904–1913. doi: 10.1210/endo-126-4-1904.

Carnes, M. *et al.* (1992) 'Pulsatile ACTH and Cortisol in Goats: Effects of Insulin-Induced Hypoglycemia and Dexamethasone', *Neuroendocrinology*, 55(1), pp. 97–104. doi: 10.1159/000126102.

Carnes, M. *et al.* (1994) 'Coincident plasma ACTH and corticosterone time series: Comparisons between young and old rats', *Experimental Gerontology*. Pergamon, 29(6), pp. 625–643. doi: 10.1016/0531-5565(94)90075-2.

Carvalho, L. A. *et al.* (2014) 'Inflammatory activation is associated with a reduced glucocorticoid receptor alpha/beta expression ratio in monocytes of inpatients with melancholic major depressive disorder', *Translational Psychiatry*. Nature Publishing Group, 4(1), pp. e344–e344. doi: 10.1038/tp.2013.118.

Cassuto, H. *et al.* (2005) 'Glucocorticoids Regulate Transcription of the Gene for Phosphoenolpyruvate Carboxykinase in the Liver via an Extended Glucocorticoid Regulatory Unit', *Journal of Biological Chemistry*, 280(40), pp. 33873–33884. doi: 10.1074/jbc.M504119200.

de Castro, M. *et al.* (1996) 'The non-ligand binding beta-isoform of the human glucocorticoid receptor (hGR beta): tissue levels, mechanism of action, and potential physiologic role.', *Molecular medicine (Cambridge, Mass.)*. The Feinstein Institute for Medical Research, 2(5), pp. 597–607. Available at: http://www.ncbi.nlm.nih.gov/pubmed/8898375 (Accessed: 23 March 2019).

Chaix, A. *et al.* (2019) 'Time-Restricted Feeding Prevents Obesity and Metabolic Syndrome in Mice Lacking a Circadian Clock Chaix et al', *Cell Metabolism*, 29, pp. 303-319.e4. doi: 10.1016/j.cmet.2018.08.004.

Chakera, A. J. and Vaidya, B. (2010) 'Addison Disease in Adults: Diagnosis and Management', *The American Journal of Medicine*. Elsevier, 123(5), pp. 409–413. doi: 10.1016/j.amjmed.2009.12.017.

Chakravarthy, M. V. *et al.* (2005) '"New" hepatic fat activates PPARα to maintain glucose, lipid, and cholesterol homeostasis', *Cell Metabolism*. Cell Press, 1(5), pp. 309–322. doi: 10.1016/J.CMET.2005.04.002.

Chakravarti, D. *et al.* (1996) 'Role of CBP/P300 in nuclear receptor signalling', *Nature*. Nature Publishing Group, 383(6595), pp. 99–103. doi: 10.1038/383099a0.

Chan, W. L. *et al.* (2013) 'How changes in affinity of corticosteroid-binding globulin modulate free cortisol concentration', *Journal of Clinical Endocrinology and Metabolism*, 98(8), pp. 3315–3322. doi: 10.1210/jc.2012-4280.

Chandola, T., Brunner, E. and Marmot, M. (2006) 'Chronic stress at work and the metabolic syndrome: prospective study.', *BMJ (Clinical research ed.)*, 332(7540), pp. 521–5. doi: 10.1136/bmj.38693.435301.80.

Charmandari, E., Nicolaides, N. C. and Chrousos, G. P. (2014) 'Adrenal insufficiency.', *Lancet (London, England)*. Elsevier, 383(9935), pp. 2152–67. doi: 10.1016/S0140-6736(13)61684-0.

Chen, W. *et al.* (2008) 'Glucocorticoid Receptor Phosphorylation Differentially Affects Target Gene Expression', *Molecular Endocrinology*, 22(8), pp. 1754–1766. doi: 10.1210/me.2007-0219.

Chen, W., Rogatsky, I. and Garabedian, M. J. (2006) 'MED14 and MED1 Differentially Regulate Target-Specific Gene Activation by the Glucocorticoid Receptor', *Molecular Endocrinology*. Narnia, 20(3), pp. 560–572. doi: 10.1210/me.2005-0318.

Chinenov, Y. *et al.* (2008) 'GRIP1-associated SET-domain methyltransferase in glucocorticoid receptor target gene expression.', *Proceedings of the National Academy of Sciences of the United States of America*. National Academy of Sciences, 105(51), pp. 20185–90. doi: 10.1073/pnas.0810863105.

Cho, E. J. *et al.* (2001) 'Opposing effects of Ctk1 kinase and Fcp1 phosphatase at Ser 2 of the RNA polymerase II C-terminal domain.', *Genes & development*. Cold Spring Harbor Laboratory Press, 15(24), pp. 3319–29. doi: 10.1101/gad.935901.

Cho, H. *et al.* (2012) 'Regulation of circadian behaviour and metabolism by REV-ERB-α and REV-ERB-β', *Nature*, 485(7396), pp. 123–127. doi: 10.1038/nature11048.

Choi, B. R. *et al.* (2006) 'Expression of glucocorticoid receptor mRNAs in glucocorticoid-resistant nasal polyps', *Experimental and Molecular Medicine*. doi: 10.1038/emm.2006.55.

Chojnacki, C. *et al.* (2012) 'Melatonin secretion and metabolism in patients with hepatic encephalopathy', *Journal of gastroenterology and hepatology*, 28(2), pp. 342–347. doi: 10.1111/jgh.12055.

Ciriaco, M. *et al.* (2013) 'Corticosteroid-related central nervous system side effects.', *Journal of pharmacology & pharmacotherapeutics*. Wolters Kluwer -- Medknow Publications, 4(Suppl 1), pp. S94-8. doi: 10.4103/0976-500X.120975.

Cohen, P. *et al.* (2002) 'Role for Stearoyl-CoA Desaturase-1 in Leptin-Mediated Weight Loss', *Science*, 297(5579), pp. 240–243. doi: 10.1126/science.1071527.

Columbano, A. *et al.* (1985) 'Occurrence of cell death (apoptosis) during the involution of liver hyperplasia.', *Laboratory investigation; a journal of technical methods and pathology*, 52(6), pp. 670–

5. Available at: http://www.ncbi.nlm.nih.gov/pubmed/4010225 (Accessed: 14 May 2019).

Conway-Campbell, B. L. *et al.* (2007) 'Proteasome-dependent down-regulation of activated nuclear hippocampal glucocorticoid receptors determines dynamic responses to corticosterone.', *Endocrinology*, 148(11), pp. 5470–7. doi: 10.1210/en.2007-0585.

Conway-Campbell, B. L. *et al.* (2010) 'Glucocorticoid ultradian rhythmicity directs cyclical gene pulsing of the clock gene period 1 in rat hippocampus', *Journal of Neuroendocrinology*, 22(10), pp. 1093–1100. doi: 10.1111/j.1365-2826.2010.02051.x.

Conway-Campbell, B. L. *et al.* (2011) 'The HSP90 molecular chaperone cycle regulates cyclical transcriptional dynamics of the glucocorticoid receptor and its coregulatory molecules CBP/p300 during ultradian ligand treatment.', *Molecular endocrinology (Baltimore, Md.)*, 25(6), pp. 944–954. doi: 10.1210/me.2010-0073.

Conway-Campbell, B. L. *et al.* (2012) 'Molecular dynamics of ultradian glucocorticoid receptor action', *Molecular and Cellular Endocrinology*. Elsevier Ireland Ltd, 348(2), pp. 383–393. doi: 10.1016/j.mce.2011.08.014.

Conway, J. R., Lex, A. and Gehlenborg, N. (2017) 'UpSetR: an R package for the visualization of intersecting sets and their properties', *Bioinformatics*. Edited by J. Hancock. Narnia, 33(18), pp. 2938–2940. doi: 10.1093/bioinformatics/btx364.

Corden, J. L. (1990) 'Tails of RNA polymerase II', *Trends in Biochemical Sciences*. Elsevier Current Trends, 15(10), pp. 383–387. doi: 10.1016/0968-0004(90)90236-5.

Cordon-Cardo, C. *et al.* (1989) 'Multidrug-resistance gene (P-glycoprotein) is expressed by endothelial cells at blood-brain barrier sites.', *Proceedings of the National Academy of Sciences*, 86(2), pp. 695–698. doi: 10.1073/pnas.86.2.695.

Core, L. J., Waterfall, J. J. and Lis, J. T. (2008) 'Nascent RNA Sequencing Reveals Widespread Pausing and Divergent Initiation at Human Promoters', *Science (New York, N.Y.)*. NIH Public Access, 322(5909), p. 1845. doi: 10.1126/SCIENCE.1162228.

Cudd, T. A. *et al.* (1995) 'Ontogeny and ultradian rhythms of adrenocorticotropin and cortisol in the late-gestation fetal horse.', *The Journal of endocrinology*, 144(2), pp. 271–83. Available at: http://www.ncbi.nlm.nih.gov/pubmed/7706980 (Accessed: 2 April 2019).

Cui, Y. *et al.* (2007) 'Loss of signal transducer and activator of transcription 5 leads to hepatosteatosis and impaired liver regeneration', *Hepatology*, 46(2), pp. 504–513. doi: 10.1002/hep.21713.

Czar, M. J. *et al.* (1995) 'Evidence that the FK506-binding immunophilin heat shock protein 56 is required for trafficking of the glucocorticoid receptor from the cytoplasm to the nucleus.', *Molecular Endocrinology*, 9(11), pp. 1549–1560. doi: 10.1210/mend.9.11.8584032.

Czeisler, C. A. *et al.* (1999) 'Stability, precision, and near-24-hour period of the human circadian pacemaker.', *Science (New York, N.Y.)*. American Association for the Advancement of Science, 284(5423), pp. 2177–81. doi: 10.1126/SCIENCE.284.5423.2177.

D'Adamio, F. *et al.* (1997) 'A new dexamethasone-induced gene of the leucine zipper family protects T lymphocytes from TCR/CD3-activated cell death', *Immunity*, 7(6), pp. 803–812. doi: 10.1016/S1074-7613(00)80398-2.

Dahlman-Wright, K. *et al.* (1991) 'Interaction of the glucocorticoid receptor DNA-binding domain with DNA as a dimer is mediated by a short segment of five amino acids.', *The Journal of biological chemistry*, 266(5), pp. 3107–12. Available at: http://www.ncbi.nlm.nih.gov/pubmed/1993683 (Accessed: 25 March 2019).

Dahlman-Wright, K. *et al.* (1995) 'Structural characterization of a minimal functional transactivation domain from the human glucocorticoid receptor.', *Proceedings of the National Academy of Sciences of the United States of America*, 92(5), pp. 1699–703. Available at: http://www.ncbi.nlm.nih.gov/pubmed/7878043 (Accessed: 25 March 2019).

Das, M. K. *et al.* (2007) 'A survey of DNA motif finding algorithms.', *BMC bioinformatics*. BioMed Central, 8 Suppl 7(Suppl 7), p. S21. doi: 10.1186/1471-2105-8-S7-S21.

Daujat, S. *et al.* (2002) 'Crosstalk between CARM1 methylation and CBP acetylation on histone H3.', *Current biology : CB*, 12(24), pp. 2090–7. Available at: http://www.ncbi.nlm.nih.gov/pubmed/12498683 (Accessed: 12 April 2019).

Davies, L. *et al.* (2008) 'Cross Talk of Signaling Pathways in the Regulation of the Glucocorticoid Receptor Function', *Molecular Endocrinology*, 22(6), pp. 1331–1344. doi: 10.1210/me.2007-0360.

Delaunay, F. and Laudet, V. (2002) 'Circadian clock and microarrays: mammalian genome gets rhythm', *Trends in Genetics*. Elsevier Current Trends, 18(12), pp. 595–597. doi: 10.1016/S0168-9525(02)02794-4.

Deroo, B. J. *et al.* (2002) 'Proteasomal inhibition enhances glucocorticoid receptor transactivation and alters its subnuclear trafficking.', *Molecular and cellular biology*. American Society for Microbiology Journals, 22(12), pp. 4113–23. doi: 10.1128/MCB.22.12.4113-4123.2002.

Deuschle, M. *et al.* (1997) 'Diurnal activity and pulsatility of the hypothalamus-pituitary-adrenal system in male depressed patients and healthy controls', *Journal of Clinical Endocrinology and Metabolism*, 82(1), pp. 234–238. doi: 10.1210/jc.82.1.234.

Diamond, M. *et al.* (1990) 'Transcription factor interactions: selectors of positive or negative regulation from a single DNA element', *Science*, 249(4974), pp. 1266–1272. doi: 10.1126/science.2119054.

Dieken, E. S. and Miesfeld, R. L. (1992) 'Transcriptional transactivation functions localized to

the glucocorticoid receptor N terminus are necessary for steroid induction of lymphocyte apoptosis.', *Molecular and cellular biology*. American Society for Microbiology Journals, 12(2), pp. 589–97. doi: 10.1128/MCB.12.2.589.

Dixon, J. R. *et al.* (2012) 'Topological domains in mammalian genomes identified by analysis of chromatin interactions', *Nature*. Nature Publishing Group, 485(7398), pp. 376–380. doi: 10.1038/nature11082.

Doane, L. D. *et al.* (2010) 'Associations between jet lag and cortisol diurnal rhythms after domestic travel.', *Health psychology : official journal of the Division of Health Psychology, American Psychological Association*. NIH Public Access, 29(2), pp. 117–23. doi: 10.1037/a0017865.

Doi, R., Oishi, K. and Ishida, N. (2010) 'CLOCK regulates circadian rhythms of hepatic glycogen synthesis through transcriptional activation of Gys2.', *The Journal of biological chemistry*. American Society for Biochemistry and Molecular Biology, 285(29), pp. 22114–21. doi: 10.1074/jbc.M110.110361.

Dolinsky, V. W. *et al.* (2004) 'Regulation of the enzymes of hepatic microsomal triacylglycerol lipolysis and re-esterification by the glucocorticoid dexamethasone', *Biochemical Journal*, 378(3), pp. 967–974. doi: 10.1042/bj20031320.

Le Drean, Y. *et al.* (2002) 'Potentiation of Glucocorticoid Receptor Transcriptional Activity by Sumoylation', *Endocrinology*, 143(9), pp. 3482–3489. doi: 10.1210/en.2002-220135.

Droste, S. K. *et al.* (2008) 'Corticosterone levels in the brain show a distinct ultradian rhythm but a delayed response to forced swim stress', *Endocrinology*, 149(7), pp. 3244–3253. doi: 10.1210/en.2008-0103.

Droste, S. K. *et al.* (2009) 'Distinct, Time-Dependent Effects of Voluntary Exercise on Circadian and Ultradian Rhythms and Stress Responses of Free Corticosterone in the Rat Hippocampus', *Endocrinology*. Narnia, 150(9), pp. 4170–4179. doi: 10.1210/en.2009-0402.

Druker, J. *et al.* (2013) 'RSUME enhances glucocorticoid receptor SUMOylation and transcriptional activity.', *Molecular and cellular biology*. American Society for Microbiology Journals, 33(11), pp. 2116–27. doi: 10.1128/MCB.01470-12.

Duma, D. *et al.* (2010) 'Sexually dimorphic actions of glucocorticoids provide a link to inflammatory diseases with gender differences in prevalence.', *Science signaling*. NIH Public Access, 3(143), p. ra74. doi: 10.1126/scisignal.2001077.

Duperrex, H. *et al.* (1993) 'Rat liver 11 beta-hydroxysteroid dehydrogenase complementary deoxyribonucleic acid encodes oxoreductase activity in a mineralocorticoid-responsive toad bladder cell line.', *Endocrinology*, 132(2), pp. 612–619. doi: 10.1210/endo.132.2.8425481.

De Duve, C. *et al.* (1949) 'LE SYSTEME HEXOSE-PHOSPHATASIQUE. 1. EXISTENCE DUNE

GLUCOSE-6-PHOSPHATASE SPECIFIQUE DANS LE FOIE', *Bulletin de la Société de Chimie Biologique*, 31(7–8), pp. 1242–1253.

Earl, E. *et al.* (2017) 'Synthetic glucocorticoid treatment causes dysregulated activation dynamics of glucocorticoid receptors in brain and pituitary', in *Brain and Neuroscience Advances: BNA 2017 Festival of Neuroscience: Abstract Book*, p. 83.

Eastman, C. I. *et al.* (2005) 'Advancing circadian rhythms before eastward flight: a strategy to prevent or reduce jet lag.', *Sleep*, 28(1), pp. 33–44. Available at: http://www.ncbi.nlm.nih.gov/pubmed/15700719 (Accessed: 15 April 2019).

Ebert-Zavos, E. *et al.* (2013) 'Biological Clocks in the Duodenum and the Diurnal Regulation of Duodenal and Plasma Serotonin', *PLoS ONE*. Edited by L. C. Lyons. Public Library of Science, 8(5), p. e58477. doi: 10.1371/journal.pone.0058477.

Edmonds, S. C. and Adler, N. T. (1977) 'Food and light as entrainers of circadian running activity in the rat', *Physiology & Behavior*, 18(5), pp. 915–919. doi: 10.1016/0031-9384(77)90201-3.

Edwards, E. M. *et al.* (2012) 'Job Strain and Incident Metabolic Syndrome Over 5 Years of Follow-Up', *Journal of Occupational and Environmental Medicine*, 54(12), pp. 1447–1452. doi: 10.1097/JOM.0b013e3182783f27.

El-Maghrabi, M. R. *et al.* (1995) 'Human Fructose-1,6-Bisphosphatase Gene (FBP1): Exon-Intron Organization, Localization to Chromosome Bands 9q22.2-q22.3, and Mutation Screening in Subjects with Fructose-1,6-Bisphosphatase Deficiency', *Genomics*. Academic Press, 27(3), pp. 520–525. doi: 10.1006/GENO.1995.1085.

Elbi, C. *et al.* (2004) 'Molecular chaperones function as steroid receptor nuclear mobility factors.', *Proceedings of the National Academy of Sciences of the United States of America*. National Academy of Sciences, 101(9), pp. 2876–81. doi: 10.1073/pnas.0400116101.

Ellero-Simatos, S. *et al.* (2012) 'Assessing the metabolic effects of prednisolone in healthy volunteers using urine metabolic profiling.', *Genome medicine*. BioMed Central, 4(11), p. 94. doi: 10.1186/gm395.

ENCODE Project Consortium (2007) 'Identification and analysis of functional elements in 1% of the human genome by the ENCODE pilot project', *Nature*, 447, pp. 799–816. doi: 10.1038/nature05874.

Engblom, D. *et al.* (2007) 'Direct glucocorticoid receptor-Stat5 interaction in hepatocytes controls body size and maturation-related gene expression'. Cold Spring Harbor Laboratory Press, 21(10). doi: 10.1101/gad.426007.

Engler, D. *et al.* (1989) 'Studies of the Secretion of Corticotropin-Releasing Factor and Arginine Vasopressin into the Hypophysial-Portal Circulation of the Conscious Sheep', *Neuroendocrinology*.

Karger Publishers, 49(4), pp. 367–381. doi: 10.1159/000125141.

Engler, D. *et al.* (1990) 'Studies of the Regulation of the Hypothalamic-Pituitary-Adrenal Axis in Sheep with Hypothalamic-Pituitary Disconnection. II. Evidence for in Vivo Ultradian Hypersecretion of Proopiomelanocortin Peptides by the Isolated Anterior and Intermediate Pituitary*', *Endocrinology*. Narnia, 127(4), pp. 1956–1966. doi: 10.1210/endo-127-4-1956.

Ensler, K. *et al.* (2002) 'Dexamethasone stimulates very low density lipoprotein (VLDL) receptor gene expression in differentiating 3T3-L1 cells', *Biochimica et Biophysica Acta (BBA) - Molecular and Cell Biology of Lipids*. Elsevier, 1581(1–2), pp. 36–48. doi: 10.1016/S1388-1981(02)00118-X.

Eriksson, P. and Wrange, Örjan (1990) 'Protein-Protein Contacts in the Glucocorticoid Receptor Homodimer Influence Its DNA Binding Properties', *The Journal of biological chemistry*, 265(6), pp. 3535–3542. Available at: http://www.jbc.org/ (Accessed: 28 March 2019).

Evan, G. I. and Littlewood, T. D. (1993) 'The role of c-myc in cell growth.', *Current opinion in genetics & development*, 3(1), pp. 44–9. Available at: http://www.ncbi.nlm.nih.gov/pubmed/8453273 (Accessed: 29 May 2019).

Exton, J. *et al.* (1976) 'Carbohydrate metabolism in perfused livers of adrenalectomized and steroid-replaced rats', *American Journal of Physiology-Legacy Content*, 230(1), pp. 163–170. doi: 10.1152/ajplegacy.1976.230.1.163.

Fardet, L., Petersen, I. and Nazareth, I. (2011) 'Prevalence of long-term oral glucocorticoid prescriptions in the UK over the past 20 years', *Rheumatology*, 50(11), pp. 1982–1990. doi: 10.1093/rheumatology/ker017.

Feelders, R. A. *et al.* (2012) 'The burden of Cushing's disease: clinical and health-related quality of life aspects', *European Journal of Endocrinology*, 167(311), pp. 311–326. doi: 10.1530/EJE-11-1095.

Feingold, K. R. and Grunfeld, C. (2000) *Introduction to Lipids and Lipoproteins*, *Endotext*. MDText.com, Inc. Available at: http://www.ncbi.nlm.nih.gov/pubmed/26247089 (Accessed: 14 May 2019).

Feldstein, A. E. *et al.* (2003) 'Hepatocyte apoptosis and fas expression are prominent features of human nonalcoholic steatohepatitis.', *Gastroenterology*, 125(2), pp. 437–43. Available at: http://www.ncbi.nlm.nih.gov/pubmed/12891546 (Accessed: 14 May 2019).

Feng, J. *et al.* (2012) 'Identifying ChIP-seq enrichment using MACS', *Nature Protocols*, 7(9), pp. 1728–1740. doi: 10.1038/nprot.2012.101.

Filipsson, H. *et al.* (2006) 'The Impact of Glucocorticoid Replacement Regimens on Metabolic Outcome and Comorbidity in Hypopituitary Patients', *The Journal of Clinical Endocrinology & Metabolism*. Narnia, 91(10), pp. 3954–3961. doi: 10.1210/jc.2006-0524.

Finck, B. N. *et al.* (2006) 'Lipin 1 is an inducible amplifier of the hepatic PGC-1α/PPARα regulatory pathway', *Cell Metabolism*. Cell Press, 4(3), pp. 199–210. doi: 10.1016/J.CMET.2006.08.005.

Finkel, T., Deng, C.-X. and Mostoslavsky, R. (2009) 'Recent progress in the biology and physiology of sirtuins', *Nature*. Nature Publishing Group, 460(7255), pp. 587–591. doi: 10.1038/nature08197.

Fitzsimons, C. P. *et al.* (2008) 'The microtubule-associated protein doublecortin-like regulates the transport of the glucocorticoid receptor in neuronal progenitor cells.', *Molecular endocrinology (Baltimore, Md.)*. The Endocrine Society, 22(2), pp. 248–62. doi: 10.1210/me.2007-0233.

Flynn, B. P., Conway-Campbell, B. L. and Lightman, S. L. (2018) 'The emerging importance of ultradian glucocorticoid rhythms within metabolic pathology', *Annales d'Endocrinologie*. Elsevier Masson, 79(3), pp. 112–114. doi: 10.1016/J.ANDO.2018.03.003.

Follenius, M. *et al.* (1987) 'Ultradian plasma corticotropin and cortisol rhythms: time-series analyses', *Journal of Endocrinological Investigation*. Springer International Publishing, 10(3), pp. 261–266. doi: 10.1007/BF03348128.

Freimuth, J. *et al.* (2010) 'Application of magnetic resonance imaging in transgenic and chemical mouse models of hepatocellular carcinoma.', *Molecular cancer*. BioMed Central, 9, p. 94. doi: 10.1186/1476-4598-9-94.

Friedbichler, K. *et al.* (2012) 'Growth-hormone-induced signal transducer and activator of transcription 5 signaling causes gigantism, inflammation, and premature death but protects mice from aggressive liver cancer', *Hepatology*, 55(3), pp. 941–952. doi: 10.1002/hep.24765.

Friedman, J. E. *et al.* (1993) *Glucocorticoids Regulate the Induction of Phosphoenolpyruvate Carboxykinase (GTP) Gene Transcription during Diabetes* The hormonal regulation of transcription of the phosphoenolpyruvate carboxykinase (GTP) (4.1.1.32)*, *THE JOURNAL OF BIOLOGICAL CHEMISTRY Q*. Available at: http://www.jbc.org/content/268/17/12952.full.pdf (Accessed: 6 April 2019).

Friedrich, N. *et al.* (2012) 'The association between IGF-I and insulin resistance: a general population study in Danish adults.', *Diabetes care*. American Diabetes Association, 35(4), pp. 768–73. doi: 10.2337/dc11-1833.

Gaitan, D. *et al.* (1995) 'Glucocorticoid receptor structure and function in an adrenocorticotropin-secreting small cell lung cancer.', *Molecular Endocrinology*. Narnia, 9(9), pp. 1193–1201. doi: 10.1210/mend.9.9.7491111.

Galigniana, M. D. *et al.* (1998) 'Heat Shock Protein 90-Dependent (Geldanamycin-Inhibited) Movement of the Glucocorticoid Receptor through the Cytoplasm to the Nucleus Requires Intact Cytoskeleton', *Molecular Endocrinology*. Narnia, 12(12), pp. 1903–1913. doi:

10.1210/mend.12.12.0204.

Galliher-Beckley, A. J. *et al.* (2008) 'Glycogen Synthase Kinase 3 -Mediated Serine Phosphorylation of the Human Glucocorticoid Receptor Redirects Gene Expression Profiles', *Molecular and Cellular Biology*, 28(24), pp. 7309–7322. doi: 10.1128/MCB.00808-08.

Galliher-Beckley, A. J., Williams, J. G. and Cidlowski, J. A. (2011) 'Ligand-independent phosphorylation of the glucocorticoid receptor integrates cellular stress pathways with nuclear receptor signaling.', *Molecular and cellular biology*. American Society for Microbiology (ASM), 31(23), pp. 4663–75. doi: 10.1128/MCB.05866-11.

Gan, Y. *et al.* (2015) 'Shift work and diabetes mellitus: a meta-analysis of observational studies', *Occupational and Environmental Medicine*, 72(1), pp. 72–78. doi: 10.1136/oemed-2014-102150.

Garbarino, S. and Magnavita, N. (2015) 'Work Stress and Metabolic Syndrome in Police Officers. A Prospective Study.', *PloS one*. Public Library of Science, 10(12), p. e0144318. doi: 10.1371/journal.pone.0144318.

Gathercole, L. L. *et al.* (2011) 'Regulation of Lipogenesis by Glucocorticoids and Insulin in Human Adipose Tissue', *PLoS ONE*, 6(10), p. 26223. doi: 10.1371/journal.pone.0026223.

Gautier-Stein, A. *et al.* (2012) 'Glucotoxicity induces glucose-6-phosphatase catalytic unit expression by acting on the interaction of HIF-1α with CREB-binding protein.', *Diabetes*. American Diabetes Association, 61(10), pp. 2451–60. doi: 10.2337/db11-0986.

Gekakis, N. *et al.* (1998) 'Role of the CLOCK protein in the mammalian circadian mechanism.', *Science (New York, N.Y.)*, 280(5369), pp. 1564–9. Available at: http://www.ncbi.nlm.nih.gov/pubmed/9616112 (Accessed: 20 May 2019).

George, C. L. *et al.* (2017) 'Ultradian glucocorticoid exposure directs gene-dependent and tissue-specific mRNA expression patterns in vivo', *Molecular and Cellular Endocrinology*. Elsevier Ireland Ltd, 439, pp. 46–53. doi: 10.1016/j.mce.2016.10.019.

George, C. L., Lightman, S. L. and Biddie, S. C. (2011) 'Transcription factor interactions in genomic nuclear receptor function', *Epigenomics*. Future Medicine Ltd London, UK , 3(4), pp. 471–485. doi: 10.2217/epi.11.66.

Gerritsen, M. E. *et al.* (1997) 'CREB-binding protein/p300 are transcriptional coactivators of p65.', *Proceedings of the National Academy of Sciences of the United States of America*. National Academy of Sciences, 94(7), pp. 2927–32. doi: 10.1073/PNAS.94.7.2927.

Gibbons, G. F. *et al.* (2004) 'Synthesis and function of hepatic very-low-density lipoprotein.', *Biochemical Society transactions*. Portland Press Limited, 32(Pt 1), pp. 59–64. doi: 10.1042/.

Giguère, V. *et al.* (1986) 'Functional domains of the human glucocorticoid receptor', *Cell*. Cell

Press, 46(5), pp. 645–652. doi: 10.1016/0092-8674(86)90339-9.

'Global IDF/ISPAD Guideline for diabetes in childhood' (2011) *International Diabetes Federation*. Available at: www.ispad.org (Accessed: 20 May 2019).

Godowski, P. J. *et al.* (1987) 'Glucocorticoid receptor mutants that are constitutive activators of transcriptional enhancement', *Nature*. Nature Publishing Group, 325(6102), pp. 365–368. doi: 10.1038/325365a0.

Gonnissen, H. K. *et al.* (2012) 'Effect of a phase advance and phase delay of the 24-h cycle on energy metabolism, appetite, and related hormones', *The American Journal of Clinical Nutrition*, 96(4), pp. 689–697. doi: 10.3945/ajcn.112.037192.

Granner, D. K. and Hargrove, J. L. (1983) 'Regulation of the synthesis of tyrosine aminotransferase : the relationship to mRNA TAT', in *Molecular and cellular biology*, pp. 113–128. Available at: file:///C:/Users/mdzbf/Desktop/art%253A10.1007%252FBF00225249.pdf.

Grøntved, L. *et al.* (2013) 'C/EBP maintains chromatin accessibility in liver and facilitates glucocorticoid receptor recruitment to steroid response elements', *The EMBO Journal*, 32(11), pp. 1568–1583. doi: 10.1038/emboj.2013.106.

Grøntved, L. *et al.* (2015) 'Transcriptional activation by the thyroid hormone receptor through ligand-dependent receptor recruitment and chromatin remodelling', *Nature Communications*, 6, p. 7048. doi: 10.1038/ncomms8048.

Grunstein, M. (1997) 'Histone acetylation in chromatin structure and transcription', *Nature*. Nature Publishing Group, 389(6649), pp. 349–352. doi: 10.1038/38664.

de Guia, R., Rose, A. J. and Herzig, S. (2014) 'Glucocorticoid hormones and energy homeostasis', *Hormone moecular biology and clinical investigation*, 19(2), pp. 117–128.

Guo, N. *et al.* (2018) 'Dentate granule cell recruitment of feedforward inhibition governs engram maintenance and remote memory generalization', *Nature Medicine*. Nature Publishing Group, 24(4), pp. 438–449. doi: 10.1038/nm.4491.

Haarman, E. G. *et al.* (2004) 'Glucocorticoid receptor alpha, beta and gamma expression vs in vitro glucocorticod resistance in childhood leukemia', *Leukemia*. Nature Publishing Group, 18(3), pp. 530–537. doi: 10.1038/sj.leu.2403225.

Hahn, S. (2004) 'Structure and mechanism of the RNA polymerase II transcription machinery', *Nature Structural & Molecular Biology*. Nature Publishing Group, 11(5), pp. 394–403. doi: 10.1038/nsmb763.

Hakim, O. *et al.* (2009) 'Glucocorticoid receptor activation of the Ciz1-Lcn2 locus by long range interactions', *Journal of Biological Chemistry*, 284(10), pp. 6048–6052. doi: 10.1074/jbc.C800212200.

Hall, R. K. *et al.* (2007) 'Insulin Represses Phosphoenolpyruvate Carboxykinase Gene

Transcription by Causing the Rapid Disruption of an Active Transcription Complex: A Potential Epigenetic Effect', *Molecular Endocrinology*. Narnia, 21(2), pp. 550–563. doi: 10.1210/me.2006-0307.

Hall, R. K., Sladek, F. M. and Granner, D. K. (1995) 'The orphan receptors COUP-TF and HNF-4 serve as accessory factors required for induction of phosphoenolpyruvate carboxykinase gene transcription by glucocorticoids.', *Proceedings of the National Academy of Sciences of the United States of America*. National Academy of Sciences, 92(2), pp. 412–6. doi: 10.1073/PNAS.92.2.412.

Haller, J *et al.* (2000) 'The active phase-related increase in corticosterone and aggression are linked.', *Journal of neuroendocrinology*, 12(5), pp. 431–6. Available at: http://www.ncbi.nlm.nih.gov/pubmed/10792582 (Accessed: 15 April 2019).

Haller, J. *et al.* (2000) 'Ultradian corticosterone rhythm and the propensity to behave aggressively in male rats', *Journal of Neuroendocrinology*, 12(10), pp. 937–940. doi: 10.1046/j.1365-2826.2000.00568.x.

Hamdi, H. *et al.* (2007) 'Glucocorticoid-induced leucine zipper: A key protein in the sensitization of monocytes to lipopolysaccharide in alcoholic hepatitis', *Hepatology*, 46(6), pp. 1986–1992. doi: 10.1002/hep.21880.

Han, Y. H. *et al.* (2009) 'The effect of MG132, a proteasome inhibitor on HeLa cells in relation to cell growth, reactive oxygen species and GSH.', *Oncology reports*, 22(1), pp. 215–21. Available at: http://www.ncbi.nlm.nih.gov/pubmed/19513526 (Accessed: 26 March 2019).

Hanniman, E. A. *et al.* (2006) 'Apolipoprotein A-IV is regulated by nutritional and metabolic stress: involvement of glucocorticoids, HNF-4a, and PGC-1a', *Journal of lipid research*, 47, pp. 2503–2514. doi: 10.1194/jlr.M600303-JLR200.

Hansen, E. J. and Juni, E. (1974) 'Two routes for synthesis of phosphoenolpyruvate from C4-dicarboxylic acids in Escherichia coli', *Biochemical and Biophysical Research Communications*. Academic Press, 59(4), pp. 1204–1210. doi: 10.1016/0006-291X(74)90442-2.

Hanson, R. W. and Garber, A. J. (1972) 'Phosphoenolpyruvate carboxykinase. I. Its role in gluconeogenesis', *The American Journal of Clinical Nutrition*. Narnia, 25(10), pp. 1010–1021. doi: 10.1093/ajcn/25.10.1010.

Harbuz, M. S. and Lightman, S. L. (1989) 'Glucocorticoid inhibition of stress-induced changes in hypothalamic corticotrophin-releasing factor messenger RNA and proenkephalin a messenger RNA', *Neuropeptides*. Churchill Livingstone, 14(1), pp. 17–20. doi: 10.1016/0143-4179(89)90029-2.

Harmanci, A., Rozowsky, J. and Gerstein, M. (2014) 'MUSIC: identification of enriched regions in ChIP-Seq experiments using a mappability-corrected multiscale signal processing framework', *Genome Biology*. BioMed Central, 15(10), p. 474. doi: 10.1186/s13059-014-0474-3.

Harris, T. D. *et al.* (2008) 'Single-molecule DNA sequencing of a viral genome.', *Science (New*

York, N.Y.), 320(5872), pp. 106–9. doi: 10.1126/science.1150427.

Hattar, S. (2002) 'Melanopsin-Containing Retinal Ganglion Cells: Architecture, Projections, and Intrinsic Photosensitivity', *Science*, 295(5557), pp. 1065–1070. doi: 10.1126/science.1069609.

Hayes, J. J., Clark, D. J. and Wolffe, A. P. (1991) 'Histone contributions to the structure of DNA in the nucleosome.', *Proceedings of the National Academy of Sciences of the United States of America*. National Academy of Sciences, 88(15), pp. 6829–33. doi: 10.1073/PNAS.88.15.6829.

Heintzman, N. D. *et al.* (2009) 'Histone modifications at human enhancers reflect global cell-type-specific gene expression', *Nature*. Nature Publishing Group, 459(7243), pp. 108–112. doi: 10.1038/nature07829.

Heinz, S. *et al.* (2010) 'Simple combinations of lineage-determining transcription factors prime cis-regulatory elements required for macrophage and B cell identities.', *Molecular cell*. NIH Public Access, 38(4), pp. 576–89. doi: 10.1016/j.molcel.2010.05.004.

Heinz, S. *et al.* (2015) 'The selection and function of cell type-specific enhancers', *Nat Rev Mol Cell Biol*. Nature Publishing Group, 16(3), pp. 144–154. doi: 10.1038/nrm3949.

van Helden, J., André, B. and Collado-Vides, J. (1998) 'Extracting regulatory sites from the upstream region of yeast genes by computational analysis of oligonucleotide frequencies.', *Journal of molecular biology*, 281(5), pp. 827–42. doi: 10.1006/jmbi.1998.1947.

Hellerstein, M. K. (1999) 'De novo lipogenesis in humans: metabolic and regulatory aspects.', *European journal of clinical nutrition*, 53 Suppl 1, pp. S53-65. Available at: http://www.ncbi.nlm.nih.gov/pubmed/10365981 (Accessed: 20 May 2019).

Hemmer, M. C. *et al.* (2019) 'E47 modulates hepatic glucocorticoid action', *Nature Communications*. Nature Publishing Group, 10(1), p. 306. doi: 10.1038/s41467-018-08196-5.

Hench, P. S. and Kendall, E. C. (1949) 'The effect of a hormone of the adrenal cortex (17-hydroxy-11-dehydrocorticosterone; compound E) and of pituitary adrenocorticotropic hormone on rheumatoid arthritis.', *Mayo Clinic proceedings. Mayo Clinic*, 24(8), pp. 181–197. doi: 12/18/2013.

Hengartner, C. J. *et al.* (1998) 'Temporal Regulation of RNA Polymerase II by Srb10 and Kin28 Cyclin-Dependent Kinases', *Molecular Cell*. Cell Press, 2(1), pp. 43–53. doi: 10.1016/S1097-2765(00)80112-4.

Henley, D E *et al.* (2009) 'Development of an automated blood sampling system for use in humans) Development of an automated blood sampling system for use in humans Development of an automated blood sampling system for use in humans', *Journal of Medical Engineering & TechnologyOnline) Journal Journal of Medical Engineering & Technology*, 33(3), pp. 199–208. doi: 10.1080/03091900802185970.

Henley, David E., Russell, G. M., *et al.* (2009) 'Hypothalamic-Pituitary-Adrenal Axis Activation

in Obstructive Sleep Apnea: The Effect of Continuous Positive Airway Pressure Therapy', *The Journal of Clinical Endocrinology & Metabolism*. Narnia, 94(11), pp. 4234–4242. doi: 10.1210/jc.2009-1174.

Henley, David E., Buchanan, F., *et al.* (2009) 'Plasma apelin levels in obstructive sleep apnea and the effect of continuous positive airway pressure therapy', *Journal of Endocrinology*, 203(1), pp. 181–188. doi: 10.1677/JOE-09-0245.

Hennighausen, L. and Robinson, G. W. (2008) 'Interpretation of cytokine signaling through the transcription factors STAT5A and STAT5B.', *Genes & development*. Cold Spring Harbor Laboratory Press, 22(6), pp. 711–21. doi: 10.1101/gad.1643908.

Hers, H. G. *et al.* (1951) 'The hexose-phosphatase system. III. Intracellular localization of enzymes by fractional centrifugation.', *Bulletin de la Société de Chimie Biologique*, 33(1–2), pp. 21–41. Available at: https://www.ncbi.nlm.nih.gov/pubmed/14935564 (Accessed: 6 April 2019).

Hertz, G. Z., Hartzell, G. W. and Stormo, G. D. (1990) 'Identification of consensus patterns in unaligned DNA sequences known to be functionally related.', *Computer applications in the biosciences : CABIOS*, 6(2), pp. 81–92. doi: 10.1093/bioinformatics/6.2.81.

Herzig, S. *et al.* (2003) 'CREB controls hepatic lipid metabolism through nuclear hormone receptor PPAR-γ', *Nature*. Nature Publishing Group, 426(6963), pp. 190–193. doi: 10.1038/nature02110.

Higgins, G. M. and Anderson, R. M. (1931) 'Experimental pathology of the liver. I. Restoration of the liver of the white rat following partial surgical removal', *Archives of pathology & laboratory medicine*, 12, pp. 186–202.

Hillgartner, F. B., Salati, L. M. and Goodridge, A. G. (1995) 'Physiological and molecular mechanisms involved in nutritional regulation of fatty acid synthesis.', *Physiological reviews*, 75(1), pp. 47–76. doi: 10.1152/physrev.1995.75.1.47.

Hillier, S. G. (2007) 'Diamonds are forever: The cortisone legacy', *Journal of Endocrinology*, pp. 1–6. doi: 10.1677/JOE-07-0309.

Hinds, T. D. *et al.* (2010) 'Discovery of glucocorticoid receptor-beta in mice with a role in metabolism.', *Molecular endocrinology (Baltimore, Md.)*. The Endocrine Society, 24(9), pp. 1715–27. doi: 10.1210/me.2009-0411.

Hoffman, B. and Liebermann, D. A. (2008) 'Apoptotic signaling by c-MYC', *Oncogene*. Nature Publishing Group, 27(50), pp. 6462–6472. doi: 10.1038/onc.2008.312.

Holaday, J. W., Martinez, H. M. and Natelson, B. H. (1977) 'Synchronized ultradian cortisol rhythms in monkeys: persistence during corticotropin infusion.', *Science (New York, N.Y.)*, 198(4312), pp. 56–8. Available at: http://www.ncbi.nlm.nih.gov/pubmed/197603 (Accessed: 2 April 2019).

Hollenberg, S. M. *et al.* (1985) 'Primary structure and expression of a functional human

glucocorticoid receptor cDNA.', *Nature*. Howard Hughes Medical Institute, 318(6047), pp. 635–41. Available at: http://www.ncbi.nlm.nih.gov/pubmed/2867473 (Accessed: 23 March 2019).

Holmstrom, S. R. *et al.* (2008) 'SUMO-Mediated Inhibition of Glucocorticoid Receptor Synergistic Activity Depends on Stable Assembly at the Promoter But Not on DAXX', *Molecular Endocrinology*, 22(9), pp. 2061–2075. doi: 10.1210/me.2007-0581.

Holstege, F. C., Fiedler, U. and Timmers, H. T. (1997) 'Three transitions in the RNA polymerase II transcription complex during initiation.', *The EMBO journal*. European Molecular Biology Organization, 16(24), pp. 7468–80. doi: 10.1093/emboj/16.24.7468.

Hong, H. *et al.* (1996) 'GRIP1, a novel mouse protein that serves as a transcriptional coactivator in yeast for the hormone binding domains of steroid receptors.', *Proceedings of the National Academy of Sciences of the United States of America*, 93(10), pp. 4948–52. Available at: http://www.ncbi.nlm.nih.gov/pubmed/8643509 (Accessed: 12 April 2019).

Hong, H. *et al.* (1997) *GRIP1, a Transcriptional Coactivator for the AF-2 Transactivation Domain of Steroid, Thyroid, Retinoid, and Vitamin D Receptors Downloaded from*, *MOLECULAR AND CELLULAR BIOLOGY*. Available at: http://mcb.asm.org/ (Accessed: 12 April 2019).

Hooper, A. J., Burnett, J. R. and Watts, G. F. (2015) 'Contemporary Aspects of the Biology and Therapeutic Regulation of the Microsomal Triglyceride Transfer Protein', *Circulation Research*, 116(1), pp. 193–205. doi: 10.1161/CIRCRESAHA.116.304637.

Hudson, W. H., Youn, C. and Ortlund, E. A. (2013) 'The structural basis of direct glucocorticoid-mediated transrepression', *Nature Structural & Molecular Biology*. Nature Publishing Group, 20(1), pp. 53–58. doi: 10.1038/nsmb.2456.

Hue, L. and Rider, M. H. (1987) 'Role of fructose 2,6-bisphosphate in the control of glycolysis in mammalian tissues.', *Biochemical Journal*. Portland Press Ltd, 245(2), p. 313. Available at: https://www.ncbi.nlm.nih.gov/pmc/articles/PMC1148124/ (Accessed: 6 April 2019).

Ichimura, M. *et al.* (2015) 'High-fat and high-cholesterol diet rapidly induces non-alcoholic steatohepatitis with advanced fibrosis in Sprague-Dawley rats', *Hepatology Research*, 45(4), pp. 458–469. doi: 10.1111/hepr.12358.

Iguchi, H., Kato, K. and Inayashi, H. (1982) 'Melatonin Serum Levels and Metabolic Clearance Rate in Patients with Liver Cirrhosis', *The Journal of Clinical Endocrinology & Metabolism*. Narnia, 54(5), pp. 1025–1027. doi: 10.1210/jcem-54-5-1025.

Iizuka, K., Miller, B. and Uyeda, K. (2006) 'Deficiency of carbohydrate-activated transcription factor ChREBP prevents obesity and improves plasma glucose control in leptin-deficient (ob/ob) mice', *American Journal of Physiology-Endocrinology and Metabolism*. American Physiological Society, 291(2), pp. E358–E364. doi: 10.1152/ajpendo.00027.2006.

Imai, E. *et al.* (1990) 'Characterization of a complex glucocorticoid response unit in the phosphoenolpyruvate carboxykinase gene.', *Molecular and cellular biology*. American Society for Microbiology (ASM), 10(9), pp. 4712–9. Available at: http://www.ncbi.nlm.nih.gov/pubmed/2388623 (Accessed: 6 April 2019).

Imai, E. *et al.* (1993) 'Glucocorticoid receptor-cAMP response element-binding protein interaction and the response of the phosphoenolpyruvate carboxykinase gene to glucocorticoids.', *The Journal of biological chemistry*, 268(8), pp. 5353–6. Available at: http://www.ncbi.nlm.nih.gov/pubmed/8449898 (Accessed: 7 April 2019).

Inouye, S. T. and Kawamura, H. (1979) 'Persistence of circadian rhythmicity in a mammalian hypothalamic "island" containing the suprachiasmatic nucleus.', *Proceedings of the National Academy of Sciences of the United States of America*. National Academy of Sciences, 76(11), pp. 5962–6. Available at: http://www.ncbi.nlm.nih.gov/pubmed/293695 (Accessed: 1 April 2019).

Ioannou, G. N. *et al.* (2009) 'Association between dietary nutrient composition and the incidence of cirrhosis or liver cancer in the united states population', *Hepatology*, 50(1), pp. 175–184. doi: 10.1002/hep.22941.

Ito, K. *et al.* (2006) 'Histone deacetylase 2–mediated deacetylation of the glucocorticoid receptor enables NF-κB suppression', *Journal of Experimental Medicine*. Rockefeller University Press, 203(1), pp. 7–13. doi: 10.1084/JEM.20050466.

Itoh, M. *et al.* (2002) 'Nuclear Export of Glucocorticoid Receptor is Enhanced by c-Jun N-Terminal Kinase-Mediated Phosphorylation', *Molecular Endocrinology*. Narnia, 16(10), pp. 2382–2392. doi: 10.1210/me.2002-0144.

Iyer, V. R. *et al.* (2001) 'Genomic binding sites of the yeast cell-cycle transcription factors SBF and MBF.', *Nature*, 409(6819), pp. 533–538. doi: 10.1038/35054095.

Jackson, D. A. *et al.* (1998) 'Numbers and organization of RNA polymerases, nascent transcripts, and transcription units in HeLa nuclei.', *Molecular biology of the cell*. American Society for Cell Biology, 9(6), pp. 1523–36. Available at: http://www.ncbi.nlm.nih.gov/pubmed/9614191 (Accessed: 29 March 2019).

Jadhav, T. and Wooten, M. W. (2009) 'Defining an Embedded Code for Protein Ubiquitination.', *Journal of proteomics & bioinformatics*. NIH Public Access, 2, p. 316. doi: 10.4172/jpb.1000091.

Jantzen, H. M. *et al.* (1987) 'Cooperativity of glucocorticoid response elements located far upstream of the tyrosine aminotransferase gene.', *Cell*, 49(1), pp. 29–38. Available at: http://www.ncbi.nlm.nih.gov/pubmed/2881624 (Accessed: 25 March 2019).

Jasper, M. S. and Engeland, W. C. (1991) 'Synchronous ultradian rhythms in adrenocortical

secretion detected by microdialysis in awake rats', *American Journal of Physiology-Regulatory, Integrative and Comparative Physiology*, 261(5), pp. R1257–R1268. doi: 10.1152/ajpregu.1991.261.5.R1257.

Jensen-Urstad, A. P. L. and Semenkovich, C. F. (2012) 'Fatty acid synthase and liver triglyceride metabolism: housekeeper or messenger?', *Biochimica et biophysica acta*. NIH Public Access, 1821(5), pp. 747–53. doi: 10.1016/j.bbalip.2011.09.017.

Jetten, A. M. (2009) 'Retinoid-Related Orphan Receptors (RORs): Critical Roles in Development, Immunity, Circadian Rhythm, and Cellular Metabolism', *Nuclear Receptor Signaling*, 7(1), p. nrs.07003. doi: 10.1621/nrs.07003.

Ji, J. Y., Jing, H. and Diamond, S. L. (2003) 'Shear stress causes nuclear localization of endothelial glucocorticoid receptor and expression from the GRE promoter.', *Circulation research*, 92(3), pp. 279–85. Available at: http://www.ncbi.nlm.nih.gov/pubmed/12595339 (Accessed: 24 May 2019).

Jia, X. *et al.* (2018) 'Dynamic development of metabolic syndrome and its risk prediction in Chinese population: a longitudinal study using Markov model.', *Diabetology & metabolic syndrome*. BioMed Central, 10, p. 24. doi: 10.1186/s13098-018-0328-3.

Jiang, Z. G., Robson, S. C. and Yao, Z. (2013) 'Lipoprotein metabolism in nonalcoholic fatty liver disease.', *Journal of biomedical research*. Education Department of Jiangsu Province, 27(1), pp. 1–13. doi: 10.7555/JBR.27.20120077.

Jitrapakdee, S. *et al.* (1997) 'Regulation of Rat Pyruvate Carboxylase Gene Expression by Alternate Promoters during Development, in Genetically Obese Rats and in Insulin-secreting Cells Multiple transcripts with 5'-end heterogeneity modulate translation', *The Journal of biological chemistry*. American Society for Biochemistry and Molecular Biology, 272(33), pp. 20522–30. doi: 10.1074/JBC.272.33.20522.

Jitrapakdee, S. *et al.* (2008) 'Structure, mechanism and regulation of pyruvate carboxylase.', *The Biochemical journal*. NIH Public Access, 413(3), pp. 369–87. doi: 10.1042/BJ20080709.

Jitrapakdee, S. and Wallace, J. C. (1999) *Structure, function and regulation of pyruvate carboxylase - alternate promoters generate multiple transcripts with the 5'-end heterogeneity*, *Biochem. J.* Available at: https://www.ncbi.nlm.nih.gov/pmc/articles/PMC1220216/pdf/10229653.pdf (Accessed: 6 April 2019).

John, K. *et al.* (2016) 'The glucocorticoid receptor: cause of or cure for obesity?', *American journal of physiology. Endocrinology and metabolism*. American Physiological Society, 310(4), pp. E249-57. doi: 10.1152/ajpendo.00478.2015.

John, S. *et al.* (2008) 'Interaction of the Glucocorticoid Receptor with the Chromatin Landscape', *Molecular Cell*, 29(5), pp. 611–624. doi: 10.1016/j.molcel.2008.02.010.

John, S. *et al.* (2011) 'Chromatin accessibility pre-determines glucocorticoid receptor binding patterns.', *Nature genetics*, 43(3), pp. 264–8. doi: 10.1038/ng.759.

Johnson, D. S. *et al.* (2007) 'Genome-wide mapping of in vivo protein-DNA interactions', *Science*, 316(5830), pp. 1497–1502. doi: 1141319 [pii]\r10.1126/science.1141319.

Jonat, C. *et al.* (1990) 'Antitumor promotion and antiinflammation: Down-modulation of AP-1 (Fos/Jun) activity by glucocorticoid hormone', *Cell*. Cell Press, 62(6), pp. 1189–1204. doi: 10.1016/0092-8674(90)90395-U.

Jones, C. G., Hothi, S. K. and Titheradge, M. A. (1993) 'Effect of dexamethasone on gluconeogenesis, pyruvate kinase, pyruvate carboxylase and pyruvate dehydrogenase flux in isolated hepatocytes', *Biochemical Journal*, 289(3), pp. 821–828. doi: 10.1042/bj2890821.

Jones, M T, Hillhouse, E. W. and Burden, J. L. (1977) 'Dynamics and mechanics of corticosteroid feedback at the hypothalamus and anterior pituitary gland.', *The Journal of endocrinology*, 73(3), pp. 405–17. Available at: http://www.ncbi.nlm.nih.gov/pubmed/194993 (Accessed: 15 November 2018).

Jones, M. T., Hillhouse, E. W. and Burden, J. L. (1977) 'Structure-activity relationships of corticosteroid feedback at the hypothalamic level', *Journal of Endocrinology*, 74(3), pp. 415–424.

Jubb, A. W. *et al.* (2016) 'Enhancer Turnover Is Associated with a Divergent Transcriptional Response to Glucocorticoid in Mouse and Human Macrophages.', *Journal of immunology (Baltimore, Md. : 1950)*. American Association of Immunologists, 196(2), pp. 813–822. doi: 10.4049/jimmunol.1502009.

Jubb, A. W. *et al.* (2017) 'Glucocorticoid Receptor Binding Induces Rapid and Prolonged Large-Scale Chromatin Decompaction at Multiple Target Loci', *Cell Reports*. Elsevier, 21(11), pp. 3022–3031. doi: 10.1016/j.celrep.2017.11.053.

Judd, L. L. *et al.* (2014) 'Adverse Consequences of Glucocorticoid Medication: Psychological, Cognitive, and Behavioral Effects', *American Journal of Psychiatry*. American Psychiatric AssociationArlington, VA, 171(10), pp. 1045–1051. doi: 10.1176/appi.ajp.2014.13091264.

Kalafatakis, K. *et al.* (2018) 'Ultradian rhythmicity of plasma cortisol is necessary for normal emotional and cognitive responses in man.', *Proceedings of the National Academy of Sciences of the United States of America*. National Academy of Sciences, 115(17), pp. E4091–E4100. doi: 10.1073/pnas.1714239115.

Kalsbeek, A. *et al.* (1992) 'Vasopressin-containing neurons of the suprachiasmatic nuclei inhibit corticosterone release', *Brain Research*. Elsevier, 580(1–2), pp. 62–67. doi: 10.1016/0006-8993(92)90927-2.

Kalsbeek, A. *et al.* (2008) 'Opposite actions of hypothalamic vasopressin on circadian corticosterone rhythm in nocturnal versus diurnal species', *European Journal of Neuroscience*, 27(4), pp. 818–827. doi: 10.1111/j.1460-9568.2008.06057.x.

Kalsbeek, A., la Fleur, S. and Fliers, E. (2014) 'Circadian control of glucose metabolism.', *Molecular metabolism*. Elsevier, 3(4), pp. 372–83. doi: 10.1016/j.molmet.2014.03.002.

Kalsbeek, A., van der Vliet, J. and Buijs, R. M. (1996) 'Decrease of endogenous vasopressin release necessary for expression of the circadian rise in plasma corticosterone: a reverse microdialysis study.', *Journal of neuroendocrinology*, 8(4), pp. 299–307. Available at: http://www.ncbi.nlm.nih.gov/pubmed/8861286 (Accessed: 2 April 2019).

Kamitani, T. *et al.* (1998) 'Covalent modification of PML by the sentrin family of ubiquitin-like proteins.', *The Journal of biological chemistry*. American Society for Biochemistry and Molecular Biology, 273(6), pp. 3117–20. doi: 10.1074/JBC.273.6.3117.

Kanamoto, R., Su, Y. and Pitot, H. C. (1991) *Hormonal Regulation of Serine Dehydratase Gene Expression in Liver and Kidney of the Adrenalectomized Rat*. Available at: https://academic.oup.com/mend/article-abstract/5/11/1661/2714261 (Accessed: 30 April 2019).

Karatsoreos, I. N. *et al.* (2011) 'Disruption of circadian clocks has ramifications for metabolism, brain, and behavior', *Proceedings of the National Academy of Sciences*, 108(4), pp. 1657–1662. doi: 10.1073/pnas.1018375108.

Karssen, A. M. *et al.* (2001) 'Multidrug resistance P-glycoprotein hampers the access of cortisol but not of corticosterone to mouse and human brain', *Endocrinology*, 142(6), pp. 2686–2694. doi: 10.1210/en.142.6.2686.

Karssen, A. M. *et al.* (2005) 'Low Doses of Dexamethasone Can Produce a Hypocorticosteroid State in the Brain', *Endocrinology*. Narnia, 146(12), pp. 5587–5595. doi: 10.1210/en.2005-0501.

Kauppi, B. *et al.* (2003) 'The Three-dimensional Structures of Antagonistic and Agonistic Forms of the Glucocorticoid Receptor Ligand-binding Domain', *Journal of Biological Chemistry*, 278(25), pp. 22748–22754. doi: 10.1074/jbc.M212711200.

Kaur, J. (2014) 'A comprehensive review on metabolic syndrome.', *Cardiology research and practice*. Hindawi Limited, 2014, p. 943162. doi: 10.1155/2014/943162.

Kendall, E. C. *et al.* (1936) 'A physiologic and chemical investigation of the suprarenal cortex', *Journal of Biological Chemistry*.

Kendall, E. C. (1949) 'Some observations on the hormone of the adrenal cortex designated compound E', *Proc Staff Meet Mayo Clin*, 24(8), pp. 181–197.

Kent, W. J. *et al.* (2002) 'The human genome browser at UCSC.', *Genome research*. Cold Spring Harbor Laboratory Press, 12(6), pp. 996–1006. doi: 10.1101/gr.229102.

Kharbanda, K. (2009) 'Alcoholic Liver Disease and Methionine Metabolism', *Seminars in Liver Disease*, 29(02), pp. 155–165. doi: 10.1055/s-0029-1214371.

Kim, H. *et al.* (2011) 'A short survey of computational analysis methods in analysing ChIP-seq data', *Human Genomics*, 5(2), pp. 117–123. doi: 10.1186/1479-7364-5-2-117.

Kim, Y. H. *et al.* (2018) 'Rev-erbα dynamically modulates chromatin looping to control circadian gene transcription.', *Science (New York, N.Y.)*. American Association for the Advancement of Science, p. eaao6891. doi: 10.1126/science.aao6891.

Kino, T. *et al.* (2005) 'G protein beta interacts with the glucocorticoid receptor and suppresses its transcriptional activity in the nucleus.', *The Journal of cell biology*. The Rockefeller University Press, 169(6), pp. 885–96. doi: 10.1083/jcb.200409150.

Kino, T. *et al.* (2007) 'Cyclin-Dependent Kinase 5 Differentially Regulates the Transcriptional Activity of the Glucocorticoid Receptor through Phosphorylation: Clinical Implications for the Nervous System Response to Glucocorticoids and Stress', *Molecular Endocrinology*. Narnia, 21(7), pp. 1552–1568. doi: 10.1210/me.2006-0345.

Kino, T. *et al.* (2009) 'Glucocorticoid receptor (GR) beta has intrinsic, GRalpha-independent transcriptional activity.', *Biochemical and biophysical research communications*. NIH Public Access, 381(4), pp. 671–5. doi: 10.1016/j.bbrc.2009.02.110.

Kino, T. (2018) 'GR-regulating Serine/Threonine Kinases: New Physiologic and Pathologic Implications.', *Trends in endocrinology and metabolism: TEM*. Elsevier, 29(4), pp. 260–270. doi: 10.1016/j.tem.2018.01.010.

Kinyamu, H. K. and Archer, T. K. (2004) 'Modifying chromatin to permit steroid hormone receptor-dependent transcription', *Biochimica et Biophysica Acta (BBA) - Gene Structure and Expression*. Elsevier, 1677(1–3), pp. 30–45. doi: 10.1016/J.BBAEXP.2003.09.015.

Kishnani, P. S. *et al.* (2014) 'Diagnosis and management of glycogen storage disease type I: a practice guideline of the American College of Medical Genetics and Genomics', *Genetics in Medicine*. Nature Publishing Group, 16(11), pp. e1–e1. doi: 10.1038/gim.2014.128.

Kiss, J. Z., Mezey, E. and Skirboll, L. (1984) 'Corticotropin-releasing factor-immunoreactive neurons of the paraventricular nucleus become vasopressin positive after adrenalectomy.', *Proceedings of the National Academy of Sciences of the United States of America*, 81(6), pp. 1854–1858. doi: 10.1073/pnas.81.6.1854.

Kitchener, P. *et al.* (2004) 'Differences between brain structures in nuclear translocation and DNA binding of the glucocorticoid receptor during stress and the circadian cycle', *European Journal of Neuroscience*, 19(7), pp. 1837–1846. doi: 10.1111/j.1460-9568.2004.03267.x.

Koh, S. S. *et al.* (2001) 'Synergistic Enhancement of Nuclear Receptor Function by p160

Coactivators and Two Coactivators with Protein Methyltransferase Activities', *Journal of Biological Chemistry*, 276(2), pp. 1089–1098. doi: 10.1074/jbc.M004228200.

Kohsaka, A. *et al.* (2007) 'High-Fat Diet Disrupts Behavioral and Molecular Circadian Rhythms in Mice', *Cell Metabolism*. Cell Press, 6(5), pp. 414–421. doi: 10.1016/J.CMET.2007.09.006.

Kojetin, D. J. and Burris, T. P. (2014) 'REV-ERB and ROR nuclear receptors as drug targets.', *Nature reviews. Drug discovery*. NIH Public Access, 13(3), pp. 197–216. doi: 10.1038/nrd4100.

Komarnitsky, P., Cho, E. J. and Buratowski, S. (2000) 'Different phosphorylated forms of RNA polymerase II and associated mRNA processing factors during transcription.', *Genes & development*, 14(19), pp. 2452–60. Available at: http://www.ncbi.nlm.nih.gov/pubmed/11018013 (Accessed: 25 May 2016).

Koohy, H. *et al.* (2014) 'A comparison of peak callers used for DNase-Seq data', *PLoS ONE*, 9(5). doi: 10.1371/journal.pone.0096303.

Vander Kooi, B. T. *et al.* (2005) 'The Glucose-6-Phosphatase Catalytic Subunit Gene Promoter Contains Both Positive and Negative Glucocorticoid Response Elements', *Molecular Endocrinology*. Narnia, 19(12), pp. 3001–3022. doi: 10.1210/me.2004-0497.

Koopman, A. D. M. *et al.* (2017) 'The Association between Social Jetlag, the Metabolic Syndrome, and Type 2 Diabetes Mellitus in the General Population: The New Hoorn Study.', *Journal of biological rhythms*. SAGE Publications, 32(4), pp. 359–368. doi: 10.1177/0748730417713572.

Kornberg, R. D. (1974) 'Chromatin structure: a repeating unit of histones and DNA.', *Science (New York, N.Y.)*, 184(139), pp. 868–871. doi: 10.1126/science.184.4139.868.

Kornberg, R. D. and Lorch, Y. (1999) 'Twenty-Five Years of the Nucleosome, Fundamental Particle of the Eukaryote Chromosome', *Cell*. Cell Press, 98(3), pp. 285–294. doi: 10.1016/S0092-8674(00)81958-3.

Kotronen, A. *et al.* (2009) 'Hepatic stearoyl-CoA desaturase (SCD)-1 activity and diacylglycerol but not ceramide concentrations are increased in the nonalcoholic human fatty liver.', *Diabetes*. American Diabetes Association, 58(1), pp. 203–8. doi: 10.2337/db08-1074.

Krämer, A. *et al.* (2014) 'Causal analysis approaches in Ingenuity Pathway Analysis', *Bioinformatics*. Narnia, 30(4), pp. 523–530. doi: 10.1093/bioinformatics/btt703.

Krett, N. L. *et al.* (1995) 'A variant glucocorticoid receptor messenger RNA is expressed in multiple myeloma patients.', *Cancer research*. American Association for Cancer Research, 55(13), pp. 2727–9. Available at: http://www.ncbi.nlm.nih.gov/pubmed/7796394 (Accessed: 23 March 2019).

Krieger, D. T. *et al.* (1971) 'Characterization of the Normal Temporal Pattern of Plasma Corticosteroid Levels', *The Journal of Clinical Endocrinology & Metabolism*. Narnia, 32(2), pp. 266–284. doi: 10.1210/jcem-32-2-266.

Kume, K. *et al.* (1999) 'mCRY1 and mCRY2 are essential components of the negative limb of the circadian clock feedback loop.', *Cell*, 98(2), pp. 193–205. Available at: http://www.ncbi.nlm.nih.gov/pubmed/10428031 (Accessed: 20 May 2019).

Kuo, T. *et al.* (2015) 'Regulation of Glucose Homeostasis by Glucocorticoids.', *Advances in experimental medicine and biology*. NIH Public Access, 872, pp. 99–126. doi: 10.1007/978-1-4939-2895-8_5.

Kuznetsova, T. *et al.* (2015) 'Glucocorticoid receptor and nuclear factor kappa-b affect three-dimensional chromatin organization.', *Genome biology*. BioMed Central, 16, p. 264. doi: 10.1186/s13059-015-0832-9.

Kyrou, I., Chrousos, G. P. and Tsigos, C. (2006) 'Stress, Visceral Obesity, and Metabolic Complications', *Annals of the New York Academy of Sciences*. John Wiley & Sons, Ltd (10.1111), 1083(1), pp. 77–110. doi: 10.1196/annals.1367.008.

van der Laan, S. *et al.* (2008) 'Chromatin immunoprecipitation scanning identifies glucocorticoid receptor binding regions in the proximal promoter of a ubiquitously expressed glucocorticoid target gene in brain', *Journal of Neurochemistry*, 106(6), pp. 2515–2523. doi: 10.1111/j.1471-4159.2008.05575.x.

van der Laan, S., de Kloet, E. R. and Meijer, O. C. (2009) 'Timing is critical for effective glucocorticoid receptor mediated repression of the cAMP-induced CRH gene.', *PloS one*. Public Library of Science, 4(1), p. e4327. doi: 10.1371/journal.pone.0004327.

Lagrost, L. *et al.* (1989) 'Evidence for high density lipoproteins as the major apolipoprotein A-IV-containing fraction in normal human serum', *Journal of lipid research*, 30, pp. 1525–1534. Available at: www.jlr.org (Accessed: 10 April 2019).

Lane, E. A. and Moss, H. B. (1985) 'Pharmacokinetics of Melatonin in Man: First Pass Hepatic Metabolism', *The Journal of Clinical Endocrinology & Metabolism*. Narnia, 61(6), pp. 1214–1216. doi: 10.1210/jcem-61-6-1214.

de Lange, P. *et al.* (2001) 'Expression in hematological malignancies of a glucocorticoid receptor splice variant that augments glucocorticoid receptor-mediated effects in transfected cells.', *Cancer research*, 61(10), pp. 3937–41. Available at: http://www.ncbi.nlm.nih.gov/pubmed/11358809 (Accessed: 23 March 2019).

Langlais, D. *et al.* (2012) 'The Stat3/GR Interaction Code: Predictive Value of Direct/Indirect DNA Recruitment for Transcription Outcome', *Molecular Cell*. Cell Press, 47(1), pp. 38–49. doi: 10.1016/J.MOLCEL.2012.04.021.

Langmead, B. and Salzberg, S. L. (2012) 'Fast gapped-read alignment with Bowtie 2', *Nat Methods*, 9(4), pp. 357–359. doi: 10.1038/nmeth.1923.

Larsson, J. *et al.* (2019) 'eulerr: Area-Proportional Euler and Venn Diagrams with Ellipses'. Comprehensive R Archive Network (CRAN). Available at: https://cran.r-project.org/web/packages/eulerr/index.html (Accessed: 22 April 2019).

Lee, D. Y. *et al.* (1993) 'A positive role for histone acetylation in transcription factor access to nucleosomal DNA', *Cell*. Cell Press, 72(1), pp. 73–84. doi: 10.1016/0092-8674(93)90051-Q.

Lee, H. L. and Archer, T. K. (1994) 'Nucleosome-mediated disruption of transcription factor-chromatin initiation complexes at the mouse mammary tumor virus long terminal repeat in vivo.', *Molecular and cellular biology*. American Society for Microbiology Journals, 14(1), pp. 32–41. doi: 10.1128/MCB.14.1.32.

Lee, H. and Schatz, M. C. (2012) 'Genomic dark matter: the reliability of short read mapping illustrated by the genome mappability score.', *Bioinformatics (Oxford, England)*. Oxford University Press, 28(16), pp. 2097–105. doi: 10.1093/bioinformatics/bts330.

Lee, W. *et al.* (1987) 'Activation of transcription by two factors that bind promoter and enhancer sequences of the human metallothionein gene and SV40', *Nature*. Nature Publishing Group, 325(6102), pp. 368–372. doi: 10.1038/325368a0.

Lee, W. *et al.* (2007) 'A high-resolution atlas of nucleosome occupancy in yeast.', *Nature genetics*, 39(10), pp. 1235–44. doi: 10.1038/ng2117.

Lehner, R. and Verger, R. (1997) 'Purification and Characterization of a Porcine Liver Microsomal Triacylglycerol Hydrolase †', *Biochemistry*, 36(7), pp. 1861–1868. doi: 10.1021/bi962186d.

Lembessis, P., Kalariti, N. and Koutsilieris, M. (2004) 'Glucocorticoid receptor function suppresses insulin-like growth factor 1 activity in human KLE endometrial-like cells.', *In Vivo*, 18(1), pp. 43–7. Available at: http://www.ncbi.nlm.nih.gov/pubmed/15011750 (Accessed: 14 May 2019).

Lemke, U. *et al.* (2008) 'The Glucocorticoid Receptor Controls Hepatic Dyslipidemia through Hes1', *Cell Metabolism*. Cell Press, 8(3), pp. 212–223. doi: 10.1016/J.CMET.2008.08.001.

Lerdrup, M. *et al.* (2016) 'An interactive environment for agile analysis and visualization of ChIP-sequencing data', *Nature Structural & Molecular Biology*. Nature Publishing Group, 23(4), pp. 349–357. doi: 10.1038/nsmb.3180.

Leu, J. I. *et al.* (2003) 'Impaired Hepatocyte DNA Synthetic Response Posthepatectomy in Insulin-Like Growth Factor Binding Protein 1-Deficient Mice with Defects in C/EBP and Mitogen-Activated Protein Kinase/Extracellular Signal-Regulated Kinase Regulation', *Molecular and Cellular Biology*, 23(4), pp. 1251–1259. doi: 10.1128/MCB.23.4.1251-1259.2003.

Li, H. *et al.* (2009) 'The Sequence Alignment/Map format and SAMtools.', *Bioinformatics (Oxford, England)*. Oxford University Press, 25(16), pp. 2078–9. doi: 10.1093/bioinformatics/btp352.

Lightman, S. (2016) *Rhythms Within Rhythms: The Importance of Oscillations for*

Glucocorticoid Hormones, *A Time for Metabolism and Hormones*. doi: 10.1007/978-3-319-27069-2_10.

Lightman, S. L. *et al.* (2002) 'Hypothalamic-pituitary-adrenal function.', *Archives of physiology and biochemistry*, 110(1–2), pp. 90–3. doi: 10.1076/apab.110.1.90.899.

Lightman, S. L. (2006) 'Patterns of exposure to glucocorticoid receptor ligand.', *Biochemical Society transactions*, 34(Pt 6), pp. 1117–8. doi: 10.1042/BST0341117.

Lightman, S. L. and Conway-Campbell, B. L. (2010) 'The crucial role of pulsatile activity of the HPA axis for continuous dynamic equilibration.', *Nature reviews. Neuroscience*. Nature Publishing Group, 11(10), pp. 710–718. doi: 10.1038/nrn2914.

Lim, H. W. *et al.* (2015) 'Genomic redistribution of GR monomers and dimers mediates transcriptional response to exogenous glucocorticoid in vivo', *Genome Research*, 25(6), pp. 836–844. doi: 10.1101/gr.188581.114.

Lin, B., Morris, D. W. and Chou, J. Y. (1998) 'Hepatocyte Nuclear Factor 1α Is an Accessory Factor Required for Activation of Glucose-6-Phosphatase Gene Transcription by Glucocorticoids', *DNA and Cell Biology*, 17(11), pp. 967–974. doi: 10.1089/dna.1998.17.967.

Linder, C. *et al.* (1976) 'Lipoprotein lipase and uptake of chylomicron triglyceride by skeletal muscle of rats', *American Journal of Physiology-Legacy Content*. American Physiological Society, 231(3), pp. 860–864. doi: 10.1152/ajplegacy.1976.231.3.860.

Linton, M. E., Fame, R. V and Young, S. G. (1993) 'Familial hypobetalipoproteinemia', *Journal of lipid research*, 34(4), pp. 521–541. Available at: www.jlr.org (Accessed: 14 May 2019).

Liu, J. and DeFranco, D. B. (1999) 'Chromatin Recycling of Glucocorticoid Receptors: Implications for Multiple Roles of Heat Shock Protein 90', *Molecular Endocrinology*. Narnia, 13(3), pp. 355–365. doi: 10.1210/mend.13.3.0258.

Loudon, A. S. *et al.* (1994) 'Ultradian endocrine rhythms are altered by a circadian mutation in the Syrian hamster.', *Endocrinology*. Narnia, 135(2), pp. 712–718. doi: 10.1210/endo.135.2.8033819.

Love, M. I., Huber, W. and Anders, S. (2014) 'Moderated estimation of fold change and dispersion for RNA-seq data with DESeq2', *Genome Biology*, 15. doi: 10.1186/s13059-014-0550-8.

Low, S. C. *et al.* (1994) '"Liver-type" 11 beta-hydroxysteroid dehydrogenase cDNA encodes reductase but not dehydrogenase activity in intact mammalian COS-7 cells.', *Journal of molecular endocrinology*, 13(2), pp. 167–74. Available at: http://www.ncbi.nlm.nih.gov/pubmed/7848528 (Accessed: 20 April 2019).

Lu, N. Z. *et al.* (2007) 'Selective Regulation of Bone Cell Apoptosis by Translational Isoforms of the Glucocorticoid Receptor', *Molecular and Cellular Biology*, 27(20), pp. 7143–7160. doi: 10.1128/MCB.00253-07.

Lu, N. Z. and Cidlowski, J. A. (2005) 'Translational Regulatory Mechanisms Generate N-Terminal Glucocorticoid Receptor Isoforms with Unique Transcriptional Target Genes', *Molecular Cell*. Cell Press, 18(3), pp. 331–342. doi: 10.1016/J.MOLCEL.2005.03.025.

Lu, Y. *et al.* (2012) 'Glucocorticoids promote hepatic cholestasis in mice by inhibiting the transcriptional activity of the farnesoid X receptor', *Gastroenterology*, 143(6), pp. 1630–1640. doi: 10.1053/j.gastro.2012.08.029.

Lu, Z., Gu, Y. and Rooney, S. A. (2001) 'Transcriptional regulation of the lung fatty acid synthase gene by glucocorticoid, thyroid hormone and transforming growth factor-beta 1.', *Biochimica et biophysica acta*, 1532(3), pp. 213–22. Available at: http://www.ncbi.nlm.nih.gov/pubmed/11470242 (Accessed: 11 April 2019).

Luedde, T., Kaplowitz, N. and Schwabe, R. F. (2014) 'Cell Death and Cell Death Responses in Liver Disease: Mechanisms and Clinical Relevance', *Gastroenterology*. NIH Public Access, 147(4), p. 765. doi: 10.1053/J.GASTRO.2014.07.018.

Luisi, B. F. *et al.* (1991) 'Crystallographic analysis of the interaction of the glucocorticoid receptor with DNA', *Nature*. Nature Publishing Group, 352(6335), pp. 497–505. doi: 10.1038/352497a0.

Luse, D. S. (2014) 'The RNA polymerase II preinitiation complex. Through what pathway is the complex assembled?', *Transcription*. Taylor & Francis, 5(1), p. e27050. doi: 10.4161/trns.27050.

Lyssenko, V. *et al.* (2009) 'Common variant in MTNR1B associated with increased risk of type 2 diabetes and impaired early insulin secretion', *Nature Genetics*. Nature Publishing Group, 41(1), pp. 82–88. doi: 10.1038/ng.288.

MacDougald, O. A. *et al.* (1994) 'Glucocorticoids Reciprocally Regulate Expression of the CCAATEnhancer-binding Protein a and 6 Genes in 3T3-Ll Adipocytes and White Adipose Tissue', *JOURNAL OF BIOLOGICAL CHEMISTRY*, 269(29), pp. 19041–19047. Available at: http://www.jbc.org/content/269/29/19041.full.pdf (Accessed: 11 April 2019).

Macfarlane, D. P., Forbes, S. and Walker, B. R. (2008) 'Glucocorticoids and fatty acid metabolism in humans: fuelling fat redistribution in the metabolic syndrome', *Journal of Endocrinology*, 197(2), pp. 189–204. Available at: https://joe.bioscientifica.com/view/journals/joe/197/2/189.xml (Accessed: 31 March 2019).

Madrigal, P. and Krajewski, P. (2012) 'Current bioinformatic approaches to identify DNase I hypersensitive sites and genomic footprints from DNase-seq data', *Frontiers in Genetics*. doi: 10.3389/fgene.2012.00230.

Mahajan, R. *et al.* (1997) 'A Small Ubiquitin-Related Polypeptide Involved in Targeting RanGAP1 to Nuclear Pore Complex Protein RanBP2', *Cell*. Cell Press, 88(1), pp. 97–107. doi:

10.1016/S0092-8674(00)81862-0.

Mahley, R. W. (1988) 'Apolipoprotein E: cholesterol transport protein with expanding role in cell biology.', *Science (New York, N.Y.)*. American Association for the Advancement of Science, 240(4852), pp. 622–30. doi: 10.1126/SCIENCE.3283935.

Malmström, R. *et al.* (1997) 'Metabolic basis of hypotriglyceridemic effects of insulin in normal men.', *Arteriosclerosis, thrombosis, and vascular biology*, 17(7), pp. 1454–64. Available at: http://www.ncbi.nlm.nih.gov/pubmed/9261280 (Accessed: 20 May 2019).

Manelli, F. and Giustina, A. (2000) 'Glucocorticoid-induced Osteoporosis', *Trends in Endocrinology & Metabolism*, 11(3), pp. 79–85. doi: 10.1016/S1043-2760(00)00234-4.

Mangiapane, E. H. and Brindley, D. N. (1986) 'Effects of dexamethasone and insulin on the synthesis of triacylglycerols and phosphatidylcholine and the secretion of very-low-density lipoproteins and lysophosphatidylcholine by monolayer cultures of rat hepatocytes.', *The Biochemical journal*. Portland Press Ltd, 233(1), pp. 151–60. Available at: http://www.ncbi.nlm.nih.gov/pubmed/3513755 (Accessed: 10 April 2019).

Marcus, F. *et al.* (1987) 'Function, structure and evolution of fructose-1,6-bisphosphatase.', *Archivos de biologia y medicina experimentales*, 20(3–4), pp. 371–8. Available at: http://www.ncbi.nlm.nih.gov/pubmed/8816077 (Accessed: 6 April 2019).

Martí, O., Martí, J. and Armario, A. (1994) 'Effects of chronic stress on food intake in rats: influence of stressor intensity and duration of daily exposure.', *Physiology & behavior*, 55(4), pp. 747–53. Available at: http://www.ncbi.nlm.nih.gov/pubmed/8190805 (Accessed: 15 May 2019).

Martin, A. D., Allan, E. H. and Titheradge, M. A. (1984) 'The stimulation of mitochondrial pyruvate carboxylation after dexamethasone treatment of rats.', *The Biochemical journal*. Portland Press Limited, 219(1), pp. 107–15. doi: 10.1042/BJ2190107.

Mason, H. L., Hoehn, W. M. and Kendall, E. C. (1938) 'Chemical studies of the auprarenal cortex IV. structures of compounds C, D, E, F, and G', *Jounral of biological chemistry*, 120, pp. 719–741. Available at: http://www.jbc.org/ (Accessed: 20 April 2019).

Massillon, D. *et al.* (1996) 'Glucose regulates in vivo glucose-6-phosphatase gene expression in the liver of diabetic rats.', *The Journal of biological chemistry*. American Society for Biochemistry and Molecular Biology, 271(17), pp. 9871–4. doi: 10.1074/jbc.271.17.9871.

Massillon, D. (2001) 'Regulation of the glucose-6-phosphatase gene by glucose occurs by transcriptional and post-transcriptional mechanisms. Differential effect of glucose and xylitol.', *The Journal of biological chemistry*. American Society for Biochemistry and Molecular Biology, 276(6), pp. 4055–62. doi: 10.1074/jbc.M007939200.

Mato, J. M., Martínez-Chantar, M. L. and Lu, S. C. (2008) 'Methionine Metabolism and Liver

Disease', *Annual Review of Nutrition*. Annual Reviews , 28(1), pp. 273–293. doi: 10.1146/annurev.nutr.28.061807.155438.

McDowell, I. C. *et al.* (2018) 'Glucocorticoid receptor recruits to enhancers and drives activation by motif-directed binding.', *Genome research*. Cold Spring Harbor Laboratory Press, 28(9), pp. 1272–1284. doi: 10.1101/gr.233346.117.

McEwen, B. S. (2007) 'Physiology and neurobiology of stress and adaptation: Central role of the brain.', *Physiological Reviews*, 87, pp. 873–904. doi: 10.1152/physrev.00041.2006.

McFarlan, S. C. *et al.* (1997) 'Characterization of an intronic hormone response element of the rat liver/skeletal muscle 6-phosphofructo-2-kinase/fructose-2,6-bisphosphatase gene', *Molecular and Cellular Endocrinology*. Elsevier, 129(2), pp. 219–227. doi: 10.1016/S0303-7207(97)00069-5.

Medina-Santillán, R. *et al.* (2013) 'Hepatic manifestations of metabolic syndrome', *Diabetes/Metabolism Research and Reviews*, p. n/a:n/a. doi: 10.1002/dmrr.2410.

Meijer, O. C. *et al.* (1998) 'Penetration of Dexamethasone into Brain Glucocorticoid Targets Is Enhanced in mdr1A P-Glycoprotein Knockout Mice [1]', *Endocrinology*. Narnia, 139(4), pp. 1789–1793. doi: 10.1210/endo.139.4.5917.

Meijer, O. C. *et al.* (2000) 'Transcriptional repression of the 5-HT1A receptor promoter by corticosterone via mineralocorticoid receptors depends on the cellular context', *Journal of Neuroendocrinology*, 12(3), pp. 245–254. doi: 10.1046/j.1365-2826.2000.00445.x.

Meijer, O. C., Buurstede, J. C. and Schaaf, M. J. M. (2019) 'Corticosteroid Receptors in the Brain: Transcriptional Mechanisms for Specificity and Context-Dependent Effects.', *Cellular and molecular neurobiology*. Springer, 39(4), pp. 539–549. doi: 10.1007/s10571-018-0625-2.

Meijsing, S. *et al.* (2009) 'DNA binding site sequence directs glucocorticoid receptor structure and activity', *Science*, 324(5925), pp. 407–410. doi: 10.1126/science.1164265.DNA.

Meijsing, S. H. *et al.* (2007) 'The ligand binding domain controls glucocorticoid receptor dynamics independent of ligand release.', *Molecular and cellular biology*. American Society for Microbiology (ASM), 27(7), pp. 2442–51. doi: 10.1128/MCB.01570-06.

Meisner, H., Loose, D. S. and Hanson, R. W. (1985) 'Effect of Hormones on Transcription of the Gene for Cytosolic Phosphoenolpyruvate Carboxykinase (GTP) in Rat Kidneyf', *Biochemistry*, 24, pp. 421–425. Available at: https://pubs.acs.org/sharingguidelines (Accessed: 6 April 2019).

Méndez-Lucas, A. *et al.* (2013) 'PEPCK-M expression in mouse liver potentiates, not replaces, PEPCK-C mediated gluconeogenesis.', *Journal of hepatology*. NIH Public Access, 59(1), pp. 105–13. doi: 10.1016/j.jhep.2013.02.020.

Menefee, A. L. and Zeczycki, T. N. (2014) 'Nearly 50 years in the making: defining the catalytic mechanism of the multifunctional enzyme, pyruvate carboxylase', *FEBS Journal*. John Wiley & Sons,

Ltd (10.1111), 281(5), pp. 1333–1354. doi: 10.1111/febs.12713.

Mersmann, H. J. and Segal, H. L. (1969) 'Glucocorticoid Control of the Liver Glycogen Synthetase-activating System', *The journal of biological chemistry*, 244(7), pp. 1701–1704. Available at: http://www.jbc.org/ (Accessed: 1 May 2019).

Michaud, K., Forget, H. and Cohen, H. (2009) 'Chronic glucocorticoid hypersecretion in Cushing's syndrome exacerbates cognitive aging', *Brain and Cognition*. Elsevier Inc., 71(1), pp. 1–8. doi: 10.1016/j.bandc.2009.02.013.

Mifsud, K. R. and Reul, J. M. H. M. (2016) 'Acute stress enhances heterodimerization and binding of corticosteroid receptors at glucocorticoid target genes in the hippocampus.', *Proceedings of the National Academy of Sciences of the United States of America*. National Academy of Sciences, p. 201605246. doi: 10.1073/pnas.1605246113.

Mikkelsen, T. S. *et al.* (2007) 'Genome-wide maps of chromatin state in pluripotent and lineage-committed cells.', *Nature*, 448(7153), pp. 553–560. doi: 10.1038/nature06008.

Miller, A. L. *et al.* (2005) 'p38 Mitogen-Activated Protein Kinase (MAPK) Is a Key Mediator in Glucocorticoid-Induced Apoptosis of Lymphoid Cells: Correlation between p38 MAPK Activation and Site-Specific Phosphorylation of the Human Glucocorticoid Receptor at Serine 211', *Molecular Endocrinology*, 19(6), pp. 1569–1583. doi: 10.1210/me.2004-0528.

Le Minh, N. *et al.* (2001) 'Glucocorticoid hormones inhibit food-induced phase-shifting of peripheral circadian oscillators.', *The EMBO journal*. European Molecular Biology Organization, 20(24), pp. 7128–36. doi: 10.1093/emboj/20.24.7128.

Moalli, P. A. *et al.* (1993) 'Alternatively spliced glucocorticoid receptor messenger RNAs in glucocorticoid-resistant human multiple myeloma cells.', *Cancer research*. American Association for Cancer Research, 53(17), pp. 3877–9. Available at: http://www.ncbi.nlm.nih.gov/pubmed/8358712 (Accessed: 23 March 2019).

Monczor, F. *et al.* (2019) 'A Model of Glucocorticoid Receptor Interaction With Coregulators Predicts Transcriptional Regulation of Target Genes.', *Frontiers in pharmacology*. Frontiers Media SA, 10, p. 214. doi: 10.3389/fphar.2019.00214.

Mooradian, A. D., Haas, M. J. and Wong, N. C. W. (2004) 'Transcriptional Control of Apolipoprotein A-I Gene Expression in Diabetes', *Diabetes*. American Diabetes Association, 53(3), pp. 513–520. doi: 10.2337/DIABETES.53.3.513.

Moore, R. L., Dai, Y. and Faller, D. V (2012) 'Sirtuin 1 (SIRT1) and steroid hormone receptor activity in cancer.', *The Journal of endocrinology*. NIH Public Access, 213(1), pp. 37–48. doi: 10.1530/JOE-11-0217.

Moore, R. Y. and Eichler, V. B. (1972) 'Loss of a circadian adrenal corticosterone rhythm

following suprachiasmatic lesions in the rat', *Brain Research*. Elsevier, 42(1), pp. 201–206. doi: 10.1016/0006-8993(72)90054-6.

Morsink, M. C. *et al.* (2006) 'The dynamic pattern of glucocorticoid receptor-mediated transcriptional responses in neuronal PC12 cells', *Journal of Neurochemistry*. John Wiley & Sons, Ltd (10.1111), 99(4), pp. 1282–1298. doi: 10.1111/j.1471-4159.2006.04187.x.

Mueller, K. M. *et al.* (2012) 'Hepatic growth hormone and glucocorticoid receptor signaling in body growth, steatosis and metabolic liver cancer development.', *Molecular and cellular endocrinology*. Elsevier, 361(1–2), pp. 1–11. doi: 10.1016/j.mce.2012.03.026.

Mukherji, A. *et al.* (2015) 'Shifting eating to the circadian rest phase misaligns the peripheral clocks with the master SCN clock and leads to a metabolic syndrome', *Proceedings of the National Academy of Sciences*, 112(48), pp. E6691–E6698. doi: 10.1073/pnas.1519807112.

Muse, G. W. *et al.* (2007) 'RNA polymerase is poised for activation across the genome.', *Nature genetics*. NIH Public Access, 39(12), pp. 1507–11. doi: 10.1038/ng.2007.21.

Nader, N., Chrousos, G. P. and Kino, T. (2009) 'Circadian rhythm transcription factor CLOCK regulates the transcriptional activity of the glucocorticoid receptor by acetylating its hinge region lysine cluster: potential physiological implications', *The FASEB Journal*. Federation of American Societies for Experimental Biology, 23(5), pp. 1572–1583. doi: 10.1096/fj.08-117697.

Nakajima, T. *et al.* (1997) 'RNA helicase A mediates association of CBP with RNA polymerase II.', *Cell*, 90(6), pp. 1107–12. Available at: http://www.ncbi.nlm.nih.gov/pubmed/9323138 (Accessed: 12 April 2019).

Narisawa, K. *et al.* (1978) 'A new variant of glycogen storage disease Type I probably due to a defect in the glucose-6-phosphate transport system', *Biochemical and Biophysical Research Communications*. Academic Press, 83(4), pp. 1360–1364. doi: 10.1016/0006-291X(78)91371-2.

Neufeld-Cohen, A. *et al.* (2016) 'Circadian control of oscillations in mitochondrial rate-limiting enzymes and nutrient utilization by PERIOD proteins.', *Proceedings of the National Academy of Sciences of the United States of America*. National Academy of Sciences, 113(12), pp. E1673-82. doi: 10.1073/pnas.1519650113.

Nevzorova, Y. A. *et al.* (2013) 'Overexpression of c-myc in hepatocytes promotes activation of hepatic stellate cells and facilitates the onset of liver fibrosis', *Biochimica et Biophysica Acta (BBA) - Molecular Basis of Disease*. Elsevier, 1832(10), pp. 1765–1775. doi: 10.1016/J.BBADIS.2013.06.001.

Newell-Price, J. *et al.* (2006) 'Cushing's syndrome', *Lancet*, pp. 1605–1617. doi: 10.1016/S0140-6736(06)68699-6.

Newton, R. and Holden, N. S. (2007) 'Separating transrepression and transactivation: a distressing divorce for the glucocorticoid receptor?', *Molecular pharmacology*. American Society for

Pharmacology and Experimental Therapeutics, 72(4), pp. 799–809. doi: 10.1124/mol.107.038794.

Nicolaides, N. C. *et al.* (2018) *Glucocorticoid Therapy and Adrenal Suppression*, *Endotext*. MDText.com, Inc. Available at: http://www.ncbi.nlm.nih.gov/pubmed/25905379 (Accessed: 31 March 2019).

Nieman, L. K. and Ilias, I. (2005) 'Evaluation and treatment of Cushing's syndrome', *The American Journal of Medicine*, 118(12), pp. 1340–1346. doi: 10.1016/j.amjmed.2005.01.059.

Nishida, S. *et al.* (1977) 'The Variations of Plasma Corticosterone/Cortisol Ratios Following ACTH Stimulation or Dexamethasone Administration in Normal Men', *The Journal of Clinical Endocrinology & Metabolism*. Narnia, 45(3), pp. 585–588. doi: 10.1210/jcem-45-3-585.

Nocito, A. *et al.* (2007) 'Serotonin Mediates Oxidative Stress and Mitochondrial Toxicity in a Murine Model of Nonalcoholic Steatohepatitis', *Gastroenterology*, 133(2), pp. 608–618. doi: 10.1053/j.gastro.2007.05.019.

Nora, E. P. *et al.* (2012) 'Spatial partitioning of the regulatory landscape of the X-inactivation centre', *Nature*. Nature Publishing Group, 485(7398), pp. 381–385. doi: 10.1038/nature11049.

O'Brien, R. M. *et al.* (1990) 'Identification of a sequence in the PEPCK gene that mediates a negative effect of insulin on transcription.', *Science (New York, N.Y.)*, 249(4968), pp. 533–7. Available at: http://www.ncbi.nlm.nih.gov/pubmed/2166335 (Accessed: 7 April 2019).

O'Brien, R. M. *et al.* (1995) 'Hepatic nuclear factor 3- and hormone-regulated expression of the phosphoenolpyruvate carboxykinase and insulin-like growth factor-binding protein 1 genes.', *Molecular and cellular biology*, 15(3), pp. 1747–58. Available at: http://www.ncbi.nlm.nih.gov/pubmed/7532283 (Accessed: 7 April 2019).

Oakley, R. H. *et al.* (1999) 'The dominant negative activity of the human glucocorticoid receptor beta isoform. Specificity and mechanisms of action.', *The Journal of biological chemistry*, 274(39), pp. 27857–66. Available at: http://www.ncbi.nlm.nih.gov/pubmed/10488132 (Accessed: 23 March 2019).

Oakley, R. H. and Cidlowski, J. A. (2013) 'The biology of the glucocorticoid receptor: New signaling mechanisms in health and disease', *Journal of Allergy and Clinical Immunology*. Mosby, 132(5), pp. 1033–1044. doi: 10.1016/J.JACI.2013.09.007.

Oakley, R. H., Sar, M. and Cidlowski, J. A. (1996) 'The human glucocorticoid receptor beta isoform. Expression, biochemical properties, and putative function.', *The Journal of biological chemistry*. American Society for Biochemistry and Molecular Biology, 271(16), pp. 9550–9. doi: 10.1074/JBC.271.16.9550.

Ogawa, H. *et al.* (2002) 'Evidence for a dimeric structure of rat liver serine dehydratase', *International Journal of Biochemistry and Cell Biology*, 34(5), pp. 533–543. doi: 10.1016/S1357-

2725(01)00146-7.

Ogawa, H. and Ansai, Y. (1995) 'Diurnal Rhythms of Rat Liver Serine Dehydratase, D-Site Binding Protein, and 3-Hydroxy-3-methylglutaryl Coenzyme A Reductase mRNA Levels Are Altered by Destruction of the Suprachiasmatic Nucleus of the Hypothalamus', *Archives of Biochemistry and Biophysics*. Academic Press, 321(1), pp. 115–122. doi: 10.1006/ABBI.1995.1375.

Ohgaki, H. *et al.* (1996) 'Molecular analyses of liver tumors in c-myc transgenic mice and c-myc and TGF-alpha double transgenic mice.', *Cancer letters*, 106(1), pp. 43–9. Available at: http://www.ncbi.nlm.nih.gov/pubmed/8827045 (Accessed: 29 May 2019).

Okabe, T. *et al.* (2016) 'REV-ERBα influences the stability and nuclear localization of the glucocorticoid receptor', *Journal of Cell Science*, (129), pp. 4143–4154. doi: 10.1242/jcs.190959.

Olefsky, J. M. *et al.* (1975) 'The effects of acute and chronic dexamethasone administration on insulin binding to isolated rat hepatocytes and adipocytes', *Metabolism*. W.B. Saunders, 24(4), pp. 517–527. doi: 10.1016/0026-0495(75)90076-1.

Olswang, Y. *et al.* (2003) 'Glucocorticoids repress transcription of phosphoenolpyruvate carboxykinase (GTP) gene in adipocytes by inhibiting its C/EBP-mediated activation.', *The Journal of biological chemistry*. American Society for Biochemistry and Molecular Biology, 278(15), pp. 12929–36. doi: 10.1074/jbc.M300263200.

Onate, S. A. *et al.* (1998) 'The steroid receptor coactivator-1 contains multiple receptor interacting and activation domains that cooperatively enhance the activation function 1 (AF1) and AF2 domains of steroid receptors.', *The Journal of biological chemistry*, 273(20), pp. 12101–8. Available at: http://www.ncbi.nlm.nih.gov/pubmed/9575154 (Accessed: 12 April 2019).

Onuma, H. *et al.* (2006) 'Correlation between FOXO1a (FKHR) and FOXO3a (FKHRL1) Binding and the Inhibition of Basal Glucose-6-Phosphatase Catalytic Subunit Gene Transcription by Insulin', *Molecular Endocrinology*. Narnia, 20(11), pp. 2831–2847. doi: 10.1210/me.2006-0085.

Osborne, C. S. *et al.* (2004) 'Active genes dynamically colocalize to shared sites of ongoing transcription', *Nature Genetics*. Nature Publishing Group, 36(10), pp. 1065–1071. doi: 10.1038/ng1423.

Oster, H. *et al.* (2016) 'The functional and clinical significance of the 24-h rhythm of circulating glucocorticoids', *Endocrine Reviews*. Oxford University Press, 38(1), p. er.2015-1080. doi: 10.1210/er.2015-1080.

Ota, T., Gayet, C. and Ginsberg, H. N. (2008) 'Inhibition of apolipoprotein B100 secretion by lipid-induced hepatic endoplasmic reticulum stress in rodents.', *The Journal of clinical investigation*. American Society for Clinical Investigation, 118(1), pp. 316–32. doi: 10.1172/JCI32752.

Ozcan, U. *et al.* (2004) 'Endoplasmic reticulum stress links obesity, insulin action, and type 2

diabetes.', *Science (New York, N.Y.)*. American Association for the Advancement of Science, 306(5695), pp. 457–61. doi: 10.1126/science.1103160.

Paakinaho, V. *et al.* (2014) 'SUMOylation regulates the chromatin occupancy and anti-proliferative gene programs of glucocorticoid receptor', *Nucleic Acids Research*. Narnia, 42(3), pp. 1575–1592. doi: 10.1093/nar/gkt1033.

Panda, S. *et al.* (2002) 'Coordinated Transcription of Key Pathways in the Mouse by the Circadian Clock', *Cell*. Cell Press, 109(3), pp. 307–320. doi: 10.1016/S0092-8674(02)00722-5.

Pariante, C. M. (2006) 'The glucocorticoid receptor: part of the solution or part of the problem?', *Journal of Psychopharmacology*. SAGE PublicationsLondon, Thousand Oaks, CA and New Delhi, 20(4_suppl), pp. 79–84. doi: 10.1177/1359786806066063.

Pariante, C. M. and Lightman, S. L. (2008) 'The HPA axis in major depression: classical theories and new developments', *Trends in Neurosciences*, 31(9), pp. 464–468. doi: 10.1016/j.tins.2008.06.006.

Park, P. J. (2009) 'ChIP-seq: advantages and challenges of a maturing technology.', *Nature reviews. Genetics*. Nature Publishing Group, 10(10), pp. 669–80. doi: 10.1038/nrg2641.

Pasieka, A. *et al.* (2016) 'Impact of Glucocorticoid Excess on Glucose Tolerance: Clinical and Preclinical Evidence', *Metabolites*. Multidisciplinary Digital Publishing Institute, 6(3), p. 24. doi: 10.3390/metabo6030024.

Pei, L. (1996) *Identification of a Negative Glucocorticoid Response Element in the Rat Type 1 Vasoactive Intestinal Polypeptide Receptor Gene* Downloaded from*, *THE JOURNAL OF BIOLOGICAL CHEMISTRY*. Available at: http://www.jbc.org/ (Accessed: 29 March 2019).

Pepke, S., Wold, B. and Mortazavi, A. (2009) 'Computation for ChIP-seq and RNA-seq studies', *Nature Methods*, 6(11s), pp. S22–S32. doi: 10.1038/nmeth.1371.

Petersons, C. J. *et al.* (2013) 'Effects of Low-Dose Prednisolone on Hepatic and Peripheral Insulin Sensitivity, Insulin Secretion, and Abdominal Adiposity in Patients With Inflammatory Rheumatologic Disease', *Diabetes Care*. American Diabetes Association, 36(9), p. 2822. doi: 10.2337/DC12-2617.

Pfaff, S. J. and Fletterick, R. J. (2010) 'Hormone binding and co-regulator binding to the glucocorticoid receptor are allosterically coupled.', *The Journal of biological chemistry*. American Society for Biochemistry and Molecular Biology, 285(20), pp. 15256–67. doi: 10.1074/jbc.M110.108118.

Phan, J. and Reue, K. (2005) 'Lipin, a lipodystrophy and obesity gene', *Cell Metabolism*, 1(1), pp. 73–83. doi: 10.1016/j.cmet.2004.12.002.

Picard, D. *et al.* (1990) 'Reduced levels of hsp90 compromise steroid receptor action in vivo',

Nature. Nature Publishing Group, 348(6297), pp. 166–168. doi: 10.1038/348166a0.

Picard, D. and Yamamoto, K. R. (1987) 'Two signals mediate hormone-dependent nuclear localization of the glucocorticoid receptor.', *The EMBO journal*, 6(11), pp. 3333–40. Available at: http://www.ncbi.nlm.nih.gov/pubmed/3123217 (Accessed: 25 March 2019).

Pierreux, C. E. *et al.* (1998) 'Inhibition by Insulin of Glucocorticoid-Induced Gene Transcription: Involvement of the Ligand-Binding Domain of the Glucocorticoid Receptor and Independence from the Phosphatidylinositol 3-Kinase and Mitogen-Activated Protein Kinase Pathways', *Molecular Endocrinology*. Narnia, 12(9), pp. 1343–1354. doi: 10.1210/mend.12.9.0172.

Plat, L. *et al.* (1999) 'Metabolic Effects of Short-Term Elevations of Plasma Cortisol Are More Pronounced in the Evening Than in the Morning [1]', *The Journal of Clinical Endocrinology & Metabolism*. Oxford University Press, 84(9), pp. 3082–3092. doi: 10.1210/jcem.84.9.5978.

Poggiogalle, E., Jamshed, H. and Peterson, C. M. (2018) 'Circadian regulation of glucose, lipid, and energy metabolism in humans', *Metabolism*. W.B. Saunders, 84, pp. 11–27. doi: 10.1016/J.METABOL.2017.11.017.

Polman, J. A. E., de Kloet, E. R. and Datson, N. A. (2013) 'Two Populations of Glucocorticoid Receptor-Binding Sites in the Male Rat Hippocampal Genome', *Endocrinology*, 154(5), pp. 1832–1844. doi: 10.1210/en.2012-2187.

Ponjavic, J. *et al.* (2006) 'Transcriptional and structural impact of TATA-initiation site spacing in mammalian core promoters', *Genome Biology*. BioMed Central, 7(8), p. R78. doi: 10.1186/gb-2006-7-8-r78.

Pooley, J. R. *et al.* (2017) 'Genome-wide identification of basic helix-loop helix and NF-1 motifs underlying GR binding sites in male rat hippocampus', *Endocrinology*, 158(5), pp. 1486–1501.

Powell, L. M. *et al.* (1987) 'A novel form of tissue-specific RNA processing produces apolipoprotein-B48 in intestine.', *Cell*, 50(6), pp. 831–40. Available at: http://www.ncbi.nlm.nih.gov/pubmed/3621347 (Accessed: 13 May 2019).

Pratt, W. B. *et al.* (2004) 'Role of hsp90 and the hsp90-binding immunophilins in signalling protein movement', *Cellular Signalling*, 16(8), pp. 857–872. doi: 10.1016/j.cellsig.2004.02.004.

Presman, D. M. *et al.* (2014) 'Live Cell Imaging Unveils Multiple Domain Requirements for In Vivo Dimerization of the Glucocorticoid Receptor', *PLoS Biology*, 12(3), p. e1001813. doi: 10.1371/journal.pbio.1001813.

Presman, D. M. *et al.* (2016) 'DNA binding triggers tetramerization of the glucocorticoid receptor in live cells', *Proceedings of the National Academy of Sciences*. National Academy of Sciences, 113(29), pp. 8236–8241. doi: 10.1073/PNAS.1606774113.

Qian, X. *et al.* (2012) 'Circadian and ultradian rhythms of free glucocorticoid hormone are

highly synchronized between the blood, the subcutaneous tissue, and the brain.', *Endocrinology*, 153(9), pp. 4346–53. doi: 10.1210/en.2012-1484.

Quinodoz, M. *et al.* (2014) 'Characteristic bimodal profiles of RNA polymerase II at thousands of active mammalian promoters.', *Genome biology*. BioMed Central, 15(6), p. R85. doi: 10.1186/gb-2014-15-6-r85.

van Raalte, D. H. *et al.* (2011) 'Low-dose glucocorticoid treatment affects multiple aspects of intermediary metabolism in healthy humans: a randomised controlled trial', *Diabetologia*, 54(8), pp. 2103–2112. doi: 10.1007/s00125-011-2174-9.

Rahl, P. B. *et al.* (2010) 'c-Myc regulates transcriptional pause release.', *Cell*. NIH Public Access, 141(3), pp. 432–45. doi: 10.1016/j.cell.2010.03.030.

Rankin, J. *et al.* (2012) 'Characterizing dynamic interactions between ultradian glucocorticoid rhythmicity and acute stress using the phase response curve', *PLoS ONE*, 7(2), p. e30978. doi: 10.1371/journal.pone.0030978.

Rao, N. A. S. *et al.* (2011) 'Coactivation of GR and NFKB alters the repertoire of their binding sites and target genes.', *Genome research*. Cold Spring Harbor Laboratory Press, 21(9), pp. 1404–16. doi: 10.1101/gr.118042.110.

Rashid, N. U. *et al.* (2011) 'ZINBA integrates local covariates with DNA-seq data to identify broad and narrow regions of enrichment, even within amplified genomic regions', *Genome Biology*, p. R67. doi: 10.1186/gb-2011-12-7-r67.

Raspé, E. *et al.* (2001) 'Transcriptional regulation of apolipoprotein C-III gene expression by the orphan nuclear receptor RORalpha.', *The Journal of biological chemistry*. American Society for Biochemistry and Molecular Biology, 276(4), pp. 2865–71. doi: 10.1074/jbc.M004982200.

Raspé, E. *et al.* (2002) 'Identification of Rev-erbalpha as a physiological repressor of apoC-III gene transcription.', *Journal of lipid research*, 43(12), pp. 2172–9. Available at: http://www.ncbi.nlm.nih.gov/pubmed/12454280 (Accessed: 15 April 2019).

Ratman, D. *et al.* (2013) *How glucocorticoid receptors modulate the activity of other transcription factors: A scope beyond tethering*, *Molecular and Cellular Endocrinology*. Elsevier. doi: 10.1016/j.mce.2012.12.014.

Raubenheimer, P. J. *et al.* (2006) 'The role of corticosterone in human hypothalamic? pituitary?adrenal axis feedback', *Clinical Endocrinology*. John Wiley & Sons, Ltd (10.1111), 65(1), pp. 22–26. doi: 10.1111/j.1365-2265.2006.02540.x.

Ray, A. and Prefontaine, K. E. (1994) 'Physical association and functional antagonism between the p65 subunit of transcription factor NF-kappa B and the glucocorticoid receptor.', *Proceedings of the National Academy of Sciences of the United States of America*. National Academy of Sciences,

91(2), pp. 752–6. doi: 10.1073/PNAS.91.2.752.

Reddy, T. E. *et al.* (2012) 'The hypersensitive glucocorticoid response specifically regulates period 1 and expression of circadian genes.', *Molecular and cellular biology*, 32(18), pp. 3756–67. doi: 10.1128/MCB.00062-12.

Reddy, T. E., Pauli, F. and Sprouse, R. O. (2009) 'Genomic determination of the glucocorticoid response reveals unexpected mechanisms of gene regulation Genomic determination of the glucocorticoid response reveals unexpected mechanisms of gene regulation', *Genome Research*, 19, pp. 2163–2171. doi: 10.1101/gr.097022.109.

Refinetti, R. and Menaker, M. (1992) *The Circadian Rhythm of Body Temperature*, *Physiology & Behavior*.

Reinke, H. and Hörz, W. (2003) 'Histones Are First Hyperacetylated and Then Lose Contact with the Activated PHO5 Promoter', *Molecular Cell*. Cell Press, 11(6), pp. 1599–1607. doi: 10.1016/S1097-2765(03)00186-2.

Reiter, F., Wienerroither, S. and Stark, A. (2017) 'Combinatorial function of transcription factors and cofactors', *Current Opinion in Genetics & Development*. Elsevier Current Trends, 43, pp. 73–81. doi: 10.1016/J.GDE.2016.12.007.

Ren, B. *et al.* (2000) 'Genome-wide location and function of DNA binding proteins.', *Science*, 290(5500), pp. 2306–2309. doi: 10.1126/science.290.5500.2306.

Renaud, J.-P. *et al.* (1995) 'Crystal structure of the RAR-γ ligand-binding domain bound to all-trans retinoic acid', *Nature*. Nature Publishing Group, 378(6558), pp. 681–689. doi: 10.1038/378681a0.

Reppert, S. M. and Weaver, D. R. (2002) 'Coordination of circadian timing in mammals', *Nature*. Nature Publishing Group, 418(6901), pp. 935–941. doi: 10.1038/nature00965.

Reue, K. and Dwyer, J. R. (2009) 'Lipin proteins and metabolic homeostasis.', *Journal of lipid research*. American Society for Biochemistry and Molecular Biology, 50 Suppl(Supplement), pp. S109-14. doi: 10.1194/jlr.R800052-JLR200.

Reul, J. M. H. M. and Kloet, E. R. DE (1985) 'Two Receptor Systems for Corticosterone in Rat Brain: Microdistribution and Differential Occupation', *Endocrinology*, 117(6), pp. 2505–2511. doi: 10.1210/endo-117-6-2505.

Revollo, J. R. *et al.* (2013) 'HES1 is a master regulator of glucocorticoid receptor-dependent gene expression.', *Science signaling*. NIH Public Access, 6(304), p. ra103. doi: 10.1126/scisignal.2004389.

Rider, M. H. *et al.* (2004) '6-phosphofructo-2-kinase/fructose-2,6-bisphosphatase: head-to-head with a bifunctional enzyme that controls glycolysis.', *The Biochemical journal*. Portland Press Ltd,

381(Pt 3), pp. 561–79. doi: 10.1042/BJ20040752.

Riu, E. *et al.* (2003) 'Overexpression of c-myc in the liver prevents obesity and insulin resistance', *The FASEB Journal*, 17(12), pp. 1715–1717. doi: 10.1096/fj.02-1163fje.

Rivers, C. *et al.* (1999) 'Insertion of an Amino Acid in the DNA-Binding Domain of the Glucocorticoid Receptor as a Result of Alternative Splicing', *The Journal of Clinical Endocrinology & Metabolism*. Narnia, 84(11), pp. 4283–4286. doi: 10.1210/jcem.84.11.6235.

Robertson, G. *et al.* (2007) 'Genome-wide profiles of STAT1 DNA association using chromatin immunoprecipitation and massively parallel sequencing', *Nature Methods*, 4(8), pp. 651–657. doi: 10.1038/nmeth1068.

Rochlani, Y. *et al.* (2017) 'Metabolic syndrome: pathophysiology, management, and modulation by natural compounds', *Therapeutic Advances in Cardiovascular Disease*. SAGE PublicationsSage UK: London, England, 11(8), pp. 215–225. doi: 10.1177/1753944717711379.

Rod, N. H. *et al.* (2009) 'Perceived stress as a risk factor for changes in health behaviour and cardiac risk profile: a longitudinal study', *Journal of Internal Medicine*, 266(5), pp. 467–475. doi: 10.1111/j.1365-2796.2009.02124.x.

Roden, M. *et al.* (1993) 'The circadian melatonin and cortisol secretion pattern in permanent night shift workers', *American Journal of Physiology-Regulatory, Integrative and Comparative Physiology*, 265(1), pp. R261–R267. doi: 10.1152/ajpregu.1993.265.1.R261.

Rombauts, S. *et al.* (1999) 'PlantCARE, a plant cis-acting regulatory element database', *Nucleic Acids Research*, pp. 295–296. doi: 10.1093/nar/27.1.295.

Van Rooyen, D. M. *et al.* (2011) 'Hepatic Free Cholesterol Accumulates in Obese, Diabetic Mice and Causes Nonalcoholic Steatohepatitis', *Gastroenterology*, 141(4), pp. 1393-1403.e5. doi: 10.1053/j.gastro.2011.06.040.

Rosenson, R. S. *et al.* (2012) 'Cholesterol efflux and atheroprotection: Advancing the concept of reverse cholesterol transport', *Circulation*. NIH Public Access, 125(15), p. 1905. doi: 10.1161/CIRCULATIONAHA.111.066589.

Rougvie, A. E. and Lis, J. T. (1988) 'The RNA polymerase II molecule at the 5' end of the uninduced hsp70 gene of D. melanogaster is transcriptionally engaged', *Cell*. Cell Press, 54(6), pp. 795–804. doi: 10.1016/S0092-8674(88)91087-2.

Rozowsky, J. *et al.* (2009) 'PeakSeq enables systematic scoring of ChIP-seq experiments relative to controls.', *Nature biotechnology*. Nature Publishing Group, 27(1), pp. 66–75. doi: 10.1038/nbt.1518.

Rui, L. (2014) 'Energy metabolism in the liver.', *Comprehensive Physiology*. NIH Public Access, 4(1), pp. 177–97. doi: 10.1002/cphy.c130024.

Russell, G. M. *et al.* (2010) 'Rapid glucocorticoid receptor-mediated inhibition of hypothalamic-pituitary-adrenal ultradian activity in healthy males.', *The Journal of neuroscience : the official journal of the Society for Neuroscience*. Society for Neuroscience, 30(17), pp. 6106–15. doi: 10.1523/JNEUROSCI.5332-09.2010.

Rybkin, I. I. *et al.* (1997) 'Effect of restraint stress on food intake and body weight is determined by time of day.', *The American journal of physiology*, 273(5 Pt 2), pp. R1612-22. Available at: http://www.ncbi.nlm.nih.gov/pubmed/9374801 (Accessed: 15 May 2019).

Rye, M. B., Sætrom, P. and Drabløs, F. (2011) 'A manually curated ChIP-seq benchmark demonstrates room for improvement in current peak-finder programs', *Nucleic Acids Research*, 39(4). doi: 10.1093/nar/gkq1187.

Ryu, H. *et al.* (2016) 'Office Workers' Risk of Metabolic Syndrome-Related Indicators', *Western Journal of Nursing Research*. SAGE PublicationsSage CA: Los Angeles, CA, 38(11), pp. 1433–1447. doi: 10.1177/0193945916654134.

Sagot, M. F. (2009) 'Spelling approximate repeated or common motifs using a suffix tree', *Lecture notes in computer science*, pp. 374–390. doi: 10.1.1.39.3583.

Sakamoto, T. *et al.* (1999) 'Mitosis and apoptosis in the liver of interleukin-6-deficient mice after partial hepatectomy', *Hepatology*, 29(2), pp. 403–411. doi: 10.1002/hep.510290244.

Saladin, Rc. *et al.* (1996) *Transcriptional induction of rat liver apolipoprotein A-I gene expression by glucocorticoids requires the glucocorticoid receptor and a labile cell-specific protein*, *Eur. J. Biochem*. Available at: https://febs.onlinelibrary.wiley.com/doi/pdf/10.1111/j.1432-1033.1996.0451u.x (Accessed: 8 April 2019).

Sandelin, A. *et al.* (2007) 'Mammalian RNA polymerase II core promoters: insights from genome-wide studies', *Nature Reviews Genetics*. Nature Publishing Group, 8(6), pp. 424–436. doi: 10.1038/nrg2026.

Sandoval, I. V and Sols, A. (1974) *Gluconeogenesis from Serine by the Serine-Dehydratase-Dependent Pathway in Rat Liver*, *Eur. J. Biochem*. Available at: https://febs.onlinelibrary.wiley.com/doi/pdf/10.1111/j.1432-1033.1974.tb03448.x (Accessed: 30 April 2019).

Sarabdjitsingh, R. A. *et al.* (2010) 'Stress responsiveness varies over the ultradian glucocorticoid cycle in a brain-region-specific manner', *Endocrinology*, 151(11), pp. 5369–5379. doi: 10.1210/en.2010-0832.

Sarabdjitsingh, R. A. *et al.* (2014) 'Ultradian corticosterone pulses balance glutamatergic transmission and synaptic plasticity.', *Proceedings of the National Academy of Sciences of the United States of America*. National Academy of Sciences, 111(39), pp. 14265–70. doi:

10.1073/pnas.1411216111.

Sarabdjitsingh, R. A. *et al.* (2016) 'Hippocampal Fast Glutamatergic Transmission Is Transiently Regulated by Corticosterone Pulsatility', *PLOS ONE*. Edited by R. Trullas. Public Library of Science, 11(1), p. e0145858. doi: 10.1371/journal.pone.0145858.

Sarnyai, Z. *et al.* (1995) 'Effects of cocaine and corticotropin-releasing factor on pulsatile ACTH and cortisol release in ovariectomized rhesus monkeys.', *The Journal of Clinical Endocrinology & Metabolism*. Narnia, 80(9), pp. 2745–2751. doi: 10.1210/jcem.80.9.7673418.

Sasse, S. K. *et al.* (2015) 'Response Element Composition Governs Correlations between Binding Site Affinity and Transcription in Glucocorticoid Receptor Feed-forward Loops.', *The Journal of biological chemistry*. American Society for Biochemistry and Molecular Biology, 290(32), pp. 19756–69. doi: 10.1074/jbc.M115.668558.

Savory, J. G. A. *et al.* (1999) 'Discrimination between NL1- and NL2-Mediated Nuclear Localization of the Glucocorticoid Receptor', *Molecular and Cellular BiologyCellular Biology*. American Society for Microbiology (ASM), 19(2), pp. 1025–1037. Available at: https://www.ncbi.nlm.nih.gov/pmc/articles/PMC116033/ (Accessed: 22 March 2019).

Sawchenko, P. E. (1987) 'Evidence for a local site of action for glucocorticoids in inhibiting CRF and vasopressin expression in the paraventricular nucleus', *Brain Research*. Elsevier, 403(2), pp. 213–224. doi: 10.1016/0006-8993(87)90058-8.

Sawchenko, P. E., Swanson, L. W. and Vale, W. W. (1984) 'Co-expression of corticotropin-releasing factor and vasopressin immunoreactivity in parvocellular neurosecretory neurons of the adrenalectomized rat.', *Proceedings of the National Academy of Sciences of the United States of America*, 81(6), pp. 1883–7. doi: 10.1073/pnas.81.6.1883.

Van Schaftingen, E. and Gerin, I. (2002) *The glucose-6-phosphatase system*, *Biochem. J*. Available at: https://www.ncbi.nlm.nih.gov/pmc/articles/PMC1222414/pdf/11879177.pdf (Accessed: 7 April 2019).

Scheer, F. A. J. L. *et al.* (2009) 'Adverse metabolic and cardiovascular consequences of circadian misalignment', *Proceedings of the National Academy of Sciences*. National Academy of Sciences, 106(11), pp. 4453–4458. doi: 10.1073/pnas.0808180106.

Scheidereit, C. *et al.* (1983) 'The glucocorticoid receptor binds to defined nucleotide sequences near the promoter of mouse mammary tumour virus.', *Nature*, 304(5928), pp. 749–52.

Scheschowitsch, K., Leite, J. A. and Assreuy, J. (2017) 'New Insights in Glucocorticoid Receptor Signaling-More Than Just a Ligand-Binding Receptor.', *Frontiers in endocrinology*. Frontiers Media SA, 8, p. 16. doi: 10.3389/fendo.2017.00016.

Schiller, B. J. *et al.* (2014) 'Glucocorticoid receptor binds half sites as a monomer and regulates

specific target genes', *Genome Biology*. BioMed Central, 15(8), p. 418. doi: 10.1186/s13059-014-0418-y.

Schmoll, D. *et al.* (1999) 'Identification of a cAMP response element within the glucose- 6-phosphatase hydrolytic subunit gene promoter which is involved in the transcriptional regulation by cAMP and glucocorticoids in H4IIE hepatoma cells.', *The Biochemical journal*. Portland Press Ltd, 338 (Pt 2)(Pt 2), pp. 457–63. Available at: http://www.ncbi.nlm.nih.gov/pubmed/10024523 (Accessed: 7 April 2019).

Schneider, H. J. *et al.* (2011) 'Prediction of incident diabetes mellitus by baseline IGF1 levels', *European Journal of Endocrinology*, 164(2), pp. 223–229. doi: 10.1530/EJE-10-0963.

Schoenfelder, S. *et al.* (2010) 'Preferential associations between co-regulated genes reveal a transcriptional interactome in erythroid cells', *Nature Genetics*. Nature Publishing Group, 42(1), pp. 53–61. doi: 10.1038/ng.496.

Schule, R. *et al.* (1988) 'Many transcription factors interact synergistically with steroid receptors', *Science*. American Association for the Advancement of Science, 232(4750), pp. 613–618. doi: 10.1126/science.3457470.

Schule, R. *et al.* (1990) 'Functional antagonism between oncoprotein c-Jun and the glucocorticoid receptor', *Cell*, 62(6), pp. 1217–1226. doi: 10.1016/0092-8674(90)90397-W.

Scott, D. K. *et al.* (1998) 'Further Characterization of the Glucocorticoid Response Unit in the Phosphoenolpyruvate Carboxykinase Gene. The Role of the Glucocorticoid Receptor-Binding Sites', *Molecular Endocrinology*. Narnia, 12(4), pp. 482–491. doi: 10.1210/mend.12.4.0090.

Scott, D. K., Mitchell, J. A. and Granner, D. K. (1996a) 'Identification and charaterization of the second retinoic acid response element in the phosphoenolpyruvate carboxykinase gene promoter.', *The Journal of biological chemistry*. American Society for Biochemistry and Molecular Biology, 271(11), pp. 6260–4. doi: 10.1074/JBC.271.11.6260.

Scott, D. K., Mitchell, J. A. and Granner, D. K. (1996b) 'The orphan receptor COUP-TF binds to a third glucocorticoid accessory factor element within the phosphoenolpyruvate carboxykinase gene promoter.', *The Journal of biological chemistry*. American Society for Biochemistry and Molecular Biology, 271(50), pp. 31909–14. doi: 10.1074/JBC.271.50.31909.

Scott, E., Carter, A. and Grant, P. (2008) 'Association between polymorphisms in the Clock gene, obesity and the metabolic syndrome in man', *International Journal of Obesity*, 32, pp. 658–662. doi: 10.1038/sj.ijo.0803778.

Selye, H. (1950) 'The phsiology and pathology of exposure to stress, a treatise based on the concepts of the general-adaption-syndrome and the diseases of adaption.', *ACTA, inc., Medical Publishers*.

Sexton, T. *et al.* (2012) 'Three-Dimensional Folding and Functional Organization Principles of the Drosophila Genome', *Cell*. Cell Press, 148(3), pp. 458–472. doi: 10.1016/J.CELL.2012.01.010.

Shearman, L. P. *et al.* (2000) 'Interacting molecular loops in the mammalian circadian clock.', *Science (New York, N.Y.)*, 288(5468), pp. 1013–9. Available at: http://www.ncbi.nlm.nih.gov/pubmed/10807566 (Accessed: 20 May 2019).

Shimizu, H. *et al.* (2010) 'Glucocorticoids increase NPY gene expression in the arcuate nucleus by inhibiting mTOR signaling in rat hypothalamic organotypic cultures', *Peptides*, 31(1), pp. 145–149. doi: 10.1016/j.peptides.2009.09.036.

Shimomura, I. *et al.* (1998) 'Nuclear sterol regulatory element-binding proteins activate genes responsible for the entire program of unsaturated fatty acid biosynthesis in transgenic mouse liver.', *The Journal of biological chemistry*. American Society for Biochemistry and Molecular Biology, 273(52), pp. 35299–306. doi: 10.1074/JBC.273.52.35299.

Shogren-Knaak, M. *et al.* (2006) 'Histone H4-K16 acetylation controls chromatin structure and protein interactions.', *Science (New York, N.Y.)*. American Association for the Advancement of Science, 311(5762), pp. 844–7. doi: 10.1126/science.1124000.

Silver, R. *et al.* (1996) 'A diffusible coupling signal from the transplanted suprachiasmatic nucleus controlling circadian locomotor rhythms', *Nature*. Nature Publishing Group, 382(6594), pp. 810–813. doi: 10.1038/382810a0.

Simic, I. *et al.* (2013) 'Phosphorylation of leukocyte glucocorticoid receptor in patients with current episode of major depressive disorder', *Progress in Neuro-Psychopharmacology and Biological Psychiatry*. Elsevier, 40, pp. 281–285. doi: 10.1016/J.PNPBP.2012.10.021.

Simmons, L. R. *et al.* (2012) 'Steroid-Induced Diabetes: Is It Just Unmasking of Type 2 Diabetes?', *ISRN Endocrinology*, 2012, pp. 1–5. doi: 10.5402/2012/910905.

van der Sluis, R. J. *et al.* (2012) 'Adrenalectomy stimulates the formation of initial atherosclerotic lesions: Reversal by adrenal transplantation', *Atherosclerosis*. Elsevier, 221(1), pp. 76–83. doi: 10.1016/J.ATHEROSCLEROSIS.2011.12.022.

Soncini, M. *et al.* (1995) 'Hormonal and nutritional control of the fatty acid synthase promoter in transgenic mice.', *The Journal of biological chemistry*. American Society for Biochemistry and Molecular Biology, 270(51), pp. 30339–43. doi: 10.1074/JBC.270.51.30339.

Spencer, T. E. *et al.* (1997) 'Steroid receptor coactivator-1 is a histone acetyltransferase', *Nature*. Nature Publishing Group, 389(6647), pp. 194–198. doi: 10.1038/38304.

Staels, B. (2006) 'When the Clock stops ticking, metabolic syndrome explodes', *Nature medicine*. Nature Publishing Group, 12(1), pp. 54–55; discussion 55. doi: 10.1038/nm0106-54.

Stahn, C. *et al.* (2007) 'Molecular mechanisms of glucocorticoid action and selective

glucocorticoid receptor agonists', *Molecular and Cellular Endocrinology*, 275(1–2), pp. 71–78. doi: 10.1016/j.mce.2007.05.019.

Stark, R. *et al.* (2014) 'A role for mitochondrial phosphoenolpyruvate carboxykinase (PEPCK-M) in the regulation of hepatic gluconeogenesis.', *The Journal of biological chemistry*. American Society for Biochemistry and Molecular Biology, 289(11), pp. 7257–63. doi: 10.1074/jbc.C113.544759.

Stavreva, D. A. *et al.* (2009) 'Ultradian hormone stimulation induces glucocorticoid receptor-mediated pulses of gene transcription.', *Nature cell biology*. Nature Publishing Group, 11(9), pp. 1093–1102. doi: 10.1038/ncb1922.

Stavreva, D. A. *et al.* (2015) 'Dynamics of chromatin accessibility and long-range interactions in response to glucocorticoid pulsing.', *Genome research*, 25(6), pp. 845–857. doi: 10.1101/gr.184168.114.

Stavreva, D. a *et al.* (2004) 'Rapid glucocorticoid receptor exchange at a promoter is coupled to transcription and regulated by chaperones and proteasomes.', *Molecular and cellular biology*, 24(7), pp. 2682–2697. doi: 10.1128/MCB.24.7.2682-2697.2004.

Stephan, F. K. and Zucker, I. (1972) 'Circadian rhythms in drinking behavior and locomotor activity of rats are eliminated by hypothalamic lesions.', *Proceedings of the National Academy of Sciences of the United States of America*. National Academy of Sciences, 69(6), pp. 1583–6. Available at: http://www.ncbi.nlm.nih.gov/pubmed/4556464 (Accessed: 6 November 2018).

Stöcklin, E. *et al.* (1996) 'Functional interactions between Stat5 and the glucocorticoid receptor', *Nature*. Nature Publishing Group, 383(6602), pp. 726–728. doi: 10.1038/383726a0.

Stoecklin, E. *et al.* (1997) 'Specific DNA binding of Stat5, but not of glucocorticoid receptor, is required for their functional cooperation in the regulation of gene transcription.', *Molecular and Cellular Biology*. American Society for Microbiology Journals, 17(11), pp. 6708–6716. doi: 10.1128/MCB.17.11.6708.

Stratakis, C. A. (2008) 'Cushing syndrome caused by adrenocortical tumors and hyperplasias (corticotropin- independent Cushing syndrome).', *Endocrine development*. NIH Public Access, 13, pp. 117–32. doi: 10.1159/000134829.

Stubbs, F. E., Flynn, B. P. and Conway-Campbell, B. L. (2018) 'FISH-ing Novel Dynamic Modes of Glucocorticoid-Induced Chromatin Reorganization', *Trends in Endocrinology & Metabolism*. Elsevier, 29(4), pp. 204–207. doi: 10.1016/j.tem.2018.02.003.

Su, Y. and Pitot, H. C. H. (1992) 'Location and characterization of multiple glucocorticoid-responsive elements in the rat serine dehydratase gene.', *Archives of biochemistry and biophysics*. Academic Press, 297(2), pp. 239–43. doi: 10.1016/0003-9861(92)90667-L.

Sun, X. *et al.* (2002) 'Circadian 5-HT production regulated by adrenergic signaling', *Proceedings*

of the National Academy of Sciences. National Academy of Sciences, 99(7), pp. 4686–4691. doi: 10.1073/PNAS.062585499.

Surjit, M. *et al.* (2011) 'Widespread Negative Response Elements Mediate Direct Repression by Agonist- Liganded Glucocorticoid Receptor', *Cell*. Cell Press, 145(2), pp. 224–241. doi: 10.1016/J.CELL.2011.03.027.

Suzuki, S. *et al.* (2018) 'SIRT1 is a transcriptional enhancer of the glucocorticoid receptor acting independently to its deacetylase activity.', *Molecular and cellular endocrinology*. NIH Public Access, 461, pp. 178–187. doi: 10.1016/j.mce.2017.09.012.

Swanson, L. W. *et al.* (1983) 'Organization of ovine corticotropin-releasing factor immunoreactive cells and fibers in the rat brain: an immunohistochemical study.', *Neuroendocrinology*, 36(3), pp. 165–186. doi: 10.1159/000123454.

Szapary, D., Huang, Y. and Simons, S. S. (1999) *Opposing Effects of Corepressor and Coactivators in Determining the Dose-Response Curve of Agonists, and Residual Agonist Activity of Antagonists, for Glucocorticoid Receptor-Regulated Gene Expression*. Available at: https://academic.oup.com/mend/article-abstract/13/12/2108/2747824 (Accessed: 12 April 2019).

Szczepaniak, L. S. *et al.* (2005) 'Magnetic resonance spectroscopy to measure hepatic triglyceride content: prevalence of hepatic steatosis in the general population', *American Journal of Physiology-Endocrinology and Metabolism*, 288(2), pp. E462–E468. doi: 10.1152/ajpendo.00064.2004.

Takeda, T. *et al.* (1998) 'Crosstalk between the interleukin-6 (IL-6)-JAK-STAT and the glucocorticoid-nuclear receptor pathway: synergistic activation of IL-6 response element by IL-6 and glucocorticoid.', *The Journal of endocrinology*, 159(2), pp. 323–30. Available at: http://www.ncbi.nlm.nih.gov/pubmed/9795374 (Accessed: 30 March 2019).

Tannin, G. M. *et al.* (1991) 'The human gene for 11 beta-hydroxysteroid dehydrogenase. Structure, tissue distribution, and chromosomal localization.', *The Journal of biological chemistry*, 266(25), pp. 16653–8. Available at: http://www.ncbi.nlm.nih.gov/pubmed/1885595 (Accessed: 20 April 2019).

Tappy, L. *et al.* (1994) 'Mechanisms of dexamethasone-induced insulin resistance in healthy humans.', *The Journal of Clinical Endocrinology & Metabolism*, 79(4), pp. 1063–1069. doi: 10.1210/jcem.79.4.7962275.

Tatham, M. H. *et al.* (2001) 'Polymeric chains of SUMO-2 and SUMO-3 are conjugated to protein substrates by SAE1/SAE2 and Ubc9.', *The Journal of biological chemistry*. American Society for Biochemistry and Molecular Biology, 276(38), pp. 35368–74. doi: 10.1074/jbc.M104214200.

Tatham, M. H. *et al.* (2011) 'Comparative Proteomic Analysis Identifies a Role for SUMO in Protein Quality Control', *Sci. Signal.* American Association for the Advancement of Science, 4(178), pp.

rs4–rs4. doi: 10.1126/SCISIGNAL.2001484.

Taves, M. D., Gomez-Sanchez, C. E. and Soma, K. K. (2011) 'Extra-adrenal glucocorticoids and mineralocorticoids: evidence for local synthesis, regulation, and function.', *American journal of physiology. Endocrinology and metabolism*. American Physiological Society, 301(1), pp. E11-24. doi: 10.1152/ajpendo.00100.2011.

Taylor, A. H. *et al.* (1996) 'Glucocorticoid increases rat apolipoprotein A-I promoter activity.', *Journal of lipid research*, 37(10), pp. 2232–43. Available at: http://www.ncbi.nlm.nih.gov/pubmed/8906599 (Accessed: 8 April 2019).

Tetel, M. J. (2009) 'Nuclear receptor coactivators: essential players for steroid hormone action in the brain and in behaviour.', *Journal of neuroendocrinology*. NIH Public Access, 21(4), pp. 229–37. doi: 10.1111/j.1365-2826.2009.01827.x.

Thompson, N. L. *et al.* (1986) 'Sequential protooncogene expression during rat liver regeneration.', *Cancer research*, 46(6), pp. 3111–7. Available at: http://www.ncbi.nlm.nih.gov/pubmed/3516391 (Accessed: 29 May 2019).

Thorgeirsson, S. S. and Santouni-Rugiu, E. (2003) 'Transgenic mouse models in carcinogenesis: interaction of c-myc with transforming growth factor α and hepatocyte growth factor in hepatocarcinogenesis', *British Journal of Clinical Pharmacology*, 42(1), pp. 43–52. doi: 10.1046/j.1365-2125.1996.03748.x.

Tian, S. *et al.* (2002) 'Small ubiquitin-related modifier-1 (SUMO-1) modification of the glucocorticoid receptor.', *The Biochemical journal*, 367(Pt 3), pp. 907–11. doi: 10.1042/BJ20021085.

Tirode, F. *et al.* (1999) 'Reconstitution of the transcription factor TFIIH: assignment of functions for the three enzymatic subunits, XPB, XPD, and cdk7.', *Molecular cell*, 3(1), pp. 87–95. Available at: http://www.ncbi.nlm.nih.gov/pubmed/10024882 (Accessed: 12 April 2019).

Tiwari, S. and Siddiqi, S. A. (2012) 'Intracellular Trafficking and Secretion of VLDL', *Arteriosclerosis, Thrombosis, and Vascular Biology*. Lippincott Williams & Wilkins Hagerstown, MD, 32(5), pp. 1079–1086. doi: 10.1161/ATVBAHA.111.241471.

Trapp, T. *et al.* (1994) 'Heterodimerization between mineralocorticoid and glucocorticoid receptor: a new principle of glucocorticoid action in the CNS.', *Neuron*, 13(6), pp. 1457–62. Available at: http://www.ncbi.nlm.nih.gov/pubmed/7993637 (Accessed: 25 March 2019).

Trinh, K. Y. *et al.* (1998) 'Perturbation of Fuel Homeostasis Caused by Overexpression of the Glucose-6-phosphatase Catalytic Subunit in Liver of Normal Rats', *Journal of Biological Chemistry*, 273(47), pp. 31615–31620. doi: 10.1074/jbc.273.47.31615.

Tronche, F. *et al.* (2004) 'Glucocorticoid receptor function in hepatocytes is essential to promote postnatal body growth'. Cold Spring Harbor Laboratory Press, 18(5). doi:

10.1101/gad.284704.

Trusca, V. G. *et al.* (2017) 'Differential action of glucocorticoids on apolipoprotein E gene expression in macrophages and hepatocytes.', *PloS one*. Public Library of Science, 12(3), p. e0174078. doi: 10.1371/journal.pone.0174078.

Turek, F. W. *et al.* (2013) 'Obesity and Metabolic Syndrome in Circadian Clock Mutant Mice', *Science*. American Association for the Advancement of Science, 1043(2005), pp. 3–6. doi: 10.1126/science.1108750.

Uhl, A. *et al.* (2002) 'Pharmacokinetics and pharmacodynamics of methylprednisolone after one bolus dose compared with two dose fractions.', *Journal of clinical pharmacy and therapeutics*, 27(4), pp. 281–7. Available at: http://www.ncbi.nlm.nih.gov/pubmed/12174030 (Accessed: 30 March 2019).

Uhlenhaut, N. H. *et al.* (2013) 'Insights into Negative Regulation by the Glucocorticoid Receptor from Genome-wide Profiling of Inflammatory Cistromes', *Molecular Cell*, 49(1). doi: 10.1016/j.molcel.2012.10.013.

Underwood, R. H. and Williams, G. H. (1972) 'The simultaneous measurement of aldosterone, cortisol, and corticosterone in human peripheral plasma by displacement analysis.', *The Journal of laboratory and clinical medicine*, 79(5), pp. 848–62. Available at: http://www.ncbi.nlm.nih.gov/pubmed/5062996 (Accessed: 13 August 2019).

Utter, M. F. and Bruce Keech, D. (1960) *Preliminary Communications Formation of Oxaloacetate from Pyruvate and*, *THE JOURNAL OF BIOLOGICAL CHEMI~TRS*. Available at: http://www.jbc.org/ (Accessed: 6 April 2019).

Vacchio, M. S., Papadopoulos, V. and Ashwell, J. D. (1994) 'Steroid production in the thymus: implications for thymocyte selection', *Journal of Experimental Medicine*, 179(6), pp. 1835–1846. doi: 10.1084/jem.179.6.1835.

Vaissière, T., Sawan, C. and Herceg, Z. (2008) 'Epigenetic interplay between histone modifications and DNA methylation in gene silencing', *Mutation Research/Reviews in Mutation Research*. Elsevier, 659(1–2), pp. 40–48. doi: 10.1016/J.MRREV.2008.02.004.

Valera, A. *et al.* (1995) 'Evidence from transgenic mice that myc regulates hepatic glycolysis.', *The FASEB Journal*, 9(11), pp. 1067–1078. doi: 10.1096/fasebj.9.11.7649406.

Vandevyver, S., Dejager, L. and Libert, C. (2014) 'Comprehensive Overview of the Structure and Regulation of the Glucocorticoid Receptor', *Endocrine Reviews*. Oxford University Press, 35(4), pp. 671–693. doi: 10.1210/er.2014-1010.

Varney, N. R., Alexander, B. and MacIndoe, J. H. (1984) 'Reversible steroid dementia in patients without steroid psychosis', *American Journal of Psychiatry*, 141(3), pp. 369–372. doi:

10.1176/ajp.141.3.369.

Vaziri, H. *et al.* (2001) 'hSIR2SIRT1 Functions as an NAD-Dependent p53 Deacetylase', *Cell*. Cell Press, 107(2), pp. 149–159. doi: 10.1016/S0092-8674(01)00527-X.

Vegiopoulos, A. and Herzig, S. (2007) 'Glucocorticoids, metabolism and metabolic diseases', *Molecular and Cellular Endocrinology*. Elsevier, 275(1–2), pp. 43–61. doi: 10.1016/J.MCE.2007.05.015.

Veldhuis, J. D. *et al.* (1989) 'Amplitude modulation of a burstlike mode of cortisol secretion subserves the circadian glucocorticoid rhythm.', *The American journal of physiology*, 257(14), pp. E6–E14.

Veldhuis, J. D. *et al.* (1990) 'Twenty-Four-Hour Rhythms in Plasma Concentrations of Adenohypophyseal Hormones Are Generated by Distinct Amplitude and/or Frequency Modulation of Underlying Pituitary Secretory Bursts*', *The Journal of Clinical Endocrinology & Metabolism*. Narnia, 71(6), pp. 1616–1623. doi: 10.1210/jcem-71-6-1616.

Verhoog, N. J. D. *et al.* (2011) 'Glucocorticoid-independent Repression of Tumor Necrosis Factor (TNF) α-stimulated Interleukin (IL)-6 Expression by the Glucocorticoid Receptor', *Journal of Biological Chemistry*. American Society for Biochemistry and Molecular Biology, 286(22), pp. 19297–19310. Available at: http://www.jbc.org/content/286/22/19297.long (Accessed: 26 March 2019).

Vicennati, V. *et al.* (2009) 'Stress-related Development of Obesity and Cortisol in Women', *Obesity*, 17(9), pp. 1678–1683. doi: 10.1038/oby.2009.76.

Vilo, J. *et al.* (2000) 'Mining for putative regulatory elements in the yeast genome using gene expression data', *Proc Int Conf Intell Syst Mol Biol*, 8, pp. 384–394. Available at: http://www.ncbi.nlm.nih.gov/htbin-post/Entrez/query?db=m&form=6&dopt=r&uid=10977099.

Visel, A. *et al.* (2009) 'ChIP-seq accurately predicts tissue-specific activity of enhancers.', *Nature*, 457(7231), pp. 854–8. doi: 10.1038/nature07730.

Vrang, N., Larsen, P. J. and Mikkelsen, J. D. (1995) 'Direct projection from the suprachiasmatic nucleus to hypophysiotrophic corticotropin-releasing factor immunoreactive cells in the paraventricular nucleus of the hypothalamus demonstrated by means ofPhaseolus vulgaris-leucoagglutinin tract tracing', *Brain Research*. Elsevier, 684(1), pp. 61–69. doi: 10.1016/0006-8993(95)00425-P.

Waite, E. J. *et al.* (2012) 'Ultradian corticosterone secretion is maintained in the absence of circadian cues.', *The European journal of neuroscience*, 36(8), pp. 3142–50. doi: 10.1111/j.1460-9568.2012.08213.x.

Walker, J. J. *et al.* (2012) 'The Origin of Glucocorticoid Hormone Oscillations', *PLoS Biology*. Edited by A. J. Vidal-Puig. Public Library of Science, 10(6), p. e1001341. doi: 10.1371/journal.pbio.1001341.

Walker, J. J. *et al.* (2014) 'Rapid intra-adrenal feedback regulation of glucocorticoid synthesis', *J. R. Soc. InterfaceJ*, 12, p. 20140875.

Walker, J. J., Terry, J. R. and Lightman, S. L. (2010) 'Origin of ultradian pulsatility in the hypothalamic–pituitary–adrenal axis', *Proceedings of the Royal Society B: Biological Sciences*. The Royal Society, 277(1688), pp. 1627–1633. doi: 10.1098/rspb.2009.2148.

Wallace, A. D. *et al.* (2010) 'Lysine 419 targets human glucocorticoid receptor for proteasomal degradation', *Steroids*, 75(12), pp. 1016–1023. doi: 10.1016/j.steroids.2010.06.015.

Wallace, A. D. and Cidlowski, J. A. (2001) 'Proteasome-mediated glucocorticoid receptor degradation restricts transcriptional signaling by glucocorticoids.', *The Journal of biological chemistry*. American Society for Biochemistry and Molecular Biology, 276(46), pp. 42714–21. doi: 10.1074/jbc.M106033200.

Wallberg, A. E. *et al.* (2000) 'Recruitment of the SWI-SNF chromatin remodeling complex as a mechanism of gene activation by the glucocorticoid receptor tau1 activation domain.', *Molecular and cellular biology*, 20(6), pp. 2004–13. Available at: http://www.ncbi.nlm.nih.gov/pubmed/10688647 (Accessed: 25 March 2019).

Wang, J.-C. *et al.* (2004) 'Chromatin immunoprecipitation (ChIP) scanning identifies primary glucocorticoid receptor target genes.', *Proceedings of the National Academy of Sciences of the United States of America*, 101(44), pp. 15603–15608. doi: 10.1073/pnas.0407008101.

Wang, Q., Carroll, J. S. and Brown, M. (2005) 'Spatial and Temporal Recruitment of Androgen Receptor and Its Coactivators Involves Chromosomal Looping and Polymerase Tracking', *Molecular Cell*. Cell Press, 19(5), pp. 631–642. doi: 10.1016/J.MOLCEL.2005.07.018.

Wang, W., Carey, J. D. and Gralla, J. D. (1992) 'Polymerase II promoter activation: closed complex formation and ATP-driven start site opening', *Science*. Science, 255(5043), pp. 540–453. Available at: http://www.ncbi.nlm.nih.gov/pubmed/3413495 (Accessed: 12 April 2019).

Wang, X. and DeFranco, D. B. (2005) 'Alternative Effects of the Ubiquitin-Proteasome Pathway on Glucocorticoid Receptor Down-Regulation and Transactivation Are Mediated by CHIP, an E3 Ligase', *Molecular Endocrinology*. Narnia, 19(6), pp. 1474–1482. doi: 10.1210/me.2004-0383.

Wang, Z., Frederick, J. and Garabedian, M. J. (2002) 'Deciphering the Phosphorylation "Code" of the Glucocorticoid Receptor *in Vivo*', *Journal of Biological Chemistry*, 277(29), pp. 26573–26580. doi: 10.1074/jbc.M110530200.

Warris, L. T. *et al.* (2016) 'Acute Activation of Metabolic Syndrome Components in Pediatric Acute Lymphoblastic Leukemia Patients Treated with Dexamethasone', *PLOS ONE*. Edited by O. R. Bandapalli. Public Library of Science, 11(6), p. e0158225. doi: 10.1371/journal.pone.0158225.

Weitsman, E. D. *et al.* (1971) 'Twenty-four Hour Pattern of the Episodic Secretion of Cortisol

in Normal Subjects', *The Journal of Clinical Endocrinology & Metabolism*. Narnia, 33(1), pp. 14–22. doi: 10.1210/jcem-33-1-14.

Weitzman, E. D. (1976) 'Circadian Rhythms and Episodic Hormone Secretion in Man', *Annual Review of Medicine*. Annual Reviews 4139 El Camino Way, P.O. Box 10139, Palo Alto, CA 94303-0139, USA, 27(1), pp. 225–243. doi: 10.1146/annurev.me.27.020176.001301.

Welsh, D. K. *et al.* (1995) 'Individual neurons dissociated from rat suprachiasmatic nucleus express independently phased circadian firing rhythms', *Neuron*. Cell Press, 14(4), pp. 697–706. doi: 10.1016/0896-6273(95)90214-7.

Welty, F. K. (2014) 'Hypobetalipoproteinemia and abetalipoproteinemia.', *Current opinion in lipidology*. NIH Public Access, 25(3), pp. 161–8. doi: 10.1097/MOL.0000000000000072.

Werner, A., Kuipers, F. and Verkade, H. J. (2013) 'Fat Absorption and Lipid Metabolism in Cholestasis'. Landes Bioscience. Available at: https://www.ncbi.nlm.nih.gov/books/NBK6420/?report=printable (Accessed: 9 April 2019).

Wetterau, J. R. *et al.* (1992) 'Absence of microsomal triglyceride transfer protein in individuals with abetalipoproteinemia.', *Science (New York, N.Y.)*, 258(5084), pp. 999–1001. Available at: http://www.ncbi.nlm.nih.gov/pubmed/1439810 (Accessed: 14 May 2019).

White, B. D. *et al.* (1994) 'Type II corticosteroid receptor stimulation increases NPY gene expression in basomedial hypothalamus of rats.', *The American journal of physiology*. American Physiological Society Bethesda, MD , 266(5 Pt 2), pp. R1523-9. doi: 10.1152/ajpregu.1994.266.5.R1523.

White, H. M., Koser, S. L. and Donkin, S. S. (2011) 'Differential regulation of bovine pyruvate carboxylase promoters by fatty acids and peroxisome proliferator-activated receptor-α agonist', *Journal of Dairy Science*. Elsevier, 94(7), pp. 3428–3436. doi: 10.3168/JDS.2010-3960.

Wiley, S. R., Kraus, R. J. and Mertz, J. E. (1992) 'Functional binding of the "TATA" box binding component of transcription factor TFIID to the -30 region of TATA-less promoters.', *Proceedings of the National Academy of Sciences of the United States of America*. National Academy of Sciences, 89(13), pp. 5814–8. Available at: http://www.ncbi.nlm.nih.gov/pubmed/1321424 (Accessed: 12 April 2019).

Wilkinson, L., Verhoog, N. J. D. and Louw, A. (2018) 'Disease and treatment associated acquired glucocorticoid resistance.', *Endocrine connections*. Bioscientifica Ltd., 7(12), p. R328. doi: 10.1530/EC-18-0421.

Windle, R. J., Wood, S. A., Lightman, S. L., *et al.* (1998) 'The Pulsatile Characteristics The pulsatile characteristics of hypothalamo-pituitary-adrenal activity in female Lewis and Fischer 344 rats and its relationship to differential stress responses.', *Endocrinology*. Narnia, 139(10), pp. 4044–4052. doi: 10.1210/endo.139.10.6238.

Windle, R. J., Wood, S. A., Shanks, N., *et al.* (1998) 'Ultradian Rhythm of Basal Corticosterone Release in the Female Rat: Dynamic Interaction with the Response to Acute Stress', *Endocrinology*. Oxford University Press, 139(2), pp. 443–450. doi: 10.1210/endo.139.2.5721.

Wolkowitz, O. M. (1994) 'Prospective controlled studies of the behavioral and biological effects of exogenous corticosteroids.', *Psychoneuroendocrinology*, 19(3), pp. 233–55. Available at: http://www.ncbi.nlm.nih.gov/pubmed/7515507.

Wu, I. *et al.* (2013) 'Selective glucocorticoid receptor translational isoforms reveal glucocorticoid-induced apoptotic transcriptomes', *Cell Death & Disease*. Nature Publishing Group, 4(1), pp. e453–e453. doi: 10.1038/cddis.2012.193.

Wurtz, J.-M. *et al.* (1996) 'A canonical structure for the ligand-binding domain of nuclear receptors', *Nature Structural Biology*. Nature Publishing Group, 3(1), pp. 87–94. doi: 10.1038/nsb0196-87.

Xing, H. *et al.* (2012) 'Genome-Wide Localization of Protein-DNA Binding and Histone Modification by a Bayesian Change-Point Method with ChIP-seq Data', *PLoS Computational Biology*. Edited by I. Ioshikhes. Public Library of Science, 8(7), p. e1002613. doi: 10.1371/journal.pcbi.1002613.

Xu, H. E. *et al.* (1999) 'Molecular Recognition of Fatty Acids by Peroxisome Proliferator–Activated Receptors', *Molecular Cell*. Cell Press, 3(3), pp. 397–403. doi: 10.1016/S1097-2765(00)80467-0.

Xu, Z. X., Viviano, C. J. and Rooney, S. A. (1995) 'Glucocorticoid stimulation of fatty-acid synthase gene transcription in fetal lung: antagonism by retinoic acid.', *The American journal of physiology*, 268(4 Pt 1), pp. L683-90. doi: 10.1152/ajplung.1995.268.4.L683.

Yang-Yen, H. F. *et al.* (1990) 'Transcriptional interference between c-Jun and the glucocorticoid receptor: Mutual inhibition of DNA binding due to direct protein-protein interaction', *Cell*, 62(6), pp. 1205–1215. doi: 10.1016/0092-8674(90)90396-V.

Yang, J. and DeFranco, D. B. (1994) 'Differential roles of heat shock protein 70 in the in vitro nuclear import of glucocorticoid receptor and simian virus 40 large tumor antigen.', *Molecular and cellular biology*. American Society for Microbiology (ASM), 14(8), pp. 5088–98. Available at: http://www.ncbi.nlm.nih.gov/pubmed/8035791 (Accessed: 22 March 2019).

Yang, J., Liu, J. and DeFranco, D. B. (1997) 'Subnuclear trafficking of glucocorticoid receptors in vitro: chromatin recycling and nuclear export.', *The Journal of cell biology*, 137(3), pp. 523–38. doi: 10.1083/jcb.137.3.523.

Yang, Y. *et al.* (2014) 'Leveraging biological replicates to improve analysis in ChIP-seq experiments.', *Computational and structural biotechnology journal*. Research Network of Computational and Structural Biotechnology, 9, p. e201401002. doi: 10.5936/csbj.201401002.

Yaribeygi, H. *et al.* (2019) 'Insulin resistance: Review of the underlying molecular mechanisms', *Journal of Cellular Physiology*. John Wiley & Sons, Ltd, 234(6), pp. 8152–8161. doi: 10.1002/jcp.27603.

Yin, L. *et al.* (2006) 'Nuclear Receptor Rev-erb Is a Critical Lithium-Sensitive Component of the Circadian Clock', *Science*. American Association for the Advancement of Science, 311(5763), pp. 1002–1005. doi: 10.1126/science.1121613.

Young, E., Carlson, N. E. and Brown, M. B. (2001) 'Twenty-Four-Hour ACTH and Cortisol Pulsatility in Depressed Women', *Neuropsychopharmacology*. Nature Publishing Group, 25(2), pp. 267–276. doi: 10.1016/S0893-133X(00)00236-0.

Yu, C. Y. *et al.* (2010) 'Genome-wide analysis of glucocorticoid receptor binding regions in adipocytes reveal gene network involved in triglyceride homeostasis', *PLoS ONE*, 5(12). doi: 10.1371/journal.pone.0015188.

Yuan, G.-C. *et al.* (2005) 'Genome-scale identification of nucleosome positions in S. cerevisiae.', *Science (New York, N.Y.)*, 309(5734), pp. 626–30. doi: 10.1126/science.1112178.

Zang, C. *et al.* (2009) 'A clustering approach for identification of enriched domains from histone modification ChIP-Seq data.', *Bioinformatics (Oxford, England)*. Oxford University Press, 25(15), pp. 1952–8. doi: 10.1093/bioinformatics/btp340.

Zani, F. *et al.* (2013) 'PER2 promotes glucose storage to liver glycogen during feeding and acute fasting by inducing Gys2 PTG and GL expression', *Molecular Metabolism*. Elsevier, 2(3), pp. 292–305. doi: 10.1016/J.MOLMET.2013.06.006.

Zhang, K. *et al.* (2012) 'Hepatic Suppression of *Foxo1* and *Foxo3* Causes Hypoglycemia and Hyperlipidemia in Mice', *Endocrinology*, 153(2), pp. 631–646. doi: 10.1210/en.2011-1527.

Zhang, P. *et al.* (2008) 'Regulation of lipin-1 gene expression by glucocorticoids during adipogenesis.', *Journal of lipid research*, 49(7), pp. 1519–1528. doi: 10.1194/jlr.M800061-JLR200.

Zhang, W. *et al.* (2012) 'Genome-wide identification of regulatory DNA elements and protein-binding footprints using signatures of open chromatin in Arabidopsis.', *The Plant cell*, 24(7), pp. 2719–31. doi: 10.1105/tpc.112.098061.

Zhang, X. *et al.* (2019) 'Unraveling the Regulation of Hepatic Gluconeogenesis', *Frontiers in Endocrinology*. Frontiers, 9, p. 802. doi: 10.3389/fendo.2018.00802.

Zhang, Y. *et al.* (2008) 'Model-based Analysis of ChIP-Seq (MACS)', *Genome Biology*. BioMed Central, 9(9), p. R137. doi: 10.1186/gb-2008-9-9-r137.

Zhang, Z. *et al.* (1997) 'STAT3 acts as a co-activator of glucocorticoid receptor signaling.', *The Journal of biological chemistry*. American Society for Biochemistry and Molecular Biology, 272(49), pp. 30607–10. doi: 10.1074/JBC.272.49.30607.

Zhao, H. *et al.* (2015) 'PARP1- and CTCF-Mediated Interactions between Active and Repressed

Chromatin at the Lamina Promote Oscillating Transcription', *Molecular Cell*, 59, pp. 984–997. doi: 10.1016/j.molcel.2015.07.019.

Zhao, L. F. *et al.* (2010) 'Hormonal regulation of acetyl-CoA carboxylase isoenzyme gene transcription.', *Endocrine journal*, 4, pp. 317–324. Available at: https://www.ncbi.nlm.nih.gov/pubmed/20139635 (Accessed: 11 April 2019).

Zheng, K., Cubero, F. J. and Nevzorova, Y. A. (2017) 'c-MYC-Making Liver Sick: Role of c-MYC in Hepatic Cell Function, Homeostasis and Disease.', *Genes*. Multidisciplinary Digital Publishing Institute (MDPI), 8(4). doi: 10.3390/genes8040123.

Zhou, P.-Z. *et al.* (2016) 'Relationship Between Glucocorticoids and Insulin Resistance in Healthy Individuals.', *Medical science monitor : international medical journal of experimental and clinical research*. International Scientific Information, Inc., 22, pp. 1887–94. doi: 10.12659/MSM.895251.

Zimmermann, P. L. N. and Rousseau, G. G. (1994) 'Liver-specific DNase I-hypersensitive sites and DNA methylation pattern in the promoter region of a 6-phosphofructo-2-kinase/fructose-2,6-bisphosphatase gene', *European Journal of Biochemistry*. John Wiley & Sons, Ltd (10.1111), 220(1), pp. 183–191. doi: 10.1111/j.1432-1033.1994.tb18613.x.

Zindy, F. *et al.* (1998) 'Myc signaling via the ARF tumor suppressor regulates p53-dependent apoptosis and immortalization', *Genes & Development*, 12(15), pp. 2424–2433. doi: 10.1101/gad.12.15.2424.